UNIVERSIDAD NACIONAL AUTÓNOMA DE MÉXICO

Maestría y Doctorado en Ciencias Bioquímicas

"Estudio de la participación de MAP cinasas en la regulación del desarrollo del embrión y de la raíz de *Arabidopsis thaliana*"

TESIS

QUE PARA OPTAR POR EL GRADO DE:

Doctor en Ciencias

PRESENTA:

Jesús Salvador López Bucio

TUTOR PRINCIPAL

Dr. Ángel Arturo Guevara García (IBT-UNAM)

MIEMBROS DEL COMITÉ TUTOR

Dr. Luis Cárdenas Torres (IBT-UNAM)

Dra. Marina Macías Silva (IFC-UNAM)

Cuernavaca Morelos. Junio, 2016

AGRADECIMIENTOS

A mi tutor, el Dr. Ángel Arturo Guevara García por haberme dado la oportunidad de formar parte de su equipo y por su valiosa aportación intelectual y personal para la realización de este trabajo de tesis y del proyecto de MAP cinasas.

Al los miembros de mi comité tutoral: la Dra. Marina Macías Silva y el Dr. Luis Cárdenas Torres por sus comentarios y sugerencias durante las evaluaciones de este trabajo de tesis.

A los miembros de mi jurado de examen:

Dr. Joseph Dubrovsky

Dra. Gladys Cassab

Dr. Alexandre Tromas

Dr. Gustavo Pedraza

Dr. Christopher Wood

Por sus comentarios y sugerencias durante la revisión de esta tesis.

Al CONACYT por la beca 332863 y por los fondos otorgados para la realización de esta tesis a través del proyecto de ciencia básica 129266.

A la Dirección General de Asuntos del Personal Académico (DGAPA) de la UNAM por los fondos otorgados a través de los proyectos IN207111 e IN207014.

Al Programa de Apoyo a los Estudios de Posgrado (PAEP) de la UNAM por los apoyos otorgados para la participación en congresos así como para la impresión de tesis.

A Jesús Omar Arriaga de la Unidad de Biblioteca del IBT-UNAM por su valioso apoyo durante el uso del equipo de videoconferencias.

Al Lic. Antonio Bolaños Guillen y a Gloria Villa Herrera de la Unidad de Docencia y Formación de Recursos Humanos del IBT-UNAM por su apoyo en los diferentes trámites realizados.

A la Dra. Patricia León y a mis compañeros de laboratorio por todo su apoyo durante la realización de este trabajo.

Esta tesis es el culmen de una etapa académica y personal que se ha realizado con el apoyo incondicional de mi Madre María del Rosario, de mis Hermanos Jóse, Gracia, Antonio, Gerardo y Luis, de mi Esposa Yunuén y de mis Hijos Eliam y Zuria.

Los admiro fervientemente y les Dedico este y todos mis logros.

ÍNDICE

TABLAS Y FIGURAS

ABREVIACIONES

ACR– *Arabidopsis* CRINKLY
ARF– AUXIN RESPONSE FACTOR
ARR– *Arabidopsis* RESPONSE REGULATOR
AS– ASYMETRIC LEAVES
ATHB– *Arabidopsis thaliana* HOMEOBOX
BD– BODENLOS
BRI– BRASSINOSTEROID INSENSITIVE
CESA– CELLULOSE SYNTHASE
CPC– CAPRICE
CTR1– CONSTITUTIVE TRIPLE RESPONSE
DRN– DORNRÖSCHEN
DRNL– DORNRÖSCHEN LIKE
ERL– ERECTA LIKE
FLS– FLAGELIN SENSING
GL**–** GLABRA
HD-ZIP– HOMEODOMAIN LEUCINE ZIPPER
IAA– AUXIN RESPONSE PROTEIN
iGluR– IONOTROPIC GLUTAMATE RECEPTOR
L-Glu– L-GLUTAMATO
MAP– MICROTUBULE ASSOCIATED PROTEIN KINASE
MAPKs– MITOGEN ACTIVATED PROTEIN KINASES
MKP– MAP KINASE PHOSPHATASE
MP– MONOPTEROS
MPK– MITOGEN ACTIVATED PROTEIN KINASE
MPKK– MITOGEN ACTIVATED PROTEIN KINASE KINASE
MPKKK– MITOGEN ACTIVATED PROTEIN KINASE KINASE KINASE
PAMPs– PATHOGEN ASSOCIATED MOLECULAR PATTERNS
PHB– PHABULOSA
PHV– PHAVOLUTA
PIN– PINFORMED
PLT– PLETHORA
PTP– PROTEIN TYROSINE PHOSPHATASE
QC– QUIESCENT CENTER
RAM– ROOT APICAL MERISTEM
RHD2– ROOT HAIR DEFICIENT
RL– RAÍCES LATERALES
RLK– RECEPTOR LIKE KINASE
ROS– REACTIVE OXIGEN SPECIES
S/T– SERINE/THREONINE
SAM– SHOOT APICAL MERISTEM
SCR– SCARECROW
SHR– SHORTROOT
SHY– SHORT HYPOCOTYL
SLR– SOLITARY ROOT
SSP– SHORT SUSPENSOR
STM– SHOOT MERISTEMLESS
TAIR– THE *Arabidopsis* INFORMATION RESOURCE
TMM– TOO MANY MOUTHS
TXY– THREONINE X TYROSINE
WER– WEREWOLF
WOX– WUSCHEL RELATED HOMEOBOX
WUS– WUSCHEL
XTH– XYLOGLUCAN ENDOTRANSGLUCOSYLASE

RESUMEN

Las plantas por su naturaleza sésil crecen ancladas al suelo y su desarrollo es altamente influenciado por estímulos de su entorno como los cambios en las condiciones ambientales y la disponibilidad de agua y nutrientes, así como por la interacción con microorganismos. En las vías de señalización, la fosforilación y defosforilacion de proteínas es una de las reacciones más importantes para regular diferentes procesos celulares. Las MAPKs (Mitogen Activated Protein Kinase) son proteínas que catalizan la fosforilación de proteínas (cinasas) a través de módulos de señalización conformados por tres diferentes MAPKs. Se ha demostrado que dichos módulos transducen la señal de diversos estimulos para inducir respuestas celulares específicas y acordes a cada condición. Recientemente se encontró que una MPK (MPK6) regula el desarrollo del embrión y de la raíz de *Arabidopsis thaliana,* sin embargo, el estudio detallado de los mecanismos modulados por esta cinasa para regular ambos programas de desarrollo, así como los otros componentes que conforman el módulo de MAPKs que opera en estos procesos, es en incipiente. En este trabajo, se determinó que la cinasa MPK6 regula procesos de división celular durante la embriogénesis temprana, ya que mutantes de pérdida de función de esta cinasa causan divisiones anormales que afectan el desarrollo del embrión y el establecimiento de la semilla, mismas que posteriormente impactan el desarrollo postgerminativo del sistema radical. Mediante análisis detallados, se encontró que la mutante *mpk6* tiene alterados tanto la proliferación como el alargamiento celular de la raíz primaria, simultáneamente se demostró que el aminoácido glutamato regula el crecimiento de la raíz primaria, así como la percepción del estímulo de la gravedad a través de una vía de señalización en la que participan la cinasa MPK6 y la fosfatasa MKP1. Finalmente, mediante un escrutinio de mutantes enfocado a fenotipos de semilla similares a los de la mutante *mpk6*, se identificó al receptor con actividad cinasa SSP1, a la MPKKK4 (YDA) y a la MPKK5, como los posibles componentes del módulo de MAPKs del que MPK6 forma parte para regular el desarrollo del embrión.

ABSTRACT

Plants, due to their sessile nature, grow anchored to a substrate and their development is highly influenced by stimuli from their environment such as, changes in weather conditions, availability of water and nutrients, as well as interaction with microorganisms. Within signaling pathways, phosphorylation and dephosphorylation of proteins is key process of plant development. MAPKs (Mitogen Activated Protein Kinase) are protein kinases (catalyzing phosphorylation of proteins) organized as signaling modules comprised of three different proteins. Has been shown that MAPK modules transduce stimuli signals to induce specific cellular responses according to each condition. Recently it was found that MPK6 regulates *Arabidopsis thaliana* embryo and root development, however, the detailed mechanisms modulated by MPK6 to regulate both developmental programs as well as other components of the MAPK module controlling these processes are unknown. In this study we determined that MPK6 regulates cellular division during early embryogenesis, since loss function mutants of MPK6 (*mpk6*) have abnormal divisions which affects embryo and seed development, these alterations have impact in the postgerminative root development. Through detailed analysis we found that *mpk6* mutant, has altered proliferation and elongation cellular in the primary root, simultaneously we expose that glutamate mediates primary root growth as well primary root gravitropic responses through a MPK6 and MKP1 participating pathway. Finally, through screening procedure focused in mutants with *mpk6*-like seed alterations, we identified that the Receptor Like Kinase (SSP1), the MPKKK4 (YDA) and the MPKK5 are posible components mediating MPK6 activity in the MAPK module that regulate embryo development.

I. INTRODUCCIÓN

I.1. *Arabidopsis thaliana*

Las plantas son organismos sésiles que han adaptado su desarrollo en función de los diversos factores de su entorno, que incluyen cambios en las condiciones ambientales como luz, temperatura, disponibilidad de agua y nutrientes, así como interacciones con otros organismos. A diferencia de los animales, el crecimiento vegetal puede durar cientos o incluso miles de años, gracias a las actividades de los meristemos apicales del brote (SAM por Shoot Apical Meristem) y de la raíz (RAM por Root Apical Meristem) (Jürgens, 2001; Alberts *et al.,* 2008; Lau *et al*., 2012).

En las últimas tres décadas, *A. thaliana* ha sido el modelo vegetal más usado para el estudio de procesos genéticos, fisiológicos, moleculares y del desarrollo, generándose un vasto conocimiento que puede ser extrapolado a otras especies. Las características principales de esta planta modelo que han favorecido su utilización son: (a) Tiene uno de los genomas vegetales más pequeños, el cual está completamente secuenciado y anotado (Nature, 408:796-815; 2000). (b) Su ciclo de vida corto, de entre 6 a 8 semanas desde la germinación hasta la producción de semillas. (c) La planta adulta es pequeña, aproximadamente 30 cm, por lo que se puede cultivar y manipular fácilmente en condiciones de laboratorio (Meyerowitz, 1989). (d) Muestra una alta eficiencia para la transformación genética, tanto por métodos biológicos como la infiltración con *Agrobacterium tumefasciens* como físico-químicos como por ejemplo la biobalística. Estas características en conjunto han conducido a la formación de colecciones de mutantes que pueden ser adquiridas por catálogo para muchos de sus genes, a través de cuya caracterización fenotípica, molecular y funcional, en diferentes condiciones experimentales ha permitido la generación de un vasto conocimiento en prácticamente todos los campos de la biología vegetal (http://www.arabidopsis.org).

I.2. Desarrollo del embrión y establecimiento de la semilla

El desarrollo post-embrionario de *A. thaliana* se divide en dos etapas, desarrollo vegetativo y desarrollo reproductivo. El desarrollo vegetativo comienza después de la germinación de la semilla y se caracteriza por la formación de una roseta de hojas que es producida por la actividad del SAM. Cuando la roseta mide alrededor de 10 cm de diámetro y dependiendo de la temperatura y el fotoperiodo, ocurre la transición a la etapa reproductiva que se caracteriza por la formación de un tallo floral (escapo) del cual se forman hojas caulinares en las que se determinan los meristemos axilares que permitirán que el tallo se ramifique; en los extremos de estas ramificaciones se forman las inflorescencias donde se lleva a cabo la fertilización de los óvulos por los granos de polen. Mediante la polinización, ocurre la formación de los frutos, denominados silicuas, las cuales contienen a las semillas que son el producto final de la embriogénesis y que darán paso a la siguiente generación (Bowman, 1994).

El desarrollo de la semilla comienza después de la doble fertilización de las células central y huevo. La célula central, da origen al endospermo que suplirá de nutrientes al embrión durante las etapas tempranas, por su parte, la célula huevo, forma al zigoto para comenzar la embriogénesis (Hehenberger *et al*., 2012; Dekkers *et al*., 2013). En las etapas tempranas de la embriogénesis, el zigoto aumenta unas tres veces su tamaño inicial y se divide en una célula basal larga y una célula apical corta, esta división es asimétrica y sus células hijas establecerán linajes con diferentes patrones de crecimiento y diferentes destinos de desarrollo (Scheres & Benfey, 1999; Jürgens, 2001; Lau *et al*., 2012). Las células del linaje apical adoptan un patrón de crecimiento isotrópico y forman al proembrión esférico, por su parte, las células del linaje basal continúan alargándose y se dividen transversalmente produciendo una fila de 7-9 células que forman al suspensor (Lukowitz *et al*., 2004). La última célula del linaje basal (hipófisis) que esta en contacto con el proembrión, eventualmente se incorpora al embrión y genera una pequeña célula hija en forma de lente que se convertirá en el centro quiescente (QC por Quiescent Center) del RAM (Jürgens, 2001; Jiang y Feldman, 2005). Suspensor que tiene diversas funciones, como generar una ruta de

transporte de nutrientes desde los tejidos maternos hacia el embrión, aunque también se le ha implicado en la producción y la distribución de diferentes fitohormonas que controlan este programa de desarrollo (Tomokazu y Goldberg, 2009; Badu *et al*., 2013). El orden de los órganos del embrión en el eje apical-basal son: el SAM, los cotiledones, el hipocotilo y el RAM. Tanto el RAM como el SAM son generados como resultado de un proceso de señalización que define un dominio embrionario apical y basal, respectivamente (Ueda *et al*., 2011). Este proceso de señalización comienza en la embriogénesis temprana y en él participan los factores de transcripción WOX (WUSCHEL RELATED HOMEOBOX) *WOX8*, *WOX9* y *WOX2,* MP (MONOPTEROS) y BD (BODENLOS), cuya expresión está coordinada por la distribución de auxinas llevadas a cabo por el transportador PIN7 (PIN-FORMED 7) (Breuninger *et al*., 2008; Ueda *et al*., 2011; Lau *et al*., 2012). En el zigoto se coexpresan los genes *WOX8* y *WOX2,* más tarde, después de las primeras divisiones celulares, *WOX2* se expresa únicamente en la célula apical, mientras que *WOX8* y *WOX9* se expresan en la célula basal (Haecker *et al*., 2004; Ueda *et al*., 2011). El transporte basal-apical de auxinas mediado por PIN7 y la posterior expresión de los genes *MP* y *BD* en la célula apical, determinan el eje de crecimiento y la polaridad apical-basal (Friml *et al*., 2003; Lau *et al*., 2012). Posteriormente, durante la etapa globular se lleva a cabo una redistribución de auxinas mediada por PIN1 y PIN4 que va desde la parte apical hacia la región basal, generando un gradiente en la célula apical del suspensor para especificar la hipófisis que más tarde dará lugar al RAM durante la especificación de la hipófisis también participan los represores de la señalización de citocininas *ARR7* y *ARR15* (*Arabidopsis* RESPONSE REGULATOR) [Friml *et al*., 2003; Müller y Sheen, 2008].

La actividad celular proliferativa del SAM está coordinada por los factores de transcripción de tipo HD-ZIP III (III HOMEODOMAIN-LEUCINE ZIPPER): PHB (PHABULOSA), PHV (PHAVOLUTA), REV (REVOLUTA), ATHB8 y ATHB15 (*Arabidopsis thaliana* HOMEOBOX), también por los factores de transcripción WUS (WUSCHEL) y STM (SHOOT MERISTEMLESS), así como por la señalización de citocininas (Capron *et al*., 2009). Finalmente, la señalización de

auxinas induce la expresión de los factores de transcripción DRN (DORNRÖSCHEN) y DRNL (DORNRÖSCHEN LIKE), así como AS1 y AS2 (ASYMMETRIC LEAVES), que controlan el desarrollo de los cotiledones (Capron *et al*., 2009). Lo anterior sugiere que un balance en las concentraciones de auxinas/citocininas es importante para la correcta funcionalidad del SAM.

Con base al número de células que forman al embrión, se consideran las siguientes etapas del desarrollo: De una sola célula (Figura 1A), dos células (Figura 1B), octante, en la cual se visualizan cuatro de ocho células en dos niveles (Figura 1C), dermatógeno, en la cual ocurre una división periclinal de cada una de las ocho células que producirá células internas y células de protodermo que dan origen a la epidermis (Figura 1D), globular temprana, en la cual se llevan a cabo divisiones de las células internas inmediatamente después de la etapa de dermatógeno que dotan al embrión de un eje reconocible (Figura 1E), triangular, en la cual se puede observar un patrón polarizado en donde se reconocen los cotiledones, el suspensor y la célula hipofiseal, que formará el QC del meristemo de la raíz primaria y las células iniciales de la columela (Figura 1F). En las etapas de corazón, de medio torpedo y de cotiledones doblados (Figura 1G-I), el hipocotilo y los cotiledones continúan su crecimiento hasta ocupar la mayor parte de la semilla. El patrón radial del hipocotilo está definido por una sola capa de células epidérmicas, una capa de córtex, una capa de endodermis y el cilindro vascular (Figura 1I).

Al final de la embriogénesis procede la maduración de la semilla, que es una estructura de propagación y dispersión, además permite al nuevo organismo resistir condiciones adversas gracias a la acumulación de proteínas, carbohidratos y lípidos de reserva. La semilla desecada carece de actividad metabólica y dentro de ella el embrión permanece en dormancia hasta que las condiciones de disponibilidad de agua y luz son adecuadas para inducir la germinación (Bewley JD, 1997; Finkelstein *et al*., 2008; Graeber *et al*., 2012).

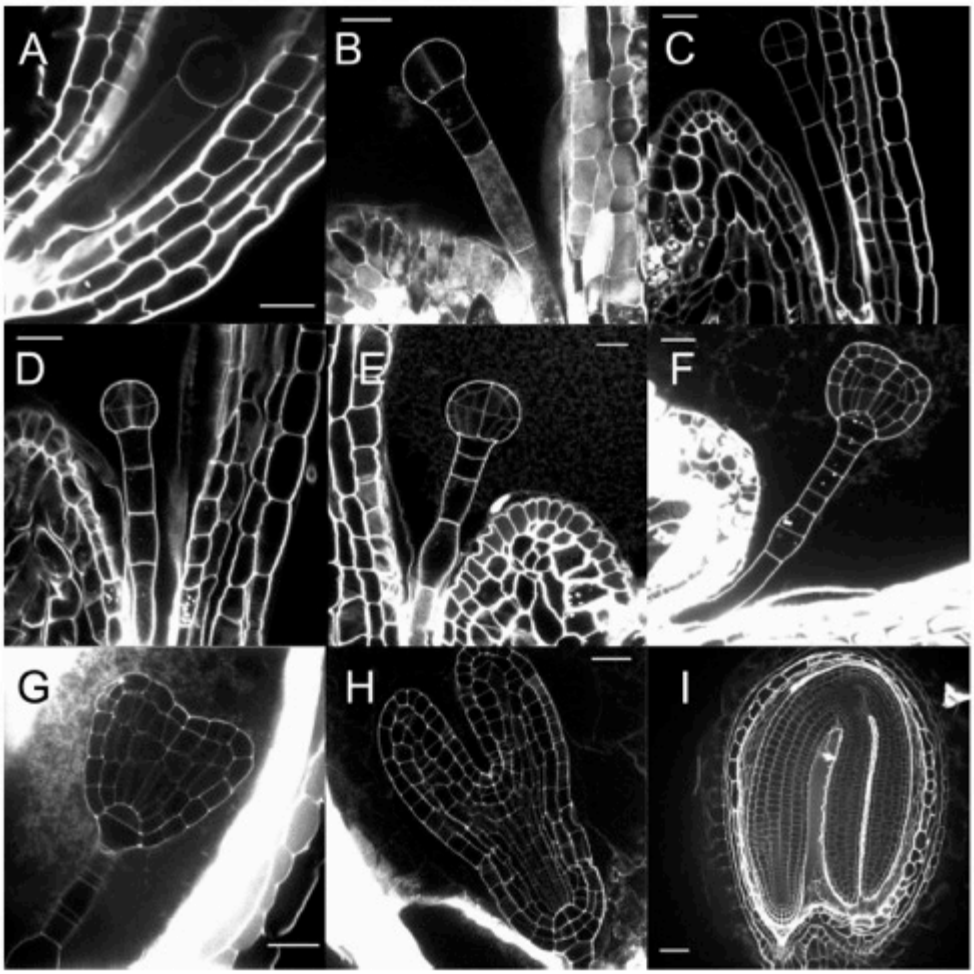

Figura 1. Desarrollo del embrión de *Arabidopsis thaliana*. Se muestran los estadios de desarrollo correspondientes a: una célula (A), dos células (B), octante (C), dermatógeno (D), globular temprana (E), triangular (F), corazón (G), medio torpedo (H) y cotiledones doblados (I) [Tomada de Capron *et al*., 2009].

I.3. Sistema radical

El sistema radical además de anclar la planta al suelo y participar en la captación de agua y nutrientes, permite establecer relaciones con los microorganismos de la rizósfera que constituyen el microbioma vegetal. El ambiente biótico y abiótico al que está expuesta regula la capacidad de ramificación de la raíz, mediante la formación de raíces laterales (RL) y pelos radicales, tanto en la raíz primaria,

como en las raíces laterales para incrementan la superficie total de absorción (López-Bucio *et al.,* 2003).

La raíz primaria de *A. thaliana* en cuya estructura se diferencian claramente las zonas de división, crecimiento y diferenciación celular, se ha utilizado como un modelo para investigaciones sobre procesos morfogenéticos. Un número pequeño de células troncales (“stem cells”) generan todos los tejidos de la raíz a través de divisiones estereotípicas seguidas de una expansión y diferenciación celular, por lo tanto el crecimiento de este órgano es el resultado de los procesos de actividad proliferativa que ocurre en el RAM y de crecimiento rápido que se lleva a cabo en la zona de elongación (Dolan *et al*., 2003; Tian *et al*., 2014). Durante estos procesos se producen células en dos direcciones (apical y basal), siendo en la parte basal más distal donde se forman las capas de tejido que conforman la cofia, estructura que cubre a la punta de la raíz y la protege de la abrasión de las partículas del suelo. Además de su función protectora, la cofia desempeña una función sensorial fundamental, ya que percibe y procesa los estímulos ambientales y modula la dirección del crecimiento de la raíz en función de la gravedad (gravitropismo), luz (fototropismo), obstáculos (tigmotropismo), gradientes de temperatura (termotropismo), humedad (hidrotropismo), nutrientes y otras sustancias químicas (quimiotropismo) [Hasenstein y Evans, 1988; Ishikawa y Evans ,1990; Ishikawa y Evans, 1993; Okada y Shimura, 1990]. La región basal de la raíz primaria está formada por diferentes tejidos, ordenados en forma radial siendo los tejidos vasculares los más internos seguidos por la endodermis, el córtex y la epidermis (Figura 2). Las células que forman los diferentes tejidos se producen a partir de las células iniciales localizadas en el ápice de la raíz internamente y en contacto con las células del QC (Figura 2). El QC presenta poca actividad mitótica y su función principal es la de mantener la organización de las células adyacentes mediante una comunicación célula-célula (Dolan *et al.,* 1993). En el RAM se pueden distinguir dos dominios: el dominio de proliferación (PD por Proliferation Domain) y el dominio de transición (TD por Transition Domain). En el dominio de proliferación las células sufren varias rondas de división mientras que en el dominio de transición, las células pierden actividad mitotica para dar paso a

una fase de expansión celular que marca el final de la zona meristemática y el inicio de la zona de elongación (Scacchi *et al*., 2010). Una vez que incrementan su tamaño, las células se diferencian en su forma y función final, este proceso está evidenciado por la aparición de los pelos radicales a partir de células epidérmicas denominadas H o tricoblastos. Por otra parte, mediante eventos de división celular en el periciclo, se forman las raíces laterales que incrementan la superficie total de exploración del suelo y contribuyen con un mejor anclaje (Malamy y Benfey, 1997; De Smet et al., 2007).

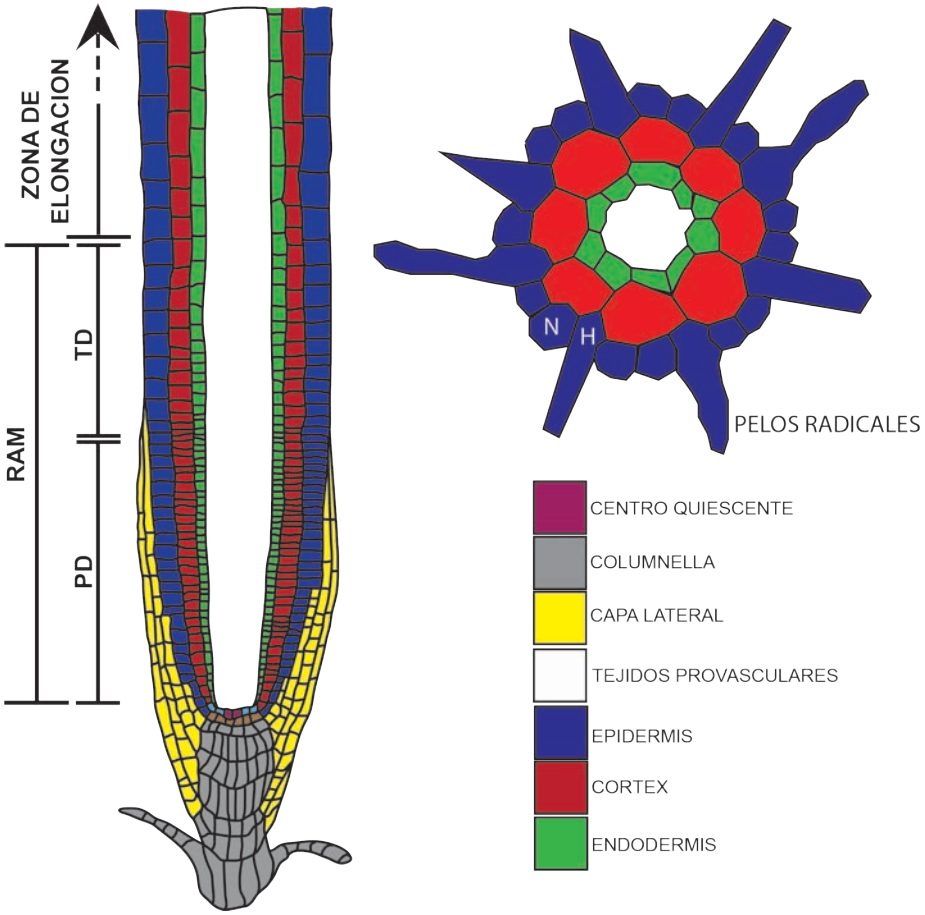

Figura 2. Organización celular de la raíz de *A. thaliana*. Se muestran los cortes longitudinal y transversal de la raíz primaria indicándose en código de colores, los diferentes tejidos que la componen. En el corte transversal se señalan los atricoblastos (N) y tricoblastos (H) que dan lugar a los pelos radicales.

A pesar del vasto conocimiento existente sobre los procesos morfológicos que se llevan a cabo en el sistema radical, realmente poco se sabe acerca de los mecanismos celulares y moleculares que participan en la regulación del desarrollo de la raíz primaria. La interacción antagónica entre las auxinas y las citocininas son determinantes para la actividad del RAM. Tanto el transporte de auxinas desde los tejidos fuente (hojas y yemas axilares) como su biosintesis en el ápice de la raíz, mantienen los gradientes necesarios para regular el funcionamiento del QC, el establecimiento de la cofia, la diferenciación de los tejidos vasculares y el mantenimiento de las células troncales (Petersson *et al*., 2009). Las auxinas inducen la expresión de genes que codifican para factores de transcripción del tipo *PLT* (*PLETHORA*) para regular la identidad y la división celular (Aida *et al*., 2004; Aloni *et al*., 2006; Grieneisen *et al*., 2007; Pirelli *et al*., 2012; Sozzani y Iyer-Pascuzzi, 2014). Además de los gradientes de auxinas para regular la expresión de los genes *PLT*, se requieren los factores de transcripción SCR (SCARECROW) y SHR (SHORTROOT) para el mantenimiento del QC y de las células troncales. SHR se transcribe en la estela de tejido provascular y se mueve a la célula inicial del córtex/endodermis y al QC, en donde induce la transcripción de SCR para controlar su funcionamiento y la identidad de las células troncales (Sabatini *et al*., 2002; Perilli *et al*., 2012; Sozzani y Iyer-Pascuzzi, 2014).

Por su parte, las citocininas promueven principalmente la diferenciación celular en el RAM. Las citocininas inducen la expresión de ARR1 (*Arabidopsis* RESPONSE REGULATOR 1) el cual induce la expresión del factor de transcripción SHY2 (SHORT HYPOCOTYL 2) que reprime la expresión de los transportadores de auxinas PIN1, PIN3 y PIN7, antagonizando así su distribución y reduciendo el tamaño del meristemo (Dello Ioio *et al*., 2007; Grieneisen *et al*., 2007; Sozzani y Iyer-Pascuzzi, 2014; Satbhai *et al*., 2015).

I.4. Las raíces laterales

Las raíces laterales se originan a partir de células del periciclo localizadas de manera opuesta a los polos del xilema que adquieren atributos de células

fundadoras (Dolan *et al.,* 1993; Dubrovsky *et al*., 2008). Estas células se dividen creando una capa de hasta 10 células de igual tamaño formando un primordio de RL en estado I. Posteriormente, las células se dividen periclinalmente formando una segunda capa celular (Estado II), donde ocurren divisiones anticlinales y periclinales para crear una estructura en forma de domo (Estados del III-VII) que eventualmente se abrirá camino por las diferentes capas celulares de la raíz hasta emerger en forma de RL (Figura 3) [Malamy y Benfey, 1997; Benková y Bielach, 2010].

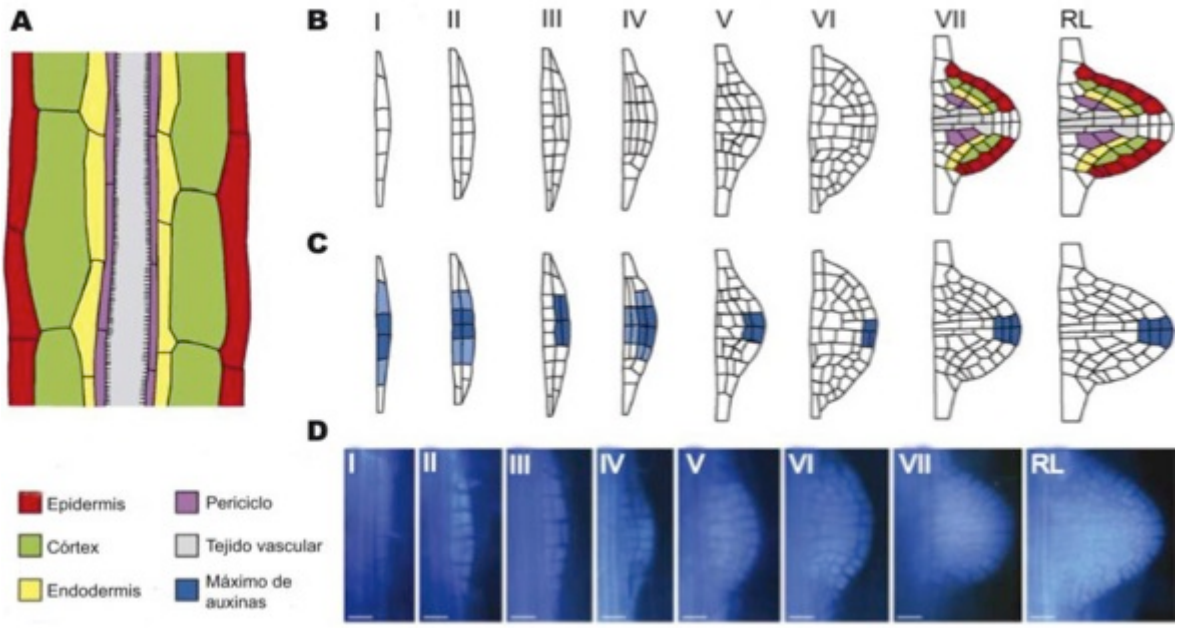

Figura 3. Formación y desarrollo de raíces laterales. Las raíces laterales se originan en la raíz primaria a partir de células del pericicio (A), pasando por siete estadios (números romanos) de desarrollo de primordios [Malamy y Benfey, 1997]) hasta la emergencia de la raíz lateral (B y D). Este proceso muestra una clara correlación con la respuesta máxima a auxinas, demostrado por el marcador *DR5:uidA* (C) [Modificado de Péret *et al.,* 2009].

Los mecanismos moleculares que median la formación de raíces laterales son poco conocidos, de éstos destacan la señalización mediada por auxinas de la cual se ha identificado a algunos de los componentes. En trabajos recientes, se ha demostrado que la acumulación local de auxinas en las células del pericicio es una

señal necesaria y suficiente para reespecificar al periciclo en células fundadoras de raíces laterales, por lo que este regulador puede ser considerado como un morfógeno en la organogénesis de la planta (Casimiro *et al*., 2001; Dubrovsky *et al*., 2008). La acumulación de auxinas en las células fundadoras activa los módulos *IAA14-ARF7* (AUXIN RESPONSE PROTEIN/AUXIN RESPONSE FACTOR) y *ARF19* y *BDL/IAA12-MP/ARF5* (BODENLOS/IAA12, MONOPTEROS/ARF5), que son factores de respuesta a auxinas que regulan positiva (*ARF7-ARF19*, *MP/ARF5*) y negativamente a *SRL/IAA14 (SOLITARY ROOT/IAA14)* y a *BDL/IAA12* durante la división celular que conduce a la iniciación de raíces laterales (De Smet *et al*., 2007; Okushima *et al*., 2007; Benková y Bielach, 2010). Adicionalmente, un receptor membranal de tipo cinasa ACR4 (*Arabidopsis* CRINKLY 4) fue identificado como un componente clave para la iniciación de raíces laterales, ya que la pérdida de su función conduce a una división celular incrementada de células del periciclo con la consecuente formación de primordios fusionados o producción de primordios ectópicos (De Smet *et al*., 2008). Adicionalmente, se sabe que ACR4 puede actuar de manera autónoma-celular y de manera no autónoma-celular. En la manera autónoma-celular, parece ser requerido para la especificación correcta del primordio de raíz lateral, mientras que de manera no autónoma-celular, antagoniza la iniciación de raíces laterales en las células del periciclo vecinas (De Smet *et al*., 2008). Por otra parte, se ha encontrado que la distribución de auxinas coordina la división y diferenciación celular en la organogénesis de primordios de raíces laterales, ya que el transportador de auxinas de localización membranal PIN1, redirige el flujo de auxinas hacia la punta del primordio (Benkova *et al.,* 2003; Benková y Bielach, 2010). Finalmente, también se sabe que el crecimiento de la raíz lateral es regulado por RNAs pequeños (sRNA, *mi*R390 y *tasi*ARF) que controlan los módulos de respuesta a auxinas *ARF2*, *ARF3* y *ARF4*. El sRNA *mi*R390 permite la producción del *tasi*ARFs que reprimen la expresión de *ARF2*, *ARF3* y *ARF4*, quienes a su vez regulan por retroalimentación positiva (*ARF2*) o negativa (*ARF3* y *ARF4*) al *mi*R390 (Marin et al., 2010).

I.5. Los pelos radicales

La epidermis de la raíz de *A. thaliana* es el tejido más externo producido a partir de células iniciales durante la embriogénesis (Dolan *et al.,* 1993; Scheres *et al.,* 1994). En las células hijas ocurren divisiones transversales que sirven para generar células adicionales dentro de la misma fila (Baum y Rost, 1996; Berger *et al.,* 1998). Ocasionalmente ocurren divisiones longitudinales anticlinales resultando en un incremento en el número de filas celulares. Durante el desarrollo de la raíz en el RAM se forman dos tipos de células epidérmicas, las células que se diferencian en pelos radicales (tricoblastos o células H), que normalmente están en contacto con dos células corticales subyacentes, y las células que no forman pelos (atricoblastos o células N), las cuales solamente están en contacto con una célula cortical (Figura 2). Los pelos radicales son extensiones con forma tubular de las células epidérmicas H que tienen diversas funciones, como la adquisición de agua y nutrientes, la interacción con microorganismos de la rizósfera y la exudación de diversas sustancias (Hofer, 1991; Cho y Cosgrove 2002). En *A. thaliana* los pelos radicales tienen aproximadamente 10 µm de diámetro y llegan a medir alrededor de 1 mm de longitud.

El desarrollo de los pelos radicales puede ser dividido en tres fases: la fase de especificación celular, la fase de iniciación y la fase de crecimiento. La fase de especificación se refiere a la distinción entre las células epidérmicas que se establecerán como tricoblasto y como atricoblasto, lo cual básicamente depende de su posición (en contacto con 1 o 2 células corticales), posteriormente se forma una protrusión en un sitio específico del tricoblasto. En los atricoblastos un complejo proteínico compuesto por WER (WEREWOLF), GL3 (GLABRA3) Y EGL (ENHANCER of GL3) induce la expresión de los genes *GL2* (*GLABRA 2*) y *CPC* (*CAPRICE*). GL2 regula la expresión de los genes *CESA5* (*CELLULOSE SYNTHASE 5*) y *XTH17* (*XYLOGLUCAN ENDOTRANSGLUCOSYLASE*) afectando la composición de la pared celular y la iniciación del pelo radical (Tominaga-Wada *et al*., 2009; Libault *et al*., 2010). Por otra parte, el factor transcripcional CPC se mueve de los atricoblastos hacia los tricoblastos en donde

inhibe la formación del complejo WER-GL3-EGL3, reprimiendo así la expresión de GL2 y la consecuente iniciación del pelo radical (Libault *et al*., 2010). Finalmente, el crecimiento del pelo ocurre mediante diversos procesos de exocitosis, de reorganización del citoesqueleto, así como de la generación de gradientes de calcio, de pH y de especies reactivas de oxígeno. Una elevada concentración de calcio induce la actividad de la NADPH oxidasa membranal RHD2 (ROOT HAIR DEFICIENT 2) incrementando la producción extracelular de especies reactivas de oxígeno que regulan la composición de la pared celular y el aumento en longitud del pelo radical (Wylmer *et al*., 1997; Bibikova *et al*., 1998; Cho y Cosgrove 2002; Monshausen *et al.,* 2007; Cárdenas, 2009; Foreman *et al*., 2003; Libault *et al*., 2010). Además de los procesos moleculares mencionados para regular el crecimiento de los pelos, se ha encontrado que las auxinas y el etileno son reguladores positivos del crecimiento de los pelos radicales, ya que los tratamientos con auxinas como con etileno lo inducen, mientras que mutantes afectadas en la respuesta de ambas fitohormonas tienen alteraciones en la longitud de estos (Pitts *et al*., 1998). Sin embargo la conección entre las auxinas y el etileno con estos procesos se desconoce.

I.6. Gravitropismo

El desarrollo y la morfología del sistema radical se ve influenciado por la disponibilidad de agua y nutrientes minerales como fósforo, nitrógeno, calcio, potasio, magnesio, azufre, fierro, manganeso y boro, así como por estímulos bióticos y abióticos, como los diferentes tipos de tropismos mencionados anteriormente (López-Bucio *et al*., 2003; Gruber *et al*., 2013). El gravitropismo es la respuesta al estímulo que ejerce la fuerza de la gravedad, las hojas y el tallo tienen un crecimiento agravitrópico (en contra del vector de la gravedad), mientras que la raíz primaria crece en dirección de la fuerza de gravedad. En la raíz primaria el gravitropismo se percibe en las células de la columela, que transmiten información hacia las células de la zona de elongación que modifican su crecimiento. Las células de la columela (estatocitos) contienen amiloplastos

cargados de almidón (estatolitos) que cuando perciben el gravitropismo sedimentan e inducen una cascada de señalización mediada por la distribución de auxinas (Vitha *et al*., 2007; Band *et al*., 2012; Baldwin *et al*., 2013). La distribución de auxinas hacia la zona de elongación es necesaria para una respuesta gravitrópica adecuada y está mediada por los transportadores de auxinas de la familia PIN (Ottenschläger *et al*., 2003; Kleine-Vehn *et al*., 2010; Brunoud *et al*., 2012). Los flujos de auxinas dependientes del estímulo de la gravedad dependen de la localización de los transportadores PIN2, PIN3 y PIN7; en tanto que las mutantes sencillas de los genes *PIN2 PIN3* y *PIN7* como la doble mutante *pin3pin7* tienen respuestas gravitrópicas alteradas (Abas *et al*., 2006; Kleine-Vehn *et al*., 2010). Hasta la fecha, se desconocen los componentes moleculares que coordinan los estímulos, la respuesta auxínica y la señalización a larga distancia entre la cofia y la zona de elongación celular de las respuestas gravitropicas. Además de la distribución de auxinas, se han observado cambios en los niveles de calcio, de las especies reactivas de oxígeno, del inositol trifosfato y del óxido nítrico que son necesarios para una adecuada respuesta a la gravedad (Perera *et al*., 2006; Mendocilla-Sato *et al*., 2014).

I.7. Vías de transducción de señales

En los organismos, la percepción correcta de los cambios en las condiciones variantes de su entorno es un importante mecanismo de supervivencia que involucra una amplia gama de vías de transducción de señales las cuales, cobran mayor importancia en las plantas dada su naturaleza sesil (Misrha *et al*., 2006; Ballhorn *et al*., 2009). De manera general, una vía de transducción de señales involucra a receptores, típicamente anclados a la membrana plasmática, aunque también pueden localizarse libres en el citoplasma o en el núcleo. Cuando un receptor interacciona con su ligando, ocurre un cambio conformacional que altera su actividad y el reconocimiento de los blancos proteínicos con los que interactúa, en consecuencia se puede inducir la producción intracelular de segundos mensajeros como el calcio, el inositol 3 fosfato y las especies reactivas de oxígeno

(ROS), que amplifican y transducen la actividad sensorial hacia efectores membranales o citoplásmicos, entre los que se incluyen proteínas G heterotriméricas y proteínas G pequeñas (Ras), fosfatasas y cinasas, siendo estas dos últimas frecuentemente responsables de activar o inactivar factores de transcripción de localización nuclear que regulan positiva o negativamente la expresión de genes, para establecer una respuesta general o específica ante el estímulo percibido (Figura 4), pudiendo así afectar tanto el crecimiento como el desarrollo (Trewavas y Malhó, 1997; Alberts *et al.,* 2008; Tuteja *et al.,* 2009). Estos sistemas de reconocimiento, transmisión y procesamiento de estímulos son referidos como vías de transducción de señales o vías de señalización.

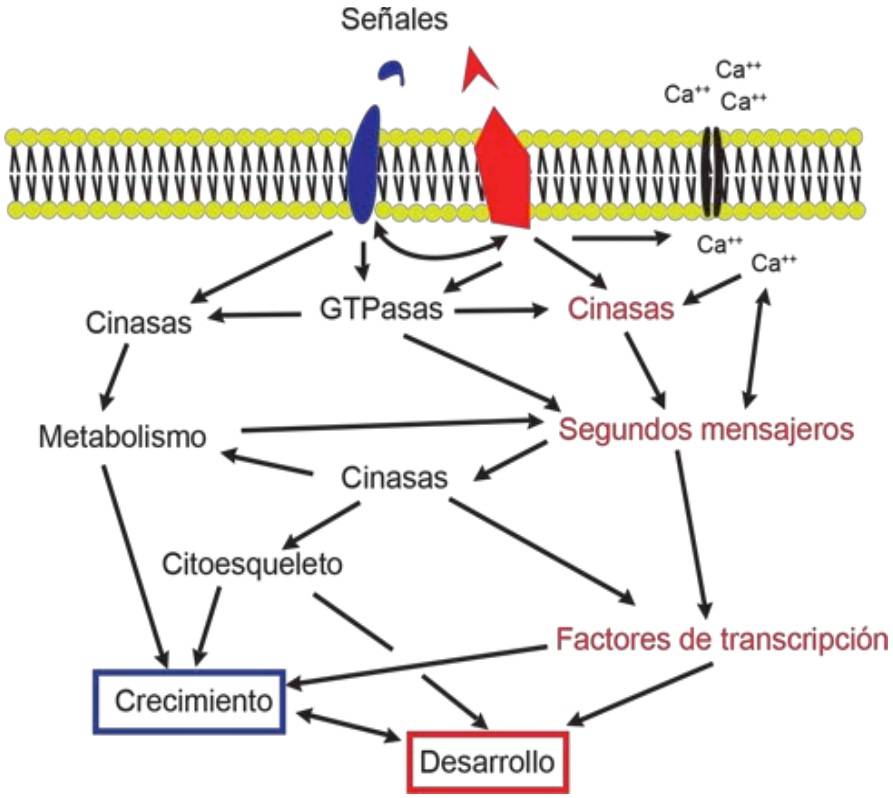

Figura 4. Intercomunicaciones en los sistemas de transducción de señales. Se muestra como una señal es reconocida por un receptor que transduce la señal al interior de la célula, dicha señal, muchas veces es procesada por segundos mensajeros (Ca^{++}) que así la pasan a proteínas efectoras para inducir una respuesta acorde al estímulo inicial (vía roja). Normalmente la transdución de la señal también implica intercomunicación entre diferentes vías (vía negra) [Adaptado de Trewavas y Malho, 1997].

Se puede pensar equivocadamente que una vía de señalización es lineal, la cual comienza con la unión de una molécula, ion o partícula a un receptor y termina con una respuesta determinada. Sin embargo, está percepción simplista es errónea ya que está bien establecido que una señal puede desencadenar más de una respuesta y que una misma respuesta puede ser activada por distintas señales, incluso es claro que existe una intrincada intercomunicación ("cross talk") entre diferentes vías de señalización que realmente constituyen redes de comunicación flexibles y complejas e incluso redundantes (Figura 4; Klipp y Liebermeister, 2006).

Los principales estudios para entender el comportamiento de las plantas ante situaciones de estrés, se basan en esclarecer la participación, función e interacciones que ocurren en las vías de señalización para modular la respuesta ante un estímulo particular. Esto sin duda representa uno de los mayores retos de investigación de la biología celular y molecular.

I.8. Mecanismos de fosforilación y defosforilación de proteínas que participan en las vías de transducción de señales

Las proteínas pueden ser modificadas postraduccionalmente, de manera rápida y reversible para regular su actividad, sus interacciones con otras proteínas, su estabilidad y su localización subcelular. En plantas se han identificado diversos tipos de modificaciones postraduccionales entre las que destacan los procesos de sumoilación, acetilación, glucosilación, ubiquitinación y fosforilación (De la Fuente van Bentem *et al*., 2007; Piquerez *et al*., 2014). Específicamente el proceso de fosforilación es llevado a cabo por proteínas con función cinasa ("protein kinases"), que catalizan la adición de grupos fosfato en residuos de aminoácidos específicos (generalmente serina, treonina o tirosina). Estas reacciones de fosforilación desempeñan un papel fundamental en las vías de señalización, ya que además de ser un proceso rápido es reversible por la acción de enzimas con actividad de fosfatasa que remueven el grupo fosfato. De esta manera, la actividad coordinada de cinasas y fosfatasas es muy útil para regular la amplitud, la especificidad y la

duración de una señal determinada de manera eficiente y sutil, además es uno los mecanismos más estudiados para el control de los procesos celulares (Mishra *et al*., 2006; De la Fuente van Bentem *et al*., 2007; Piquerez *et al*., 2014). Las más de 1500 cinasas anotadas en el genoma de *A. thaliana*, se han clasificado en familias y subfamilias en función de su similitud con cinasas de otros organismos eucariontes (Lehti-Shiu y Shiu, 2012).

I.9. MAPKs (Mitogen Activated Protein Kinases)

Las MAPKs (por "Mitogen Activated Protein Kinases") son proteínas con actividad de cinasa altamente conservadas en los organismos eucariontes, que conforman módulos para la transducción de señales que en general controlan la división y la diferenciación celular (Mishra *et al.,* 2006; Hamel *et al*., 2006; Xu y Zhang, 2015). Un módulo de MAPKs funciona mediante eventos de fosforilación secuencial que inicia cuando la primer cinasa del módulo, una MPKKK (Mitogen-activated Protein Kinase Kinase Kinase) es activada para activar a la segunda cinasa, una MPKK (Mitogen-activated Protein Kinase Kinase) mediante la fosforilación de los aminoácidos S/T ubicados en el motivo de activación S/T-X_{3-5}-S/T; una vez activa la MPKK, fosforila a la última cinasa del módulo, una MPK (Mitogen-activated Protein Kinase) en los aminoácidos T y Y localizados en el motivo de activación TXY (Jonak *et al*., 2002; Zhang *et al*., 2006). Las MPKs puede fosforilar a diferentes tipos de proteínas que regulan respuestas celulares específicas que afectan el metabolismo y la expresión genética (Figura 5) [MAPK group, 2002; Nakagami *et al*., 2005; Mishra *et al*., 2006].

La primer MAPK fue descubierta en el año 1986 en células de mamíferos y fue denominada MAP-2 Kinase (por Microtubule Associated Protein-2 Kinase), posteriormente esta enzima se relacionó con proteínas que son fosforiladas en respuesta a mitógenos y se renombró como MAPK (Sturgill y Ray, 1986; Mishra *et al*., 2006). En plantas, la primer MAPK se describió en 1993 en chícharo y a partir de entonces se han encontrado en diversas especies vegetales como alfalfa, tabaco, arroz, petunia y en *Arabidopsis*, donde desempeñan un importante papel

en la regulación de diversos procesos celulares (Kovtun *et al*., 2000; Asai *et al*., 2002; Nakagami *et al*., 2005; Bush y Krisan, 2007; Cho *et al*., 2008; Lampard *et al*., 2009; Taj *et al*., 2010; Lopez-Bucio *et al*., 2014; Xu y Zhang, 2015).

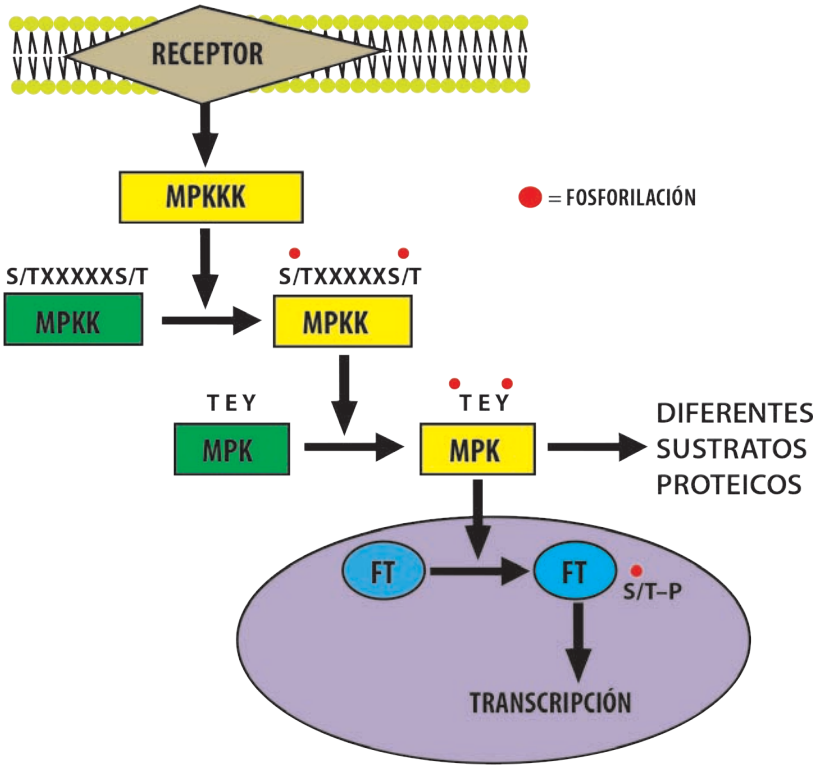

Figura 5. Cascada de señalización de MAPKs. Se puede apreciar en forma general el modo de operar de la cascada, desde que el receptor activado desencadena respuestas que llevan a la activación de la cascada de MAPKs pasando por la MPKKK, la MPKK y la MPK, hasta la fosforilación de sus blancos, que pueden ser factores de transcripción en el núcleo o bien, a otros sustratos, como fosfatasas, lipasas e incluso a otras cinasas (Adaptado de Hirt, 2000). ST=aminoácidos que se fosforilan en la MPKK (serina/treonina), TEY=motivo de aminoácidos que se fosforilan en la MPK (treonina ácido-glutámico tirosina), S/T–P=motivo de fosforilación en el sustrato (serina/treonina–prolina) y FT=factor de transcripción.

De acuerdo a homologías de secuencia con MAPKs de mamíferos se ha establecido que el genoma de *A. thaliana* contiene 90 MAPKs, de las cuales 60 corresponden a la familia de las MPKKKs, 10 a la familia de las MPKKs y 20 a la de las MPKs. Dentro de cada familia, los miembros se identifican por numeración simple y con base en sus características estructurales se subdividen en grupos

(MAPK group, 2002; Hamel *et al*., 2006). Debido a que las MAPKs operan en módulos y a que el número de miembros de la familia de las MPKKs es menor al número de integrantes de las familias MPKKK y MPK, resulta evidente que las MPKKs pueden ser activadas por más de una MPKKK y a su vez activar a más de una MPK, conformando una complicada red de intercomunicación entre varias rutas de señalización que confluyen en diferentes puntos (MAPK group, 2002; Jonak *et al*., 2002; Zhang *et al*., 2006; Xu y Zhang, 2015). En cuanto a su estructura, destaca que en el amino terminal de las MPKKs, tanto de *A. thaliana* como de otras plantas, se encuentra el dominio de unión a MPKs ([K/R][K/R][K/R]x(1-5)[L/I]x[L/I]) que es característico por sus dominios de residuos básicos [R/K] e hidrofóbicos [L/I] (MAPK group, 2002). Por su parte, las MPKs contienen en el extremo C-terminal un dominio CD altamente conservado, que funciona como el sitio de unión a MPKKs, a fosfatasas y otros sustratos proteínicos; este dominio contiene la secuencia de aminoácidos [LH][LHY]Dxx[DE]xx[DE]EPxC, que incluye dos residuos ácidos (D y E) que son cruciales para la interacción con el grupo de residuos de aminoácidos básicos (K y R) presentes en las MPKKs. A la fecha, se ha determinado que módulos particulares de MAPKs se requieren para la transducción de señales de respuesta a estrés biótico y abiótico, a fitohormonas, así como para regular el crecimiento, la diferenciación y la muerte celular (Jonak *et al*., 2002; Zhang *et al*., 2006; Xu y Zhang, 2015).

Las MAPKs cinasas más estudiadas son MPK3 y MPK6, entre ellas se ha reportado redundancia funcional en la señal que transmiten y la respuesta que inducen (Bush y Krisan 2007). Por ejemplo, en respuesta a peróxido de hidrógeno las MPKK4 y MPKK5 activan a las MPKs 3 y 6 (Kovtun *et al*., 2000), por su parte las MPKK7 y MPKK9 regulan el desarrollo de estomas a través de la activación de las MPKs 3 y 6 (Lampard *et al*., 2009). La redundancia funcional de las MPKs también se ha evidenciado a nivel de los sustratos que fosforilan, tal y como lo demuestran estudios de proteómica en los que se ha demostrado que las cinasas MPK3 y MPK6 comparten 26 sustratos (Feilner *et al*., 2005). Adicionalmente, Popescu *et al*. (2008) utilizando un “microarreglo de proteínas de alta densidad”

conteniendo 2158 proteínas impresas determinaron que MPK6 puede utilizar como sustrato a 186 proteínas, el 40% de las cuales (68) también pueden ser fosforiladas por MPK3. Por otra parte, mediante experimentos de dos híbridos se demostró que estas mismas cinasas interactúan *in vivo* con las fosfatasas PTP1, MKP1 y MKP2, así como con los factores de transcripción EIN3 y SPEECHLESS (Andreasson y Ellis, 2010).

La actividad de todas las enzimas con actividad de cinasas está regulada por desfosforilación mediada por proteínas con actividad de fosfatasa. Particularmente un módulo de MAPKs puede ser regulado a diferentes niveles por la acción de distintas fosfatasas, como las específicas de tirosina (PTPs), las específicas de serina/treonina y las denominadas duales específicas de treonina/tirosina (DSPs). Es un hecho que la regulación de las MPKs, corresponde en gran medida a la de las MKPs (por MAP kinase phosphatase) que las inactivan mediante la desfosforilación de los residuos de aminoácidos treonina y tirosina localizados en motivo de activación T-X-Y (Hyeong *et al*., 2011). En el genoma de *A. thaliana*, contrastando con los 20 miembros que conforman la familia de las MPKs, sólo hay 5 miembros que representan a la familia de las MKPs (DsPTP1, IBR5, PHS1, MKP1 y MKP2) [Bartels *et al*., 2010], siendo la fosfatasa DsPTP1 la primera que, mediante ensayos *in vitro*, se demostró que inactiva a una MPK (MPK4) [Gupta *et al.,* 1998]. También a través de ensayos *in vitro*, se demostró que la fosfatasa MKP2 desfosforila tanto a MPK3 como a MPK6. La inactivación del gen *MKP2* mediante RNA de interferencia (*RNAi-mkp2*), resultó en líneas hipersensibles a tratamiento con ozono, lo cual fue asociado con la activación de MPK3 y MPK6 (Lee y Ellis, 2007). Por su parte, la fosfatasa IBR5 interacciona con MPK12, tanto *in vitro* como *in vivo*, durante la regulación de la respuesta a auxinas (Lee *et al*., 2009). Así mismo, en ensayos *in vitro* e *in vivo* se ha demostrado que la fosfatasa PHS1 interacciona con MPK12 y MPK18 para regular funciones relacionadas a microtúbulos (Walia *et al.,* 2009). Finalmente, en ensayos *in vitro* e *in vivo* se ha encontrado que la fosfatasa MKP1 interacciona con las MPK3, MPK4 y MPK6, particularmente esta fosfatasa regula a MPK6 en la respuesta a PAMPs (Pathogen-Associated molecular patterns), así como a MPK3 y MPK6 en

respuesta a estrés con radiación UV-B (Andreason y Ellis 2010; Bartels *et al*., 2010).

I.10. Receptores tipo cinasa

Las vías de señalización mediadas por ligando-receptor han recibido especial atención y varios receptores con actividad de cinasa RLK (por Receptor Like Kinases) han sido implicados en la percepción de señales extracelulares para controlar diferentes procesos del desarrollo y el crecimiento de las plantas. En mamíferos, la percepción de los ligandos está mediada por receptores transmembranales capaces de fosforilar aminoácidos tirosina y serina/treonina. Estos receptores contienen un dominio extracelular que reconoce a un ligando específico y un dominio citoplásmico con actividad cinasa que transmite el mensaje. De manera general, la unión de un ligando al receptor induce su dimerización, su autofosforilación y una subsecuente fosforilación de proteínas señalizadores que actúan río abajo (Shiu y Bleecker, 2001).

A diferencia de los de mamíferos, los receptores con actividad cinasa reportados en plantas, identificados por su alta semejanza en la organización de sus dominios a los receptores de cinasas de tirosina de mamíferos, tienen una actividad de fosforilación específica en aminoácidos serina/treonina. En *A. thaliana* se han encontrado más de 600 receptores de tipo cinasa, lo que representa alrededor del 2% del genoma de esta planta. Dichos receptores, se han relacionado a distintos procesos de respuesta a estrés biótico y abiótico, así como con la respuesta a patógenos, eventos de simbiosis, la respuesta a fitohormonas y la actividad meristemática (Osakabe *et al*., 2013).

Los RLKs transducen la señal mediante la fosforilación de sus proteínas blanco, entre las que se incluye a los módulos de señalización de MAP cinasas (Asai *et al*., 2002; Lukowitz *et al.,* 2004; Lampard *et al.,* 2009; Bayer *et al.,* 2009). En la respuesta de *A. thaliana* activada por el receptor de tipo cinasa FLS2 (FLAGELIN SENSING 2), opera el módulo de MAP cinasas (MPKKK1, MPKK4/MPKK5 y MPK3/MPK6) para transducir la señal y finalmente activar a los factores de

transcripción WRKY22/WRKY29, que regulan la transcripción de los genes de respuesta inmune (Asai *et al*., 2002). Durante el desarrollo de estomas, el receptor TMM (TOO MANY MOUTHS), que carece de un dominio intracelular canónico, se ha propuesto funciona junto con el receptor de tipo cinasa ERL1 (ER LIKE 1) para transducir su señal al módulo de MAP cinasas compuesto por: YDA (MPKKK4), MPKK4/MPKK5 y MPK3/MPK6 (Lampard *et al.,* 2009). Este tipo de heterodimerizaciones entre receptores, como el que se da por los TMM y ERL1 es muy común en mamíferos (Schlessinger, 2000; Shpak *et al*., 2005). Este mismo módulo de MAPKs (YDA, MPKK4/MPKK5 y MPK3/MPK6) participa transduciendo la señal del RLK-ER para regular la proliferacion celular durante el desarrollo de las inflorescencias (Meng *et al*., 2012). Así mismo, durante el proceso de alargamiento del cigoto en la embriogénesis, se ha determinado que la activación de YDA requiere del receptor de tipo cinasa SSP1 (SHORT SUSPENSOR 1) [Bayer *et al.,* 2009; Lukowitz *et al.,* 2004]. Esto, se ha evidenciado por que tanto mutantes del gen *SSP1* como de *YDA*, producen embriones que no se alargan de manera normal y en los que las dos células hijas en la parte basal tienen un tamaño reducido, no crecen y frecuentemente se dividen en planos anormales, que resultan en un suspensor mal formado, por lo tanto, un embrión deforme que en muchos casos no llega a desarrollarse. Interesantemente este mismo fenómeno ocurre en la mutante *mpk6*, lo que sugiere que SSP1 podría ser el receptor que activa al módulo de MAP cinasas del que forman parte YDA y MPK6, que controla el desarrollo del embrión (Lukowitz *et al.,* 2004; Bayer *et al.,* 2009; Jeong *et al.,* 2010).

II. ANTECEDENTES

A pesar de que existen 90 MAPKs anotadas en el genoma de *A. thaliana*, existen escasos ejemplos de su función, principalmente en lo referente a todos los componentes que conforman un módulo determinado y de hecho hasta la actualidad solo se han identificado cuatro módulos en los cuales se ha identificado a todos sus componentes, y corresponden al módulo que regula la respuesta a flagelina y que esta compuesto por: MPKKK1, MPKK4/MPKK5 y MPK3/MPK6; el que regula la respuesta a etileno compuesto por: CTR1, MPKK9 y MPK3/MPK6; así como el que regula el desarrollo de estomas y de las inflorescencias en el cual participan: la MPKKK4–YDA, MPKK4/MPKK5 y MPK3/MPK6 (Asai *et al*,. 2002; Yoo *et al*., 2008; Lampard *et al*., 2009; Meng *et al*., 2012; Xu y Zhang, 2015).

Mediante estudios de proteómica se ha evidenciado que las MPK3 y MPK6 comparten alrededor de 100 sustratos (Feilner *et al*., 2005; Popescu *et al*., 2008). Y mediante experimentos de dos híbridos se ha demostrado que estas cinasas interactúan con las fosfatasas PTP1, MKP1 y MKP2 y con los factores de transcripción EIN3 y SPEECHLESS (Andreasson y Ellis, 2010).

A pesar de la evidente redundancia funcional que tienen las cinasas MPK3 y MPK6, se ha reportado que la mutación de una de ellas (*mpk6*) resulta en defectos en el desarrollo del embrión resultando en semillas explotadas (“burst seeds”) que hacen que el embrión sea expulsado de la testa, esta mutante también muestra defectos en el desarrollo del sistema radical de *A. thaliana,* el cual, se caracteriza por formar una raíz primaria corta, así como un mayor número de raíces laterales y de raíces adventicias (Bush y Krysan, 2007; Müller *et al.*, 2010).

III. HIPÓTESIS

Este trabajo está enfocado en dos programas de desarrollo relacionados, pero claramente independientes, por lo que su planteamiento se realizó en función de las siguientes hipótesis:

1) Dado que MPK6 está involucrada en la regulación del desarrollo del sistema radical y en el entendido de que la regulación de todos los programas desarrollo están mediados por reguladores del crecimiento, se plantea que: la **MPK6 es un componente de una vía de señalización controlada por reguladores del crecimiento vegetal involucrada en el desarrollo del sistema radical.**

2) Como la cinasa MPK6 es componente de un módulo de señalización y su pérdida de función resulta en tres fenotipos de semilla, entonces: **dichos fenotipos pueden utilizarse como marcadores para identificar a otros componentes del módulo en el que opera MPK6 para regular este programa de desarrollo**.

IV. OBJETIVOS

IV.1. General

Caracterizar la participación de la cinasa MPK6 en el desarrollo del embrión y del sistema radical así como identificar a los reguladores del crecimiento vegetal que estén controlando estos procesos mediante la participación de MPK6 en *Arabidopsis*

IV.2. Específicos

1. Caracterizar fenotípicamente el programa de desarrollo del embrión en mutantes afectadas en la cinasa MPK6 y compararlo con las plantas de tipo silvestre.

2. Determinar si las alteraciones en el desarrollo embrionario causadas por la pérdida de función en *MPK6* afectan la arquitectura de la raíz.

3. Evaluar si los fenotipos de raíz causados por la pérdida de función en MPK6 tienen relación con la respuesta a reguladores del crecimiento vegetal.

4. Identificar componentes potenciales de la cascada de fosforilación en la que participa *MPK6* para regular el desarrollo del embrión de *A. thaliana*.

V. RESULTADOS Y DISCUSIÓN

V.1. MPK6 está involucrada en el desarrollo del embrión y la semilla

Las MAPKs funcionan mediante eventos de fosforilación secuencial de al menos tres componentes (MPKKK, MPKK y MPK) que se activan en respuesta a varios tipos de estímulos bióticos y abióticos, así como por fitohormonas para regular diversos procesos celulares. Información de diversos grupos de investigación, habían demostrado que la mutación en MPK6 afecta los programas de desarrollo del embrión y de la raíz de *Arabidopsis thaliana* sin que se hubiese establecido una correlación entre estas alteraciones fenotípicas. En particular, se había demostrado que las mutantes de *Arabidopsis mpk6* presentan semillas que expulsan el embrión, por lo que su fenotipo fue denominado de semillas protruídas ("burst seeds", Bush y Krysan, 2007). En un reporte independiente, se describió un fenotipo de raíz corta para esta mutante (Müller *et al.*, 2009), lo cual sugiere que, al menos en estos procesos del desarrollo, la función de la MPK6 no puede ser reemplazada por alguna otra MPK, descartando así la redundancia funcional descrita para MPK6/MPK3 para otros procesos.

Mediante análisis fenotípicos detallados se encontró que la mutante *mpk6*, adicionalmente a los fenotipos de semillas explotadas (Figura 6A y 6E) [Bush y Krysan, 2007], tiene otros dos fenotipos de semilla: 1) deformes, con testas arrugadas y apariencia de uva-pasas, por lo que se definieron como "Raisin seeds" (Figura 6A y 6D) y 2) semillas que parecen fenotípicamente normales, pero que realmente son más grandes que las semillas de tipo silvestre, por lo que se definieron como "Wild-type bigger seeds" (Figura 6A y 6C). Estos fenotipos son estables a través de diferentes generaciones manteniendo una proporción de 70% semillas "Wild-type bigger", 23% de semillas "Raisin" y 7% de semillas "Burst" (Figura 6C-E). Con la idea de establecer los fenómenos que pudieran estar determinando estos fenotipos, se realizaron análisis microscópicos comparativos durante la embriogenesis de *mpk6* y de plántas de tipo silvestre (Figura 7A, B, D, I), encontrándose que la mutante *mpk6* produce divisiones ectópicas en el

suspensor previo al establecimiento de la hipófisis que dará lugar al desarrollo del RAM (Root Apical Meristem) [Figura 7C]. Más tarde, durante la etapa de corazón, la mutante *mpk6* produce un exceso de células que resultan en órganos más grandes y deformes (Cotiledones y RAM) que parecen impactar tanto en el tamaño, como la forma de la semilla (Figura 7E-H). Particularmente, los fenotipos de semillas deformes indican que MPK6 es un componente clave para el desarrollo del embrión, posiblemente a través de la señalización o el transporte de auxinas (Lau *et al*., 2012). Esto porque el fenotipo de la mutante *mpk6* es el resultado de divisiones ectopicas en el suspensor durante la embriogenesis temprana y la sobreproducción de células durante etapas subsecuentes de la embriogénesis. Alternativamente, las alteraciones durante desarrollo del embrión y los fenotipos de semilla de la mutante *mpk6,* pueden ser consecuencia de defectos en el desarrollo del endospermo, cuya celularización es crucial para la embriogénesis y para el desarrollo de la testa (Hehenberger *et al*., 2012).

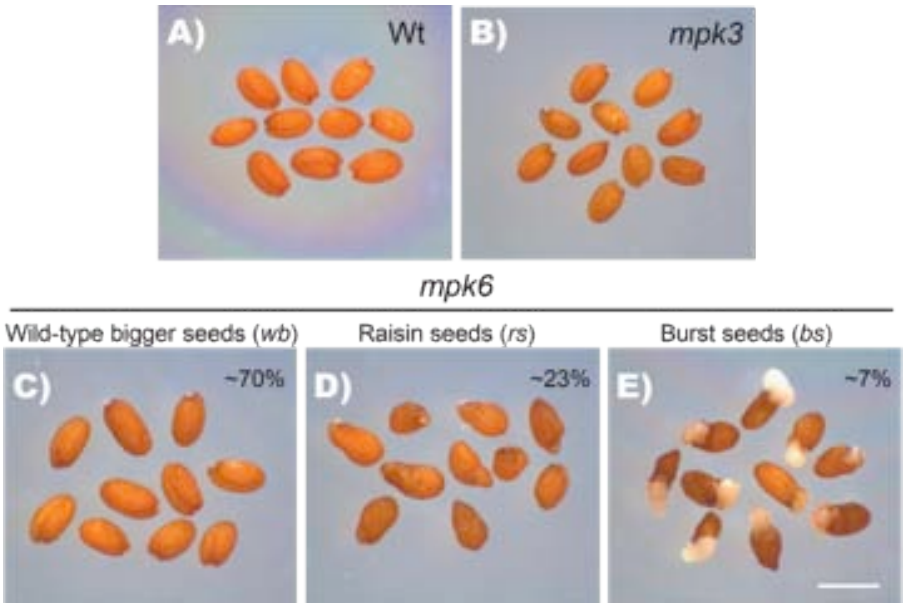

Figura 6. Fenotipo de semillas de la mutante *mpk6*. Comparadas con las semillas provenientes de plantas de tipo silvestre (A) y de la mutante *mpk3* (B), en las semillas provenientes de la mutante *mpk6* se pueden identificar tres fenotipos que se definieron como “Wild-type bigger” (*wb*) “Raisin” (*rs*) y “Burst” (*bs*) en proporciones de 70, 23 y 7 % respectivamente (C-D). Escala=500µm. n=1000.

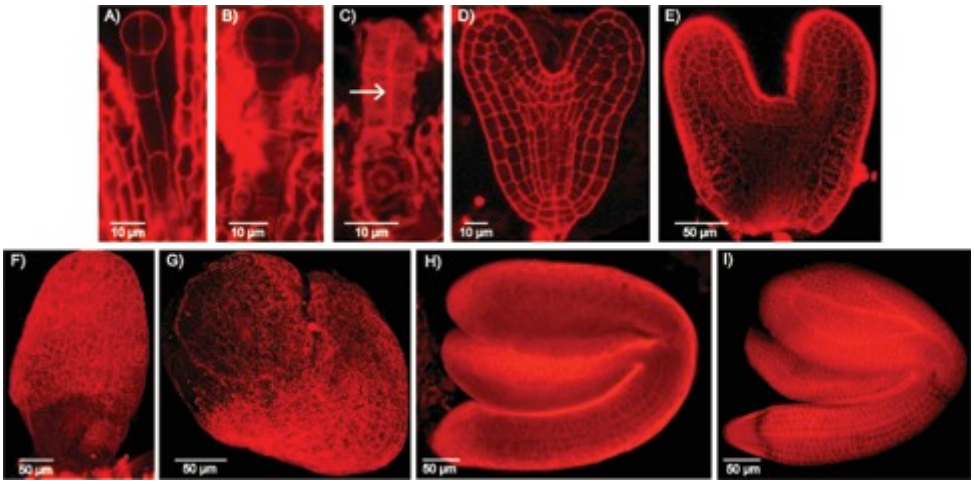

Figura 7. Defectos durante la embriogénesis de la mutante *mpk6*. Las imágenes de microscopía confocal de embriones teñidos con yoduro de propidio muestran que la mutante *mpk6* tiene divisiones periclinales en el suspensor (Flecha en C) durante etapas tempranas de la embriogénesis, así como una aparente mayor producción celular en estadíos subsecuentes (E-H) en comparación con embriones de tipo silvestre (A, B, D e I). Escalas A-D= 10µm, E-I= 50µm.

V.2. MPK6 participa en la regulación del desarrollo del sistema radical

El fenotipo del sistema radical de la mutante *mpk6* se describió como una raíz primaria corta y con una mayor producción de raíces laterales y adventicias (Müller *et al.*, 2009). Para conocer si las diferentes clases de semillas producidas por la mutante *mpk6* pudieran producir plántulas con alteraciones en el desarrollo de la raíz, se realizó una comparación fenotípica detallada entre plantas silvestres de *Arabidopsis* con mutantes *mpk6*. Se encontró que las plantas que provienen de semillas “explotadas” no desarrollan raíz primaria, aunque alrededor del 20% de estás plántulas pueden completar su ciclo de vida a través de la formación de raíces adventicias (Figura 8B y 8C). Por otra parte, las plantas que provienen de semillas “raisin” desarrollan una raíz primaria corta con aparentemente más raíces laterales (Figuras 8B y 8D), un fenotipo muy similar al reportado por Müller *et al.*, (2009), mientras que las plantas que provienen de semillas sin daño aparente en el embrión, desarrollan una raíz primaria más larga, con un mayor número de raíces laterales también de mayor tamaño a las de plantas tipo silvestre, así como

un mayor número de pelos radicales, los cuales también son más largos que los de plantas de tipo silvestre (Figuras 8D, 9A-C y 10A-C).

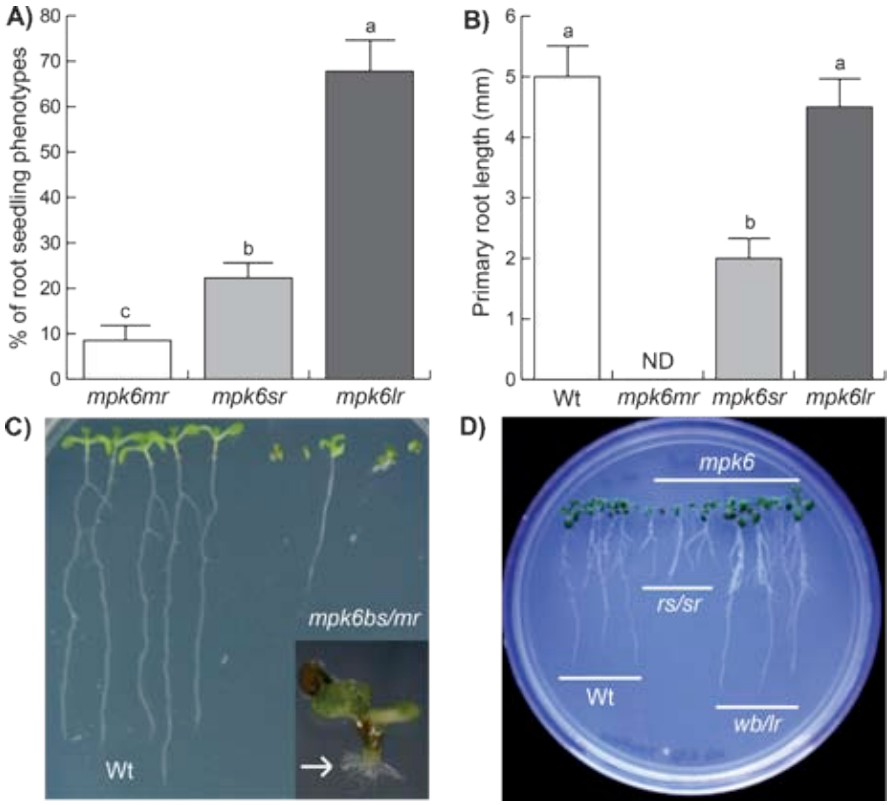

Figura 8. Fenotipos de la raíz primaria de la mutante *mpk6.* En comparación con plantas de tipo silvestre, el 7% de las plantas de la mutante *mpk6* no desarrollan raíz primaria, el 23% desarrollan una raíz primaria corta y alrededor del 73% desarrollan una raíz primaria aparentemente normal (A y B). Cuando se separan las semillas de la mutante *mpk6* por fenotipos (Figura 6) se tiene que las plántulas provenientes de semillas "Burst" no desarrollan raíz primaria, si bien algunos individuos desarrollan raíces adventicias (Recuadro en C). Por su parte, las plántulas provenientes de semillas "Raisin" y semillas "Wild type Bigger" desarrollan una raíz primaria corta y una raíz primaria aparentemente más larga, respectivamente (C y D). *mpk6mr=mpk6-minus root*, m*pk6sr=mpk6-short root*, *mpk6lr=mpk6-longer root*, *mpk6bs/mr=mpk6-burst seed/minus root*, *rs/sr=raisin seed/short root*, *wb/lr=wild type biger/longer root*. Las barras representan el error estándar de una n=20 plantas de 10 días después de germinación. Las distintas letras sobre las barras representan diferencias significativas con una P≤ 0.001.

Interesantemente, los porcentajes de los fenotipos de ausencia de raíz primaria (7%), de raíz primaria corta (23%) y de raíz primaria más larga (70%) [Figura 8A], correlacionan con los fenotipos de semillas explotadas (7%), de semillas "Raisin" (23 %) y de semillas "Wild type bigger" (70%). Estas observaciones sugieren

fuertemente que los fenotipos de raíz primaria y de desarrollo del embrión, parecen estar relacionados. Particularmente, con base a que el fenotipo de raíz primaria de mayor tamaño, parece ser independiente de daños en el desarrollo del embrión, puede concluirse que MPK6 funciona como un regulador negativo del desarrollo de la raíz primaria. A este respecto, como el establecimiento de la radícula es embrionario, mientras que el desarrollo de la raíz primaria es postembrionario y depende de procesos celulares de división en el RAM, así como de crecimiento en la zona de elongación, es posible que el fenotipo de raíz primaria larga de las plántulas provenientes de semillas *mpk6* "Wild type bigger", se deba alteraciones de división o de elongación celular.

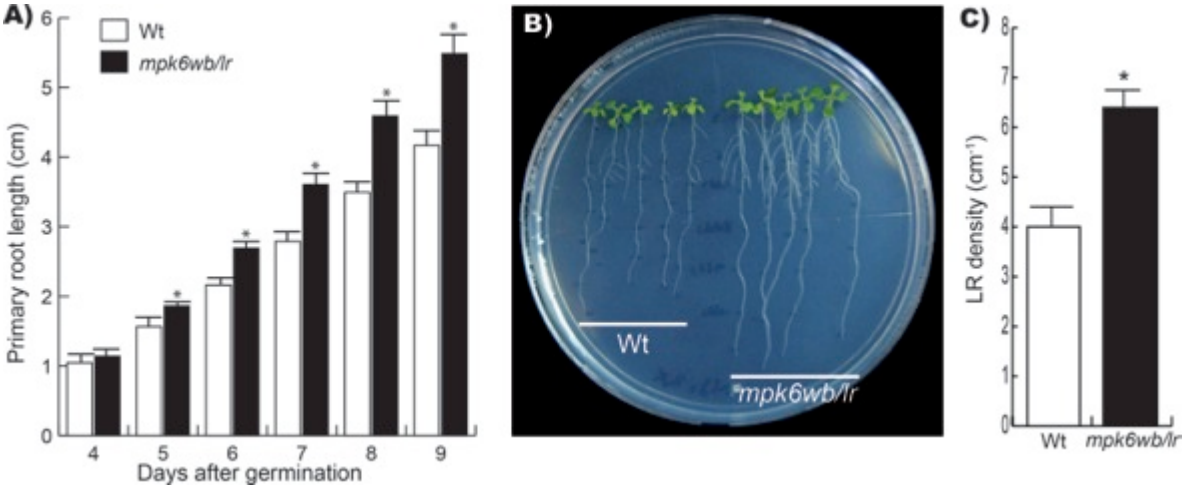

Figura 9. Fenotipos del sistema radical de plantas *mpk6* "wild type bigger". En comparación con plantas de tipo silvestre las plantas provenientes de semillas "wb" tienen una raíz primaria más larga que se distingue a partir de los 5 días después de germinación (A y B), así como una mayor densidad de raíces laterales (C). Las barras representan el error estándar de una n=20. Los asteriscos representan diferencias estadísticas significativas con una P≤ 0.001.

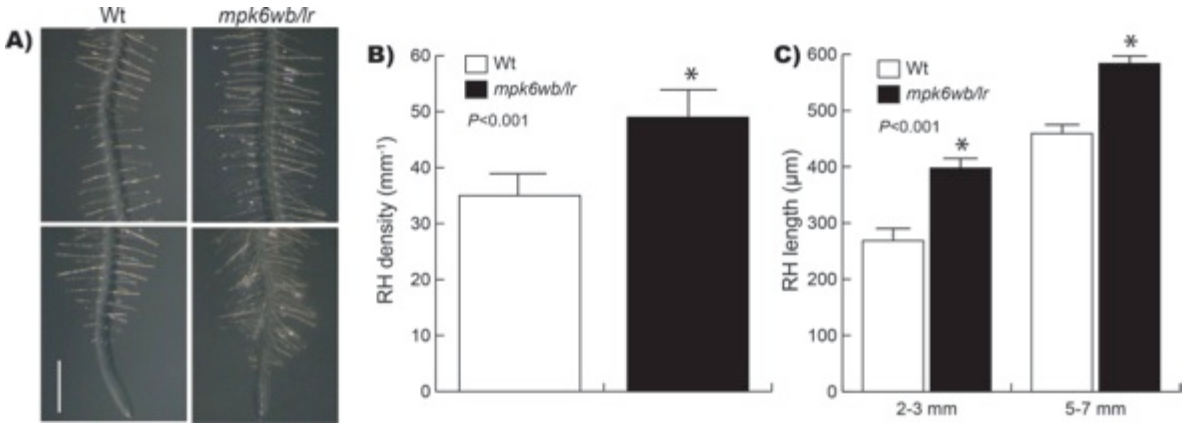

Figura 10. Producción de pelos radicales en la mutante *mpk6.* Comparadas con plantas de tipo silvestre la mutante *mpk6* produce más pelos radicales. Se muestra el fenotipo de dos regiones de la raíz primaria (A), la densidad de los pelos radicales (B) y la longitud de los pelos radicales completamente alargados (C) en la planta de tipo silvestre y en la mutante *mpk6.* Escala= 1mm. Las barras representan el error estándar de una n= 20 Plántulas de 10 días después de germinación. Los asteriscos representan diferencias estadísticas significativas con una P≤ 0.001.

V.3. El fenotipo de raíz primaria de *mpk6* depende de alteraciones en los procesos de división, diferenciación y alargamiento celular

Para profundizar sobre la participación de MPK6 en los procesos de división, diferenciación y alargamiento celular, se realizó un análisis comparativo detallado de las zonas de crecimiento (RAM+zona de elongación; Figura 11) de las raíces primarias de la mutante *mpk6* y de plántulas de tipo silvestre. Los resultados de este análisis mostraron que la mutante *mpk6* tiene un mayor número de células en el dominio de proliferación, así como una mayor longitud del dominio de transición del RAM (Figura 11). Adicionalmente, el análisis de la tasa de crecimiento demostró que la raíz primaria de *mpk6* crece más rápido y que tiene una tasa mayor de producción celular que el de plantas tipo silvestre (Figuras 12A y 12C). Tanto los datos del desarrollo del embrión, en el cual se puede observar un execeso de producción celular, como los del desarrollo de la raíz primaria, que muestra un mayor número de células en el dominio de proliferación, así como una mayor tasa de producción celular, sugieren fuertemente que MPK6 es un regulador negativo de la división celular. De hecho, existen reportes sobre la

participación de MAPKs durante la división celular (Jonak *et al*., 1993; Calderini *et al*., 1998) sin embargo, la participación detallada de la cinasa MPK6 durante este proceso se desconoce.

Por otra parte, análisis de la longitud de las células corticales en la zona de diferenciación, mostraron que las células de la mutante *mpk6* son más largas que las células de las plántulas de tipo silvestre (Figura 12B). Estos resultados (mayor longitud de células corticales) aunados a la mayor longitud de los pelos radicales que tipifican a la mutante *mpk6*, sugieren que MPK6 es un regulador negativo del alargamiento celular. El alargamiento celular es regulado en parte por la dinámica del citoesqueleto, trabajos recientes demuestran la participación de MAPKs durante este proceso, especificamente la cinasa MPK6 se ha encontrado asociada a la γ-tubulina, en donde fosforila a la proteína EB1c durante la citocinesis (Kohoutová *et al*., 2015). Por esta razón, no puede descartarse que la MPK6 regule procesos de alargamiento celular, a través de modular la dinámica del citoesqueleto.

En conjunto, los resultados de los análisis de raíz demuestran que el tamaño exacerbado de la raíz primaria de la mutante *mpk6* comparado con plantas de tipo silvestre, está determinado por alteración de los procesos de división, diferenciación y alargamiento celular.

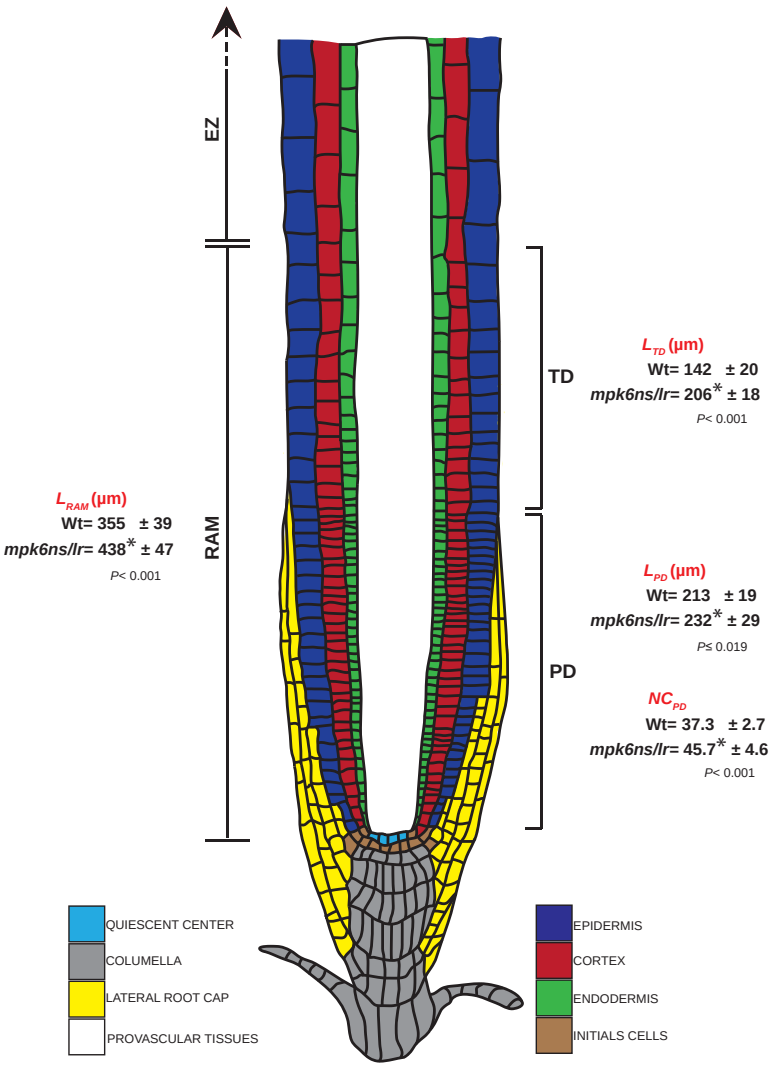

Figura 11. RAM de la raíz primaria de la mutante *mpk6.* En comparación con meristemos de plantas de tipo silvestre la mutante *mpk6* tiene un mayor número de células en el dominio de proliferación NC_{PD} (Number of Cell in PD), así como una mayor longitud tanto de los dominios de proliferación (L_{PD}) y de transición (L_{TD}), así como del RAM (L_{RAM}). EZ (Elongation Zone), TD (Transition Domain), PD (Proliferation Domain), los códigos de colores muestran los diferentes tejidos del RAM.

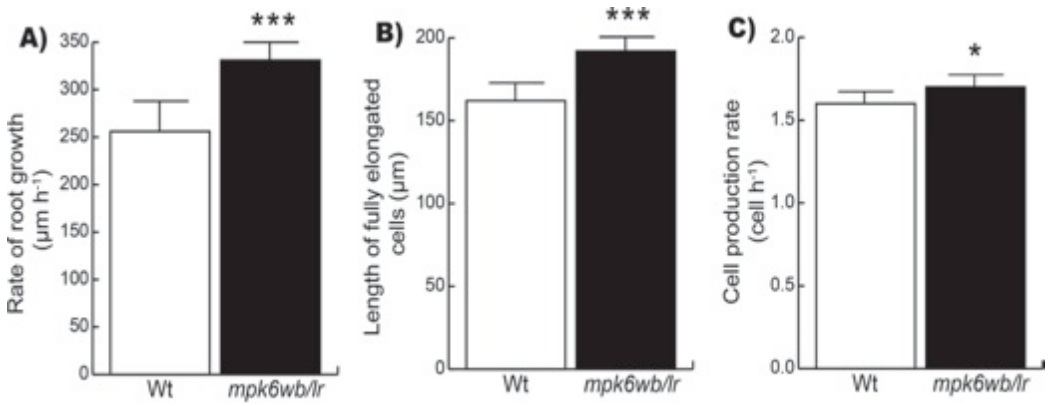

Figura 12. Parámetros de la raíz primaria de la mutante *mpk6.* En comparación con raíces de tipo silvestre la raíz de la mutante *mpk6* tiene una mayor tasa de crecimiento (A), así como una mayor longitud celular (B) y una mayor tasa de producción celular. Las barras representan el error estándar de una n=12. Plántulas de 8 días después de germinación. Los Asteriscos representan diferencias estadísticas significativas ***P≤ 0.001, **P≤0.03 y *P≤0.05.

Los resultados anteriores fueron reportados en la siguiente publicación:

López-Bucio JS, Dubrovsky JG, Raya-González J, Ugartechea-Chirino Y, López-Bucio J, de Luna-Valdez LA, Ramos-Vega M, León P, Guevara García AA (2014). *Arabidopsis thaliana* mitogen-activated protein kinase 6 is involved in seed formation and modulation of primary and lateral root development. *Journal of Experimental Botany* 65:169-183. **APÉNDICE 1.**

Dichos resultados implican el cumplimiento de los dos primeros objetivos de esta investigación cuyas principales conclusiones son que:

1) El principal fenotipo asociado a la pérdida de función de la cinasa MPK6, es el de una semilla más grande que la de las plantas tipo silvestre que está directamente asociado a un fenotipo de raíz primaria más larga con mayor número y mayor longitud tanto de raíces laterales como de pelos radicales.

2) La MPK6 participa en el establecimiento de la semilla regulando procesos de división celular durante el desarrollo del embrión.

3) La MPK6 regula el desarrollo post-embrionario de la raíz primaria, así como la producción de raíces laterales y de pelos radicales.

4) Los fenotipos postembrionarios del desarrollo de la raíz primaria de la mutante *mpk6*, dependen de alteraciones en los procesos de división, diferenciación y alargamiento celular.

V.4. Búsqueda del regulador del crecimiento a través del cual MPK6 ejerce su función sobre el programa de desarrollo de la raíz primaria.

Los reguladores del desarrollo vegetal, también llamadas fitohormonas, están involucrados en controlar todos los procesos morfológicos y fisiológicos que van desde la embriogénesis pasando por el crecimiento vegetativo, reproductivo y finalmente la senescencia, hasta las respuestas de estrés biótico y abiótico. Entre los principales reguladores del crecimiento se incluyen a las auxinas, las citocininas, el ácido abscísico, el etileno, los brasinosteroides, el ácido jasmónico, el ácido salicílico, las giberelinas y el óxido nítrico, los cuales actúan frecuentemente de manera conjunta con efectos sinérgicos o antagónicos para modular el desarrollo de las plantas (Santner *et al*., 2009). Además de las fitohormonas clásicas mencionadas, se ha encontrado que otras moléculas como los azúcares, las lactonas y algunos aminoácidos, también son capaces de modular el desarrollo de las plantas (Rolland *et al*., 2006; Walch-Liu *et al*., 2006; Ortíz-Castro *et al*., 2008).

Las auxinas y citocininas se han establecido como los principales reguladores del desarrollo del sistema radical (Dello Ioio *et al*., 2007; Overvoorde *et al*., 2010; Lee *et al*., 2012). Sin embargo, otros reguladores como es el caso del etileno, el ácido abscísico, el ácido jasmónico y el óxido nítrico, también se han relacionado a la regulación de este programa de desarrollo (Lee *et al*., 2012).

Es una realidad que las alteraciones del programa de desarrollo de la raíz que muestra la mutante *mpk6* podrían estar relacionados con la respuesta a uno o más reguladores del crecimiento. En ese sentido, estudios previos en la búsqueda de la

(s) fitohormona (s) que requieran la acción de MPK6 para ejercer sus efectos sobre los programas de desarrollo del embrión y de la raíz, ha sido extensa, pero en términos generales infructuosa. Ciertamente las auxinas, las citocininas y el ácido jasmónico, por mencionar algunas con efectos claros, son fitohormonas que afectan el desarrollo de la raíz de *A. thaliana,* pero sus efectos parecen ser, al menos en parte independientes de la función de MPK6, ya que la mutante *mpk6*, responde de manera similar que las plantas tipo silvestre al tratamiento con estos y otros reguladores del crecimiento (Figura 13).

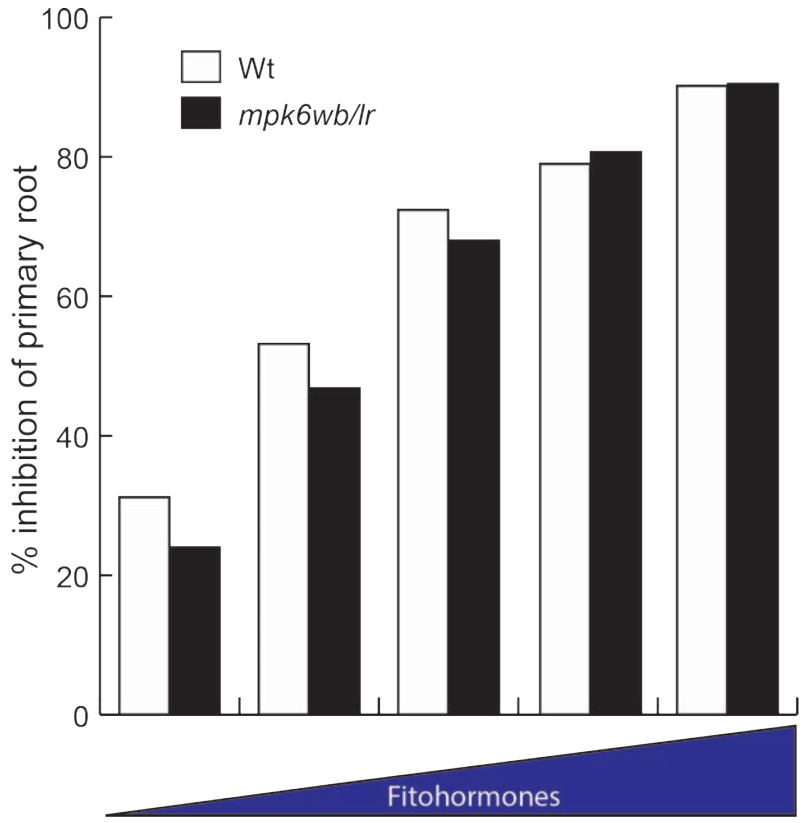

Figura 13. Efecto de las fitohormonas sobre el desarrollo de la raíz primaria. La gráfica ejemplifica el efecto inhibitorio de diferentes fitohormonas sobre el crecimiento de la raíz primaria tanto de las plantas de tipo silvestre como de la mutante *mpk6*. Las plantas fueron tratadas con auxinas (Ácido Indol Acetico 0, 0.001, 0.01, 0.1 y 1µM), citocininas (kinetina 0, 2, 4, 8, 16 µM), etileno (Ácido 1-aminociclopropano-1-carboxilico 0, 0.3, 0.6, 1.2 y 2.4 µM), ácido abscisico (0, 0.3, 0.6, 1.2 y 2.4 µM), ácido jasmonico (metil–jasmonato 0, 1, 2, 4 y 8 µM) y óxido nítrico (nitroprusiato de sodio 0, 10, 20, 30, 40 µM). n=20 plantas germinadas y crecidas durante 10 en cada tratamiento.

En los últimos años se ha encontrado que el desarrollo del sistema radical de las plantas está bajo el contról de múltiples y variadas señales como son las lactonas, que regulan el llamado “quorum sensing” de microorganismos, la decanamida, los azúcares, algunos ciclodipéptidos (ciclo-L-Prolina-L-Valina, ciclo-L-Prolina-L-Fenilalanina y cilco-L-Prolina-L-tirosina) y aminoácidos, como el ácido glutámico, así como por la disponibilidad de nutrientes e incluso la presencia de metales pesados en el suelo (Lopéz-Bucio *et al*., 2003; Walch-Liu *et al*., 2006; MacGregor *et al*., 2008; Ortíz-Castro *et al*., 2008; Ortíz-Castro *et al*., 2011; López-Bucio *et al*., 2015). De tal manera, puesto que la función de MPK6 está claramente involucrada en el control del desarrollo del sistema radical, queda abierta la posibilidad de algunas de las señales descritas, e incluso otras por descubrir, operen a través de una cascada de MAPKs en las que participe MPK6.

V.5. El glutamato regula el desarrollo de la raíz primaria de *A. thaliana* mediante una vía de señalización en la que participan la cinasa MPK6 y la fosfatasa MKP1

Recientemente se reportó que el Glutamato (L-Glu), uno de los aminoácidos constituyentes de proteínas, que es un conocido neurotransmisor en sistemas animales, así como una fuente de nitrógeno orgánico para las plantas, actúa como una señal que modula el desarrollo del sistema radical de *A. thaliana* (Walch-Liu *et al*., 2006). Los efectos del suministro de L-Glu al medio de cultivo ocasionan, una inhibición en el crecimiento de la raíz primaria y un incremento en la formación de raíces laterales en *A. thaliana*, efectos mediados por la función de la MAP cinasa MPKKK1 y del receptor de glutamato GLR3.4 (Walch-Liu *et al*., 2006; Forde *et al*., 2013; Vincill *et al*., 2013). Los receptores de glutamato actúan como canales de calcio (Ca^{++}) cuya activación dirige incrementos del Ca^{++} citoplásmico que a su vez induce la actividad de las cinasas MPK3 y MPK6 (Kwaaitaal *et al*., 2011). Por otra parte, se ha demostrado que MPK6 forma parte de una vía de señalización en respuesta a flagelina en la que también participa MPKKK1 que recientemente se ha asociado a las respuestas de las plantas al glutamato (Forde *et al*., 2013). Con

base a estos antecedentes, se decidió explorar los efectos del L-Glu sobre el programa de desarrollo de la raíz de *A. thaliana* afectado por la pérdida de función de la enzima MPK6 mediante la realización de experimentos de dosis respuesta sobre plantas tipo silvestre y la mutante *mpk6*. Adicionalmente, para complementar el estudio de los efectos del glutamato sobre el desarrollo de la raíz primaria posiblemente mediado por MPK6, en los experimentos se incluyó a una mutante de la fosfatasa MKP1. Esta fosfatasa, es un conocido regulador de la actividad de la MPK6 en respuesta a luz UV y a PAMPs (Andreason y Ellis 2010; Barteles *et al*., 2010), pero además, interesantemente la mutante corrrespondiente (*mkp1*) muestra fenotipos de raíz opuestos a los que tipifican a la mutante *mpk6*, es decir, la mutante *mkp1* tiene una raíz primaria corta con menos raíces laterales y menos pelos radicales (Figura 14 y 15A). Los resultados de estos análisis mostraron que mientras la mutante *mpk6* es resistente al efecto de inhibición de la raíz primaria que causa el L-Glu en plantas de tipo silvestre, la mutante *mkp1* es hipersensible al tratamiento con este aminoácido (Figura 15A-C).

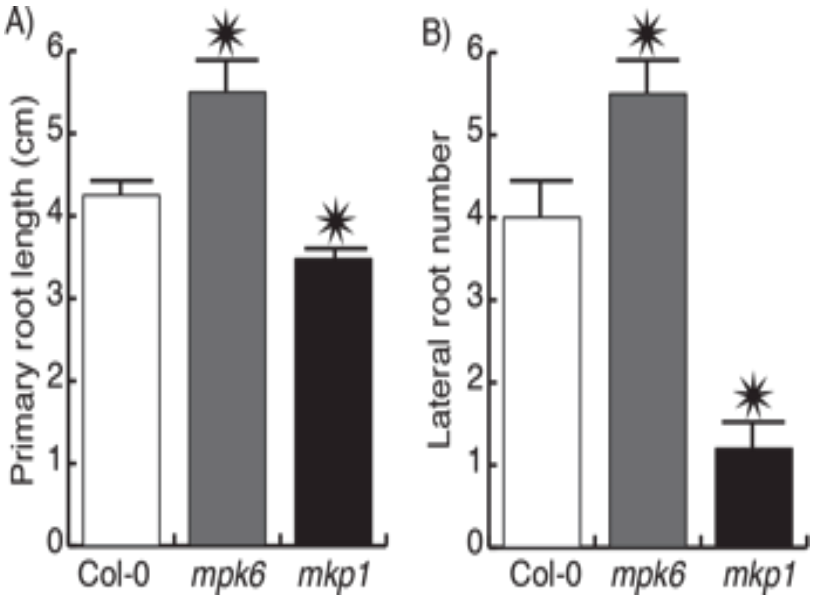

Figura 14. Sistema radical de las mutantes *mpk6* y *mkp1.* En comparación con plantas de tipo silvestre (Col-0) las mutantes *mpk6* y *mkp1* tienen fenotipos contrarios tanto en la longitud de la raíz primaria (A) como en el número de raíces laterales (B). Las barras representan el error estándar de una n=20 plántulas de 8 días después de germinación. Los asteriscos representan diferencias estadísticas significativas con una P≤ 0.001 en relación con las plantas de tipo silvestre.

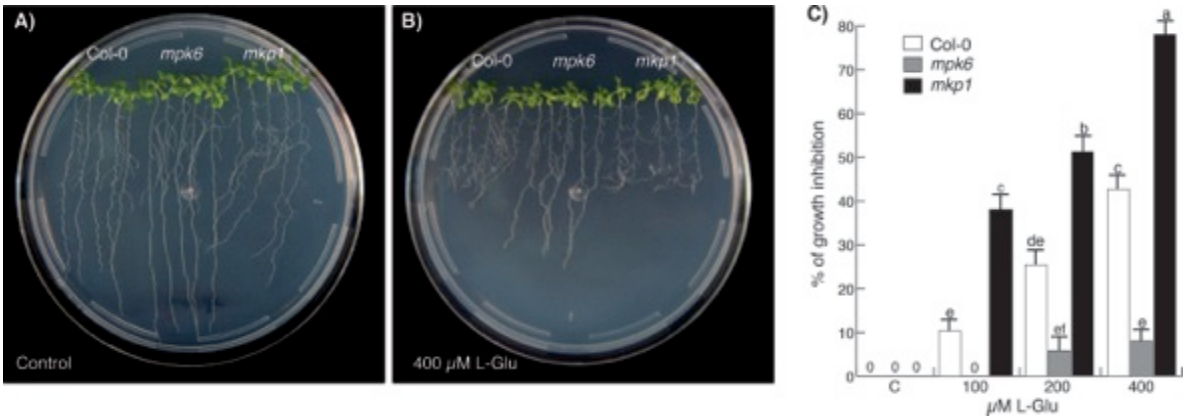

Figura 15. Respuesta del sistema radical a tratamientos con L-Glutamato (L-Glu). En comparación con plantas de tipo silvestre (Col-0) la mutante *mpk6* muestra resistencia mientras que la mutante *mkp1* muestra mayor sensibilidad a los efectos inhibitorios de 400μM de L-Glu sobre el desarrollo de la raíz primaria. Las plantas fueron crecidas durante 5 días en medio MS 0.2X y después fueron transferidas a medio MS 0.2X fresco (A) o suplementado con 400μM de L-Glu (B). En la gráfica se muestra al porcentaje de inhibición del crecimiento de la raíz primaria de las plántulas indicadas en concentraciones crecientes de L-Glu (C). Las barras representan el error estándar de una n=36 de plantas de 10 días después de germinación (5 días con tratamiento).

Estos resultados indican que tanto MPK6 como MKP1, están involucradas en el mecanismo de regulación del crecimiento de la raíz primaria mediada por glutamato. Es decir, parece que el glutamato hace uso de un módulo de MAPKs para transducir la señal que afecta el crecimiento de la raíz primaria. Podría inferirse que otro de los componentes potenciales de este módulo de MAPKs sería MPKKK1. Sin embargo, a este respecto debe considerase que ya se demostró que la participación de MPKKK1 en la respuesta al glutamato es independiente de su actividad de cinasa (Forde *et al*., 2013). En todo caso, la búsqueda de otros componentes del módulo que opera para controlar las respuestas al L-Glu es un campo de investigación abierto.

V.6. El glutamato regula respuestas al gravitropismo afectando el contenido de almidón, así como la señal de auxinas en el RAM a través de la actividad de MPK6 y MKP1

En el estudio referido, también se encontró que el L-Glu afecta la percepción de la fuerza de gravedad induciendo respuestas alteradas caracterizadas por una desviación del crecimiento con respecto al vector de la gravedad en plantas de tipo silvestre. Por su parte, las mutantes *mpk6* y *mkp1* son resistentes más sensibles respectivamente, a estos efectos del L-Glu (Figura 16 y Tabla 1).

Se ha establecido que los amiloplastos presentes en la columela de la raíz funcionan como estatolitos para una adecuada percepción del estímulo de la gravedad, de esta manera, los cambios en la densidad y sedimentación de los amiloplastos son factores determinantes para el control de las respuestas gravitrópicas de la raíz primaria (Kiss *et al*., 1989; Sack, 1997; Blancaflor *et al*., 1998; Tsugeki y Fedoroff, 1999; Paciorek *et al*., 2005). Por otra parte, también se ha demostrado que la redistribución de auxinas desde el RAM hacia la zona de elongación es importante para inducir el alargamiento celular diferencial que dirige el crecimiento de la raíz en dirección del vector de la gravedad. Dicha redistribución esta mediada por los transportadores de auxinas presentes en la membrana plasmática de las células de los tejidos provasculares (PIN1), de las células de la columnella (PIN3 y PIN7) y de las células de la epidermis y del córtex (PIN2) [Ottenschläger *et al*., 2003; Kleine-Vehn *et al*., 2010; Brunoud *et al*., 2012; Baldwin *et al*., 2013].

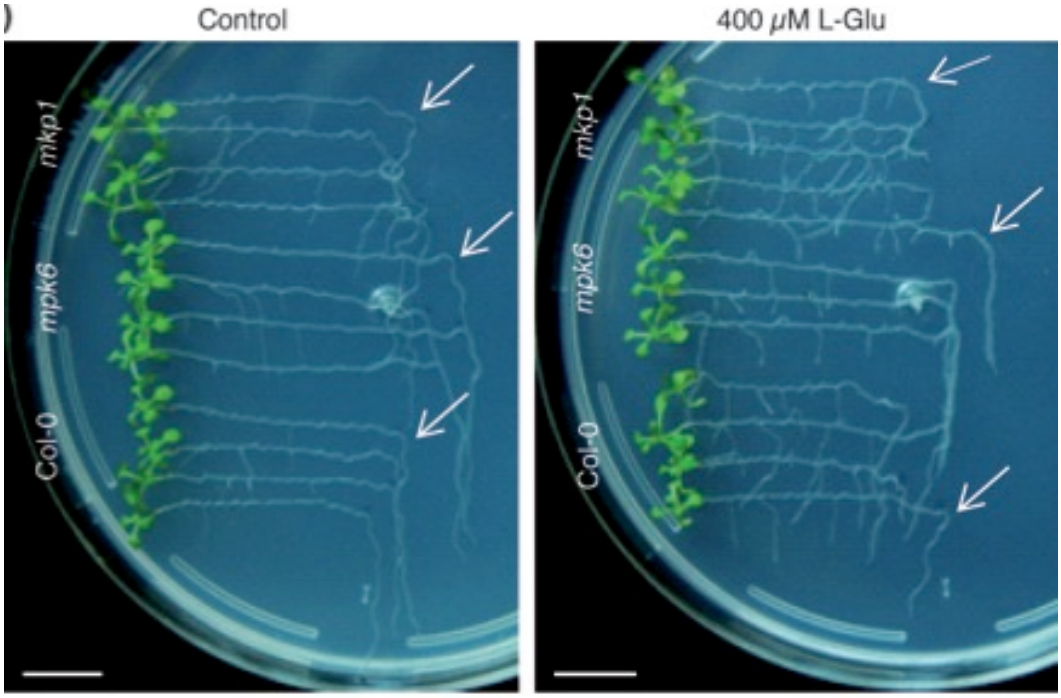

Figura 16. Efecto del L-Glu sobre la respuesta gravitrópica de la raíz primaria. El estímulo de la gravedad forma un ángulo de aproximadamente 90^0 en la raíz primaria de plantas de tipo silvestre (Col-0) mientras que en las mutantes *mpk6* y *mkp1* los angulos formados son de aproximadamente 82^0 y 99^0 respectivamente (A). En los tratamientos con 400μM de L-Glu, la formación del ángulo en respuesta al estímulo de gravedad es aproximadamente de 110^0 en las plantas de tipo silvestre, de 90^0 en la mutante *mpk6* y de 130^0 en la mutante *mkp1*. Las flechas indican el ángulo que se forma en la raíz primaria después de 4 días de girar la placa 90^0. n=16.

Tabla 1. comportamiento de la raíz primaria ante el estímulo de la gravedad en tratamientos con L-Glu.

Control	400 μM L-Glu
Col-0 $89^0 \pm 2$	Col-0 $111^0 \pm 3$
mpk6 $82^0 \pm 1$	*mpk6* $88^0 \pm 1$
mkp1 $99^0 \pm 2$	*mkp1* $127^0 \pm 1$

Bajo este razonamiento, para profundizar en el estudio del efecto del glutamato sobre la percepción de la fuerza gravedad, se analizaron sobre plantas tipo silvestre y las mutantes *mpk6* y *mkp1*, tanto la estructura del estatocito, como la distribución de la señal de auxinas en el RAM, en respuesta al tratamiento con

este aminoácido. El análisis demostró que el glutamato afecta la estructura del estatocito de las plantas de tipo silvestre y de la mutante *mkp1*, cuyo contenido de almidón en la columela es muy similar, mientras que el estatocito de la mutante *mpk6*, que de por si tiene una mayor densidad de almidón en la columela, es prácticamente insensible a los efectos del L-Glu. (Figura 17).

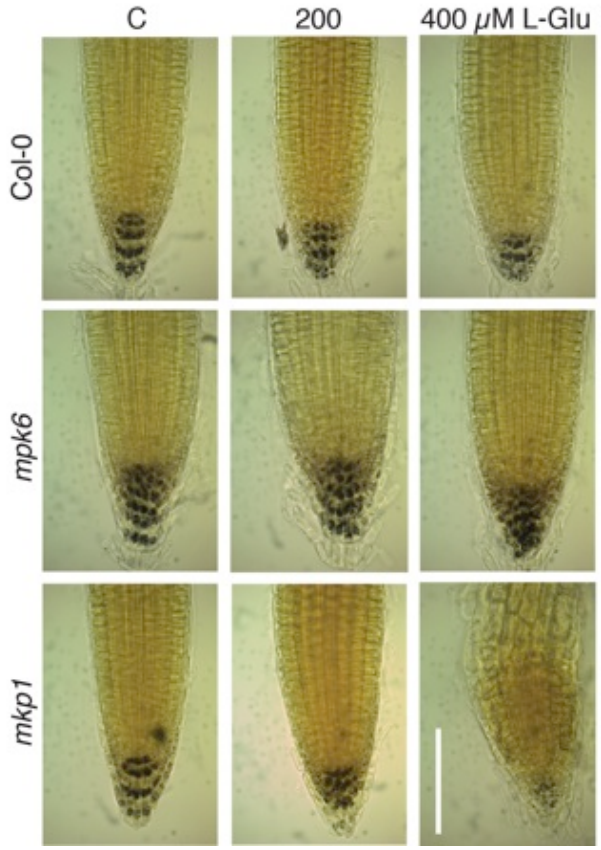

Figura 17. Tinciones del almidón en la columella en tratamientos con L-Glu. La columella de las plantas de tipo silvestre (Col-0) en condiciones control muestran una tinción de almidón característica la cual disminuye en los tratamientos con 200 y 400μM de L-Glu. En la mutante *mpk6* la tinción del almidón parece no modificarse en los tratamientos, mientras que en la mutante *mkp1* la tinción del almidón se ve severamente afectada en 400μM de L-Glu. Raíces de plántulas de 8 DDG teñidas con lugol. n=12.

Adicionalmente, las tinciones de almidón en la columela durante el tratamiento con 400μM de L-Glu, también ponen en evidencia la mayor sensibilidad de la mutante *mkp1*, a los efectos de este aminoácido, que en este caso resulta en un agotamiento del meristemo apical, caracterizado por la presencia de células

alargadas y diferenciadas, que dirige el crecimiento determinado de la raíz primaria (14B y C) [Reyes-Herández *et al*., 2014].

Los análisis de la respuesta a auxinas a nivel transcripcional en los tratamientos con L-Glu, se realizaron sobre cruzas de las mutantes *mpk6* y *mkp1* con la línea reportera de respuesta a auxinas (*DR5::GFP*) la cual es un marcador de la distribución auxínica usando la línea marcadora como control. Los resultados muestran que tanto la línea de tipo silvestre (*DR5::GFP*), como las mutantes *mpk6* y *mkp1*, muestran una distribución de auxinas característica localizada en tejidos provasculares y en las células de la columela (Ottenschläger *et al*., 2003). Interesantemente, esta distribución de auxinas claramente se modifica en respuesta al tratamiento con L-Glu. En las plantas de tipo silvestre el L-Glu causa una alteración en la distribución de auxinas en los tejidos provasculares y en la columela, así como una respuesta diferencial en la que la señal se detecta en un sólo costado de la capa lateral de la raíz. El patrón asimétrico de auxinas como el que encontramos en nuestros resultados que se acumulan en un sólo costado de la capa lateral de la raíz, es típico de plantas graviestimuladas (Paciorek *et al*., 2005). Por su parte, en la mutante *mpk6* los tratamientos con L-Glu solamente muestra cambios sutiles en la distribución de auxinas en la columela y en la capa lateral de la raíz, mientras que en la mutante *mkp1* bajo tratamiento con L-Glu, la distribución auxínica únicamente se localiza en una región muy limitada en las células provasculares vecinas al centro quiescente y está ausente en las células de la columela (Figura 18). Previamente se describió que la distribución de auxinas a 2 días de tratamiento con L-Glu no cambia, sin embargo, la intensidad de fluorescencia de la línea DR5::GFP si disminuye lo que sugiriendo que la disminución del máximo de auxinas es responsable de la inhibición de la raíz primaria (Walch-Liu et al., 2006).

Los datos presentados aquí muestran que el glutamato afecta el gravitropismo de la raíz alterando el contenido de almidón, así como la distribución de auxinas en el RAM. Ambas alteraciones dependen de la participación de la cinasa MPK6 y de la fosfatasa MKP1.

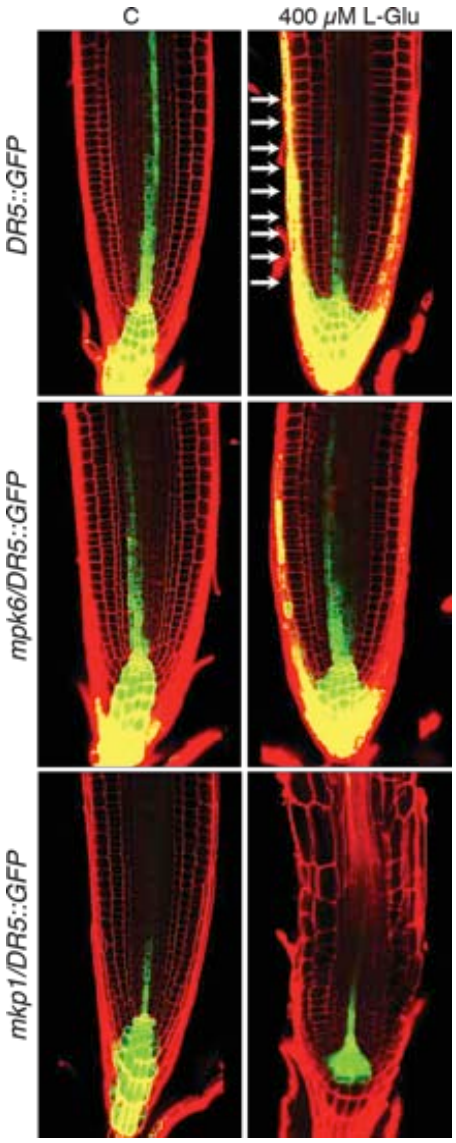

Figura 18. Señal auxínica en el RAM en respuesta a L-Glu. La línea *DR5::GFP* muestra un patrón de expresión de la GFP característico el cual se afecta en los tratamientos con 400μM de L-Glu. En la cruza mutante *mpk6 x DR5::GFP* la afección causada por el tratamiento es más sutil mientras que en la cruza de la mutante *mkp1* x *DR5::GFP*, el patrón de expresión de la GFP se ve severamente afectado por el tratamiento. n=10.

Particularmente la alteración en la distribución de auxinas en respuesta a los tratamientos de glutamato podría ser una consecuencia del efecto de este aminoácido en la expresión y/o localización de los transportadores de auxinas PIN1, PIN2, PIN3 y PIN7, mediada por la acción de la cinasa MPK6 y la fosfatasa

MKP1. Actualmente, esta posibilidad está siendo explorada haciendo uso de líneas reporteras *PIN1::PIN1:GFP* y *PIN2::PIN2:GFP* en los fondos mutantes *mpk6* y *mkp1*.

V.7. El glutamato regula la actividad de la MPK6

Está reportado que el glutamato induce la entrada de calcio al interior de la célula a través de receptores tipo iGluR causando la activación de las cinasas MPK3 y MPK6 (Kwaaitaal *et al*., 2011). Los resultados mostrados en la Figura 19A corroboran la activación de ambas cinasas en respuesta a glutamato. Sin embargo, es importante destacar que la activación de la MPK3 no se requiere para regular el desarrollo de la raíz primaria, ya que la mutante nula correspondiente (*mpk3*), se comporta igual que plantas tipo silvestre en cuanto a la inhibición del crecimiento de la raíz primaria que causa el L-Glu (Figura 20A-C).

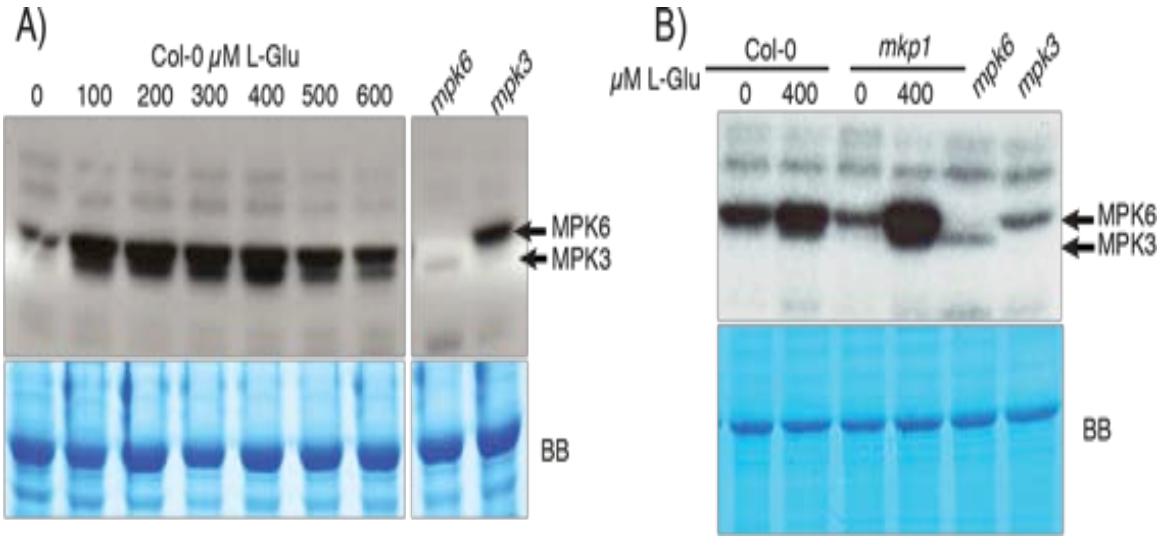

Figura 19. Efecto del L-Glu sobre la actividad de MPK6. Los ensayos de fosforilación *in vitro* muestran la actividad de las cinasas MPK6 y de MPK3, la cual se ve inducida en distintas concentraciones de L-Glu en plantas de tipo silvestre (Col-0), esta actividad esta ausente en las respectivas mutantes *mpk6* y *mpk3* (A). La actividad de ambas cinasas se ve más inducida en el fondo mutante *mkp1* en tratamientos de 400µM de L-Glu (B). Como control de carga se muestra el gel teñido con azul brillante (Brillant Blue/BB). Como referencia identidad de las cinasas se incluyeron ensayos de fosforilación sobre las mutantes *mpk3 y mpk6.*

Interesantemente, la actividad de MPK6 se ve más inducidad en la mutante *mkp1* (Figura 19C), apoyando la idea de que MPK6 es uno de los blancos de esta fosfatasa. Estos resultados indican que los efectos del L-Glu glutamato sobre la raíz primaria, están de alguna manera relacionados con la actividad de la MPK6 y de la MKP1.

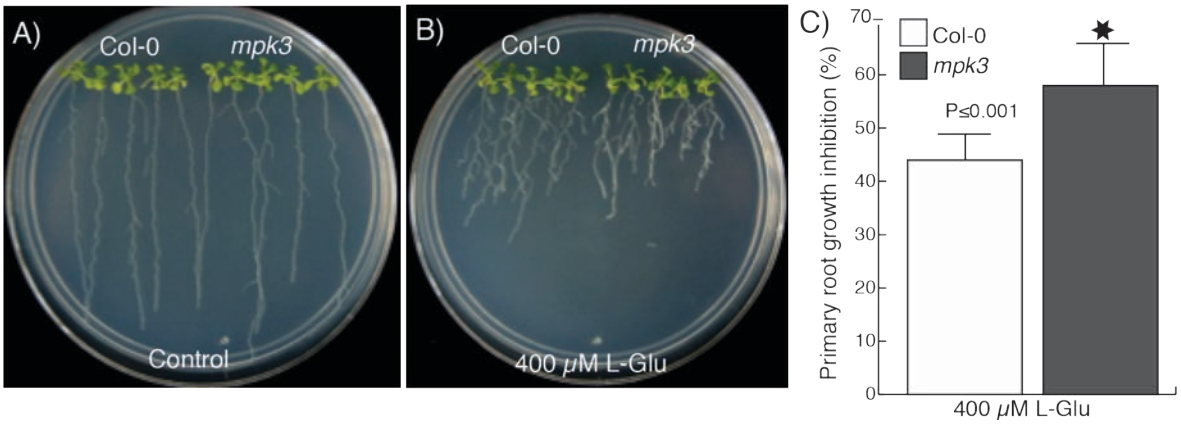

Figura 20. Respuesta de la mutante *mpk3* al L-Glu. En comparación con las plantas de tipo silvestre (Col-0) la mutante *mpk3* muestra significativamente menor inhibición del crecimiento de la raíz primaria en los tratamientos con L-Glu (A-C). Las plantas fueron germinadas y crecidas durante 10 días en medio MS 0.2X (A) o en medio MS 0.2X suplementado con 400μM de L-Glu (B). En la gráfica se muestra al porcentaje de inhibición del crecimiento de la raíz primaria de las plántulas indicadas en 400μM de L-Glu (C). Las barras representan el error estándar de una n=24 plantas.

Con los resultados de los análisis sobre la participación de la cinasa MPK6 y la fosfatasa MKP1 en la vía de señalización de respuesta a glutamato se escribió el siguiente reporte que fue sometido para su publicación en *Plant Journal*:

López-Bucio JS, Lopez-Bucio J, Raya-González J, Ramos-Vega M, León P, Guevara-García AA. Mitogen Activated Protein Kinase 6 and MAP Kinase Phosphatase 1 mediate *Arabidopsis* root responses to glutamate.

Con el cual se cumple el tercer objetivo de este trabajo y se concluye que:

1) El L-Glu regula el desarrollo de la raíz primaria de *A. thaliana* a través de la acción de la cinasa MPK6 y de la fosfatasa MKP1.

2) El L-Glu regula la respuesta gravitrópica afectando el contenido de almidón y la distribución de auxinas del RAM, mediante un proceso en el que participan la cinasa MPK6 y la fosfatasa MKP1.

V.8. Una vía de señalización conformada por RLK/SSP1, MPKKK4/YDA, MPKK5, y MPK6 parece estar involucrada en la regulación del desarrollo del embrión de *A. thaliana*.

Con respecto al cuarto objetivo de esté trabajo, enfocado a identificar posibles componentes de un módulo de MAPK (MPKKK y MPKK) y de receptores con actividad de cinasa (RLK, por "Receptor-Like Kinase"), que potencialmente pudieran estar actuando de manera coordinada con MPK6 para controlar el desarrollo del embrión/semilla de *A. thaliana*, utilizando como criterio de escrutinio los fenotipos de semilla de la mutante *mpk6,* se encontró que los genes *SSP1* (RLK), *YDA* (MPKKK) y *MPKK5*, produce fenotipos de similares a los mostrados por la mutante *mpk6* (Figura 21). El escrutinio consistió en el análisis fenotípico de mutantes para cinco MPKKKs, nueve MPKKs y ocho RLKs obtenidas del banco de TAIR (The *Arabidopsis* Information Resource). Interesantemente, previamente se reportó que un módulo de MAPKs compuesto por YDA (MPKKK4), MPKK5/MPKK9 y MPK3/MPK6, regula el desarrollo de los estomas y de las inflorescencias en *A. thaliana* (Lampard *et al*., 2009; Meng *et al*., 2012). Así, los resultados aquí presentados obtenidos con una estrategia experimental diferente, confirman que las MAPKs MPKKK4/MPKK5/MPK6 conforman un módulo de señalización aparentemente implicado en la regulación de los programas de desarrollo de estomas y del embrión. En el caso del embrión/semilla dicho módulo podría ser activado por el receptor tipo cinasa SSP1.

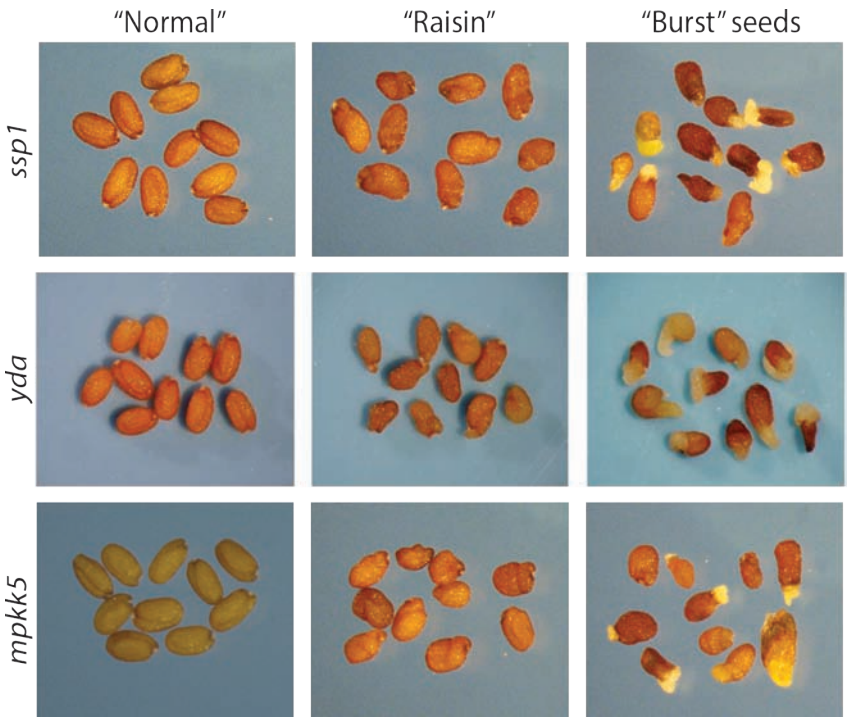

Figura 21. Mutantes con fenotipos de semillas similares a la mutante *mpk6*. Mutantes en un receptor de tipo cinasa (*ssp1*), en una MPKKK (*yda*/MPKKK4) y en una MPKK (*mpkk5*) muestran los fenotipos de semillas normales, deformes y explotados quecaracterizan a la mutante *mpk6*.

La complementación fenotípica de las mutantes referidas con una versión constitutivamente activa de la enzima MPK6 ($MPK6_{CA}$), que está en curso, pretende demostrar de manera inequívoca la participación de estas proteínas en el mismo módulo de señalización. De tal manera, los datos de nuestro y otros grupos de investigación, muestran que no obstante la diversidad de MAPKs y las numerosas combinaciones potenciales con que se puede conformar un módulo de señalización, aquel compuesto por MPKKK4, MPKK5 y MPK6, parece funcionar para distintos programas de desarrollo operando en diferentes tejidos vegetales.

VI. PERSPECTIVAS

Las principales perspectivas de este trabajo son:

1) Determinar los componentes del módulo de MAPKs que opera para regular el desarrollo del sistema radical en respuesta a L-Glu. En el entendido de que MPKKK1 y MPK6, están corroboradas para participar en esta vía de señalización, el componente faltante del módulo podría identificarse a través del análisis de las respuestas al glutamato de las mutantes para las MPKKs que disponemos.

2) Verificar la funcionalidad del módulo MPKKK4/MPKK5/MPK6 en la regulación del programa de desarrollo del embrión, mediante la complementación fenotípica ya referida.

3) Buscar blancos potenciales de este módulo mediante la estrategia de secuenciación masiva RNAseq sobre los fondos mutantes de los genes candidatos.

4) Caracterizar la participación de la cinasa MPK6 en los procesos de desarrollo de las raíces laterales y de los pelos radicales. Inicialmente a través de una caracterización fenotípica detallada de la mutante a estos respectos y complementada con estrategias bioquímicas, genéticas y moleculares, como las utilizadas a lo largo de este trabajo para el estudio de la participación de esta cinasa en el programa de desarrollo de la raíz primaria.

VII. COLABORACIONES

De manera paralela al desarrollo de este trabajo, se participó haciendo trabajo experimental para otros proyectos del grupo y de otros grupos de investigación. Estas colaboraciones resultaron en la publicación de los tres artículos internacionales referidos a continuación:

1) De Luna-Valdez LA, Martínez-Batallar AG, Hernández-Ortiz M, Encarnación-Guevara S, Ramos-Vega M, **López-Bucio JS**, León P, Guevara-García AA (2014). Proteomic analysis of chloroplast biogenesis (clb) mutants uncovers novel proteins potentially involved in the development of *Arabidopsis thaliana* chloroplast. *Journal of Proteomics* 111:148-164. **APÉNDICE 1**.

2) Contreras-Cornejo HA, **López-Bucio JS**, Mendez-Bravo A, Macias-Rodriguez L, Ramos-Vega M, Guevara-García AA, Lopez-Bucio J (2015). Mitogen-Activated Protein Kinase 6 and ethylene and auxin signaling pathways are involved in *Arabidopsis* root-system architecture alterations by *Trichoderma atroviride***.** *Molecular Plant-Microbe Interactions* 28:701-710. **APÉNDICE 1**.

3) López-García CM, Raya-González J, **López-Bucio JS**, Guevara-García AA, López-Bucio J. ALTERED MERISTEM PROGRAM 1 is involved in seed coat, root hair and trichome development in *Arabidopsis*. *Journal of Plant Growth Regulation* **(Aceptado-APÉNDICE 1).**

Adicionalmente se colaboró en la escritura de los dos siguientes capítulos de libros internacionales:

1) Contreras-Cornejo HA, Macias-Rodriguez L, Lopez-Bucio JS, Lopez-Bucio J, (2014). Enhanced Plant Immunity Using Trichoderma en: Maria Tuohy Biotechnology and Biology of Trichoderma. Vijai G. Gupta. Elsevier. p. 495-504.

2) Macias-Rodriguez L, Contreras-Cornejo HA, Lopez-Bucio JS, Lopez-Bucio J, (2015). Recent advancements in the role of volatile organic compounds from fungi en: Sreenivasaprasad S. Fungal Biomolecules: Sources, Applications and Recent Developments. Chichester. Wiley. p. 87-99.

VIII. MATERIALES Y MÉTODOS

Como material vegetal se utilizó *Arabidopsis thaliana* del ecotipo Columbia-0 como parental silvestre y líneas mutantes por inserción de T-DNA para los genes MPK6/SALK_127507, MPK3/SALK_151594, SSP1/CS16376, *MPKKK4/SALK_053981, MPKK5/CS874712, así como la línea reportera DR5*::GFP (Ottenschläger *et al*., 2003), que fue introducida en los fondos mutantes *mpk6* y *mkp1* mediante cruzas dirigidas.

Para su siembra en placas de cultivo, las semillas fueron esterilizadas con una solución de hipoclorito de sodio comercial (cloralex) al 20%, seguido de 3 enjuagues con agua destilada estéril. Las semillas esterilizadas fueron conservadas en agua y sometidas a un tratamiento de estratificación durante 3 días a 4^0 C. Las semillas fueron sembradas en placas de Petri con medio MS 0.2X y 1% de sacarosa solidificado con agar bacteriológico (Caisson, Laboratories, North Logan, UT, USA) como medio control o suplementadas con las concentraciones de L-Glutamato indicadas como tratamiento. Para el crecimiento de plántulas las placas se incubaron en una cámara de crecimiento a una temperatura de 21^0C y un fotoperiodo de 16/8 horas de luz/oscuridad bajo una intensidad de luz a 105 µmol $m^{-2}s^{-1}$. Las sales de MS, la sacarosa y el L-Glutamato, fueron adquiridos de Sigma (Sigma-Aldrich, St Louis, MO, USA).

VIII.1. Análisis del desarrollo del embrión y de la forma de la semilla

Tanto semillas de plantas de tipo Silvestre como de la mutante *mpk6* fueron disectadas de silicuas de diferente edad y se fijaron en una solucion de 50% metanol y 10% ácido acético durante 2 días, posteriormente con la ayuda de agujas de insulina los embriones se disectaron de la testa de la semilla y se aclararon (Solución de aclarado I) durante un día, después de su aclarado, los embriones se tiñeron con yoduro de propidio y se montaron en portaobjetos para su analisis por microscopia confocal (Ugartechea-Chirino *et al*., 2010).

Las semillas fueron identificadas y separadas como Normales, deformes y explotadas, las fotos de estos fenotipos fueron capturadas en un microscopio estereoscopico Nikon SMZ1500 equipado con una camara digital SIGHT DS-File.

VIII.2. Analisis del crecimiento

La longitud de la raíz primaria fue determinado con la ayuda de una regla a diferentes días de edad, la densidad de las raíces laterales fue calculada dividiendo el número total de raicés laterales entre la longitud (cm) de la zona de formación de raices laterals, las imagines representativas fueron capturadas con una camara digital EOS REBEL XSi. La longitud del RAM, de los dominios de proliferación y de transición, de las células corticales completamente alargadas así como el número de células en el dominio de proliferación fueron determinados en un microscopio optico Zeiss Axiovert 200M con la ayuda de un micrometro de objetivo a partir de plantas de 5 y 8 días después de germinar que fueron aclaradas (Solución de aclarado II) y montadas en portaobjetos (Dubrovsky *et al.,* 2009). La tasa de producción celular (CPR) fue calculada con la formula $CPR=V/_{e}^{-1}$ el la cual V=crecimiento de la raíz primaria (µm h^{-1}) durante 24 horas y l_e es la longitud (µm) de las celulas corticales completamente alargadas. La densidad de los pelos radicales fue calculada dividiendo el número total de pelos radicales por milimetro, la longitud de los pelos radicales fue determinada un microscopio optico Zeiss Axiovert 200M con la ayuda de un micrometro de objetivo. Los análisis de respuesta gravitropica fueron determinados creciendo plantas durante 5 días en pocisión vertical, posteriormente fueron tranferidas a placas con medio MS 0.2X fresco y a placas con medio MS 0.2X suplementado con 400µM de L-Glu y se dejaron en posición vertical durante 3 días para después inducir la respuesta gravitropica girando las placas 90^0 en contra de las manecillas del reloj, la respuesta al gravitropismo se determinó midiendo el ángulo formado por las raíces de las plantas.

VIII.3. Tinción de los amiloplastos

Para determinar el contenido de almidón de la raíz primaria, las plantas se fijaron con paraformaldehído al 5% durante 24 horas y posteriormente se tiñeron con solución de lugol (Yodo 0.5%, yoduro de potasio 1% en agua destilada), se enjuagaron con agua destilada, se montaron en un portaobjetos y se analizaron en un microscopio óptico Nikon Eclipse E600 equipado con una cámara digital SIGHT DS-File, con la que se tomaron registros fotográficos de plántulas representativas.

VIII.4. Análisis confocal de proteínas fluorescentes

Para el análisis de microscopía confocal de las raíces, las plantas fueron transferidas del medio de crecimiento a una solución de yoduro de propidio durante un minuto, posteriormente fueron montadas con agua destilada en un portaobjetos para su posterior análisis en un microscopio confocal Olympus FV1000. Para las imágenes de yoduro de propidio se utilizó iluminación de 568/610 nm de energías de exitación/emisión, mientras que las energías de exitación/emisión, para observar a la proteína verde fluorescente, fueron de 488/523 nm, respectivamente. La imagen final fue construida en el programa ImageJ (National Institutes of Health, USA).

VIII.5. Ensayo de fosforilación *in vitro*

Los ensayos de fosforilación *in vitro* se utilizaron para determinar la actividad de la MPK6, para esto, se preparó un gel de poliacrilamida al 10% de condiciones desnaturalizantes al cual se le añadió 250 µg/mL de la proteína Mielina Básica Bovina la cual es un sustrato de fosforialción de la MPK6. En este gel, se fraccionaron extractos proteicos de plantas de *Arabidopsis* tratadas con diferentes concentraciones de L-Glu, al finalizar la corrida, el gel se sometió a incubaciones de 3 horas en un buffer de renaturalización (Tris HCL 25 mM pH 7.5, DTT 1 mM,

Na3VO4 0.1mM, NaF 5mM en agua destilada) para posteriormente incubarse durante 2 horas en un buffer de reacción (Tris HCL 25 mM pH 7.5, EGTA 2mM, MgCl2 0.12 mM, DTT 1 mM, Na3VO4 0.1mM, ATP 200 nM, γ-ATP^{32}P 50 µCi en agua destilada) el cual contiene ATP frio y ATP radiactivo (γ-ATP^{32}P) como donadores de grupo fosfato, el ATP no incorporado se elimina mediante lavados sucesivos con buffer de lavado (5% de acido tricloroacetico y 1% de pirofosfato de sodio en agua destilada). Posteriormente el gel se seca a 120^{0} C con vacío y se utiliza para exponer películas radiográficas para finalmente revelar la señal de autorradiografía evidenciada por la aparición de bandas las cuales servirán para el análisis de los resultados.

IX. BIBLIOGRAFÍA CITADA

Abas L, Benjamins R, Malenica N, Paciorek T, Wisniewska J, Moulinier-AnzolaJC, Sieberer T, Friml J, Luschnig C (2006). Intracellular trafficking and proteolysis of the *Arabidopsis* auxin-efflux facilitator PIN2 are involved in root gravitropism**.** *Nature Cell Biology* 8:249-256.

Aida M, Beis D, Heidstra R, Willemsen V, Blilou I, Galinha C, Nussaume L, Noh YS, Amasino R, Scheres B (2004). The *PLETHORA* genes mediate patterning of the *Arabidopsis* root stem cell niche. Cell 119:109-120.

Aloni R, Aloni E, Langhans M, Ullrich C (2006). Role of cytokinin and auxin in shaping root architecture: regulating vascular differentiation, lateral root initiation, root apical dominance and root gravitropism. *Annals of Botany* 97:883-893.

Alberts B, Johnson A, Lewis J, Raff M, Roberts K, Walker P (2008). Mechanisms of cell comunication in “Molecular Biology of the Cell” 5th edition, San Francisco CA *Garland Science*.

Andreason E, Ellis B (2010). Convergence and specificity in the *Arabidopsis* MAPK nexus. *Trends in Plant Science* 15:106-113.

Asai T, Tena G, Plotnikova J, Wilmann MR, Chiu WL, Gomez-Gomez L, Boller T, Ausubel FM, Sheen J (2002). MAP kinase signaling cascade in *Arabidopsis* innate immunity. *Nature* 415 28 february 2002.

Badu y, Musielak T, Henschen A, Bayer M (2013). Suspensor length determines developmental progression of the embryo in *Arabidopsis*. *Plant Physiology* 162:1448-1458.

Baldwin K, Strohm AK, Masson PH (2013). Gravity sensing and siganling transduction in vascular plant primary roots. *American Journal of Botany* 100:126-142.

Ballhorn DJ, Kautz S, Heil M, Hegeman AD (2009). Analyzing plant defenses in nature. *Plant Signaling & Behavior* 4:743-745.

Band LR, Wells DM, Larrieu A, Sun J, Middleton AM, French AP, Brunoud G, Mendocilla Sato E, Wilson MH, Péret B, Oliva M, Swarup R, Sairanen I, Parry G, Ljung K, Beekman T, Garibaldi JM, Stelle M, Owen MR, Vissenberg K, Hodgman C, Pridmore TP, King JR, Vemoux T, Bennett MJ (2012). Root gravitropism is regulated by a transient lateral auxin gradient controlled by a tipping-point mechanism. *Proceedings of the National Academy of Sciences* 109:4668-4673.

Barteles S, González Besteiro MA, Lang D, Ulm R (2010). Emerging functions for plant MAP kinase phosphatases. *Trends in Plant Science* 15:322-329.

Baum SF, Rost TL (1996). Root apical organization in *Arabidopsis thaliana*. I. Root cap and protoderm. *Protoplasma* 192:178-188.

Bayer M, Nawy T, Giglione C, Galli M, Meinnel T, Lukowitz W (2009). Paternal control of embryonic patterning in *Arabidopsis thaliana*. *Science* 323:1485

Benková E, Michniewicz M, Sauer M, Teichmann T, Seifertová D, Jürgens G, Friml J (2003). Local, efflux-dependent auxin gradients as a common module for plant organ formation. *Cell* 115:591-602.

Benková E, Bielach A (2010). Lateral root organogénesis: from cell to organ. *Current Opinion in Plant Biology* 13:1-7.

Berger F, Hung CY, Dolan L, Schiefelbein J (1998). Control of cell division in the root epidermis of *Arabidopsis thaliana*. *Developmental Biology* 194:235-245.

Bewley JD (1997). Seed germination and dormancy. *The Plant Cell* 9:1055-1066.

Bibikova TN, Jacob T, Dashe I, Gilroy S (1998). Localized changes in apoplastic and cytoplasmic pH are associated with root hair development in *Arabidopsis thaliana*. *Development* 125:2925-2934.

Blancaflor EB, Fasano JM, Gilroy S (1998). Mapping the functional roles of cap cells in the response of *Arabidopsis* primary roots to gravity. *Plant Physiology* 116:213-222.

Bowman J (1994). Vegetative development in "*Arabidopsis:* An Atlas of Morphology and Development" 1st edition, New York, E.U.A. Editorial Springer-Verlag.

Breuninger H, Rikirsch E, Hermann M, Ueda M, Laux T (2008). Differential expression of WOX genes mediates apical-basal axis formation in the *Arabidopsis* embryo. *Developmental Cell* 14:867-876.

Brunoud G, Wells DM, Oliva M, Larrieu A, Mirabet V, Burrow AH, Beeckman T, Kepinski S, Traas J, Bennett MJ, Vernoux T (2012). A novel sensor to map auxin response and distribution at high spatio-temporal resolution. *Nature* 482:103-106.

Bush SM, Krysan PJ (2007). Mutational evidence that the *Arabidopsis* MAP kinase MPK6 is involved in anter, inflorescence, and embryo development. *Journal of Experimental Botany* 58:2181-2191.

Calderini O, Bogre L, Vicente O, Binarova P, Heberle-Bors E, Wilson C (1998). A cell cycle regulated MAPK kinase wuth a possible role in cytokinesis in tobacco cells. *Jornal of Cell Science* 111:3091-3100.

Capron A, Chatfield S, Provart N, Berleth T (2009). Embryogenesis: Pattern formation from a single cell. *The Arabidopsis Book* doi:10.1199/tab.0051.

Cárdenas L (2009). New findings in the machanisms regulating polar growth in root hair cells. *Plant Signaling & Behavior* 4:1, 4-8.

Casimiro I, Marchant A, Bhalerao RP, Beeckman T, Dhooge S, Swarup R, Graham N, Inzé D, Sandberg G, Casero PJ, Bennett M (2001). Auxin transport promotes *Arabidopsis* lateral root initiation. *The Plant Cell* 13:843-852.

Cho HT, Cosgrove DJ (2002). Regulation of root hair initiation and expansin gene expression in *Arabidopsis*. *The Plant Cell* 14:3237-3253.

Cho SK, Larue CT, Chevalier D, Wang H, Jinn TL, Zhang S, Walker JC (2008). Regulation of floral organ abscision in *Arabidopsis thaliana. Proceedings of the National Academy of Sciences* 105:15629-15634.

De la Fuente van Bentem S, Hirt H (2007). Using phosphoproteomics to reveal signalling dynamics in plants. *Trends in Plant Science* 12:1360-1385.

De Smet I, Tetsumura T, De Rybel B, Frei dit Frey N, Laplaze L, Casimiro I, Swarup R, Naudts M, Vanneste S, Audenaert D, Inzé D, Bennett MJ, Beckman T (2007). Auxin-dependent regulation of lateral root positioning in the basal meristem of *Arabidopsis. Development* 134:681-690.

De Smet I, Vassileva V, De Rybel B, Levesque MP, Grunewald W, van Damme D, van Noorden G, Naudts M, van Isterdael G, de Clercq R, Wang JY, Meuli N,

Vanneste S, Friml J, Hilson P, Jürges G, Ingram GC, Inzé D, Benfey PN, Beeckman T (2008). Receptor-like kinase ACR4 restricts formative cell divisions in the *Arabidopsis* root. *Science* 322:594-597.

Dello Ioio R, Scaglia Linhares F, Scacchi E, Casamitjana-Martinez E, Heidstra R, Costantino P, Sabatini S (2007). Cytokinins determine *Arabidopsis* root-meristem size by controlling cell differentiation. *Current Biology* 17:678-682.

Dekkers BJW, Pearce S, van Bolderen-Veldkamp RP, Marshall A, Widera P, Gilbert J, Drost HG, Bassel GW, Müller K, King JR, et al. (2013). Transcriptional dynamics of two seed compartments with opposing roles in *Arabidopsis* seed germination. *Plant Physiology* 163:205-215.

Dolan L, Janmaat K, Willemsen V, Linstead P, Poethig S, Roberts K, Scheres B (1993). Cellular organization of the *Arabidopsis thaliana* root. *Development* 119:71-84.

Dubrovsky JG, Sauer M, Napsucialy-Mendivil S, Ivanchenko MG, Friml J, Shishkova S, Celenza J, Benková E (2008). Auxin acts as a local morphogenetic trigger to specify lateral root founder cells. *Proceedings of the National Academy of Sciences* 105:8790-8794.

Feilner T, Hultschig C, Lee Justin, Meyer S, Immink RGH, Koenig A, Possling A, Seitz H, Beveridge A, Scheel D, Cahill DJ, Lehrach H, Kreutzberger J, Kersten B (2005). High throughput identification of potential *Arabidopsis* mitogen-activated protein kinases substrates. *Molecular & Cellular Proteomics* 4:1558-1568.

Figueiredo DD, Köhler C (2014). Signalling events regulating seed coat development. *Biochemical Society Transactions* 42:358-363.

Finkelstein R, Reeves W, Ariizumi T, Steber C (2008). Molecular aspects of seed dormancy. *Annual Review of Plant Biology* 59:387-415.

Friml J, Vieten A, Sauer M, Weijers D, Schuwarz H, Hamann T, Offringa R, Jüergens G (2003). Efflux-dependent auxin gradient establish the apical-basal axis of *Arabidopsis*. *Nature* 426:147-153.

Forde BG, Cutler SR, Zaman N, Krysan P (2013). Glutamate signalling via a MEKK1 kinase-dependent pathway induces changes in *Arabidopsis* root architecture. *The Plant Journal* 75:1-10.

Foreman J, Demidchik V, Bothwell JH, Mylona P, Miedema H, Torres MA, Linstead P, Costa S, Brownlee C, Jones JD, Davies JM, Dolan L (2003). Reactive oxygen species produced by NADPH oxidase regulate plant cell growth. *Nature* 422:442-446.

Graeber K, Nakabayashi K, Miatton E, Leubner-Metzger G, Soppe WJJ (2012). Molecular mechanisms of seed dormancy. *Plant Cell and Environment* 35:1769-1786.

Grieneisen VA, Xu J, Marée AFM, Hogeweg P, Scheres B (2007). Auxin transport is sufficient to generate a maximum and gradient guiding root growth. *Nature* 449:1008-1013.

Gruber BD, Giehl RFH, Friedel S, von Wirén N (2013). Plasticity of the *Arabidopsis* root system under nutrient deficiences. *Plant Physiology* 163:161-179.

Gupta R, Huang Y, Kieber J, Luan S (1998). Identification of a dual-specificity protein phosphatase that inactivates a MAP kinase from *Arabidopsis*. *The Plant Journal* 16:581-589.

Haecker A, Groß-Hart R, Geiges B, Sarkar A, Breuninger H, Herrmann M, Laux T (2004). Expression dynamics of *WOX* genes mark cell fate decisions during early embryonic patterning in *Arabidopsis thaliana*. *Development* 131:657-668.

Hamel LP, Nicole MC, Sritubtim S, Morency MJ, Ellis M, Ehlting J, Beaudoin N, Barbazuk B, Klessig D, Lee J, Martin G, Mundy J, Ohashi Y, Scheel D, Sheen J, Xing T, Zhang S, Seguin A, Ellis B (2006). Ancient signals: comparative genomics of plant MAPK and MAPKK gene families. *Trends in Plant Science* 11:192-198.

Hasenstein KH, Evans ML (1988). The effect of cations on hormone transport in primary roots of *Zea mays*. *Plant Physiology* 86:890-894.

Hehenberger E, Kradolfer D, Köhler C (2012). Endosperm cellularization defines an important developmental transition formembryo development. *Development* 139:2031-2039.

Hofer RM (1991). Root hairs in “Plant roots the hidden half” 4th eddition. Boca raton, FL Taylor and Francis group.

Hyeong CP, Eun HS, Xuan CN, Kyunghee L, Kyung EK, Ho SK, Sang ML, Sun HK, Dong WB, Dae-Jin Y, Woo SC (2011). *Arabidopsis* MAP kinase phosphatase 1 is phosphorylated and activated by its substrate AtMPK6. *Plant Cell Reports* 30:1523-1531.

Ishikawa H, Evans ML (1990). Stimulation of root growth by mechanical impedance is independent of the root cap. *American Society for Gravitational and Space Research* 4 (Abstract No. N-14):105.

Ishikawa H, Evans ML (1992). Induction of curvature in maize roots by calcium or by thigmostimulation: role of the postmitotic isodiametric growth zone. *Plant Physiology* 100:762-768.

Jeong S, Bayer M, Lukowitz W (2010). Taking the very first steps: from polarity to axial domains in the early *Arabidopsis* embryo. *Journal of Experimental Botany* 62:1687-1697.

Jiang K, Feldman LJ (2005). Regulation of root apical meristem development. *Annual Review of Cell and Developmental Biology* 21:485-509.

Jonak C, Páy A, Bögre L, Hirt H, Heberle-Bors E (1993). The plant homologue of MAP kinase is expressed in a cell cycle-dependent and organ-specific manner. *The Plant Journal* 3:611-617.

Jonak C, Ökrés L, Bögre L, Hirt H (2002). Complexity, croos talk and integration of plant MAP kinase signaling. *Current Opinion in Plant Biology* 5:415-424.

Jürgens G (2001). Apical-basal pattern formation in *Arabidopsis* embryogenesis. *The EMBO Journal* 20:3609-3616.

Kiss JZ, Hertel R, Sack FD (1989). Amyloplasts are necessary for full gravitropic sensitivity in roots of *Arabidopsis thaliana*. *Planta* 177:198-206.

Kleine-Vehn J, Ding Z, Jones AR, tasaka M, Morita MT, Friml J (2010). Gravity-induced PIN transcytosis for polarization of auxin fluxes in gravity sensing root cells. *Proceedings of the National Academy of Sciences* 107:22344-22349.

Klipp E, Liebermeister W (2006). Mathematical modeling of intracelular signaling pathways. *BMC Neuroscience* 7:S10.

Kovtun Y, Chiu WL, Tena G, Sheen J (2000). Functional analysis of oxidative stress-activated mitogen-activated protein kinase cascade in plants. *Proceedings of the National Academy of Sciences* 97:6.

Kohoutová L, Kourová H, Nagy SK, Volc J, Halada P, Mészáros T, Meskiene I. Bögre L, Binarová P (2015). The *Arabidopsis* mitogen-activated protein kinase 6 is associated with γ-tubulin on microtubules, phosphorylates EB1c and maintains spindle orientation under nitrosative stress. *New Phytologist* 207:1061-1074.

Kwaaitaal M, Huisman R Maintz J, Reinstädler A, Panstruga R (2011). Ionotropic glutamate receptor (iGluR)-like channels mediate MAMP-induced calcium influx in *Arabidopsis thaliana*. *Biochemical Journal* 440:355-365.

Lau S, Slane D, Herud O, Kong J, Jürgens G (2012). Early embryogenesis in flowering plants: setting up the basic body pattern. *Annual Review of Plant Biology* 63:483-506.

Lampard GR, Lukowitz W, Ellis BE, Bergmann D (2009). Novel and expanded roles for MAPK signaling in *Arabidopsis* stomatal cell fate revealed by cell type-specific manipulations. *The Plant Cell* 21:3506-3517.

Lee JS, Ellis B (2007). *Arabidopsis* MAPK phosphatase 2 (MKP2) positively regulates oxidative stress tolerance and inactivates the MPK3 and MPK6 MAPKs. *Journal of Biological Chemistry* 282:25020-25029.

Lee JS, Wang S, Sritubtim S, Chen JG, Ellis B (2009). *Arabidopsis* mitogen-activated protein kinase MPK12 interacts whit the MAPK phosphatase IBR5 and regulates auxin signaling. *The Plant Journal* 57:975-985.

Lee Y, Lee W, Kim SH (2012). Hormonal regulation of stem cell maintenance in roots. *Journal of Experimental Botany* 64:1153-1165.

Lehti-Shiu MD, Shiu SH (2012). Diversity, classification and function of plant protein kinase superfamily. *Philosophical Transactions of the Royal Society* 367:2619-2639.

Libault M, Brechenmacher L, Cheng J, Xu D, Stacey G (2010). Root hair systems biology. *Trends in Plant Science* 15:641-650.

López-Bucio J, Cruz-Ramírez A, Herrera-Estrella L (2003). The role of nutrient availability in regulating root architecture. *Current Opinion in Plant Biology* 6:280-287.

López-Bucio J, Ortíz-Castro R, Ruíz-Herrera LF, Juárez CV, Hernández-Madrigal F, Carreón-Abud Y, Martínez-Trujillo M (2015). Chromate induces adventitious root formation via auxin signaling and SOLITARY-ROOT/IAA14 gene function in *Arabidopsis thaliana*. *Biometals* 28:353-365.

López-Bucio JS, Dubrovsky JG, Raya-González J, Ugartechea-Chirino Y, López-Bucio J, de Luna-Valdez LA, Ramos-Vega M, León P, Guevara García AA (2014). *Arabidopsis thaliana* mitogen-activated protein kinase 6 is involved in seed fromation and modulation of primary and lateral root developement. *Journal of Experimental Botany* 65:169-183.

Lukowitz W, Roeder A, Parmenter D, Somerville C (2004). A MAPKK kinase gene regulates extra embryonic cell fate in *Arabidopsis*. *Cell* 116:109-119.

MacGregor DR, Deak KI, Ingram PA, Malamy JE (2008). Root system architecture in *Arabidopsis* grown in culture is regulated by sucrose uptake in the aerial tissues. *The Plant Cell* 20:2643-2660.

Malamy JE, Benfey PN (1997). Organization and cell differentiation in lateral roots of *Arabidopsis thaliana*. *Development* 124:33-44.

MAPK Group (2002). Mitogen-activated protein kinase cascades in plants: a new nomenclature. *Trends in Plant Science* 7:301-308.

Marin E, Jouannet V, Hertz A, Lokerse AS, Weijers D, Vaucheret H, Nassaume L, Crespi MD, Maizel A (2010). miR390, *Arabidopsis* TAS3 tasiRNAs, and their AUXIN RESPONSE FACTOR TARGETS define an autorregulatory network quantitatively regulating lateral root growth. *The Plant Cell* 22:1104-1117.

Mayerowitz EM (1989). *Arabidopsis*, a useful weed. *Cell* 56:263-269.

Mendocilla Sato E, Hijazi H, Bennett MJ, Vissenberg K, Swarup R (2014). New insights into root gravitropic signalling. *Journal of Experimental Botany* 53:333-340.

Meng X, Wang H, He Y, Liu Y, Walker JC, Torii KU, Zhang S (2012). A MAPK cascade downtream of ERECTA receptor-like protein kinase regulates *Arabidopsis* inflorescence architecture by promoting localized cell proliferation. *The Plant Cell* 24:4948-4960.

Mishra NS, Tuteja R, Tuteja N (2006). Signaling through MAP kinase networks in plants. *Archives of Biochemistry and Biophysics* 452:55-68.

Monshausen GB, Bibikova TN, Masserli MA, Shi C, Gilroy S (2007). Oscillations in extracellular pH and reactive oxygen species modulate tip growth of *Arabidopsis* root hairs. *Proceedings of the National Academy of Sciences* 104: 20996-21001.

Müller B, Sheen J (2008). Cytokinin and auxin interaction in root stem-cell specification during early embryogenesis. *Nature* 453:1094-1097.

Müller J, Beck M, Mettbach U, Komis G, Hause G, Menzel D, Samaj J (2009). *Arabidopsis* MPK6 is involved in cell division plane control during early root development, and localizes to the pre-prophase band, phragmoplast, trans-golgi network and plasma membrane. *The plant Journal*. 61:34-248.

Nakagami H, Pitzschke A, Hirt H (2005). Emerging MAP kinase pathways in plant stress signaling. *Trends in Plant Science* 10:339-346.

Okada K, Shimura Y (1990). Reversible root tip rotation in *Arabidopsis* seedlings induced by obstacle-touching stimulus. *Science* 250:274-276.

Okushima Y, Fukaki H, Onoda M, Theologis A, Tasaka M (2007). ARF7 and ARF19 regulate lateral root formation via direct activation of *LBD/ASL* genes in *Arabidopsis*. *The Plant Cell* 19:118-130.

Osakabe Y, Yamaguchi-Shinozaki K, Shinozaki K, Phan Tran LS (2013). Sensing the environment: key roles of membrane-localized kinases in plant perception and response to abiotic stress. *Journal of Experimental Botany* 64:445-458.

Ortíz–Castro R, Martíneaz-Trujillo M, López-Bucio J (2008). N-acyl-L-homoserine lactone: a class of bacterial quorum-sensing signals alter post-embryonic root development in *Arabidopsis thaliana*. *Plant Cell and Environment* 31:1497-1509.

Ortíz-Castro R, Díaz-Pérez C, Martínez-Trujillo M, del Río RE, Campos-García J, López-Bucio J (2011). Transkingdom signaling base don bacterial cyclodipeptides with auxin activity in plants. *Proceedings of National Academy of Sciences* 108:7253-7258.

Ottenschläger I, Wolff P, Wolverton C, Bhalerao RP, Sandberg G, Ishikawa H Evans M, Palme K (2003). Gravity-regulated differential auxin transport from columella to lateral root cap cells. *Proceedings of National Academy of Sciences* 100:2987-2991.

Overvoorde P, Fukaki H, Beeckman T (2010). Auxin control of root development. *Cold Spring Harbor Perspectives in Biology* 2:a001537.

Paciorek T, Zazímalová E, Ruthardt N, Petrásek J, Stierhof YD, Kleine-Vehn J, Morris DA, Emans N, Jürgens G, Geldner N, Friml J (2005). Auxin inhibits endocitosis and promotes its own eflus from cells. *Nature* 435:1251-1256.

Perera IY, Hung CY, Brady S, Muday GK, Boss WF (2006). A universal role for Inositol 1,4,5-triphosphate-mediated signaling in plant gravitropism. *Plant Physiology* 140:746-760.

Péret B, de Rybel B, Casimiro I, Benková E, Swarup R, Laplaze L, Beeckman T, Bennett MJ (2009). *Arabidopsis* lateral root development: an emerging story *Trends in Plant Science* 14:7.

Petersson SV, Johansson AI, Kowalczyk M, Makoveychuk A, Wang JY, Moritz T, Grebe M, Benfey PN, Sandberg G, Ljung K (2009). An auxin gradient and maximum in the *Arabidopsis* root apex shown by high-resolution cell-specific analysis of IAA distribution and synthesis. *The plant Cell* 21:1659-1668.

Piquerez SJ, Balmuth AL, Sklenár J, Jones AME, Rathjen JP Ntoukakis V (2014). Identification of post-translational modifications of plant protein complexes. *Journal of Visualized Experiments* 84:1-10.

Pirelli S, Di Mambro R, Sabatini S (2012). Growth and development of the root apical meristem. *Current Opinion in Plant Biology* 15:17-23.

Pitts RJ, Cernac A, Estelle M (1998). Auxin and ethylene promote root hair elongation in *Arabidopsis*. *The Plant Journal* 16:553-560.

Popescu SC, Popescu GV, Bachan S, Zhang Z, Gerstein M, Snyder M, Dinesh-Kumar SP (2008). MAPK target networks in *Arabidopsis thaliana* revealed using functional protein microarrays. *Genes and Development* 23:80-92.

Reyes-Hernández JB, Srivastava AV, Ugartechea-Chirino Y, Shishkova S, Ramos-Parra PA, Lira-Ruan V, Díaz de la Garza RI, Dong G, Moon JC, Blancaflor EB, Dubrovsky JG (2014). The root indeterminacy-to-determinacy developmental switch is operated through a folate-dependent pathway in *Arabidopsis thaliana*. *New Phytologist* 202:1223-1236.

Rolland F, Baena-González E, Sheen J (2006). Sugar sensing and signaling in plants: conserved and novel mechanisms. *Annual Review in Plant Biology* 57:675-709.

Sabatini S, Heidstra R, Wildwater M, Scheres B (2002). SACRECROW is involved in positioning the stem cell niche in the *Arabidopsis* root meristem. *Genes and Development* 17:354-358.

Sack FD (1997). Plastids and gravitropic sensing. *Planta* 203:S63-S68.

Santner A, Calderon-Villalobos LIA, Stelle M (2009). Plant hormones are versatile chemical regulators of plant growth. *Nature Chemical Biology* 5:301-307.

Satbhai SB, Ristova D, Wolfgang B (2015). Underground tuning: quantitative regulating root growth. *Journal of Experimental Botany* 66:1099-1112.

Scacchi E, Salinas P, Gujas B, Santuari L, Krogan N, Ragni L, Berleth T, Hardtke CS (2010). Spatio-temporal sequence of cross-regulatory events in root

meristem growth. *Proceedings of National Academy of Sciences* 107: 22734-22739.

Scheres B, Wolkenfelt H, Willemsen V, Terlouw M, Lawson E, Dean C, Weisbeek P (1994). Embryonic origin of the *Arabidopsis* primary root and root meristem initials. *Development* 120:2475-2487.

Scheres B, and Benfey PN (1999). Asymmetric cell divisions in plants. *Annual Reviews in Plant Physiology and Plant Molecular Biology.* 50:505–537.

Schlessinger J (2000). Cell signaling by receptor tyrosine kinases. *Cell* 103:211-225.

Shiu R, Bleeker A (2001). Plant receptor-like kinase gene family: diversity, function, and signaling. *Science Signaling STKE* 2001:re22.

Sozzani R, Iyer-Pascuzzi A (2014). Postembryonic control of root meristem growth and development. *Current Opinion in Plant Biology* 17:7-12.

Shpak ED, McAbee JM, Pillitteri LJ, Torii KU (2005). Stomatal patterning and differentiation by synergistic interactions of receptor kinases. *Science* 309:290-293.

Sturgill TW, Ray LB (1986). Muscle proteins related to microtubule associated protein-2 are substrates for an insulin stimulatable kinase. *Biochemical and Biophysical Research Communications* 134:565-571.

Taj G, Agarwal P, Grant M, Kumar A (2010). MAPK machinery in plants recognition and response to different stresses through multiple signal transduction pathways. *Plant Signaling and Behavior* 5:1370-1378.

Tian H, De Smet I, Ding Z (2014). Shaping a root system: regulating lateral versus primary root growth. *Trends in Plant Science* 19:426-431.

Tominaga-Wada R, Iwata M, Sugiyama J, Kotake T, Ishida T, Yokoyama R, Nishitani K, Okada K, Wada T (2009). The GLABRA2 homeodomain protein directly regulates *CESA* and *XTH17* gene expression in *Arabidopsis* roots. *The Plant Journal* 60:564-574.

Tomokazu K, Golberg RB (2009). The suspensor: not just suspending the embryo. *Trends in Plant Science* 15:1.

Trewavas AJ, Malhó R (1997). Signal perception and transducción: the origin of the phenotype. *The Plant Cell* 9:1181-1195.

Tsugeki R, Fedoroff N (1999). Genetic ablation of root cap cells in *Arabidopsis*. *Proceedings of National Academy of Sciences* 96:12941-12946.

Tuteja N (2009). Signaling through G protein coupled receptors. *Plant Signaling and Behavior* 4: 942-947.

Ueda M, Zhang Z, Laux T (2011). Transcriptional activation of *Arabidopsis* axis patterning genes *WOX8/9* links zygote polarity to embryo development. Developmental Cell 20:264-270

Ugartechea-Chirino Y, Swarup R, Swarup K, Péret B, Whitworth M, Bennett M, Bougourd S (2010). The AUX1 LAX family of auxin influx carriers is required for the establishment of embryonic root cell organization in *Arabidopsis thaliana*. *Annals of Botany* 105:277-289.

Vincill ED, Clarin AE, Molenda JN, Spalding EP (2013). Interacting glutamate receptor-like proteins in phloem regulate lateral root initiation in *Arabidopsis. The Plant Cell* 25:1304-1313.

Vitha S, Yang M, Sack FD, Kiss JZ (2007). Gravitropism in the *starch excess* mutant of *Arabidopsis thaliana*. *American Journal of Botany* 94:590-598.

Walch-Liu P, Liu LH, Remans T, Tester M, Forde BG (2006). Evidence that L-Glutamate can act as an exogenous signal to modulate root growth and branching in *Arabidopsis thaliana*. *The Plant Cell Physiology* 47:1045-1057.

Walia A, Lee JS, Wasteneys G, Ellis B (2009). *Arabidopsis* mitogen activated protein kinase MPK18 mediates cortical microtubule functions in plant cells. *The Plant Journal* 59:565-575.

Wylmer CL, Bibikova TN, Gilroy S (1997). Cytoplasmic free calcium distributions during the development of root hairs of *Arabidopsis thaliana*. *Plant Journal* 12:427-439.

Xu J, Zhang S (2015). Mitogen-activated protein kinase cascades in signaling plant growt and development. *Trends in Plant Science* 20:56-64.

Yoo SD, Cho YH, Tena G, Xiong Y, Sheen J (2008). Dual control of nuclear EIN3 by bifurcate MAPK cascades in C2H4 signalling. *Nature* 451:789-796.

Zhang T, Liu Y, Yang T, Zhang L, Xu S, Xue L, An L (2006). Diverse signals converge at MAPK cascades in plant. *Plant Physiology and Biochemistry* 44:274-283.

X. APÉNDICE 1

Journal of Experimental Botany, Vol. 65, No. 1, pp. 169–183, 2014
doi:10.1093/jxb/ert368 Advance Access publication 11 November, 2013
This paper is available online free of all access charges (see http://jxb.oxfordjournals.org/open_access.html for further details)

Journal of Experimental Botany
www.jxb.oxfordjournals.org

RESEARCH PAPER

Arabidopsis thaliana mitogen-activated protein kinase 6 is involved in seed formation and modulation of primary and lateral root development

J. S. López-Bucio[1], J. G. Dubrovsky[1], J. Raya-González[2], Y. Ugartechea-Chirino[3], J. López-Bucio[2], L. A. de Luna-Valdez[1], M. Ramos-Vega[1], P. León[1] and A. A. Guevara-García[1,*]

[1] Instituto de Biotecnología, Universidad Nacional Autónoma de México, Apartado Postal 510-3, 62250 Cuernavaca, Morelos, México
[2] Instituto de Investigaciones Químico-Biológicas, Universidad Michoacana de San Nicolás de Hidalgo, Edificio A-1´, CP 58030 Morelia, Michoacán, México
[3] Departamento de Ecología Funcional, Instituto de Ecología, Universidad Nacional Autónoma de México, Ciudad Universitaria, 3er circuito exterior SN, Del. Coyoacán, México D.F. 04510, México

* To whom correspondence should be addressed. E-mail: aguevara@ibt.unam.mx

Received 13 June 2013; Revised 10 September 2013; Accepted 2 October 2013

Abstract

Mitogen-activated protein kinase (MAPKs) cascades are signal transduction modules highly conserved in all eukaryotes regulating various aspects of plant biology, including stress responses and developmental programmes. In this study, we characterized the role of MAPK 6 (MPK6) in *Arabidopsis* embryo development and in post-embryonic root system architecture. We found that the *mpk6* mutation caused altered embryo development giving rise to three seed phenotypes that, post-germination, correlated with alterations in root architecture. In the smaller seed class, mutant seedlings failed to develop the primary root, possibly as a result of an earlier defect in the division of the hypophysis cell during embryo development, but they had the capacity to develop adventitious roots to complete their life cycle. In the larger class, the MPK6 loss of function did not cause any evident alteration in seed morphology, but the embryo and the mature seed were bigger than the wild type. Seedlings developed from these bigger seeds were characterized by a primary root longer than that of the wild type, accompanied by significantly increased lateral root initiation and more and longer root hairs. Apparently, the increment in primary root growth resulted from an enhanced cell production and cell elongation. Our data demonstrated that MPK6 plays an important role during embryo development and acts as a repressor of primary and lateral root development.

Key words: *Arabidopsis*, embryo development, MAP kinases, MPK6, plant signalling, root development.

Introduction

Mitogen-activated protein kinase (MAPK) cascades are signal transduction modules that are highly conserved in eukaryotes (Zhang *et al.*, 2006). A MAPK module consists of at least three kinases: a MPKKK, a MPKK, and a MPK, which activate downstream targets by phosphorylation. The last kinase of the module, a MPK, is able to phosphorylate several substrates, including transcription factors, to regulate gene expression (Andreasson and Ellis, 2009). MAPKs are known regulators of biotic and abiotic stress responses, hormone perception, and developmental programmes (Colcombet and Hirt, 2008; Suarez-Rodriguez *et al.*, 2010).

Abbreviations: CPR, cell production rate; DAG, days after germination; IAA, indole-3-acetic acid; LR, lateral root; LRP, lateral root primordium; MAPK, mitogen-activated protein kinase; MPK6, *Arabidopsis thaliana* mitogen-activated protein kinase 6; NO, nitric oxide; PD, proliferation domain; PR, primary root; RAM, root apical meristem; RH, root hair; TD, transition domain.

The *Arabidopsis* genome encodes 20 different MPKs (MAPK Group, 2002), from which MPK3, MPK4, and MPK6 play important roles both in stress and developmental responses (Colcombet and Hirt, 2008). In particular, MPK6 has been found to participate in bacterial and fungal resistance (Nuhse *et al.*, 2000; Asai *et al.*, 2002; Menke *et al.*, 2004; Wan *et al.*, 2004; Zhou *et al.*, 2004; Zhang *et al.*, 2007), in mutualistic interactions (Vadassery *et al.*, 2009), in priming of stress (Beckers *et al.*, 2009), and in regulation of plant architecture (Bush and Krysan, 2007; Müller *et al.*, 2010).

Functional redundancy is common among MAPKs. Particularly, MPK3 and MPK6 participate in biotic and abiotic stress resistance as well as in developmental processes (Lee and Ellis, 2007; Hord *et al.*, 2008; Lampard *et al.*, 2009; Liu *et al.*, 2010). MPK4/MPK6 and even MPK3/MPK4/MPK6 have been shown to act redundantly in osmotic, touch, wounding, and defence responses (Ichimura *et al.*, 2000; Droillard *et al.*, 2004; Meszaros *et al.*, 2006; Brader *et al.*, 2007). MPKs are proposed to act through common downstream targets and upstream activators (Feilner *et al.*, 2005; Merkouropoulos *et al.*, 2008; Andreasson and Ellis, 2009; Popescu *et al.*, 2009), but the interaction of these pathways is poorly understood. The MPK6 loss-of-function mutant displays alterations in the embryo and early root development, indicating that, at least for these processes, the function of this kinase cannot be substituted by any other MPK (Bush and Krysan, 2007; Müller *et al.*, 2010; Wang *et al.*, 2010).

The first evidence demonstrating that MPK6 (and/or MPK3) is involved in embryo development was reported by Wang *et al.* (2007), who showed that *mpk3*$^{-/-}$ *mpk6*$^{-/-}$ double mutants die at the embryo stage and a viable double mutant (*mpk6*$^{-/-}$ MPK3RNAi) is developmentally arrested at the cotyledon stage. In a different study, Bush and Krysan (2007) reported that several development programmes are influenced by MPK6. In that work, it was observed that *mpk6* null mutant alleles had defects in anther and embryo development, and displayed reduced male fertility. The observed *mpk6* phenotypes display variable penetrance, probably influenced by the growth conditions. Additionally, mutations in the *MPK6* gene have been linked to protrusion of the embryo detected in about 7% of the seeds from an *mpk6* homozygous population (Bush and Krysan, 2007).

Post-embryonic root development is regulated by multiple plant hormones, nutrient availability, and environmental signals (Fukaki and Tasaka, 2009; López-Bucio *et al.*, 2003). The primary root (PR) originates from the embryo and gives rise to many lateral roots (LRs) during vegetative growth, and each of these will produce more LRs. The quantity and placement of these structures among other factors determine the root system architecture (RSA), and this in turn plays a major role in determining whether a plant will survive in a particular environment (Casimiro *et al.*, 2003; Dubrovsky and Forde, 2012). A further adaptation to increase water and nutrient absorption is performed by root hairs (RHs). These are long tubular-shaped epidermal cell extensions covering roots and increase their total absorptive surface (Datta *et al.*, 2011). Auxin (indole-3-acetic acid, IAA) is recognized as the key hormone controlling both RSA and RH development, whereas cytokinins are regulators of PR growth and LR formation (Fukaki and Tasaka, 2009; De Smet *et al.*, 2012).

Current challenges are focused on determining the signalling events for which cell identity regulators are connected with hormone receptors to coordinate stress and development responses. Recently, MPK6 was proposed to be involved in early root development, possibly through altering cell division plane control and modulating the production of second messengers, such as nitric oxide (NO) in response to hydrogen peroxide (Müller *et al.*, 2010; Wang *et al.*, 2010). It was observed that *mpk6-2* and *mpk6-3* mutants produced more and longer LRs than wild-type seedlings after application of a NO donor or H_2O_2 (Wang *et al.*, 2010). However, the hormonal responses underlying these root alterations and the role of MPK6 in these processes are still unknown. Thus, independent data support the participation of MPK6 in both shoot and root development, but no relationship has been established between embryo and root phenotypes in *mpk6* mutants, nor the impact of earlier root development alterations in the configuration of post-embryonic root architecture.

In this study, we provided physiological and molecular evidence that seedlings defective in two independent *mpk6* mutant alleles showed three distinct classes of seed phenotype, which correlated with alterations in cell division and elongation processes that affected root architecture. These alterations were independent of MPK3. These data indicate that MPK6 is an essential component of early signalling processes linked to proper embryo development and maintenance of *Arabidopsis* RSA.

Materials and methods

Additional details are available in Supplementary Methods at *JXB* online.

Plant material and growth conditions

Arabidopsis thaliana Heyhn wild-type and mutant plant lines were in the Columbia-0 (Col-0) ecotype. *MPK6* (At2g43790) T-DNA insertion lines (SALK_073907 and SALK_127507) were obtained from the Salk T-DNA collection (Alonso *et al.*, 2003) and provided by TAIR (http://arabidopsis.org). Both mutant lines were described previously as *mpk6-2* and *mpk6-3* (Liu and Zhang, 2004). The *MPK3* T-DNA insertion line (SALK_151594), was kindly donated by Dr Shuqun Zhang from Missouri University, USA (Wang *et al.*, 2007). The transgenic line *ABI4*::*GUS* (Söderman *et al.*, 2000) was kindly provided by Dr Ruth Finkelstein from the University of California, USA. This marker gene was introduced into the *mpk6-2* background by crossing homozygous plants. Surface-sterilized seeds were incubated at 4 °C for 3 d to break dormancy and then grown on agar (0.8%, w/v, Bacto™ Agar, BD Difco, Sparks, MD, USA) solidified 0.2× MS medium (Caisson, Laboratories, Noth Logan, UT, USA) with 1% (w/v) sucrose. Kinetin and IAA were purchased from Sigma (Sigma-Aldrich, St Louis, MO, USA) and added to the medium at the indicated concentration. Seedlings were grown on vertically oriented Petri dishes maintained in growth chambers at 21 °C under a 16:8 h light:darkness photoperiod under 105 µmol m^{-2} s^{-1} light intensity. For seed production, plants were grown in Metro-Mix 200 (Grace Sierra, Milpitas, CA, USA) in a growth room at 23 °C under a 16/8 h photoperiod and a light intensity of 230 µmol m^{-2} s^{-1}.

Embryo analysis

Wild-type and *mpk6-2* mutant embryos were processed as described previously (Ugartechea-Chirino *et al.*, 2010). Briefly, ovules were dissected from the silique and punched with a needle in order to favour contact between the embryos and the staining solutions. Embryos were fixed for 1–7 d with 50%, v/v, methanol, 10%, v/v, acetic acid. They were rinsed and incubated at room temperature for 30–45 min in 1% periodic acid. After a second rinse, they were incubated for 2 h in pseudo-Schiff's reagent (1.9 g of sodium metabisulfite in 97 ml of H_2O and 3 ml of 5 M HCl with 0.1 mg ml^{-1} of propidium iododide). Embryos were rinsed again and transferred to a drop of chloral hydrate (80 g of chloral hydrate in 30 ml of H_2O) on a microscope slide. Excess chloral hydrate was removed, and the embryos were mounted in Hoyer's solution (30 g of gum arabic, 200 g of chloral hydrate, 20 g of glycerol in 50 ml of H_2O). Mounted embryos were cleared in Hoyer's solution for at least a week before confocal imaging.

Seed size analysis

Dry seeds were measured individually using ImageJ (http://rsb.info.nih.gov/ij) with a set scale tool to establish a 1 mm reference on a micrometer image taken with a Nikon SMZ1500 stereomicroscope equipped with a digital SIGHT DS-Fi1c camera. Seed stereomicroscope images were then analysed with ImageJ using the 1 mm reference. Seed weight was obtained by weighting a batch of 100 seeds placed in Eppendorf tubes in an analytical balance.

Growth analysis

Photographs of representative seedlings were taken with an EOS REBEL XSi digital camera (Canon, Tokyo, Japan). The growth of PRs was registered using a ruler. LR number was determined counting all LRs emerged from the PRs under the Nikon SMZ1500 stereomicroscope. LR density, LR primordium (LRP) density, length of cortical cells, LR initiation index, length of root apical meristem (RAM), length of proliferation domain (PD), length of transition domain (TD), and number of cells in the PD (NC_{PD}) were determined on cleared roots as described previously (Dubrovsky *et al.*, 2009; Dubrovsky and Forde, 2012; Ivanov and Dubrovsky, 2013). Position of the most distal (rootward) LRP and the most distal LR as well the number of LRPs in the LR formation and the branching zones was determined on cleared root preparations under a Zeiss Axiovert 200M microscope (Zeiss, Oberkochen, Germany), equipped with differential interferential contrast optics. Cortical cell length was determined for 10 cells per root on cleared preparations using an ocular micrometer. Images of RHs and etiolated seedling images were taken under a Nikon SMZ1500 stereomicroscope equipped with a digital SIGHT DS-Fi1c camera. RH density (number of RHs mm^{-1}) and RH length were determined from roots mounted in H_2O on microscope slides and observed under a Zeiss Axiovert 200M microscope. Cell production rate (CPR) was calculated with the equation $CPR=Vl_e^{-1}$, where V (μm h^{-1}) is the rate of root growth during the last 24 h before the termination of the experiment and l_e (μm) is the length of fully elongated cortical cells, whereas cell-cycle duration (T, hours) was calculated with the equation $T=(NC_{PD}\times l_e\times \ln 2)/V^{-1}$ in accordance with Ivanov and Dubrovsky (1997). This method is applicable to steady-state growing roots. One condition of steady-state growing roots is a linear increase in the root length. We analysed root growth during the last 24 h in seedling samples 5 and 8 d after germination (DAG) and found that at both time points the growth in both the mutant and the wild-type was stabilized (see Results). Another condition was a constant number of cells in the meristem (Ivanov and Dubrovsky, 1997). As the transition domain of the RAM has not been defined previously, the number of meristematic cells in the cited work corresponds to the NC_{PD} in the current study. To verify if the NC_{PD} was constant during the analysed time periods, we estimated this parameter in samples at t_0 (24 h prior to termination of the experiments) and found no statistical differences in the NC_{PD} within the same genotype at t_0 and at final time points. This preliminary analysis permitted us to apply the above equation for estimation of average cell-cycle time in the PD. Criteria for defining the PD and TD have been described (Ivanov and Dubrovsky, 2013). Briefly, the PD comprises cells that maintain proliferation activity and the TD comprises cells that have very low probability of cell proliferation but grow at the same rate as cells in the PD and have not yet started rapid elongation. As no marker lines have yet been proposed to identify these domains, we determined the domains based on relative changes in the cell lengths analysed on cleared root preparations. In the PD, the cell length commonly varies no more than 2-fold, and in the TD cells are longer than the longest cells in the PD. The distance from the quiescent centre to the point where a cortical cell becomes longer than the longest cell in the PD was considered to be the border between the PD and the TD. In the elongation zone, the cell length starts steadily to increase simultaneously in all tissues. The point where this increase can be observed was defined as the distal (rootward) border between the TD and elongation zone. All measurements were done with an ocular micrometer.

All experimental data were analysed statistically with SigmaPlot 11 (Systat Software, San Jose, CA, USA). Student's *t*-test or Tukey's post-hoc test were used for testing differences in growth and root developmental responses, as indicated. The number of independent experiments in each case is indicated in the corresponding figure legend.

Results

Mutation of the MPK6 *gene causes three distinct and stable seed phenotypes*

Through a careful phenotypic analysis of two independent *mpk6* T-DNA insertion null mutant lines (SALK_073907 and SALK_127507) (Supplementary Fig. S1A at *JXB* online), we corroborated that the protruding embryo phenotype, previously described by Bush and Krysan (2007), was present in the homozygous seed populations from both mutant alleles. Closer inspection of the seeds from these mutants showed three segregating phenotypically distinctive classes. In the larger class (~70%, *mpk6wb*/*w*ild-type-like *b*igger seeds) the lack of MPK6 did not cause any evident alteration in seed morphology, but the seeds were significantly bigger than those from wild-type plants (Figs 1C and 2). The second class (~23%, *mpk6rs*/raisin-like *s*eed phenotype) included seeds with rough coats (Fig. 1D). Finally, the smaller class (~7%, *mpk6bs*/*b*urst *s*eed phenotype) included seeds with protruding embryos from the seed coat (Fig. 1E). It is important to point out that the rough coat phenotype was not uniform, as we observed some seeds that looked more affected than others (Fig. 1D). However, in this study, all of them were pooled together within the same class. In contrast to the heterogeneous phenotype of the rough coat seeds, the other two seed phenotypes were clearly recognized. To determine whether all three *mpk6* seed phenotypes were linked to the *MPK6* mutation, we performed crosses between a homozygous *mpk6-2* mutant with pollen from wild-type (Col-0) plants. In the F1 progeny of these crosses, no phenotypic alterations were evident. Interestingly, in seedlings from all three different seed classes obtained from *mpk6* homozygous mutant populations, MPK6 activity was absent, and this was observed consistently in at least three subsequent generations of homozygous *mpk6*

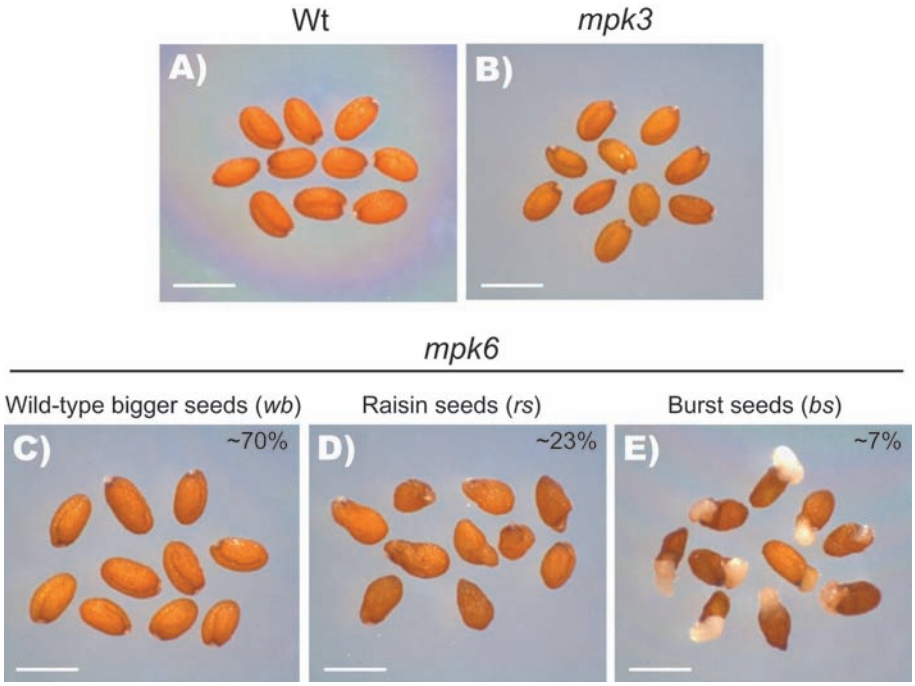

Fig. 1. *MPK6* mutation causes three different seed phenotypes. (A, B) Seeds from wild-type plants (Wt, Col-0) (A) and *mpk3* mutant (B) are shown for comparison to stable and distinguishable *mpk6* mutant seed phenotypes. (C) Seeds resembling the wild type but with a bigger seed phenotype (*mpk6wb*). (D) Seeds displaying a rough coat raisin-like seed phenotype (*mpk6rs*). (E) Embryos protruding from the seed coat burst seed phenotype (*mpk6bs*), described previously by Bush and Krysan (2007). For the pictures, seeds from each class were pooled, but the proportion of each phenotype, obtained from 1000 analysed *mpk6* seeds through several generations, is indicated. Bars, 500 µm.

seedlings from the referred seed phenotypes (Supplementary Fig. S1B).

For a better inspection of seed structure, a *pABI4::GUS* transgene encoding β-glucuronidase (GUS), expressed in embryos (Bossi *et al.*, 2009; Söderman *et al.*, 2000), was introduced into the *mpk6-2* homozygous line. We found that in homozygous *mpk6 pABI4::GUS* F3 populations, all three seed phenotypes were present (Supplementary Fig. S2, at *JXB* online). Previous studies have demonstrated redundancy between MPK6 and MPK3 (Lee and Ellis, 2007; Hord *et al.*, 2008; Lampard *et al.*, 2009; Liu *et al.*, 2010). However, a null *mpk3* mutant allele (SALK_100651) did not display any distinguishable seed phenotype when grown side by side with wild-type or *mpk6* seedlings (Figs 1B and 2), nor was the exacerbated MPK3 activity on *mpk6* seedlings (Supplementary Fig. S1B) able to compensate the *mpk6* phenotypes. Therefore, we concluded that the defects observed in seed morphology were caused specifically by a mutation in *MPK6* and they were apparently independent of *MPK3*.

mpk6 *seed phenotypes are linked to root developmental alterations*

To analyse whether the observed alterations in *mpk6* seeds affected post-germination development, we compared the early seedling growth of wild-type and *mpk6* homozygous mutant populations. Initially, we included *mpk3* seeds in our analysis, but we did not find any phenotypic alteration in *mpk3* mutant seeds or root seedlings (data not shown). Inspection of seedlings at 2 DAG demonstrated that it was possible to differentiate three different root phenotypes within the *mpk6* seedlings. Around 70% of the population analysed displayed PRs of greater length than WT seedlings (*l*onger *r*oot; *mpk6lr*). Additionally, roughly 20% of the seedlings displayed *s*hort *r*oots (*mpk6sr*), whereas around 10% of the seedlings did not develop PRs (*m*inus *r*oots; *mpk6mr*) (Fig. 3A, B). Although a previous report has already documented defects in root formation in the *mpk6-2* (SALK_073907) mutant (Müller *et al.*, 2010), no further analysis of these morphological alterations in the root architecture or their relationship with earlier embryonic alterations was performed. Interestingly, the proportion of each of the three root phenotypes correlated with those proportions observed from the seed phenotypes described previously (Figs 1C–E and 3A), suggesting that they may be related.

To analyse if *mpk6* mutant seed phenotypes had any effect on the post-germination development, the different classes of seed from this mutant were separated and germinated independently. The root morphology from each seed population was then compared with that of wild-type seedlings. Surprisingly, a high proportion of the *mpk6bs* seeds germinated *in vitro*, indicating that, in spite of the protrusion from the seed coat, these embryos were viable (Fig. 3C). However, around 80% of these germinated seedlings failed to develop PRs and most of them died a few days after germination. Those seedlings that survived all developed adventitious roots (Fig. 3C, inset) and were able to complete their life cycle and produce seeds. The progeny from these *mpk6bs* seedlings segregated again

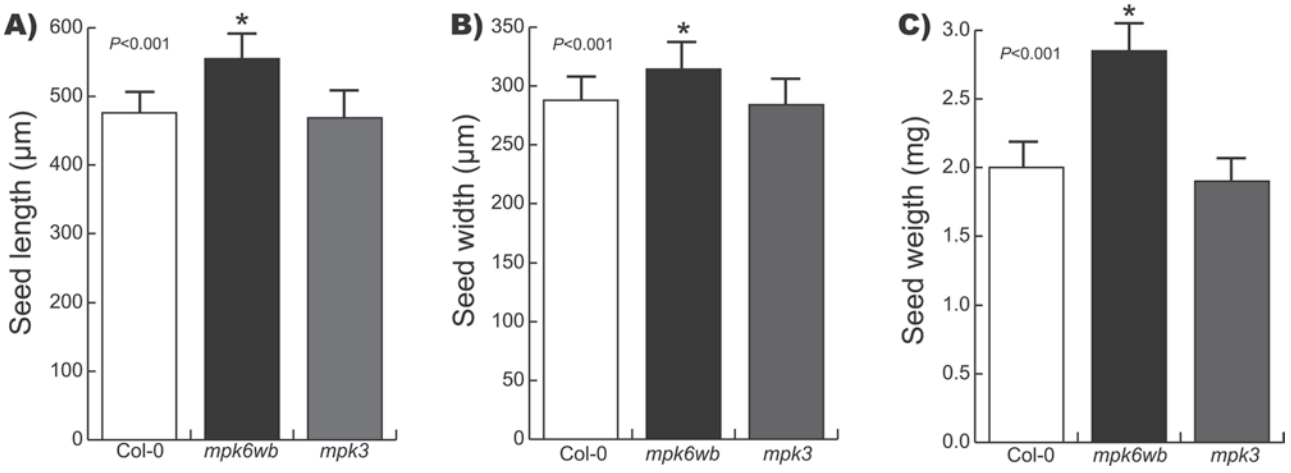

Fig. 2. *mpk6* mutant produces seeds bigger than the wild-type. The *mpk6* seeds were longer (A), wider (B), and heavier (C) than wild-type (Col-0) and *mpk3* seeds. Error bars represent the mean ±standard error (SE) from 500 seedlings analysed at each line. Asterisk indicates Student's *t*-test statistically significant differences at *P* values indicated.

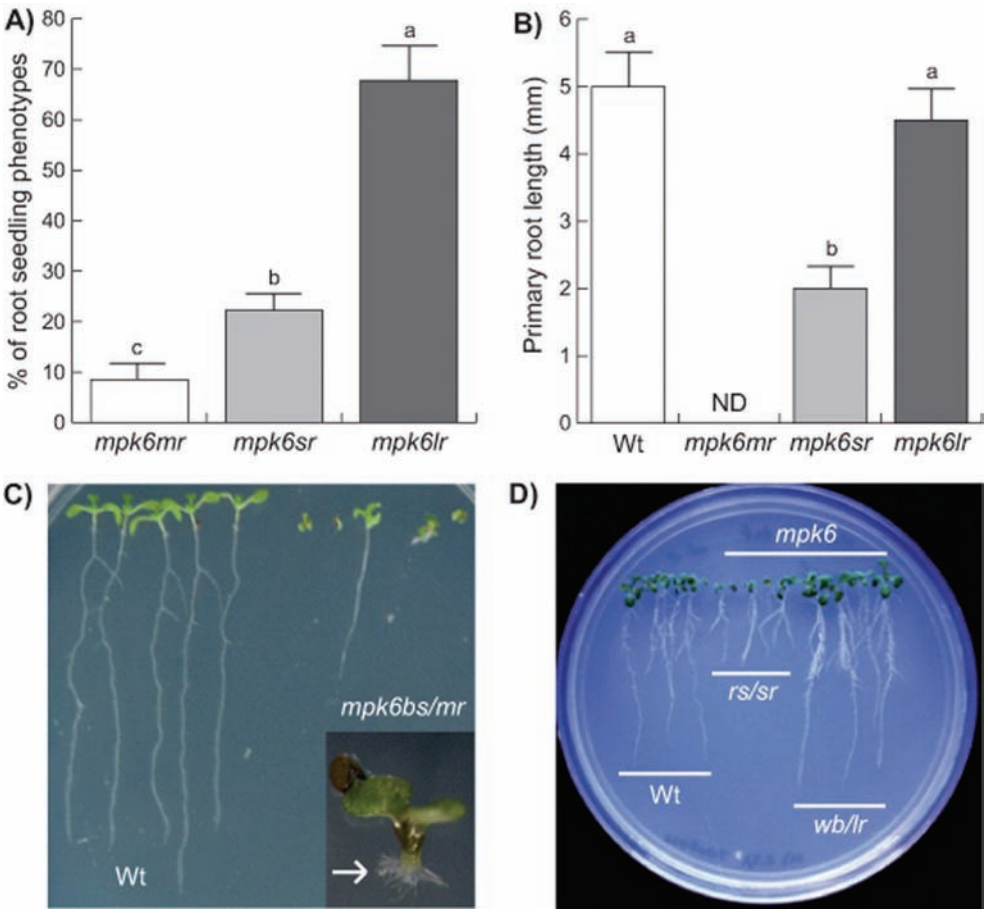

Fig. 3. *mpk6* mutant displays three different root phenotypes. The *mpk6* mutant displayed three root phenotypes each related to the seed morphology: seedlings lacking PR (minus root; *mpk6mr*), seedlings with short roots (*mpk6sr*), and seedlings with PR longer than wild-type root (*mpk6lr*). (A) Proportion of 6 DAG seedlings in each *mpk6* root mutant class.(B) PR length in 2 DAG wild-type (Wt) and the three *mpk6* root mutant classes seedlings. Notice that in this developmental stage the root length of the later *mpk6lr* phenotype is similar to that of the wild-type. Error bars represent the mean±SE from data obtained from three independent experiments, each performed with 120 (A) or 100 (B) seedlings. Different letters on the bars indicate Tukey's post-hoc test statistical difference at $P \leq 0.001$. (C) Seedlings lacking PR (minus root) developed from *mpk6bs* seeds (*mpk6bs/mr*); some of these seedlings were able to produce adventitious roots (white arrow). (D) Seeds at 6 DAG *mpk6rs* (*rs/sr*) and *mpk6wb* (*wb/lr*) develop shorter and longer PRs compared with the wild-type roots.

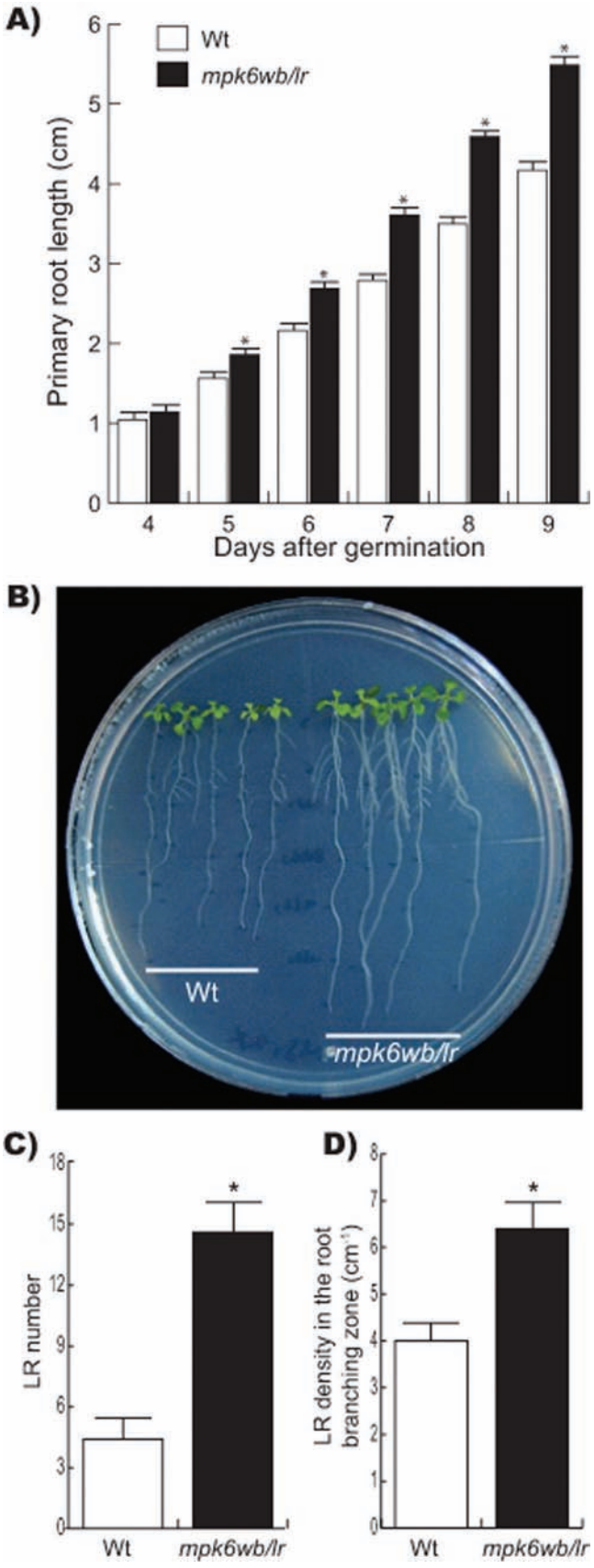

Fig. 4. *mpk6* mutant has altered primary root development, more LRs and higher LR density. (A) Primary root length changes with time. Starting from 5 DAG, statistically significant differences were observed between wild-type (Wt) and *mpk6wb/lr* PR length. Error bars represent the mean ±SE from 30 seedlings analysed at each indicated DAG. The experiment was repeated three times with similar results. Asterisk indicates Student's *t*-test statistically significant differences at $P \leq 0.001$. (B) Representative photograph of wild-type and *mpk6wb/lr* 8 DAG seedlings. Notice that *mpk6wb/lr* seedlings had longer PRs, and more and longer LRs than the wild-type seedlings. (C, D) LR number (C) and LR density (D) were obtained from the root branching zone of wild-type and *mpk6wb/lr* mutant. Error bars in (C) represent the mean ±SE from 60 seedlings analysed at 8 DAG from three independent experiments and in (D) represents the mean ±SE from 12 seedlings at 6 DAG from two independent experiments. Asterisk indicates Student's *t*-test statistically significant differences at $P \leq 0.001$.

into all three seed phenotypes shown in Fig. 1 with similar proportions (data not show). Marked differences were also observed in root development of the seedlings derived from the *mpk6wb* and *mpk6rs* seed types when compared with wild-type seedlings. Seedlings at 6 DAG derived from *mpk6rs* displayed shorter roots than the wild-type, and those derived from *mpk6wb* had longer roots (Fig. 3D). In particular, analysing the rate of growth of the PR of *mpk6wb/lr*, we found that, starting from 5 DAG, it was greater in the mutant than in wild-type seedlings (Fig. 4A). The data described so far clearly demonstrated that MPK6 plays an important role in root development and that these root phenotypes are linked with particular seed phenotypes. Besides a longer root, *mpk6wb/lr* seedlings grown *in vitro* also clearly developed more LRs (Fig. 4B). We next decided to explore the participation of MPK6 in LR development, quantifying the number of LRs and LR density in *mpk6wb/lr* and wild-type plants. These analyses demonstrated that *mpk6wb/lr* seedlings contained a higher number of LRs and a greater LR density in the root branching zone (Fig. 4C, D). These data indicated that MPK6 acts as a negative regulator of LR formation.

mpk6 *mutant has embryo development defects*

The longer root phenotype of the *mpk6wb/lr* mutant could be a result of differences in germination time compared with that of wild-type. We found that this was not the case, as both wild-type and *mpk6wb* seeds had similar germination times (data not shown) and similar root length during the first days after germination (Figs 3B and 4A). Thus an alternative hypothesis is that the short-root phenotype and the inability to form PRs are associated with defects during embryo development and do not represent alterations in the vegetative root developmental programme. To test this idea, we analysed the morphology of a total of 239 *mpk6* embryos representing all stages of embryonic development from two independent experiments (Fig. 5). During early embryogenesis, the suspensor uppermost cell is recruited to the embryo proper and acquires hypophyseal identity (Jürgens, 2001). Mutant lines defective in generating this cell lineage often produce rootless seedlings (Peris *et al.*, 2010; Jeong *et al.*, 2011). Microscopic analyses of early *mpk6* embryos showed ectopic divisions in the suspensor at the time when

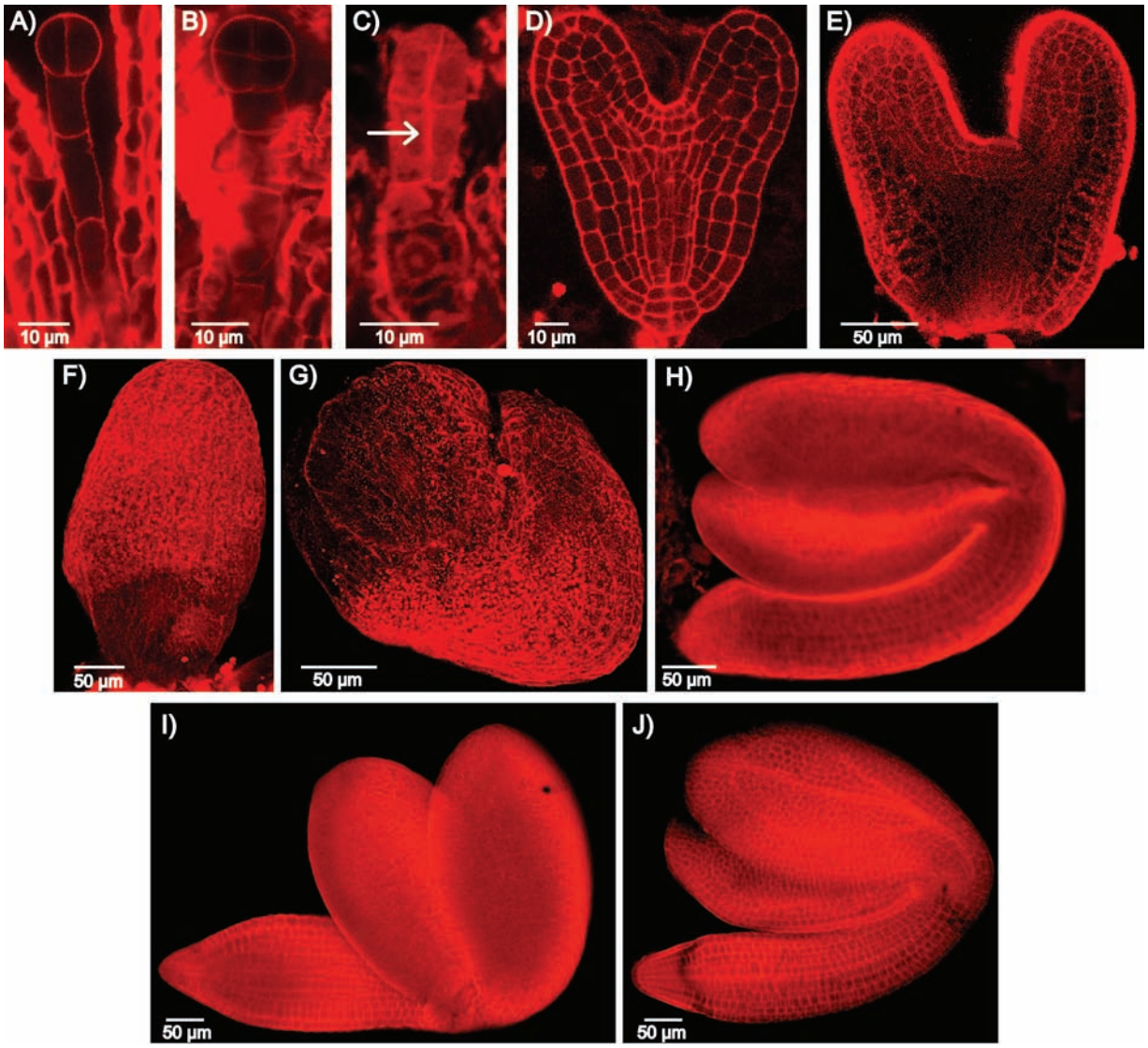

Fig. 5. *mpk6* cell organization is affected throughout embryonic development. Cell organization in wild-type (Col-0) and *mpk6* embryos. (A, B) Representative two- to four-cell (A) and eight-cell (B) wild-type embryos during their first three rounds of cell divisions. (C) Two-cell *mpk6* embryo showing ectopic periclinal cell division in the uppermost suspensor cell (arrow). This embryo failed to establish the transversal cell division plane necessary to generate an eight-cell embryo proper. (D) Wild-type heart-stage embryo. (E–G) Immature *mpk6* embryos showing arrested development at the heart (E), torpedo (F), or bent cotyledon (G) stages. (H) *mpk6* embryo with complete embryonic organogenesis at the bent cotyledon stage. (I, J) Representative *mpk6* (I) and wild-type (J) embryos at mature stage. Propidium iodide pseudo-Schiff staining of the cell wall (red) was carried out according to Ugartechea-Chirino *et al.* (2010). Bars are as indicated.

the hypophyseal cell should be specified. Seven out of 23 embryos observed between the one-cell and globular stages had ectopic divisions either in the suspensor or in the embryo proper (Fig. 5C). Later during development, 24% of the embryos were arrested at the heart stage embryo and did not proceed to develop hypocotyl and root (Fig. 5E), while 18% showed arrested development but developed hypocotyl and root (Fig. 5F–G) and 71% achieved complete embryonic organogenesis by the bent cotyledon stage (Fig. 5H). Interestingly, at the mature stage, *mpk6* embryos seemed to be bigger than the wild-type (Fig. 5I, J). Considering that *mpk6* developed several short siliques, with few seeds and many abortion events (Supplementary Fig. S3 at *JXB* online), we estimated that the frequency of these *mpk6* embryo developmental patterns correlated roughly with the frequencies observed for the burst, the raisin-like and the bigger phenotypes of mature seeds, respectively.

MPK6 is involved in the control of RSA

RSA is an important trait determining plant productivity. At present, little is known about the intrinsic mechanisms that control root growth and branching. To analyse the role that MPK6 has over RSA, we performed experiments to compare PR growth, LR formation, and RH development in wild-type and *mpk6* mutants. As they apparently do not have embryo alterations that can affect the post-germination development, to do this analysis we used only the big seed phenotype that

was also associated with long roots (*mpk6wb/lr*). LR number and length were important determinants of RSA and both were affected in the *mpk6wb/lr* mutant (Fig. 4C, D). LRs develop from the parent root through the specification of pericycle founder cells. After activation, these cells undergo repeated rounds of cell division leading to the formation of a LRP that eventually emerges as a new LR (Laskowski *et al.*, 1995; Malamy and Benfey, 1997; Dubrovsky *et al.*, 2001). A strict analysis of LR development must take into account all LR initiation events (Dubrovsky and Forde, 2012). Thus, the densities of all LR initiation events (LR and LRP) in the branching zone and in the branching zone plus LR formation zone (the latter comprises the root portion from the most rootward primordium to the most rootward emerged root) were also analysed. As shown in Fig. 6A, B, both the LR and LRP densities were significantly higher in the *mpk6wb/lr* mutant than in wild-type roots. As the fully elongated cortical cells in the *mpk6wb/lr* mutant could be longer than those from the wild type, the cell length in the LR formation zone (Fig. 6C) and the LR initiation index (Fig. 6D) were also evaluated. The latter parameter permits evaluation of LR initiation on a cellular basis and estimates the number of LR initiation events per root portion comprising 100 cortical cells of average length in a file (Dubrovsky *et al.*, 2009). This analysis also confirmed that LR initiation was significantly higher in the *mpk6wb/lr* mutant compared with wild-type seedlings. These data together strongly supported the conclusion that MPK6 acts as a negative regulator of LR initiation in *Arabidopsis*.

RHs differentiate from the root epidermal cells in a cell-position-dependent manner, increasing the total surface of roots (Tominaga-Wada *et al.*, 2011). Based on our previous results, we were interested to determine the effect of the *MPK6* mutation on RH differentiation. As shown in Fig. 7, the total number of RHs was significantly increased in the mutant compared with wild-type seedlings (Fig. 7A, B). These data indicated that the loss of function of MPK6 resulted in more and longer RHs. Moreover, we also found that the length of RHs in two different zones of the PR (2–3 and 5–7 mm root portions from the root tip) was also increased in the *mpk6wb/lr* mutant (Fig. 7C). These data also showed an important role of MPK6 in the differentiation and subsequent growth of RHs.

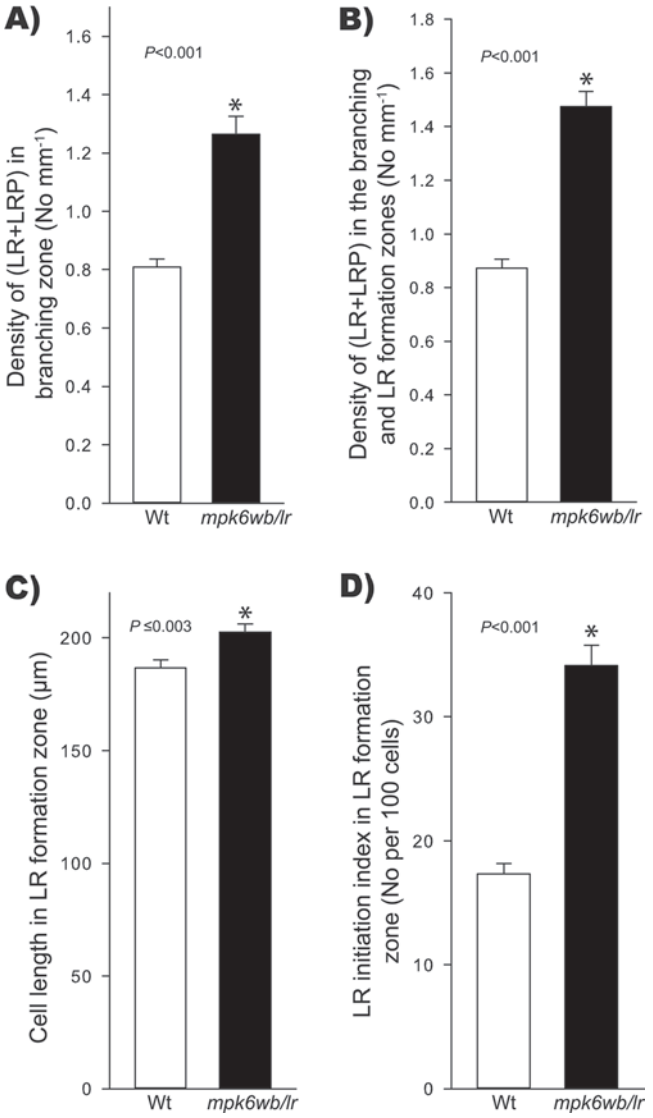

Fig. 6. The *mpk6wb/lr* mutant has increased LR initiation. LR formation in wild-type (Wt) and *mpk6wb/lr* seedlings. (A) Density of LRs and LRP in the primary root branching zone. (B) Density of LRs and LRP in branching and in LR formation zones. (C) Cortical cell length in the LR formation zone. For each individual root, 10 fully elongated cortical cells were measured. (D) LR initiation index in the LR formation zone. Error bars represent mean ±SE of 23 roots from two independent experiments. Asterisks mark Student's *t*-test significant differences at the *P* values indicated.

mpk6 *primary root growth alterations are multifactorial*

Cell division, elongation, and differentiation are closely linked cellular processes that determine PR growth. The RAM comprises two different zones: the PD, where high cell proliferation activity and a relatively slow growth takes place, and the TD, where cell proliferation probability is low but cell growth is maintained at a similar level to that found in the PD (Ivanov and Dubrovsky, 2013). After cells leave the RAM, they enter into the elongation zone, where rapid cell elongation takes place. To elucidate the contribution of cell division and elongation to the longer root phenotype of the *mpk6wb/lr* mutant, a detailed morphometric analysis of both PD and TD was conducted on 5 DAG plants. We observed that, while the size of the TD in the *mpk6wb/lr* mutant was 45% greater than that in the wild-type, the PD was 9% greater in the *mpk6wb/lr* mutant (Table 1). We also found that the number of cells, the rate of root growth, the fully elongated cell length, and cell production were also increased in *mpk6wb/lr* PRs compared with those of wild-type (Table 1 and Fig. 8A–C). A significant decrease (13%) in cell-cycle duration over time (5–8 DAG) was found in mutant seedlings (Student's *t*-test at $P \leq 0.001$), whereas in the wild type, no changes in cell-cycle duration were found during the same period (Fig. 8D). These results indicated that both cell production and cell elongation have a significant impact on the accelerated root growth found in the *mpk6wb/lr* mutant.

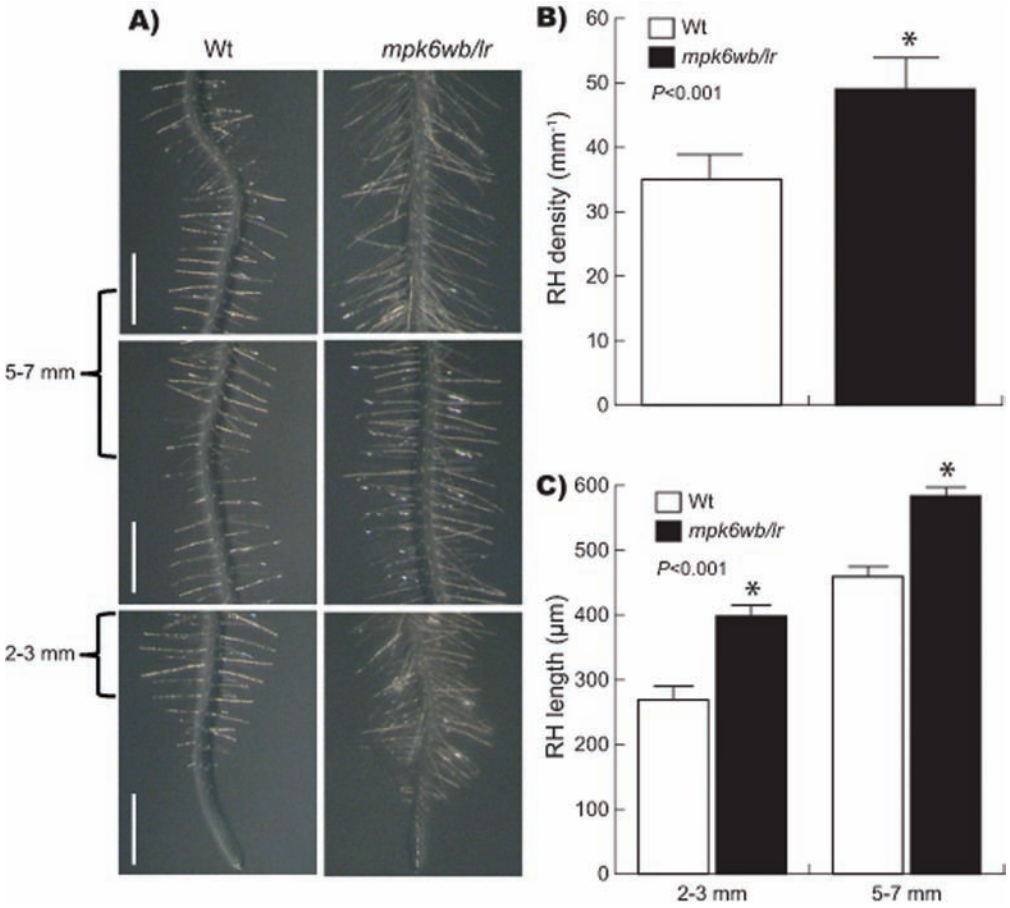

Fig. 7. The *mpk6wb/lr* mutant develops more and longer RHs. (A) RHs formed along ~1 cm from the tip of the PR from representative 6 DAG seedlings. Bars, 1 mm). (B) The RH density in 6 DAG seedlings from 2–3 and 5–7 mm root segments measured from the root tip. (C) Comparative quantification of RH length in the same root segments as in (B). Error bars represent the mean ±SE from 30 seedlings in three independent experiments. Asterisks mark Student's *t*-test significant differences at the *P* values indicated.

Table 1. *Wild-type (Col-0) and mpk6wb/lr RAM comparative analysis*

Genotype	RAM length (µm)	Difference (%)	TD length (µm)	Difference (%)	PD length (µm)	Difference (%)	NC_{PD}	Difference (%)
Col-0	355 ± 39	–	142 ± 20	–	213 ± 19	–	37.3 ± 2.7	–
mpk6wb/lr	438 ± 47*	23	206 ± 18*	45	232 ± 29**	9	45.7 ± 4.6*	22

Combined data were used from two independent experiments (n=24).
*Student's *t*-test significant differences at $P < 0.001$.
**Student's *t*-test significant differences at $P \leq 0.019$.

Discussion

MPK6 is essential for embryogenesis and root development

The central role that MAPK signalling has over different aspects of plant development is well accepted (Andreasson and Ellis, 2009; Suarez-Rodriguez *et al.*, 2010). However, the dissection of the particular function of each of the MAPK proteins has been difficult due to the partial redundancy among them. Using a genetic strategy, MPK6 has been associated with pathogen resistance (Menke *et al.*, 2004) and anther, inflorescence, embryo, and root development (Bush and Krysan, 2007; Müller *et al.*, 2010; Wang *et al.*, 2010). In particular, with respect to embryo and root development, previous analysis focused on embryo protruding seeds (Bush and Krysan, 2007), short-root seedlings (Müller *et al.*, 2010), and LR development in response to NO treatment (Wang *et al.*, 2010). In this work, we performed a detailed analysis of seed morphology and its correlation with root development in *mpk6* mutants. Three phenotypic classes of seed were identified in the progeny of homozygous *mpk6* plants, including seeds with a normal appearance but bigger than wild-type seeds, seeds with rough coats, and seeds with protruding embryos, each giving rise to seedlings with totally different root growth and development patterns (Figs 1–4). A previous work reported that the *mpk6* mutant displayed a

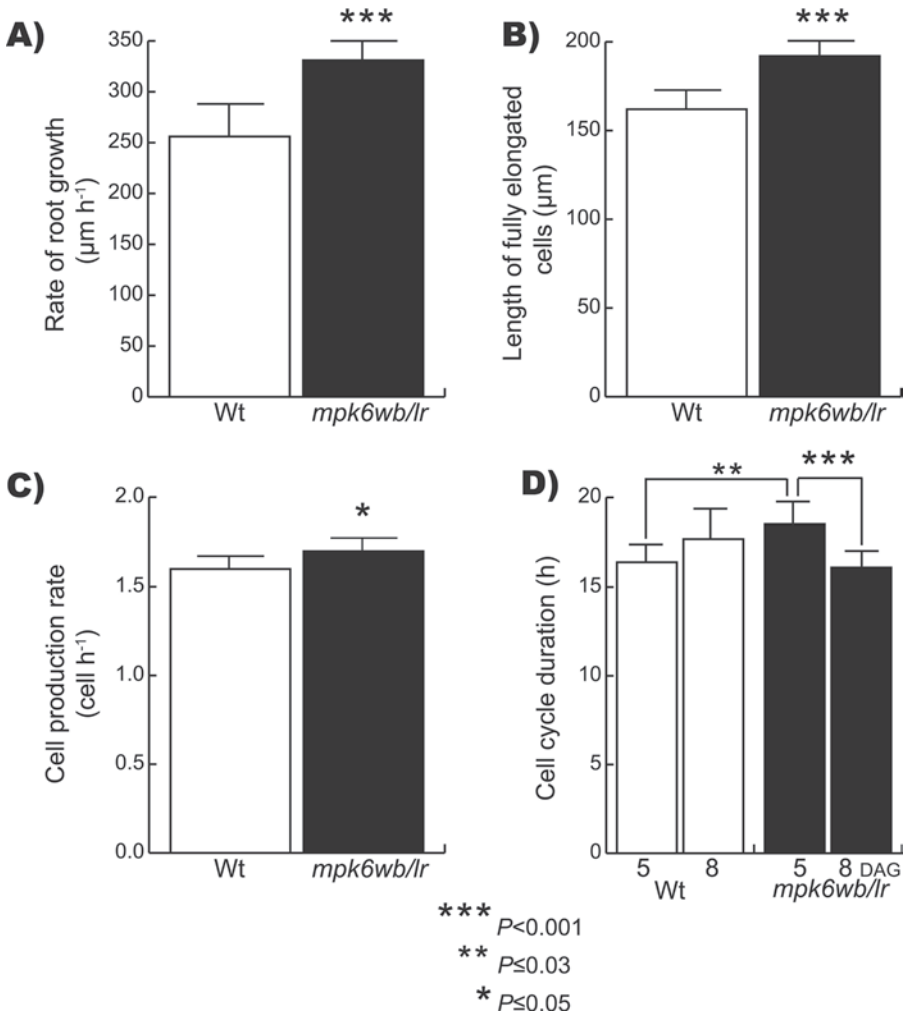

Fig. 8. Quantitative analysis of the wild-type (Wt) and *mpk6wb/lr* primary root growth and development. (A–C) Comparison between wild-type and *mpk6wb/lr* of root growth rate (A), length of fully elongated cells (B) and cell production rate (C) from 5 DAG seedlings. Error bars represent the mean ±SE from 24 seedlings in two independent experiments. (D) Cell-cycle duration (*T*) in wild-type and *mpk6wb/lr* at 5 and 8 DAG. In 5 DAG seedlings, *T* is the mean ±SE from 24 roots in two independent experiments. In 8 DAG seedlings, *T* is the mean ±SE from 12 roots in one experiment. Asterisks indicate Student's *t*-test significant differences at the *P* values indicated.

reduced fertility phenotype with variable penetrance depending on growth conditions, but the environmental variable affecting that phenotype remained to be determined (Bush and Krysan, 2007). However, the seed and root phenotypes reported here were reproducible in at least four generations of the progenies of homozygous *MPK6* from two independent null alleles (SALK_073907 and SALK_127507) grown under conditions of 21 °C, long days (16/8 h light/dark), 105 µmol m^{-2} s^{-1} of light intensity, and 45–60% of relative humidity at ~1580 m above sea level.

Between 500 and 1000 *Arabidopsis* loci have been related to embryo-defective phenotypes (Meinke *et al.*, 2009), and several of these include members of the MAPK cascade. For example, mutations in the *MPKKK4* (*YDA*) protein kinase gene cause defects in embryo development (http://www.seedgenes.org). Since the identification of *YDA* as a gene required for embryonic cell fates, it has been suggested that a MAPK signalling pathway is involved in *Arabidopsis* embryogenesis (Lukowitz *et al.*, 2004). Interestingly, the *yda/emb71* ethyl methanesulfonate heterozygous mutant, affected in the *YDA* gene (At1g63700), displays a similar embryo-protruding phenotype to that observed in *mpk6* (Lukowitz *et al.*, 2004; Meinke *et al.*, 2009). *MPKKK4* and *MPK6* are components of a common MAPK cascade involved in regulation of the embryo (Bush and Krysan, 2007) and in stomata developmental programmes (Wang *et al.*, 2007). The *yda* mutant has defects in hypophysis development similar to that observed in *mpk6bs* mutants (Fig. 5) (Lukowitz *et al.*, 2004; Meinke *et al.*, 2009). The phenotypes observed during early embryogenesis suggest that MPK6 acts as a repressor of cell proliferation involved in the establishment of embryonic polarity (Fig. 5C). This MPK6 role seems to be maintained throughout development because the *mpk6* mature embryos that achieved complete organogenesis were larger than their wild-type counterparts (Fig. 5I, J). The molecular and cellular mechanisms regulating seed development and size are complex (Sun *et al.*, 2010). Potential targets (transcription factors) and activators (leucine-rich repeat receptor kinases),

but not MAPKs were previously involved in that process (Sun *et al.*, 2010). The data from this study further confirm that both YDA and MPK6 are components of a MAPK cascade involved in the regulation of the embryo developmental programme, as already proposed (Bush and Krysan, 2007). The components acting up- and downstream of these MAPKs remain to be identified. In addition, our data support the suggestion that the failure to form a PR and the short-root phenotypes are consequences of *mpk6* mutant embryo development defects. Therefore, without considering the pleiotropic effects caused by embryo defects, the PR phenotype that can be directly associated with the loss of *MPK6* function is a long PR. Notably, this *mpk6* long PR was observed previously (Takahashi *et al.*, 2007), and in the *Arabidopsis* Hormone Database (http://ahd.cbi.pku.edu.cn) *MPK6* is included as one of the 79 genes related to a long-root phenotype.

Previous analysis made on *mpk6* short-root seedlings showed that the loss of *MPK6* function resulted in a slight but significant reduction in the number of LRs, suggesting that MPK6 is a positive regulator of LR formation (Müller *et al.*, 2010). In contrast, the data shown here using only *mpk6* mutants germinated from seeds without embryo damage demonstrated that the longer PRs had increased numbers of LRs and RHs (Figs 4 and 7). These apparent contradictory results could be explained from the different seed classes produced in the *mpk6* mutant progenies. These observations highlight how critical is to perform detailed analyses of the phenotypes associated with a gene mutation in different organs and under strictly controlled growth conditions.

MPK6 is a negative regulator of primary root growth

The comparisons of the RAM TDs and PDs and the fully elongated cell lengths between wild-type and *mpk6* mutant roots revealed that both cell division and elongation are altered in PRs of *mpk6* mutant (Table 1 and Fig. 8). Moreover, the number of cells in the *mpk6wb/lr* PD was also higher compared with that in the wild type (Fig. 6) and correlated with lower cell-cycle duration in this mutant (Fig. 8), supporting an important role of MPK6 in controlling cell proliferation and suggesting that its loss of function has a direct consequence in the long-root phenotype. For more than a decade, experimental evidence has supported the involvement of MAPKs in the regulation of cell-cycle progression in yeast (Gustin *et al.*, 1998; Strickfaden *et al.*, 2007), animals (Aliaga *et al.*, 1999; Rodríguez *et al.*, 2010), and plants (Calderini *et al.*, 1998; Jonak *et al.*, 2002; Suarez-Rodriguez *et al.*, 2010).

Regulation of plant cell division and growth is associated with microtubule reorganization, which is assisted with the action of microtubule-associated proteins. Previous reports have shown that some microtubule-associated proteins are regulated by reversible phosphorylation through MAPK cascades (Komis *et al*, 2011). For example, a MAPK from *M. sativa* (MKK3) is indispensable for spindle microtubule reorganization during mitosis (Bögre *et al.*, 1999) and the *Arabidopsis* MPK4 has been shown to be essential for the correct organization of microtubules through the phosphorylation of microtubule-associated protein 65-1 (Beck *et al.*, 2010). Additionally, the *Arabidopsis* MPK18 has been demonstrated to interact physically with a dual-specificity MAPK phosphatase (PROPYZAMIDE HYPERSENSITIVE 1/PHS1) to conform to a reversible phosphorylation/dephosphorylation switch that regulates cortical microtubule formation (Walia *et al.*, 2009). Phosphorylation of a MAP3K (NPK1) by cyclin-dependent kinases has been proposed to be critical for the appropriate cytokinesis progression in *Arabidopsis* (Sasabea *et al.*, 2011). Expression of *MPK6* has been shown to be strong in both the RAM PD and TD, specifically during the pre-prophase band and in the phragmoplast, where it controls cell division plane specification (Müller *et al.*, 2010). Epigenetic modifications like methylation or deacetylation of histones have also been suggested to regulate root development (Fukaki *et al.*, 2006; Krichevsky *et al.*, 2009). Interestingly, in animal systems, MAPK mediates histone phosphorylation, which in turns drives acetylation of histone H3, impacting on gene transcription (Clayton *et al.*, 2000). It remains to be addressed whether a similar regulatory mechanism operates in plant systems.

MPK6 regulates LR initiation

RSA is determined primarily by the spatio-temporal regulation of lateral root initiation events (Bielach *et al.*, 2012). Mutants having increased number of LRs are relatively infrequent compared with those with reduced number of LRs (De Smet *et al.*, 2006), although an increased number of LRs does not necessary indicate an increase in LR initiation (Dubrovsky and Forde, 2012). The participation of MAPK cascades in LR formation was documented by the phenotypes observed in mutants of MPK4 and its upstream activator MEKK1-1, both displaying from a slight to a severe reduction in LR density (Nakagami *et al.*, 2006; Su *et al.*, 2007). Previous studies have also shown that MPK3 and MPK6 are activated in response to the same signals as MEKK1/MPK4, supporting a possible role of these kinases in the LR development programme (Ichimura *et al.*, 2006; Suarez-Rodriguez *et al.*, 2007). However, our results demonstrated that the role of MPK6 in LR development is opposite to that of MPK4 (and MEKK1). The observation that the *mpk6wb/lr* long PR phenotype is accompanied by an increase in LR initiation (Figs 4C, D and 6), fully demonstrated that MPK6 acts as a negative regulator of LR initiation. The clearest examples of increased LR initiation are the mutants related to auxin homeostasis and signalling (Zhao, 2010). CEGENDUO, a subunit of SCF E3 ligase, has a negative role in auxin-mediated LR formation (Dong *et al.*, 2006). MAPK cascades have been found to directly or indirectly affect auxin signalling (Mockaitis and Howell, 2000; Takahashi *et al.*, 2007), which could alter LR formation. Cytokinin is a negative regulator of LR initiation. Decreased endogenous cytokinin concentration in protoxylem-adjacent pericycle cells results in increased LR initiation; in contrast, when the cytokinin concentration in these cells is increased, LR initiation is repressed (Laplaze *et al.*, 2007). In this context, the *mpk6* mutant shows a phenotype of decreased

endogenous cytokinin content. Altogether, these findings highlight the complexity of the MAPK cascades in root morphogenesis. However, an increase in cell production in the PR meristem and increased LR initiation in *mpk6wb/lr* both indicate a link between cell proliferation and its regulation by MPK6. Stress and development responses are tightly coordinated by MPKs, but their interaction is still poorly understood. As few research studies have focused on the interplay between development and environmental stresses, our findings highlight the power of studying root processes in terms of unravelling MPK signalling interactions.

MPK6 is important for RH formation

Our data also demonstrated that MPK6 is a negative regulator of RH development, as its mutation resulted in an increase in the number and size of RHs (Fig. 7). Multiple cellular factors regulate RH growth and development, including vesicle exocytosis, calcium (Ca^{2+}) homeostasis, reactive oxygen species and cytoskeleton modifications (Cardenas, 2009). Ca^{2+} is a universal second messenger, which, through interactions with Ca^{2+} sensor proteins, performs important roles in plant cell signalling (Batistič and Kudla, 2012). These sensor proteins include calmodulins, calmodulin-like proteins, Ca^{2+}-dependent protein kinases, calcineurin B-like proteins, and their interacting kinases, among others. Several genes implicated in RH differentiation have been identified; one of them, *OXIDATIVE SIGNAL INDUCIBLE 1* (*OXI1*) from *Arabidopsis*, is required for MPK6 activation by reactive oxygen species (Rentel *et al.*, 2004). The MPKKK1 (MEKK1) also has been involved in reactive oxygen species homeostasis (Nakagami *et al.*, 2006) and apparently, together with MKK2 and MPK4/MPK6, constitutes a MAPK cascade that participates in several stress responses (Ichimura *et al.*, 2000). In alfalfa, stress-induced MAPK (SIMK), an *Arabidopsis MPK6* orthologue, performs an important role in RH tip growth (Šamaj *et al.*, 2002). The alfalfa SIMK protein seems to be a positive regulator of RH growth, as treatment of plants with the MAPK inhibitor UO126 resulted in aberrant RHs, whereas the overexpression of SIMK in tobacco induced a rapid growth of these cells (Šamaj *et al.*, 2002). These results contrast with our observations of the function of MPK6 and highlight a specific role of each member of the MAPK cascade in a particular developmental process.

Possible role of MPK6 in hormone responses

As the precise mechanism underlying the root developmental alterations in *mpk6* seedlings is still unknown, we hypothesized that *mpk6wb/lr* root architectural phenotypes might result from altered responses to auxins or cytokinins, as these hormones control RSA (Perilli *et al.*, 2012). Thus, to determine whether MPK6 could affect PR responses to auxins or cytokinin, we evaluated the PR growth of wild-type and *mpk6wb/lr* mutant seedlings in response to the exogenous addition of IAA and kinetin. We observed that, at low concentrations of IAA (0.03–0.125 µM) and kinetin (0.25–2 µM), *mpk6wb/lr* was slightly insensitive and slightly hypersensitive, respectively, to the inhibitory effects of these hormones on PR growth. However, these differences were not clear at higher concentrations (0.25–0.5 µM IAA and 4–16 µM kinetin) of both hormones (Supplementary Fig. S4 at *JXB* online). These assays showed that *mpk6wb/lr* PR is not insensitive to the exogenous addition of these two plant growth regulators, suggesting that the observed root length differences in the *mpk6* mutant cannot be explained by different sensitivities to auxin or cytokinins. This observation agrees with the finding that the root growth-inhibition response to several hormones of the MPKKK mutant *yda*, which acts upstream of MPK6, is normal (Lukowitz *et al.*, 2004).

In summary, the results presented here indicate that MPK6 is a negative regulator of at least three developmental programmes in the root, namely PR growth, LR formation, and RH development, which probably occurs through regulation of cell division and elongation processes. Understanding the signalling events regulated by MPK6 activity during root development will ultimately require identification of the up- and downstream components, as well as the signal (or combination of signals) turning on and off phosphorylation of the MAPK cascade and impacting on RAM behaviour.

Supplementary data

Supplementary data are available at *JXB* online.

Supplementary Methods.

Supplementary Figure S1. *mpk6* is a null mutant.

Supplementary Figure S2. *mpk6* seed phenotypes are stable.

Supplementary Figure S3. *mpk6* siliques are shorter than wild type and contain many aborted seeds.

Supplementary Figure S4. Effect of auxin and cytokinins on primary root growth.

Acknowledgements

The authors thank Shuqun Zhang and Ruth Finkelstein for providing seeds of the homozygous *mpk3* mutant line and *pABI4::GUS* line, respectively. We also thank Patricia Jarillo for technical support, Karina Jiménez Durán (USAI, Fac. Química, UNAM), and Selene Napsucialy-Mendivil for expert technical assistance; Alma Lidia Martínez, Juan Manuel Hurtado, Roberto Rodríguez Bahena, and Arturo Ocádiz for computer support; and Paul Gaytan and Eugenio López for oligonucleotide synthesis. This work was supported by UNAM-DGAPA-PAPIIT (grants IN217111 to AGG, IN208211 to PL, and IN204312 to JGD) and CONACYT-México (CB-129266 to AGG, 127546 to PL, and 127957 to JGD).

References

Aliaga JC, Deschênes C, Beaulieu JF, Calvo EL, Rivard N. 1999. Requirement of the MAP kinase cascade for cell cycle progression and differentiation of human intestinal cells. *American Journal of Physiology—Gastrointestinal and Liver Physiology* **277,** G631–G641.

Alonso JM, Stepanova AN, Leisse TJ, *et al.* 2003. Genome-wide insertional mutagenesis of *Arabidopsis thaliana. Science* **301,** 653–657.

Andreasson E, Ellis B. 2009. Convergence and specificity in the Arabidopsis MAPK nexus. *Trends in Plant Science* **15,** 106–113.

Asai T, Tena G, Plotnikova J, Willmann MR, Chiu WL, Gomez-Gomez L, Boller T, Ausubel FM, Sheen J. 2002. MAP kinase signalling cascade in Arabidopsis innate immunity. *Nature* **415,** 977–983.

Batistič O, Kudla J. 2012. Analysis of calcium signaling pathways in plants. *Biochimica et Biophysica Acta* **1820,** 1283–1293.

Beck M, Komis G, Muller J, Menzel D, Šamaj J. 2010. Arabidopsis homologs of nucleus- and phragmoplast-localized kinase 2 and 3 and mitogen-activated protein kinase 4 are essential for microtubule organization. *Plant Cell* **22,** 755–771.

Beckers GJ, Jaskiewicz M, Liu Y, Underwood WR, He SY, Zhang S, Conrath U. 2009. Mitogen-activated protein kinases 3 and 6 are required for full priming of stress responses in *Arabidopsis thaliana. Plant Cell* **21,** 944–953.

Bielach A, Podlešáková K, Marhavý P, Duclercq J, Cuesta C, Müller B, Grunewald W, Tarkowski P, Benková E. 2012. Spatiotemporal regulation of lateral root organogenesis in Arabidopsis by cytokinin. *Plant Cell* **24,** 1–15.

Bögre L, Calderini O, Binarova P, *et al.* 1999. A MAP kinase is activated late in plant mitosis and becomes localized to the plane of cell division. *Plant Cell* **11,** 101–113.

Bossi F, Cordoba E, Dupré P, Santos-Mendoza M, San Román C, León P. 2009 The Arabidopsis ABA-INSENSITIVE (ABI) 4 factor acts as a central transcription activator of the expression of its own gene, and for the induction of ABI5 and SBE2.2 genes during sugar signaling. *The Plant Journal* **59,** 359–374.

Brader G, Djamei A, Teige M, Palva ET, Hirt H. 2007. The MAP kinase kinase MKK2 affects disease resistance in Arabidopsis. *Molecular Plant–Microbe Interaction* **20,** 589–596.

Bush SM, Krysan PJ. 2007. Mutational evidence that the Arabidopsis MAP kinase MPK6 is involved in anther, inflorescence, and embryo development. *Journal of Experimental Botany* **58,** 2181–2191.

Calderini O, Bogre L, Vicente O, Binarova P, Heberle-Bors E, Wilson C. 1998. A cell cycle regulated MAP kinase with a possible role in cytokinesis in tobacco cells. *Journal of Cell Science* **111,** 3091–3100.

Cardenas L. 2009. New findings in the mechanisms regulating polar growth in root hair cells. *Plant Signaling and Behavior* **4,** 4–8.

Casimiro I, Beeckman T, Graham N, Bhalerao R, Zhang H, Casero P, Sandberg G, Bennett MJ. 2003. Dissecting Arabidopsis lateral root development. *Trends in Plant Science* **8,** 165–171.

Clayton AL, Rose S, Barratt MJ, Mahadeva LC. 2000. Phosphoacetylation of histone H3 on c-fos- and c-jun-associated nucleosomes upon gene activation. *EMBO Journal* **17,** 3714–3726.

Colcombet J, Hirt H. 2008. Arabidopsis MAPKs: a complex signalling network involved in multiple biological processes. *Biochemical Journal* **413,** 217–226.

Datta S, Kim CM, Pernas M, Pires N, Proust H, Tam T, Vijayakumar P, Dolan L. 2011. Root hairs: development, growth and evolution at the plant–soil interface. *Plant and Soil* **346,** 1–14.

De Smet I, Vanneste S, Inzé D, Beeckman T. 2006. Lateral root initiation or the birth of a new meristem. *Plant Molecular Biology* **60,** 871–887.

De Smet I, White PJ, Bengough AG, *et al.* 2012. Analyzing lateral root development: how to move forward. *Plant Cell* **24,** 15–20.

Dong L, Wang L, Zhang Y, Zhang Y, Deng X, Xue Y. 2006. An auxin-inducible F-Box protein CEGENDUO negatively regulates auxin-mediated lateral root formation in Arabidopsis. *Plant Molecular Biology*, **60,** 599–615.

Droillard MJ, Boudsocq M, Barbier-Brygoo H, Lauriere C. 2004. Involvement of MPK4 in osmotic stress response pathways in cell suspensions and plantlets of Arabidopsis thaliana: activation by hypoosmolarity and negative role in hyperosmolarity tolerance. *FEBS Letters* **574,** 42–48.

Dubrovsky JG, Forde BG. 2012. Quantitative analysis of lateral root development: pitfalls and how to avoid them. *Plant Cell* **24,** 4–14.

Dubrovsky JG, Rost TL, Colon-Carmona A, Doerner P. 2001. Early primordium morphogenesis during lateral root initiation in *Arabidopsis thaliana*. *Planta* **214,** 30–36.

Dubrovsky JG, Soukup A, Napsucialy-Mendivil S, Jeknic Z, Ivanchenko MG. 2009. The lateral root initiation index: an integrative measure of primordium formation. *Annals of Botany* **103,** 807–817.

Feilner T, Hultschig C, Lee J, *et al.* 2005. High throughput identification of potential Arabidopsis mitogen-activated protein kinases substrates. *Molecular and Cellular Proteomics* **4,** 1558–1568.

Fukaki H, Taniguchi N, Tasaka M. 2006. PICKLE is required for SOLITARY-ROOT/IAA14-mediated repression of ARF7 and ARF19 activity during Arabidopsis lateral root initiation. *The Plant Journal* **48,** 380–389.

Fukaki H, Tasaka M. 2009. Hormone interactions during lateral root formation. *Plant Molecular Biology* **69,** 437–449.

Gustin MC, Albertyn J, Alexander M, Davenport K. 1998. MAP kinase pathways in the yeast *Saccharomyces cerevisiae*. *Microbiology and Molecular Biology Reviews* **62,** 1264–1300.

Hord CL, Sun YJ, Pillitteri LJ, Torii KU, Wang H, Zhang S, Ma H. 2008. Regulation of Arabidopsis early anther development by the mitogen-activated protein kinases, MPK3 and MPK6, and the ERECTA and related receptor-like kinases. *Molecular Plant* **1,** 645–658.

Ichimura K, Casais C, Peck SC, Shinozaki K, Shirasu K. 2006. MEKK1 is required for MPK4 activation and regulates tissue-specific and temperature-dependent cell death in Arabidopsis. *Journal of Biological Chemistry* **281,** 36969–36976.

Ichimura K, Mizoguchi T, Yoshida R, Yuasa T, Shinozaki K. 2000. Various abiotic stresses rapidly activate Arabidopsis MAP kinases ATMPK4 and ATMPK6. *The Plant Journal* **24,** 655–665.

Ivanov VB, Dubrovsky JG. 1997. Estimation of the cell-cycle duration in the root meristem: a model of linkage between cell-cycle duration, rate of cell production, and rate of root growth. *International Journal of Plant Sciences* **158,** 757–763.

Ivanov VB, Dubrovsky JG. 2013. Longitudinal zonation pattern in plant roots: conflicts and solutions. *Trends in Plant Science* **18,** 237–243.

Jeong S, Palmer MT, Lukowitz W. 2011. The RWP-RK factor GROUNDED promotes embryonic polarity by facilitating YODA MAP kinase signaling. *Current Biology* **21,** 1268–1276.

Jonak C, Okresz L, Bogre L, Hirt H. 2002. Complexity, cross talk and integration of plant MAP kinase signalling. *Current Opinion in Plant Biology* **5,** 415–424.

Jürgens G. 2001. Apical–basal pattern formation in Arabidopsis embryogenesis. *EMBO Journal* **20,** 3609–3616.

Komis G, Illés P, Beck M, Šamaj, J. 2011. Microtubules and mitogen-activated protein kinase signalling. *Current Opinion in Plant Biology* **14,** 650–657.

Krichevsky A, Zaltsman A, Kozlovsky SV, Tian GW, Citovsky V. 2009. Regulation of root elongation by histone acetylation in Arabidopsis. *Journal of Molecular Biology* **385,** 45–50.

Lampard GR, Lukowitz W, Ellis BE, Bergmann DC. 2009. Novel and expanded roles for MAPK signaling in Arabidopsis stomatal cell fate revealed by cell type-specific manipulations. *Plant Cell* **21,** 3506–3517.

Laplaze L, Benkova E, Casimiro I, *et al.* 2007.Cytokinins act directly on lateral root founder cells to inhibit root initiation. *Plant Cell* **19,** 3889–3900.

Laskowski MJ, Williams ME, Nusbaum HC, Sussex IM. 1995. Formation of lateral root meristems is a two-stage process. *Development* **121,** 3303–3310.

Lee JS, Ellis BE. 2007. Arabidopsis MAPK phosphatase 2 (MKP2) positively regulates oxidative stress tolerance and inactivates the MPK3 and MPK6 MAPKs. *Journal of Biological Chemistry* **282,** 25020–25029.

Liu XM, Kim KE, Kim KC, *et al.* 2010. Cadmium activates Arabidopsis MPK3 and MPK6 via accumulation of reactive oxygen species. *Phytochemistry* **71,** 614–618.

Liu Y, Zhang S. 2004. Phosphorylation of 1-aminocyclopropane-1-carboxylic acid synthase by MPK6, a stress-responsive mitogen-activated protein kinase, induces ethylene biosynthesis in Arabidopsis. *Plant Cell* **16,** 3386–3399.

López-Bucio J, Cruz-Ramírez A, Herrera-Estrella L. 2003. The role of nutrient availability in regulating root architecture. *Current Opinion in Plant Biology* **6,** 280–287.

Lukowitz W, Roeder A, Parmenter D, Somerville C. 2004. A MAPKK kinase gene regulates extra-embryonic cell fate in Arabidopsis. *Cell* **116,** 109–119.

Malamy JE, Benfey P. 1997. Organization and cell differentiation in lateral roots of *Arabidopsis thaliana*. *Development* **124,** 33–44.

MAPK Group. 2002. Mitogen-activated protein kinase cascades in plants: a new nomenclature. *Trends in Plant Science* **7,** 301–308.

Meinke D, Sweeney C, Muralla R. 2009. Integrating the genetic and physical maps of *Arabidopsis thaliana*: identification of mapped alleles of cloned essential (EMB) genes. *PloS One* **4,** e7386.

Menke FL, van Pelt JA, Pieterse CM, Klessig DF. 2004. Silencing of the mitogen-activated protein kinase MPK6 compromises disease resistance in Arabidopsis. *Plant Cell* **16,** 897–907.

Merkouropoulos G, Andreasson E, Hess D, Boller T, Peck SC. 2008. An Arabidopsis protein phosphorylated in response to microbial elicitation, AtPHOS32, is a substrate of MAP kinases 3 and 6. *Journal of Biological Chemistry* **283,** 10493–10499.

Meszaros T, Helfer A, Hatzimasoura E, *et al.* 2006. The Arabidopsis MAP kinase kinase MKK1 participates in defence responses to the bacterial elicitor flagellin. *The Plant Journal* **48,** 485–498.

Mockaitis K, Howell SH. 2000. Auxin induces mitogenic activated protein kinase (MAPK) activation in roots of Arabidopsis seedlings. *The Plant Journal* **24,** 785–796.

Müller J, Beck M, Mettbach U, Komis G, Hause G, Menzel D, Samaj J. 2010. Arabidopsis MPK6 is involved in cell division plane control during early root development, and localizes to the pre-prophase band, phragmoplast, trans-Golgi network and plasma membrane. *The Plant Journal* **61,** 234–248.

Nakagami H, Soukupova H, Schikora A, Zarsky V, Hirt H. 2006. A Mitogen-activated protein kinase kinase kinase mediates reactive oxygen species homeostasis in Arabidopsis. *Journal of Biological Chemistry* **281,** 38697–38704.

Nuhse TS, Peck SC, Hirt H, Boller T. 2000. Microbial elicitors induce activation and dual phosphorylation of the *Arabidopsis thaliana* MAPK 6. *Journal of Biological Chemistry* **275,** 7521–7526.

Perilli S, Di Mambro R, Sabatini S. 2012. Growth and development of the root apical meristem. *Current Opinion in Plant Biology* **15,** 17–23.

Peris CI, Rademacher EH, Weijers D. 2010. Green beginnings—pattern formation in the early plant embryo. *Current Topics in Developmental Biology* **91,** 1–27.

Popescu SC, Popescu GV, Bachan S, Zhang Z, Gerstein M, Snyder M, Dinesh-Kumar SP. 2009. MAPK target networks in *Arabidopsis thaliana* revealed using functional protein microarrays. *Genes and Development* **23,** 80–92.

Rentel MC, Lecourieux D, Ouaked F, *et al.* 2004. OXI1 kinase is necessary for oxidative burst-mediated signalling in Arabidopsis. *Nature* **427,** 858–861.

Rodríguez J, Calvo F, González JM, Casar B, Andrés V, Crespo, P. 2010. ERK1/2 MAP kinases promote cell cycle entry by rapid, kinase-independent disruption of retinoblastoma–lamin A complexes. *Journal of Cell Biology* **191,** 967–979.

Šamaj J, Ovecka M, Hlavacka A, *et al.* 2002. Involvement of the mitogen-activated protein kinase SIMK in regulation of root hair tip growth. *EMBO Journal* **21,** 3296–3306.

Sasabea M, Boudolfb V, De Veylderb L, Inzéb D, Genschikd P, Machida Y. 2011. Phosphorylation of a mitotic kinesin-like protein and a MAPKKK by cyclin-dependent kinases (CDKs) is involved in the transition to cytokinesis in plants. *Proceedings of the National Academy of Sciences, USA* **108,** 17844–17849.

Söderman EM, Brocard IM, Lynch TJ, Finkelstein RR. 2000. Regulation and function of the Arabidopsis *ABA-insensitive4* gene in seed and abscisic acid response signaling networks. *Plant Physiology* **124,** 1752–1765.

Strickfaden SC, Winters MJ, Ben-Ari G, Lamson RE, Tyers M, Pryciak PM. 2007. A Mechanism for cell cycle regulation of MAP kinase signaling in a yeast differentiation pathway. *Cell* **128,** 519–531.

Su SH, Suarez-Rodriguez MC, Krysan P. 2007. Genetic interaction and phenotypic analysis of the Arabidopsis MAP kinase pathway mutations *mekk1* and *mpk4* suggests signaling pathway complexity. *FEBS Letters* **581,** 3171–3177.

Suarez-Rodriguez MC, Adams-Phillips L, Liu Y, Wang H, Su SH, Jester PJ, Zhang S, Bent AF, Krysan PJ. 2007. MEKK1 is required for flg22-induced MPK4 activation in Arabidopsis plants. *Plant Physiology* **143,** 661–669.

Suarez-Rodriguez MC, Petersen M, Mundy J. 2010. Mitogen-activated protein kinase signaling in plants. *Annual Review of Plant Biology* **61,** 621–649.

Sun X, Shantharaj D, Kang X, Ni M. 2010. Transcriptional and hormonal signaling control of Arabidopsis seed development. *Current Opinion in Plant Biology* **13,** 611–620.

Takahashi F, Yoshida R, Ichimura K, Mizoguchi T, Seo S, Yonezawa M, Maruyama K, Yamaguchi-Shinozaki K, Shinozaki K. 2007. The mitogen-activated protein kinase cascade MKK3–MPK6 is an important part of the jasmonate signal transduction pathway in Arabidopsis. *Plant Cell* **19,** 805–818.

Tominaga-Wada R, Ishida T, Wada T. 2011. New insights into the mechanism of development of Arabidopsis root hairs and trichomes. *International Review of Cell and Molecular Biology* **286,** 67–105.

Ugartechea-Chirino Y, Swarup R, Swarup K, Péret B, Whitworth M, Bennett M, Bougourd S. 2010. The AUX1 LAX family of auxin influx carriers is required for the establishment of embryonic root cell organization in *Arabidopsis thaliana*. *Annals of Botany* **105,** 277–289.

Vadassery J, Ranf S, Drzewiecki C, Mithofer A, Mazars C, Scheel D, Lee J, Oelmuller R. 2009. A cell wall extract from the endophytic fungus *Piriformospora indica* promotes growth of Arabidopsis seedlings and induces intracellular calcium elevation in roots. *The Plant Journal* **59,** 193–206.

Walia A, Lee JS, Wasteneys G, Ellis B. 2009. Arabidopsis mitogen-activated protein kinase MPK18 mediates cortical microtubule functions in plant cells. *The Plant Journal* **59,** 565–675.

Wan J, Zhang S, Stacey G. 2004. Activation of a mitogen-activated protein kinase pathway in Arabidopsis by chitin. *Molecular Plant Pathology* **5,** 125–135.

Wang H, Ngwenyama N, Liu Y, Walker JC, Zhang S. 2007. Stomatal development and patterning are regulated by environmentally responsive mitogen-activated protein kinases in Arabidopsis. *Plant Cell* **19,** 63–73.

Wang, P, Du Y, Li Y, Ren D, Song CP. 2010. Hydrogen peroxide-mediated activation of MAP kinase 6 modulates nitric oxide biosynthesis and signal transduction in Arabidopsis. *Plant Cell* **22,** 2981–2998.

Zhang T, Liu Y, Yang T, Zhang L, Xu S, Xue L, An L. 2006. Diverse signals converge at MAPK cascades in plant. *Plant Physiology and Biochemistry* **44,** 274–283.

Zhang X, Dai Y, Xiong Y, DeFraia C, Li J, Dong X, Mou Z. 2007. Overexpression of Arabidopsis MAP kinase kinase 7 leads to activation of plant basal and systemic acquired resistance. *The Plant Journal* **52,** 1066–1079.

Zhao Y. 2010. Auxin biosynthesis and its role in plant development. *Annual Review of Plant Biology* **61,** 49–64.

Zhou F, Menke FL, Yoshioka K, Moder W, Shirano Y, Klessig DF. 2004. High humidity suppresses *ssi4*-mediated cell death and disease resistance upstream of MAP kinase activation, H_2O_2 production and defense gene expression. *The Plant Journal* **39,** 920–932.

JOURNAL OF PROTEOMICS 111 (2014) 148–164

Available online at www.sciencedirect.com

ScienceDirect

www.elsevier.com/locate/jprot

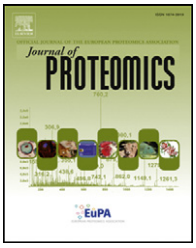

Proteomic analysis of chloroplast biogenesis (*clb*) mutants uncovers novel proteins potentially involved in the development of *Arabidopsis thaliana* chloroplasts☆

L.A. de Luna-Valdez[a], *A.G. Martínez-Batallar*[b], *M. Hernández-Ortiz*[b], *S. Encarnación-Guevara*[b], *M. Ramos-Vega*[a], *J.S. López-Bucio*[a], *P. León*[a], *A.A. Guevara-García*[a,*]

[a]*Instituto de Biotecnología, Universidad Nacional Autónoma de México, Apartado Postal 510-3, 62214 Cuernavaca, Morelos, Mexico*
[b]*Centro de Ciencias Genómicas, Universidad Nacional Autónoma de México, Av. Universidad 565, Chamilpa, 62210 Cuernavaca, Morelos, Mexico*

ARTICLE INFO

Available online 19 August 2014

Keywords:
Chloroplast development
Comparative proteomics
clb mutants
Arabidopsis thaliana

ABSTRACT

Plant cells outstand for their ability to generate biomass from inorganic sources, this phenomenon takes place within the chloroplasts. The enzymatic machinery and developmental processes of chloroplasts have been subject of research for several decades, and this has resulted in the identification of a plethora of proteins that are essential for their development and function. Mutant lines for the genes that code for those proteins, often display pigment-accumulation defects (e.g., albino phenotypes). Here, we present a comparative proteomic analysis of four chloroplast-biogenesis affected mutants (*cla1-1*, *clb2*, *clb5*, *clb19*) aiming to identify novel proteins involved in the regulation of chloroplast development in *Arabidopsis thaliana*. We performed 2D-PAGE separation of the protein samples. These samples were then analyzed by computational processing of gel images in order to select protein spots with abundance shifts of at least twofold, statistically significant according to Student's *t*-test ($P < 0.01$). These spots were subjected to MALDI-TOF mass-spectrometry for protein identification. This process resulted in the discovery of three novel proteins potentially involved in the development of *A. thaliana* chloroplasts, as their associated mutant lines segregate pigment-deficient plants with abnormal chloroplasts, and altered mRNA accumulation of chloroplast-development marker genes.

Biological significance
This report highlights the potential of using a comparative proteomics strategy for the study of biological processes. Particularly, we compared the proteomes of wild-type seedlings and four mutant lines of *A. thaliana* affected in chloroplast biogenesis. From this proteomic

☆ This article is part of a Special Issue entitled: Proteomics, mass spectrometry and peptidomics, Cancun 2013. Guest Editors: César López-Camarillo, Victoria Pando-Robles and Bronwyn Jane Barkla.

DOI of original article: http://dx.doi.org/10.1016/j.dib.2014.07.001.

* *Corresponding author.*
E-mail addresses: ldeluna@ibt.unam.mx (L.A. de Luna-Valdez), angelmb@ccg.unam.mx (A.G. Martínez-Batallar), magda@ccg.unam.mx (M. Hernández-Ortiz), encarnac@ccg.unam.mx (S. Encarnación-Guevara), mramos@ibt.unam.mx (M. Ramos-Vega), lopbucio@ibt.unam.mx (J.S. López-Bucio), patricia@ibt.unam.mx (P. León), aguevara@ibt.unam.mx (A.A. Guevara-García).

http://dx.doi.org/10.1016/j.jprot.2014.07.003

analysis it was possible to detect common mechanisms in the mutants to respond to stress and cope with heterotrophy. Notably, it was possible to identify three novel proteins potentially involved in the development or functioning of chloroplasts, also it was demonstrated that plants annotated to carry T-DNA insertions in the cognate genes display pigment-deficient phenotypes, aberrant and underdeveloped chloroplasts, as well as altered mRNA accumulation of chloroplast biogenesis marker genes.

This article is part of a Special Issue entitled: Proteomics, mass spectrometry and peptidomics, Cancun 2013. Guest Editors: César López-Camarillo, Victoria Pando-Robles and Bronwyn Jane Barkla.

1. Introduction

Among eukaryotes, plant cells are notable for their ability to generate biomass from CO_2 and sunlight via the process known as photosynthesis. This process takes place in the membranes and compartments of a remarkable organelle, the chloroplast. Given their ability to perform photosynthesis, chloroplasts represent the main source of food (sugars) for plant cells and are the keystone for the entire food chain sustaining animal life. The chloroplasts are not only responsible for the production of carbon resources, they are also the biosynthesis site of many other important metabolites, such as amino acids, lipids, hormones, vitamins, and isoprenoids [1–3]. These functions make chloroplasts an essential organelle for the development and survival of plants. Thus, abnormal development of chloroplasts often results in lethality [4–7].

Thus far, several mutant lines harboring defects in chloroplast development have been isolated, and the mutated genes have been found to encode for several different components of the plastid machinery for protein import, isoprenoid biosynthesis, RNA processing, protein maturation, plastid gene expression, thylakoid biogenesis, chloroplast to nucleus signaling, and other important processes [8–19]. Examples include the chloroplast-biogenesis (*clb*) mutants, which were originally isolated based on the phenotypes of impaired pigment accumulation, rendering plants albino, yellow, or pale green [19]. In vitro cultured *clb* mutants contain underdeveloped chloroplasts, showing reduced organelle diameter, low accumulation of thylakoid membranes, low levels of photosynthetic pigments, and deficiencies in the expression of several nuclear and chloroplast encoded genes. Several *clb* mutants have been fully characterized, and the genes affected in such mutants are now known. For instance, *cla1-1*, *clb4*, and *clb6* mutant plants are affected in the expression of deoxy-xylulose-5-phosphate synthase (DXS1), hydroxy-3-methylbut-2-enyl diphosphate synthase (HDS), and hydroxy-3-methylbut-2-enyl diphosphate reductase (HDR), respectively; these three enzymes each catalyze a different step in the chloroplastic pathway for isoprenoid biosynthesis (Fig. 1A, B) [9,10,19]. Other *clb* mutants, such as *clb19*, affect the expression of a PPR domain-containing protein known to be involved in the editing of the *ClpP* and *rpoA* plastid mRNAs (Fig. 1A, B), which code for the catalytic subunit of the main protease complex in plastids and the α-subunit of the plastid-encoded RNA polymerase, respectively [19]. Another characterized *clb* mutant is *clb2*, whose affected locus was very recently assigned in our laboratory using next-generation sequencing methods, to a homogentisate prenyltransferase gene, which is known to be involved in the biosynthesis of plastoquinone 9 (Fig. 1A, B; unpublished data) [19,20]. Finally, during the time of production of this research, the *clb5* mutant line was found to be affected in the expression of ZDS (ζ-carotene desaturase) enzyme, which is responsible of the biosynthesis of the essential carotenoid lycopene [21]. Despite all the information that has been obtained through the characterization of *clb* mutants, there are still some *clb* lines (*clb1 and clb3*) whose characterization is still under investigation.

A

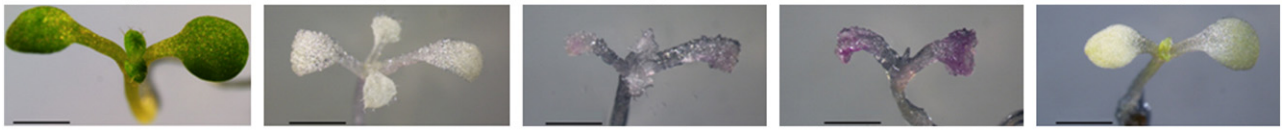

B

Locus	Mutant	Description	Phenotype	Reference
At4g15560	*cla1-1*	1-deoxy-D-xylulosa 5-phosphate synthase; chloroplastic pathway for isoprenoid synthesis.	Albino	Mandel M *et al*, 1996.
At1g05750	*clb19*	Pentatricopeptide repeat protein; editing of clpP and rpoA plastid transcripts.	Yellow	Chateigner-Boutin A *et al*, 2009.
At3g11945	*clb2*	Homogentisate prenyl transferase; plastoquinone-9 biosynthesis.	Albino	Gutiérrez-Nava M *et al*, 2004. Tian L *et al*, 2007.
At3g04870	*clb5*	ζ-carotene desaturase; carotenoid biosynthesis.	Albino	Gutiérrez-Nava M *et al*, 2004. Avendaño-Vázquez A *et al*, 2014.

Fig. 1 – Seedlings used in this analysis. A) Wild-type (Wt; 8 DAG) and mutant (16 DAG) seedling phenotypes. Plants were germinated and grown in vitro and collected after the emergence of the first pair of true leaves. B) Loci affected by the *clb* mutations under analysis; a short description of the affected proteins is included. Scale bar represents 10 μm.

Since these chloroplasts are essential for plant development, an understanding of the precise mechanisms underlying their development has been the subject of intense research by several groups around the world, and a plethora of experimental strategies have been applied to explore this phenomenon; this has been extensively described in recent reviews [22,23]. In the past few years, proteomics has been successfully used as the main tool to identify key proteins for many different biological processes, such as cancer, human fertility, and abiotic stress responses in crops [24–29]. Given the degree of success of proteomic approaches, it is not surprising to find that several efforts have been made to determine chloroplast proteomes for different plant species, including Arabidopsis, rice, maize, and wheat [30–36]. In Arabidopsis, studies have been conducted to compare the proteomes of several albino mutants, such as *ppi2*, *ffc1-2*, and *clpr4*, against the proteome of wild-type plants [37–39].

In 2012, proteomic studies took one step further in plant biology, and a study was conducted to compare the proteomes of three independent pigment-defective mutants; the results were insight into the molecular phenomena affected in such albino plants and a better understanding of several key chloroplastic processes [40]. However, from these studies it was not possible to identify specific proteins involved in chloroplast biogenesis. In this work, we perform a similar comparative analysis using four pigment-defective *clb* mutants. To accomplish this, protein extracts from mutant seedlings of four *clb* mutant lines (*cla1-1*, *clb2*, *clb5*, and *clb19*) were resolved in a 2-D PAGE then digitized to generate a super-image. A robust set of comparisons was conducted to select those protein spots that showed differences in their abundance of at least twofold and were statistically significant according to Student's *t*-test ($P < 0.01$). Mass spectrometry (MS) was then used to identify the protein associated with each selected spot. Several of the identified proteins were chosen as candidates for important functions in chloroplast biogenesis. The progeny of the available mutant lines of the candidate proteins were screened for pigment-deficient phenotypes. With this strategy, we identified three mutant lines that segregate pigment-defective seedlings. The initial characterization of those mutants demonstrated that they affect the expression of specific chloroplastic and nonchloroplastic proteins that are allegedly involved in plastid biogenesis.

2. Materials and methods

2.1. Plant material and growth conditions

Arabidopsis thaliana heterozygous mutant lines corresponding to *cla1-1* (At4g15560; [9]), *clb2* (At3g11945; [19]), *clb19* (At1g05750; [19]), *clb5* ([19,21]), *emb1241* (SALK_045238), *pbp1* (SAIL_773_D06), and *atrabe1b* (SALK_069644) were used in this study. Seeds were surface-sterilized using the solutions of 100% C_2H_6O and 1% NaClO, then cultured on 0.5× Murashige & Skoog media supplemented with 0.05 g/l 2-(N-morpholino)ethanosulfonic acid, 0.5 g/l sucrose, 100 mg/l myo-inositol, 1 mg/l nicotinic acid, 1 mg/l pyridoxine-HCl, 10 mg/l thiamine-HCl, and 8 g/l phyto agar. Seedlings from the four mutant lines that presented the wild-type phenotype and the first pair of true leaves were harvested after 8 days of culture. These were then pooled for processing as the wild-type protein samples used in this study. In order to minimize the effect of using plants in different developmental stages (detection of development-related proteins), pigment-deficient plants were collected after 16 days of culture; at this time, all the seedlings display at least the first pair of true leaves. Three biologically independent seedling batches were generated for further processing.

2.2. Extraction and quantitation of total protein

Total protein extracts were prepared according to the phenol extraction protocol reported by Hurkman & Tanaka [41]; the adjustments made to the original protocol are described here. Briefly, the starting plant material was 1 g of mutant or wild-type seedlings grown in vitro on GM medium, seedlings were ground in a mortar using liquid nitrogen and re-suspended in extraction buffer (0.7 M sucrose; 0.5 M Tris; 30 mM HCL; 50 mM EDTA; 0.1 MKCl, 12 mg/ml PVPP (Polyvinylpolypyrrolidone) and 2% β-mercaptoethanol). An equal volume of water-saturated phenol was added followed by centrifugation (6000 g for 10 min) to separate the phases. The phenol phase was re-extracted with one volume of extraction buffer then precipitated with 5 volumes of 0.1 M ammonium acetate in methanol at −20 °C overnight. The protein precipitate was washed three times with 0.1 M ammonium acetate in methanol and once with 80% acetone at −20 °C. The pellets were air dried under vacuum and re-suspended in lysis buffer (8 M Urea; 2 M Thiourea, 4% (w/v) CHAPS; 2% ampholines (1.5% pH range 5–7 and 0.5% pH range 3–10) and 60 mM DTT). Determination of protein concentration in the extracts was determined by colorimetric assays as reported by Encarnación et al., 2005 [41].

2.3. 2-D PAGE and protein visualization

500 μg (analytical gels) or 750 μg (preparative gels) of total protein extracts were separated in 12% acrylamide gels under denaturating conditions. The first dimension was run using ampholytes in the range of pH 3 to 10 and enriched in pH 4 to 8. After 2-D electrophoresis, gels were fixed and stained using colloidal Coomassie brilliant blue, following [42]. The stained gels were digitalized using a GS-800 densitometer (Bio-Rad Hercules, CA, EUA) and the image analysis software PD-Quest 8.0.1 (Bio-Rad Hercules, CA, EUA).

2.4. In silico processing of gel images

Images from 2-D gels of three biologically independent protein extracts from mutants (*cla1-1*, *clb2*, *clb5*, and *clb19*) and wild-type plants were generated and processed using the PD-Quest 8.0.1 software (Bio-Rad, Hercules CA). Protein spots in all replicates were detected automatically by the software, and the detection was then improved by the manual addition of missing spots and the removal of erroneously detected spots. Normalization of gel images was performed using the local regression model normalization method provided by PD-Quest software. Furthermore, in order to properly compare the samples, the gel images were adjusted to fit a common distortion model; this was done by matching spots

that were common to all the gel images. The gel images from the different protein samples were compared to each other in order to generate a robust data set containing all the spots represented in the samples with 98% statistical confidence ($P < 0.01$) in a Student's *t*-test. Finally, the protein spots in the statistical data set displaying ± twofold abundance change were selected as candidates for the MS analysis.

2.5. MALDI-TOF mass spectrometry and protein identification

The selected protein spots were manually excised from the preparative gels. The samples were alkylated, reduced, and trypsin-digested prior to their elution and MS analysis. Samples of digested protein spots were automatically transferred to MALDI-TOF (Matrix-Assisted Laser Desorption/Ionization-Time of Flight; Autoflex, Bruker Daltonics, Billerica, MA, USA) using Proteineer SP and SPII systems (software SPcontrol 3.1.48.0v; Bruker Daltonics, Breme, Germany). The Bruker Daltonics Autoflex system was operated in the delayed extraction and reflectron mode, and the resolution threshold was set to a signal-to-noise ratio of 1500. The specific protocols can be accessed in [42]. The m/z spectra were searched against the *A. thaliana* NCBInr (http://www.ncbi.nlm.nih.gov/guide/proteins/), SwissProt (http://www.isb-sib.ch/), and IPI (http://www.ebi.ac.uk/IPI/IPIarabidopsis.html) databases, using the Mascot (http://www.matrixscience.com) and Profound (http://prowl.rockefeller.edu) search engines. The Mascot engine was used to query NCBInr and SwissProt databases, while Profound was used to query NCBInr and IPI databases; both search engines were operated using a mass tolerance of 200 ppm, with cysteine carbamidomethylation as the constant modification and methionine oxidation as the variable modification. The significance threshold was set to $P < 0.05$ for the Mascot search.

2.6. In silico analysis of the identified proteins

Subcellular localizations were determined by manual query of the SUBA database (http://suba.plantenergy.uwa.edu.au/). Functional clustering of the identified proteins was performed using the Functional annotation tool available at DAVID (http://david.abcc.ncifcrf.gov/home.jsp) [43], and clustering was carried out using the annotations available at the Protein Information Resource (http://pir.georgetown.edu/pirwww/index.shtml) and Gene Ontology (http://www.geneontology.org/) databases. Stringency of the classification was set on medium and the rest of the options were set as default. Reconstruction of metabolic pathways was achieved using the metabolism overview pathways in the MapMan 3.5.1 software (http://mapman.gabipd.org/web/guest/mapman) with the Ath_AGI_TAIR9_Jan2010 mappings. MapMan was fed an array of data containing, for each protein, the $\log_2$ of the ratio of the detected abundance in each mutant over that registered in wild-type plants.

2.7. Northern blot, gene expression analysis

Total RNA was prepared from 12-day-old wild-type plants (Wassilewskija ecotype) and 16-day-old mutants cultured on GM media by extraction with TRIzol® Reagent (Life technologies, Carlsbad, CA USA). 5 μg of total RNA were subjected to electrophoresis in 1.2% (w/v) gels and transferred to Hybond-N + nylon membrane (GE Healthcare Life Sciences, Pittsburgh, PA, USA). RNA-Probe Hybridization was carried out under high-stringency conditions according to a previously described protocol [19]. Molecular probes were radiolabeled using ^{32}P with the Megaprime DNA labeling system (GE Healthcare Life Sciences). DNA probes used to monitor expression of *rrn16S* (AtCg00920), *accD* (AtCg00500), *psbA* (AtCg00020), and *RBCS* (At1g67090) genes were specific fragments from the corresponding genes; an *RPL21* (At1g35680) probe was obtained by DNA digestion (*SalI-NotI*) of the 146E8 clone from the ABRC stock center (http://www.arabidopsis.org).

2.8. Electron microscopy

Leaf or cotyledon samples were fixed for 1 h each in 4% paraformaldehyde and 2.5% glutaraldehyde. They were then washed in 100 mM Na-cacodylate buffer (EMS, Hatfield, PA, USA) at pH 6.5. Postfixation was performed in 1% OsO4 (EMS) in the same buffer at 4 °C for 1 h in the dark at room temperature. After the aldehyde fixation, the samples were washed with Na-cacodylate buffer and distilled water. Samples were dehydrated in a graded series of ethanol solutions followed by two changes in anhydrous propylene oxide, infiltrated in a graded series of epon-araldita resin (EMS) in propylene oxide, and finally left in a 100% embedding medium for 6 to 12 h at room temperature. Polymerization of specimens was made in molds at 60 °C for at least 24 h. Semithin (1 μ) and ultrathin (60 nm) specimens were sectioned in a LEICA (Wetzlar, Germany) ultramicrotome. Semithin sections were stained with 1% w/v toluidine blue made in 1% w/v aqueous borax solution for the digitalization of images in an Axio Scope ZEISS (Thornwood, NY, USA) microscope. Ultrathin sections were stained with 4% w/v uranyl acetate in 70% v/v ethanol followed by Reynold's lead citrate for digitalization of images in a JEOL 1200EXII Transmission Electron Microscope/GATAN (Warrendale, PA. USA).

3. Results

3.1. Sample comparison and protein identification

Total protein extracts (500 μg) from three biologically independent batches of wild-type plants and *cla1-1*, *clb2*, *clb5*, and *clb19* mutant lines were fractionated in 2-D PAGE gels; they were then stained with Coomassie blue. The gel images were processed as stated in the Material and Methods section. In this analysis, it was possible to detect more than 700 protein spots for each sample (Fig. 2A); with very few exceptions, most of the spots detected were shared between the different samples analyzed (Fig. 2A). Reproducibility of the experiments was assessed by calculating the mean coefficient of variation (CV) for each replicate group. Gel images from the *clb2* and Wt protein extracts displayed the lowest CVs, which were 29.41 and 29.52, respectively. On the other hand, images from the *cla1-1*, *clb5*, and *clb19* protein samples scored slightly higher CVs (30.3, 35.19, and 33.89, respectively; [44]).

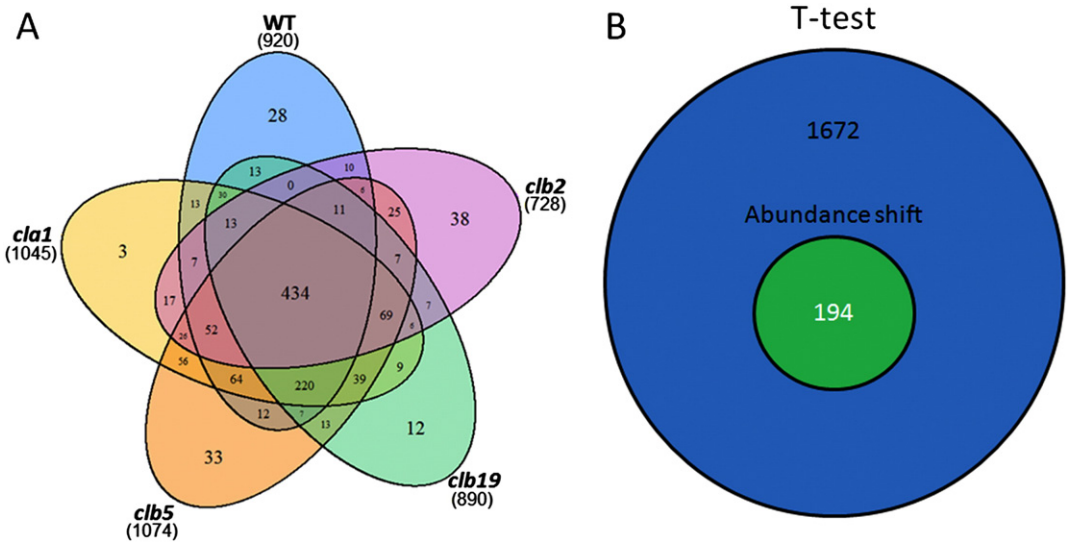

Fig. 2 – Venn diagrams depicting relationships existing between the detected spots. A) Venn diagram showing the total peptide spots detected on each mutant line and wild-type (Wt) under analysis, numbers indicate the total amount of spots detected in each protein sample; the intersections between the different subsets of spots are indicated by color. B) A Venn diagram is shown depicting the number of spots that displayed an abundance change of at least ±twofold (smaller green circle) and the total number of spots represented with a statistical confidence level of 98% (Student's *t*-test; $P < 0.01$) (larger blue circle). Null hypothesis for the Student's *t*-test states that the means of the tested populations (spots) are equal.

The total number of protein spots detected in this study is in agreement with the number of spots detected in a similar analysis of albino plants [45]. A *t*-test ($P < 0.01$) applied to the detected spots revealed that the presence in the gels of 1672 individual protein spots was statistically significant among all the samples (Fig. 2B), while only 194 spots displayed ± twofold differential abundance (Fig. 2B). Considering that the changes in the abundance of the protein spots between the analyzed mutants and wild-type protein samples might be related to differential regulation of chloroplast biogenesis, the dataset of the 194 protein spots identified to have changed their abundance in the samples was further analyzed using mass spectrometry.

Mass spectrometry analysis and subsequent database queries using different search engines resulted in the identification of 136 spots. A major constraint in the identification of proteins was the quality of the spectra. In some cases, different spots were identified as the same protein, which was probably due to posttranslational modifications, and the MS and bioinformatic analysis resulted in the identification of 96 unique proteins. Table 1 lists the identified proteins along with the data related to the search engine results and to their abundance in each mutant line.

3.2. The identified proteins have different subcellular localizations

Putative subcellular localization of the 96 MS-identified proteins was determined using the information available at the SUBA database (http://suba.plantenergy.uwa.edu.au/). As shown in Fig. 3, the list includes proteins with several subcellular localizations, such as the endoplasmic reticulum, cytoplasm, peroxisome, vacuole, nucleus, mitochondrion, plasma membrane, and chloroplast. We note that few of these proteins were predicted to have extracellular localization. However, the vast majority (37%; Fig. 3) of the analyzed proteins are presumably targeted to chloroplasts. This result supports the conclusion that the multicomparison method used in the present study efficiently detects changes in the abundance of chloroplast proteins, and similar results have been found in other proteomics studies of pigment-deficient mutants [45]. It is important to note that using the information available at SUBA, some proteins are predicted to be targeted to several cellular compartments, and further discrimination between the localizations was not possible due to lack of relevant data. The information related to the subcellular localization of each identified protein is available in Table 1.

3.3. The identified proteins cluster into stress-related groups and positively affect catabolic pathways

In order to discover proteins whose abundance shifted in all the mutants analyzed, the abundance of all the identified proteins in mutant plants was compared to their abundance in wild-type plants. Through this comparative analysis, 43 out of the 96 proteins were found down- and 42 up-regulated in at least three *clb* mutants. Inconsistent results were found among the mutants for eleven proteins [44]. The three protein sets (down-regulated, up-regulated, and inconsistent) were independently subjected to DAVID's (http://david.abcc.ncifcrf.gov/home.jsp) functional annotation tool (as described in the Material and Methods section). This method resulted in the generation of several functional clusters, as shown in Fig. 4.

The up-regulated protein subset formed only two groups with enrichment scores over the threshold (ES > 5), these groups represented functionalities related to abiotic stress

Table 1 – Proteins identified by mass spectrometry.

ID	Uniprot ID	Function	Subcellular localization	Mutant lines available	Spot abundance in WT (O. D.)	Spot abundance in *clb* mutants (O. D.)				Coverage (%)	Matched spectra	Unmatched spectra
						cla1-1	*clb5*	*clb19*	*clb2*			
At1g67090	P10795	RBCS-1A; RuBisCO small subunit 1A.	Chloroplast	Yes	2031.00	501	310	141	n. d.	29	6	9
At1g13950	Q9XI91	EIF-5A; traduction initiation factor 5A.	Cytoplasm/nucleus	Yes	624	996	2459	448	1852	29	5	28
At3g52960	Q949U7	Probable peroxiredoxin.	Chloroplast	Yes	n. d.	428	86	353	n. d.	31	7	13
At3g16640	P31265	TCPTP; translationally controlled tumour protein.	Chloroplast/nucleus/ membrane	Yes	264	239	261	223	232	60	8	13
At5g06290[a]	Q9C5R8	2-Cys peroxiredoxin A; reactive oxygen species detoxification.	Chloroplast	Yes	89	70	28	79	n. d.	32	5	8
At3g11630[a]	Q96291	2-Cys peroxiredoxin B; reactive oxygen species detoxification.	Chloroplast	Yes	186	158	62	203	42	32	5	6
At5g20720	O65282	CPN20; chaperonin 20.	Chloroplast	Yes	450	748	350	812	213	46	8	12
At1g06680	Q42029	PSBP-1; photosystem II P-1 subunit.	Chloroplast	No	715	51	n. d.	90	409	45	6	16
At1g19570	Q9FWR4	DHAR1; dehydroascorbate reductase.	Chloroplast/mitochondrion/ peroxisome/membrane	Yes	156	152	182	68	135	43	7	19
At3g01500[a]	Q56X90	Carbonic anhydrase 1 enzyme.	Chloroplast	No	470	110	n. d.	217	691	34	8	19
At1g07890[a]	C0Z2H6	Ascorbate peroxidase 1.	Chloroplast/membrane	Yes	624	996	2459	448	1852	42	6	16
At2g37220[a]	Q9ZUU4	Probable RNA binding protein cp29.	Chloroplast	Yes	233	258	30	223	42	21	6	8
At3g50820	Q9S841	PSBO2; photosystem II O-2 subunit.	Chloroplast	Yes	787	259	1234	187	1081	23	6	21
At2g37660	C0Z300	NADP binding protein.	Chloroplast	Yes	177	180	113	271	n. d.	36	8	15
At5g14740[a]	P42737	CA2; carbonic anhydrase 2 enzyme.	Cytoplasm	Yes	469	169	117	296	30	41	10	22
At5g17710[a]	Q94K56	EMB1241; Embryo deficient 1241; GrpE domain containing protein.	Chloroplast	Yes	65	43	38	42	n. d.	20	7	16
At1g20020	Q8W493	FNR2: ferredoxin NADP(+) oxidoreductase 2.	Chloroplast	Yes	305	91	70	142	n. d.	24	12	10
At5g66190	B9DI26	Ferredoxina NADP(H) oxidoreductase, leaf isoform.	Chloroplast	Yes	305	117	112	198	n. d.	37	11	16
At1g66430	Q9C524	PfkB-like carbohydrate kinase.	Chloroplast	Yes	69	42	83	52	44	21	7	15
At1g09340[a]	Q9SA52	CSP41B; RNA binding protein. Chloroplast RNA 23S metabolism.	Chloroplast/peroxisome	Yes	316	79	40	173	n. d.	32	10	18
At3g26650	P25856	Glyceraldehyde-3-phosphate dehydrogenase A subunit.	Chloroplast/membrane	Yes	304	120	156	352	n. d.	19	8	8
At4g04640	Q9SUI9	Chloroplast ATP synthase γ subunit precursor.	Chloroplast/membrane	No	405	65	73	91	121	21	7	9
At3g04120	P25858	Glyceraldehyde-3-phosphate dehydrogenase C subunit 1.	Membrane/nucleus/ mitochondrion/cytoplasm	Yes	221	126	212	219	295	37	10	10
At3g63140[a]	Q9LYA9	CSP41A; RNA binding protein. Chloroplast RNA 23S metabolism.	Chloroplast	Yes	307	115	87	120	n. d.	20	7	11
At5g65670[a]	D3K0E6	Indol-3-acetic acid induced protein 9.	Chloroplast/nucleus	Yes	65	29	n. d.	52	13	30	6	7
At1g04410	P93819	Malate dehydrogenase enzyme.	Chloroplast/nucleus/Vacuole	Yes	437	863	1136	775	969	26	7	12
At3g52930	Q9LF98	Probable fructose bisphosphate aldolase enzyme.	Chloroplast/nucleus/Vacuole	Yes	440	702	1120	524	669	48	12	18
At2g43750	P47999	OASB; o-acetylserine (thiol) liase B.	Chloroplast/mitochondrion	Yes	70	48	31	92	52	27	7	6
At4g38970	Q944G9	Probable fructose bisphosphate aldolase enzyme.	Chloroplast	Yes	932	607	210	987	192	22	7	12
At2g21330	Q9SJU4	Probable fructose bisphosphate aldolase enzyme.	Chloroplast	Yes	499	253	26	383	31	24	7	16
At1g35720[a]	Q9SYT0	Annexin; calcium-dependent membrane binding protein.	Chloroplast/membrane/ peroxisome	Yes	119	292	862	147	807	38	11	22
At1g79550	Q9SAJ4	Phosphoglycerate kinase enzyme.	Chloroplast/nucleus/ membrane/vacuole	Yes	207	348	314	293	469	25	7	8
At2g39730	P10896	RuBisCO activase enzyme.	Chloroplast/membrane	Yes	732	601	496	776	113	22	9	17

(continued on next page)

Table 1 (*continued*)

ID	Uniprot ID	Function	Subcellular localization	Mutant lines available	Spot abundance in WT (O. D.)	Spot abundance in *clb* mutants (O. D.)				Coverage (%)	Matched spectra	Unmatched spectra
						cla1-1	*clb5*	*clb19*	*clb2*			
At4g20360[a]	P17745	ATRABE1B; translation elongation factor. Homologous to RAB E1B.	Chloroplast/nucleus	Yes	622	843	284	896	183	22	8	13
At1g43670	Q9MA79	Fructose-1,6-bisphosphatase enzyme.	Chloroplast	Yes	163	56	52	97	97	27	7	9
At1g32060	P25697	Phosphoribulose kinase enzyme.	Chloroplast	Yes	516	239	102	633	49	25	11	17
At5g35630	B9DGD1	GS2; glutamin synthetase 2 enzyme.	Chloroplast/mitochondrion	Yes	873	585	216	1223	235	28	8	14
At4g05390	Q9M0V6	Ferredoxin NADP + reductase enzyme.	Chloroplast	Yes	234	52	42	150	34	24	6	17
At5g55220	Q8S9L5	Trigger factor-family protein.	Chloroplast	Yes	138	41	23	n. d.	n. d.	24	13	18
At4g01050	Q9M158	TROL; thylakoid rhodanasa-like protein. Flavoprotein anchor to thylakoid membrane.	Chloroplast	Yes	133	19	n. d.	50	n. d.	18	7	5
At4g24280	Q9STW6	cpHsc70-1; chloroplast heat shock 70-1 protein. Protein import.	Chloroplast/nucleus/ membrane	Yes	314	512	160	507	178	17	13	18
At5g49910	Q9LTX9	cpHsc70-2; chloroplast heat shock 70-2 protein. Protein import.	Chloroplast/membrane	Yes	232	153	82	82	58	13	9	19
AtCg00120	P56757	ATP synthase CF1 α subunit.	Chloroplast/nucleus/ membrane	Yes	121	39	n. d.	46	9	20	8	8
At3g17390	Q9LUT2	MTO3; methionine adenosyltransferase enzyme.	Nucleus/membrane	Yes	398	519	822	419	536	20	5	4
At3g09260[a]	Q9SR37	PYK10; β glucosidase.	Endoplasmic reticulum/ nucleus/membrane	Yes	585	1517	3693	1654	2450	16	8	16
At1g50480	Q9SPK5	THFS; formyltetrahydrofolate synthase enzyme.	Chloroplast/membrane	Yes	94	143	152	156	282	16	9	11
At1g29880[a]	O23627	Probable glycyl-tRNA synthetase enzyme.	Cytoplasm/mitochondrion/ membrane	Yes	95	85	60	75	44	13	9	5
At3g48870[a]	Q9SXJ7	HSP93-III; homologous to the regulatory subunit of Clp protease.	Chloroplast/membrane/ mitochondrion	Yes	89	98	36	97	33	11	7	9
At1g62750	Q9SI75	SCO1; snowy cotyledon. translation elongation factor G.	Chloroplast/mitochondrion	Yes	149	73	19	75	27	20	12	17
At3g56700	B9TSP7	Fatty acid reductase 6 enzyme.	Chloroplast/mitochondrion	Yes	179	15	42	105	34	19	7	32
At5g02500	P22953	HSC70-1; heat shock 70-1 cognate protein.	Chloroplast/nucleus/ peroxisome	Yes	504	316	379	167	n. d.	20	9	14
AtCg00490	O03042	RuBisCO large subunit.	Chloroplast	Yes	1326	865	404	184	173	19	9	11
AtCg00480	P19366	ATP synthase CF1 β subunit.	Chloroplast/membrane	Yes	104	85	n. d.	205	n. d.	21	8	10
At4g23670	Q9SUR0	Major latex protein-related.	Vacuole/membrane	Yes	624	996	2459	448	1852	43	12	18
At3g16450[a]	O04311	Probable lectin; mannose binding protein.	Nucleus/extracellular	Yes	183	99	220	55	223	46	11	14
At3g16420[a]	O04314	PBP1; PYK10 binding protein.	Nucleus/extracellular	Yes	76	107	279	177	219	30	7	14
At1g16080	C0Z2K9	Unknown.	Chloroplast	Yes	74	129	158	76	156	22	5	8
At5g55190[a]	Q8H156	RAN GTPase.	Membrane	Yes	260	471	153	732	223	20	5	19
At4g37930	Q9SZJ5	SHM1; serine transhydroxymethyl transferase 1 enzyme.	Chloroplast/nucleus/ mitochondrion	Yes	390	114	125	380	n. d.	22	12	8
At4g35090[a]	P25819	CAT2; catalase 2 enzyme.	Chloroplast/mitochondrion/ peroxisome	Yes	242	226	304	624	413	31	15	12
At3g22200	Q9LIE2	HER1; aminotransferase enzyme.	Mitochondrion/vacuole	Yes	86	96	134	101	242	13	5	8
At5g17920	O50008	METS; cobalamine-independent methionine synthase enzyme.	Chloroplast/membrane/ cytoplasm/vacuole	Yes	966	1908	1991	1609	1210	17	10	13
At2g26080	O80988	GLDP2; glycine decarboxylase P-2 enzyme.	Chloroplast/mitochondrion	Yes	23	n. d.	43	n. d.	n. d.	10	9	12
At3g60750	Q9LZY8	Transketolase enzyme.	Chloroplast	Yes	499	472	173	661	478	13	7	14
At3g12580[a]	Q9LHA8	HSP70; heat shock 70 protein.		Yes	89	244	154	251	259	12	7	8

			Mitochondrion/vacuole/ membrane									
At3g15950[a]	Q712H0	TSA1; TSK-associated protein like.	Endoplasmic reticulum/ peroxisome	Yes	41	101	693	64	742	19	15	29
At1g42970	P25857	Glyceraldehyde-3-phosphate dehydrogenase B subunit.	Chloroplast	Yes	393	286	157	611	117	17	7	16
At1g65930	Q9SRZ6	Isocitrate dehydrogenase enzyme.	Chloroplast/membrane	Yes	338	709	1083	719	780	23	9	13
At5g07440	Q38946	GDH2; glutamate dehydrogenase subunit 2.	Mitochondrion/vacuole	Yes	75	164	162	280	140	22	11	19
At2g36530	P25696	LOS2; enolase.	Extracellular	Yes	1654	1487	1757	1058	1149	27	10	14
At5g08670	Q8H135	ATP synthase β subunit.	Mitochondrion/peroxisome	Yes	1275	1011	1133	941	1031	33	14	22
At1g64190	Q9SH69	6-phosphogluconate dehydrogenase enzyme.	Chloroplast/membrane	Yes	n. d.	137	163	228	n. d.	25	10	10
At3g16400[a]	Q9SDM9	Mirosinase binding protein.	Extracellular	Yes	157	378	313	216	902	24	9	24
At3g03250	Q9M9P3	UDP-glucose pyrophosphorylase enzyme.	Membrane	Yes	187	161	199	188	153	20	8	13
At2g24200	P30184	Aminopeptidase enzyme.	Chloroplast/membrane/ vacuole	Yes	52	213	190	180	283	20	7	7
At2g28000	P21238	CPN60; 60 kDa chaperonin α.	Chloroplast/mitochondrion	Yes	335	614	178	591	403	53	10	23
At1g77510	Q9SRG3	ATPDIL1-2; disulfide isomerase enzyme.	Endoplasmic reticulum/ vacuole	Yes	60	79	85	125	97	15	7	7
At3g19170[a]	Q9LJL3	PREP1; zinc-dependent protease. Transit peptide degradation.	Chloroplast/mitochondrion	Yes	83	95	71	149	54	14	12	7
At1g22530[a]	Q56ZI2	Patellin II; membrane-trafficking events during cytokinesis.	Plasma membrane	Yes	14.7	9.5	7.7	11.9	11.3	18	10	8
At1g78900	O23654	VHA-A; catalytic subunit of the peripheral V1 complex of vacuoler ATPase.	Plasma membrane/vacuole	Yes	173.2	310.9	257.7	347.9	198.1	58	37	44
At3g25230	Q38931	FKBP62; co-chaperone that modulates thermotolerance by interacting with HSP90.	Plasma membrane/ cytoplasm	Yes	86.1	33.9	67.4	46.4	41.2	15	8	12
At3g16460	O04310	JACALIN-RELATED LECTIN 34; mannose-binding lectin superfamily protein.	Peroxisome	Yes	n. d.	71.1	316.5	n. d.	907.7	35	21	36
At1g76030	P11574	VHA-B1; non-catalytic subunit of the peripheral V1 complex of vacuoler ATPase.	Chloroplast/membrane/ vacuole	Yes	120.4	231.7	190.4	219	613.3	34	13	25
At3g09440	O65719	HSC70-3; heat shock 70-3 cognate protein.	Membrane	Yes	240.6	523.5	704.6	402.6	736.1	41	23	18
At2g05710	Q9SIB9	ACO2; catalyzes the isomerization of citrate to isocitrate via cis-aconitate.	Chloroplast/mitochondrion/ membrane	Yes	227.3	151.8	287.1	200.7	452.7	37	27	30
At3g02090	Q42290	Beta-MPP; cleaves (transit peptides) from Mitochondrionl protein precursors.	Mitochondrion	Yes	150	190.9	267.8	178.7	526	48	20	40
Atmg01190	P92549	ATPA; mitochondrionl membrane ATP synthase.	Mitochondrion	Yes	392.7	716.8	1036.7	608.5	929	42	18	34
At1g59720[a]	Q0WQW5	CCR28; pentatricopeptide repeat protein. Editing of multiple plastid transcripts.	Chloroplast	Yes	59.3	91.2	167	82.5	126.3	13	9	16
At3g16430[a]	O04313	Jacalin-related lectin 31.	Extracellular	Yes	n. d.	n. d.	n. d.	n. d.	87.9	44	13	29
At3g19160	Q9LJL4	IPT8; adenylate dimethylallyltransferase 8 enzyme.	Chloroplast	Yes	n. d.	18.5	n. d.	n. d.	130.2	15	3	14
At1g48090	NA	Calcium-dependent lipid-binding protein.	Chloroplast/membrane	Yes	50.1	n. d.	62.9	n. d.	90.6	13	36	125
At2g39310	O80950	Myrosinase-binding protein-like.	Membrane	Yes	n. d.	51.3	n. d.	n. d.	510.9	32	12	10
At1g65840	Q8H191	PAO4; flavoenzyme. Oxidation of the secondary amino group of spermine.	Peroxisome	Yes	n. d.	14.3	45.4	n. d.	64.4	29	8	26
At5g04110	Q8VY11	GYRB3; DNA gyrase B3.	Membrane	Yes	208.2	257	330.9	204.9	423	15	7	44
At4g34050	O49499	CCOAOMT1; caffeoyl-CoA O-methyltransferase 1 enzyme.	Unknown	Yes	73.9	123.7	148	89.2	195.9	32	9	16
At1g71330	Q9FVV9	NAP5; probable non-intrinsic ABC protein 5.	Membrane	Yes	21	57.4	59.6	61.3	107	13	5	25

n. d. (not detected).
O. D. (optic density).
[a] CLB-related protein candidates.

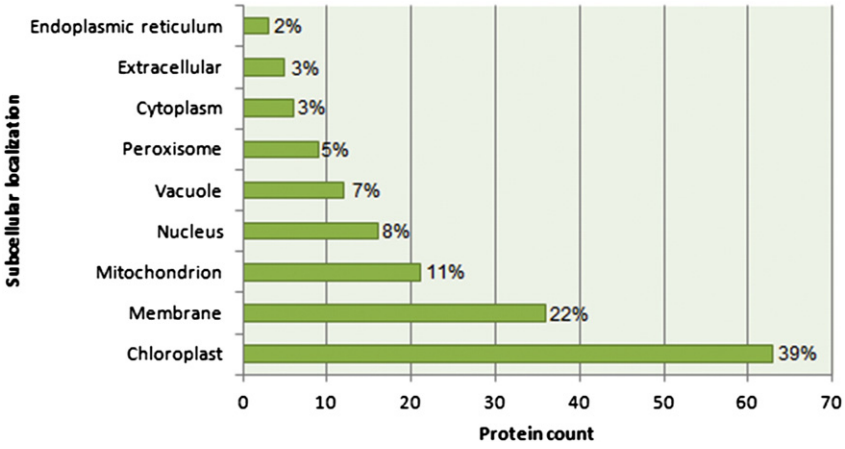

Fig. 3 – Predicted subcellular localization of proteins. The graph shows the number of proteins annotated for each subcellular compartment. The fraction of proteins in each localization is also indicated. Information was retrieved from the SUBA database (http://suba.plantenergy.uwa.edu.au/).

responses and included peroxidases such as CATALASE 2 and ANNEXIN D1 (Fig. 4A, B). In contrast, the down-regulated protein subset clustered in at least five groups with significant enrichment scores ([44]; ES > 5). Three of the most significant clusters include a chloroplast-related group (Fig. 4C) and two stress-related functional groups (Fig. 4D, E). Finally, the subset of proteins whose abundance shift was not consistent among the mutant plants formed two small clusters related to chloroplasts (Fig. 4F) and to abiotic stress (Fig. 4G); both clusters displayed enrichment scores under the significance threshold. These subsets displayed enrichment of different GO terms that link the proteins in each subset to common molecular processes.

Further analysis using MapMan 3.5.1R2 software (http://mapman.gabipd.org/web/guest) revealed that several metabolic processes are clearly affected in the *clb* mutant plants. For instance, it is clear that functions related to sucrose synthesis, photosynthetic light reactions and the Calvin cycle display strong down-regulation in the mutant lines compared to their behavior in the wild-type plants (Fig. 5). While functions related to catabolic processes, such as glycolysis, mitochondrial electron transport, the citric acid cycle, metabolism of some amino acids, and NH_3 homeostasis showed evident up-regulation in the different mutant backgrounds (Fig. 5). Details about the specific functions represented by each bin in Fig. 5 can be found in [44].

From the presented data, it is possible to speculate that the lack of fully functional plastids in pigment-deficient mutants such as *clb* and *apg* dramatically alters the plants' stress responses and the affected plants are capable of modulating their metabolism in order to adapt to heterotrophy.

3.4. *Identification of putative novel chloroplast biogenesis regulators*

All the proteins identified in this analysis (listed in Table 1) were manually annotated for their function (Description, Table 1), subcellular localization and availability of mutant lines using databases such as TAIR (http://www.arabidopsis.org/), UniProtKB (http://www.uniprot.org/), and SUBA. The list of 96 proteins was screened in the search for novel chloroplast biogenesis-related proteins. In that screening, those proteins with no mutant lines available, as well as those with annotated roles related to primary metabolism, chloroplast development, or chloroplast function, were discarded (Fig. 6A). We also excluded proteins whose predicted subcellular localization was not chloroplastic, except for some endoplasmic reticulum proteins, since recent evidence has demonstrated that at least one protein is transported to chloroplasts via an endoplasmic reticulum–Golgi pathway [46]. Furthermore, the specific function of each protein was assessed to identify proteins participating in important processes of the development or functioning of the chloroplasts, such as mRNA editing, chloroplast gene expression, and importation of proteins.

Taking into account the information presented in Table 1 and the screening parameters described above, we selected 26 candidate proteins to investigate as possible chloroplast biogenesis-related proteins. Available mutant lines for the 26 selected candidates were obtained from the Arabidopsis Biological Resource Center (Table 1), and a phenotypic screening was conducted in the search of plants displaying a pigment-deficient phenotype, which has been unequivocally associated to defects in the development or function of chloroplasts. Three mutant lines from this collection segregated pigment-deficient seedlings in their progeny. The *emb1241* (TAIR: At5g17710; SALK_045238) and *pbp1* (TAIR: At3g16420; SAIL_773_D06) mutants segregated albino and yellow phenotypes, respectively, while the *atrabe1b* (TAIR: At4g20360; SALK_069644) mutant segregated seedlings with slight variegation in cotyledons (Fig. 6B). Interestingly, none of these mutants have been previously characterized for their defects in the biogenesis or function of chloroplasts. Along with these putative novel chloroplast biogenesis regulators, several proteins were identified with known functions in chloroplast biogenesis or function, such as RBCS, CPN60, SCO1, and RuBisCO activase (Table 1).

3.5. *Expression levels of chloroplast development marker genes on mutant lines*

To obtain a more detailed characterization of the chloroplast defects in each of the selected mutants, the expression of several chloroplast- and nuclear-encoded marker genes related

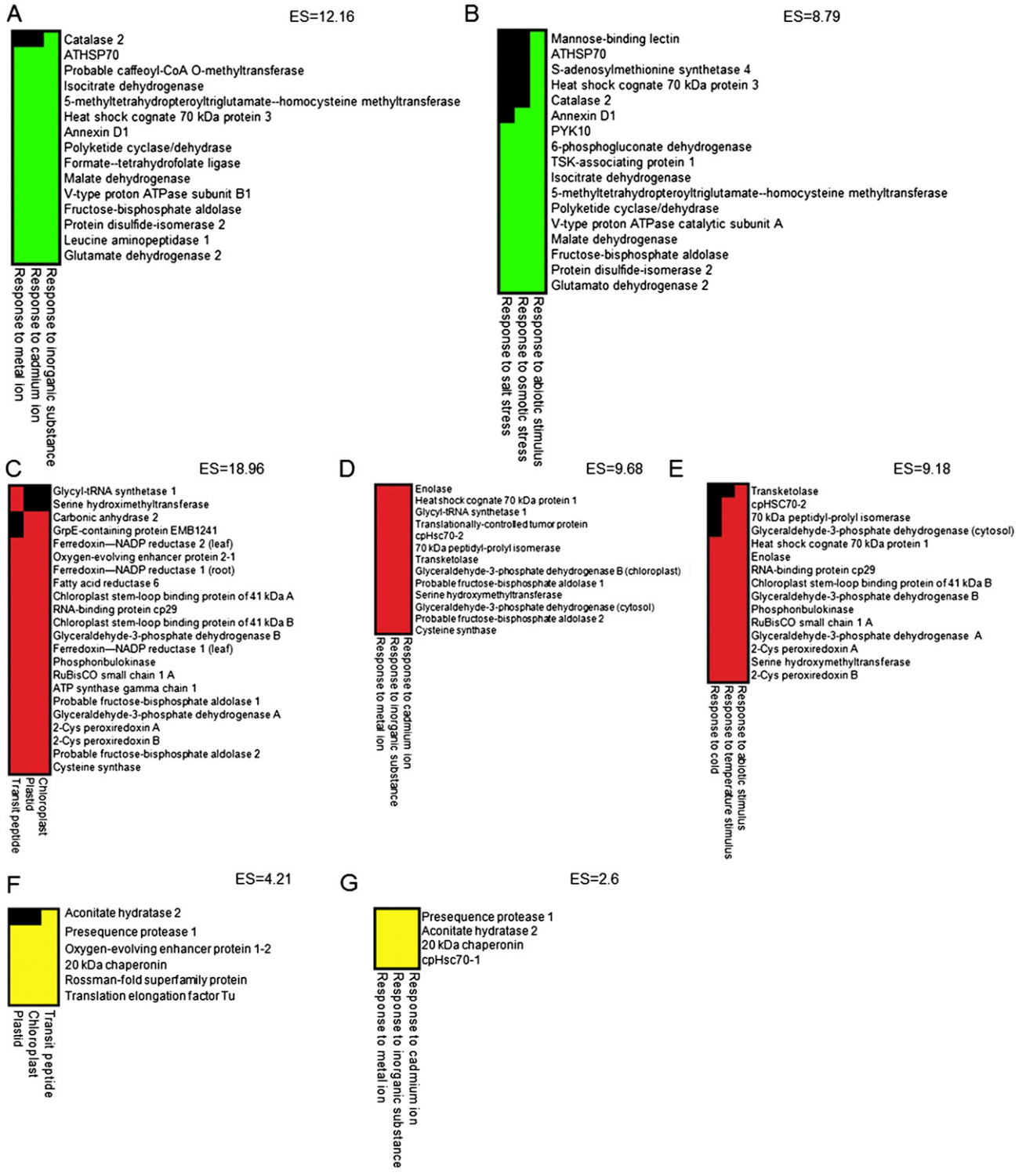

Fig. 4 – Functional clustering of the identified proteins. Significant clusters are shown of up- (A, B) and down-regulated (C, D, E) proteins, according to DAVID's functional annotation tool (http://david.abcc.ncifcrf.gov/home.jsp). Two nonsignificant clusters formed by the proteins with inconsistent abundance (F, G) are also displayed. The protein names on each cluster are shown at the right side, the corresponding GO terms are shown at the bottom of the corresponding panel, and the enrichment scores (ES) are shown at the top. The Enrichment Score is the geometric mean (in −log scale) of member's p-values in a corresponding annotation cluster.

to chloroplast functionality or development was determined. For this analysis, we choose the plastid- and the nuclear-encoded genes associated with chloroplast development, as shown in Table 2. As can be seen in Fig. 7, the different mutant lines under analysis display different expression levels of each marker gene; the *emb1241* and *pbp1* mutants clearly displayed

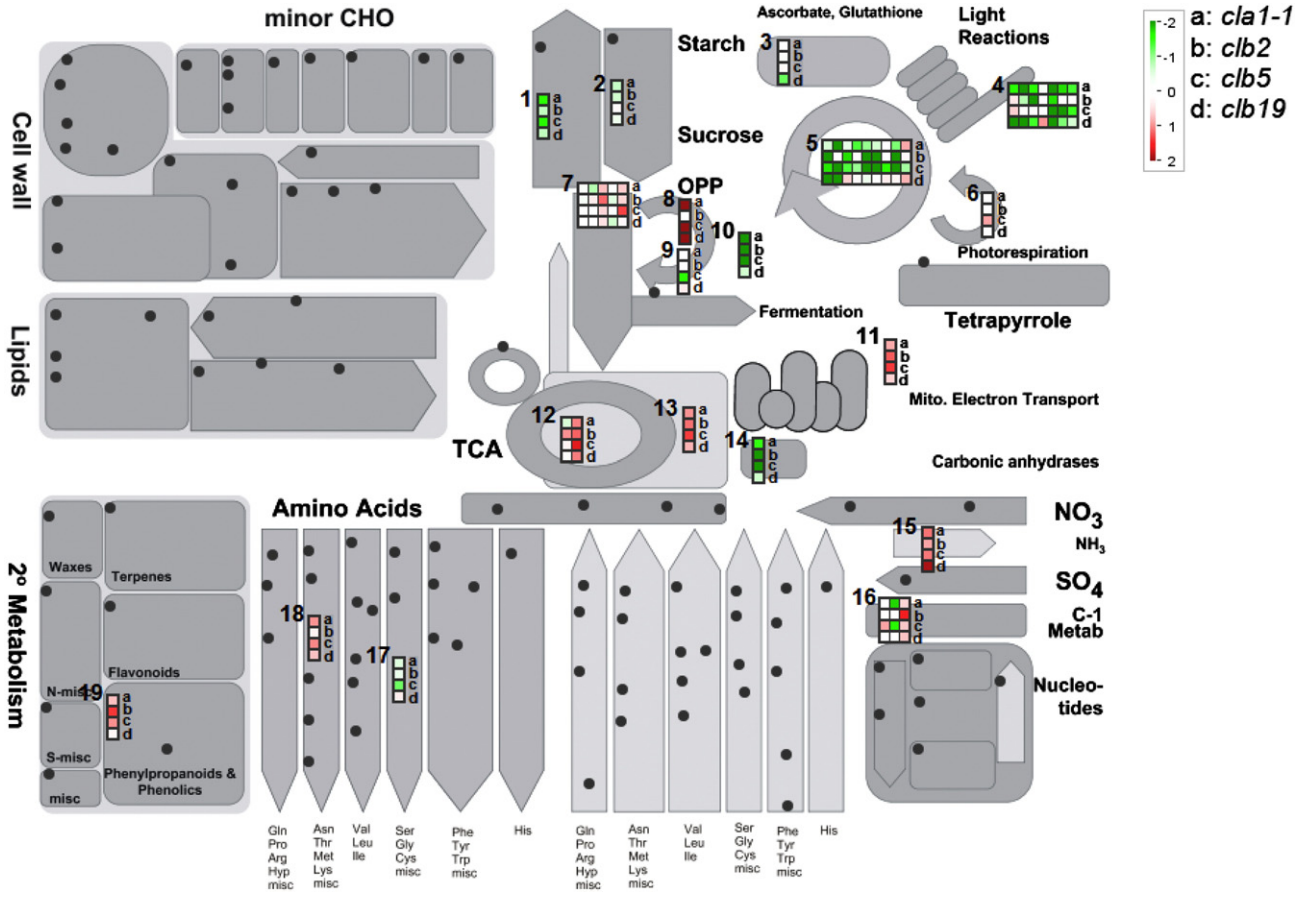

Fig. 5 – Mapping the identified proteins to metabolic pathways. The protein list (Table 1) was mapped to a database containing all the metabolic pathways of *Arabidopsis thaliana* using MapMan 3.5.1R2 software (http://mapman.gabipd.org/web/guest); matches between functions annotated in the database for a given pathway and the protein functionalities of the analyzed protein list are shown as a bin or group of bins (colored squares), whose color corresponds to its abundance level in each mutant compared to the wild-type levels. Abundance data is plotted using a $\log_2$ scale.

the strongest down-regulation of most marker genes, while the *atrabe1b* mutant showed expression levels closer to those of the wild-type (Fig. 7A, B). Compared to the wild-type expression levels, the *emb1241* mutant plants showed strong down-regulation of *psbA* (44%), *RBCS* (34%), *rrn16S* (43%), and *RPL21* (30%) genes; in a similar way, the expression levels of *psbA* (33%), *RBCS* (50%), and *rrn16S* (60%) marker genes displayed severe down-regulation in the *pbp1* mutant. On the other hand, mild down-regulation of *RPL21* (80%) was detected in *pbp1* mutants, as well as mild down-regulation of *accD* in both *emb1241* (95%) and *pbp1* (79%) plants.

Finally, the *atrabe1b* mutants displayed only small differences, if any, in the expression levels of most marker genes compared to those from the wild-type; *psbA* transcript levels did not display changes, compared to the wild-type plants, while *rrn16S* (106%) and *accD* (75%) genes showed a very slight increase and mild down-regulation of mRNA accumulation, respectively. Interestingly, in this mutant a substantial increase in *RBCS* (129%) and *RPL21* (152%) transcript levels was observed. These results indicate that the *embl241* and *pbp1* mutant lines are most affected for chloroplast biogenesis, while the *atrabe1b* line is least affected.

3.6. Chloroplast ultrastructure of mutant lines

Finally, to further access the developmental defects associated with each of these mutations, the ultrastructure of the plastids in each mutant line was analyzed using electron microscopy (Fig. 8). Compared to the wild-type plant, the *atrabe1b* mutant was found to be heteroplastidic, containing both wild-type-like and malformed plastids (Fig. 8). In the case of *emb1241* and *pbp1*, both mutants contain plastids of small size in which the development was arrested at an early stage (Fig. 8). Plastids in the *pbp1* mutant contain undeveloped internal membranes with long, single, linear membranes and have dense vesicles. In the case of *emb1241*, the plastids seemed to be arrested earlier since they lacked almost all internal membranes (Fig. 8).

4. Discussion

In this study, several different yet related mutant plants were compared using a classical proteomics workflow coupled with

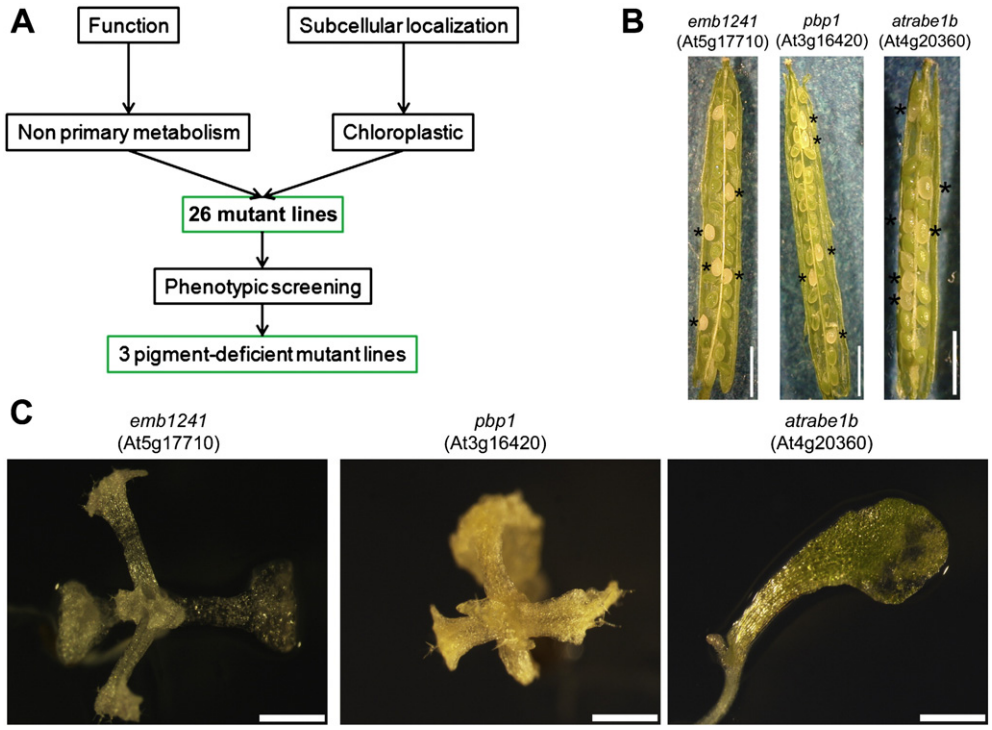

Fig. 6 – Screening the mutants for CLB-related proteins. The pipeline followed for the screening of the protein list is depicted (A). Criteria used for the candidate selection are shown in boxes. The 26 acquired mutant lines subjected to phenotypic screening are shown in Table 1. Siliques (B) and 16 day-old seedling (C) from the three mutant lines found to segregate plants with pigment accumulation defects (*emb1241*: albino; *pbp1*: yellow; *atrabe1b*: variegated) are shown. Scale bars represent 25 mm (B) and 10 μm (C).

phenotype screenings and a human-driven functional assessment; this resulted in the successful identification of proteins related to the development or functions of chloroplasts. Several of the identified proteins have known functions in the chloroplast machinery for protein import, photosynthesis, and other important chloroplast-related processes; such is the case for RBCS, CPN60, SCO1, and RuBisCO proteins (Table 1) [47–50]. Since these proteins are known to affect chloroplast development or function, we concluded that their presence among the 96 identified proteins validates our strategy. Furthermore, it was also possible to identify three proteins with mutant lines that displayed pigment-defective phenotypes and whose functions in chloroplast function have not yet been explored.

The up-regulated proteins cluster into two abiotic stress-related groups, one containing proteins related to ion stress (Fig. 4A; including response to Cd^{2+} ion) and the second one related to salt and osmotic stress (Fig. 4B); also, the down-regulated and inconsistent protein sets formed clusters that contain proteins related to the same ion stress (Fig. 4D, G). Similar results were reported by Motohashi et al. in 2012, when they compared the proteomes of 3 pigment-deficient mutants (*apg1–3*) and wild-type plants, one of the enriched GO terms consistently found to be 5 to 10 times up-regulated in

Table 2 – Chloroplast development molecular marker probes.

Monitored events	Molecular probe	Gene ID	Coding genome	Description
Early transcriptional activity				
	rrn16S	AtCg00920	Plastid	16S rRNA; highly expressed in proplastids.
	rpl21	At1g35680	Nucleus	Ribosomal protein L21; expressed early after seed imbibition.
Late transcriptional activity				
	accD	AtCg00500	Plastid	Acetyl-CoA carboxylase; chloroplast lipid biosynthesis; only transcribed by NEP[a]
Late chloroplast function				
	psbA	AtCg00020	Plastid	Photosystem II reaction center D1 protein.
	RBCS	At1g67090	Nucleus	RuBisCO small subunit.

[a] Nuclear-encoded RNA polymerase.

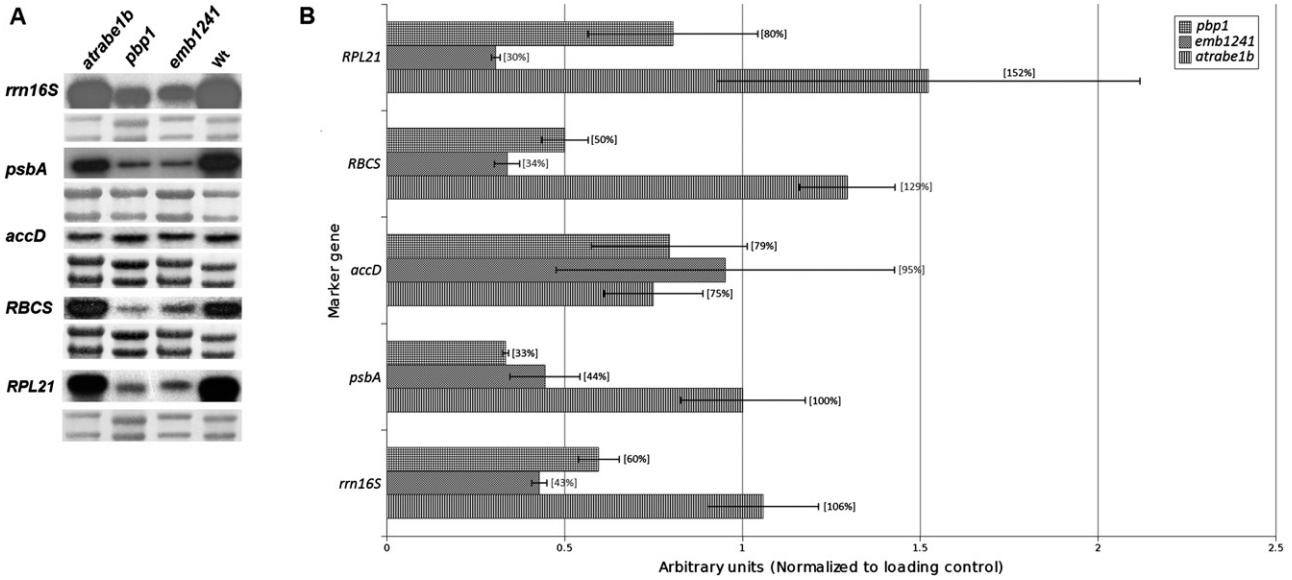

Fig. 7 – CLB marker gene expression analysis. A) Northern-blot hybridization of molecular probes for indicated marker gene on total RNA extracts from *atrabe1b*, *pbp1*, *emb1241*, and the wild-type (Wt) Wassilewskija (WS) ecotype. B) Densitometry analysis of Northern-blot hybridization, the ratio of the expression level of each probe in the mutants against the wild-type plants is shown (normalized to the corresponding loading controls; methylene blue staining; panels under each probe signal). For all mutants, the percentage of expression of each molecular probe compared to the wild-type plants is shown inside brackets: *rrn16S* (16S rRNA), *psbA* (Photosystem II reaction center D1 protein), *accD* (Acetyl-CoA carboxylase), *RBCS* (RuBisCO small subunit), *RPL21* (Ribosomal protein L21). A more detailed description of molecular probes is shown in Table 2. Error bars represent the mean ± standard error (SE) from data obtained from five independent experiments.

the *apg1–3* mutants was the response to Cd^{2+} ion [40]. There may not be a straightforward reason why all these pigment-deficient mutants display similar regulation of the response to ion stress, but it is possible that chloroplasts have molecular mechanisms that sense divalent cations (essential or toxic) in the cellular environment, such as Cd^{2+} and Mg^{2+}, and modulate the expression of proteins whose function might be affected by the intracellular levels of such ions. At the transcriptional level,

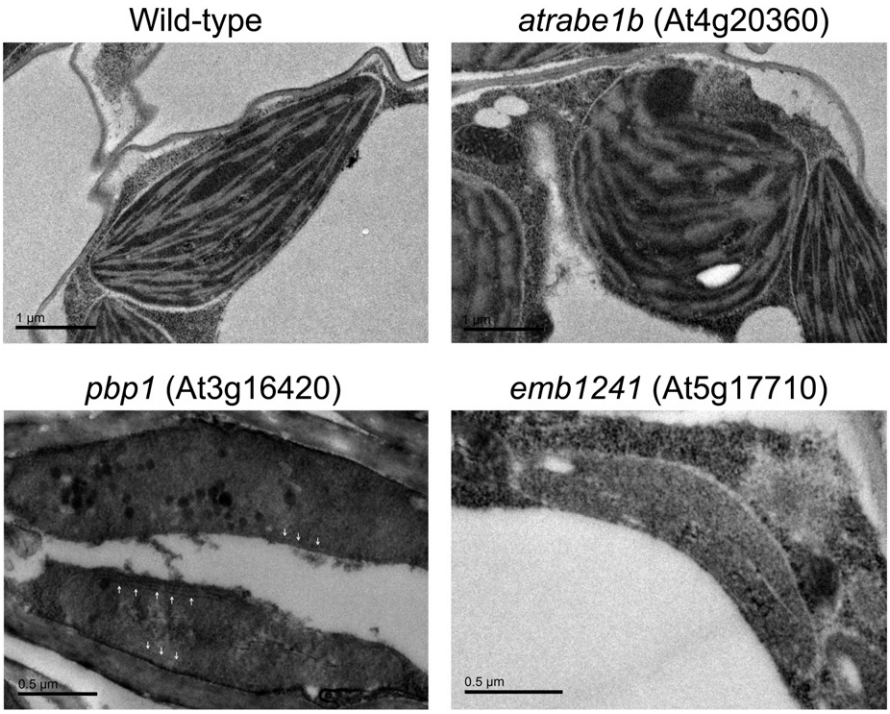

Fig. 8 – Ultrastructure of mutant plastids. Ultrastructure of mutant plastids was resolved by electron microscopy of leaves (*pbp1* and *emb1241*) or cotyledons (wild-type like and *atrabe1b*) from 16-day-old plants. Arrows indicate endomembranes.

evidence has been found that Mg^{2+} regulates the stability of chloroplastic mRNAs, such as *psbA*, *rbcL*, and *rrn16S* [51], strongly suggesting the existence of ion-sensing molecular mechanisms that might regulate protein accumulation in chloroplasts. Moreover, the down-regulated protein subset contains proteins that cluster due to temperature stress; also, Motohashi et al. reported the down-regulation of proteins related to responses to fungus and water deprivation in the *apg1–3* mutants [40]. Considering that data, it seems likely that chloroplasts function as stress-processing components, gathering information about the cellular conditions and modulating the expression of cpDNA- and nucleus-encoded genes. In the absence of properly developed chloroplasts (as in the case of the *clb* and *apg* mutants), the correct regulation of such genes and their products would be lost.

Further bioinformatic analysis of the protein list revealed that all four mutant lines display strong down-regulation of photosynthetic functions, both light-dependent and light-independent reactions (Fig. 5); at the same time, molecular processes involved in catabolic pathways show up-regulation in the mutant lines, clearly indicating that pigment-deficient plants (including *apg* mutants [40]) are forced to adopt a heterotrophic lifestyle. These results correlate with similar data reported by Motohashi et al. and directly reflect at the molecular level the impairment in chloroplast assembly displayed by the *clb* and *apg* mutants. Other processes consistently affected in the *clb* mutants are those related to amino acid metabolism and NH_3 homeostasis; the catabolism of glycogenic amino acids such as methionine is enhanced in mutant plants (Fig. 5, [44] Table S2 probably due to the possibility that its carbon skeleton can be assimilated into glucose, making this amino acid a valuable source of energy in the heterotrophic cellular environment; similar results were obtained by Motohashi et al., through the analysis of *apg1–3* mutants [40].

The data presented in Figs. 7 and 8 corroborate at the molecular and cellular levels the pipeline presented in Fig. 6; this validates assessment of function as a critical step when screening for proteins implicated in certain phenomena. Our gene expression and microscopic analyses demonstrated that *emb1241* and *pbp1* mutant lines had altered (earlier) chloroplast biogenesis, compared to *atrabe1b*. The *atrabe1b* mutant is able to assemble both normal and malformed plastids, even though the malformed plastids are able to generate considerable amounts of endomembranes and probably remain functional (Fig. 8). Given the low expression levels of the two early transcriptional activity marker genes (Fig. 7) and the complete lack of endomembranes in the plastids (Fig. 8), we concluded that the *emb1241* mutant is affected earliest in the chloroplast developmental processes, followed by the *pbp1* mutant. The slight down-regulation of *accD* transcript levels in *pbp1* mutants, along with the incipient formation of endomembranes in their plastids (Fig. 8), indicate that plastids in the *pbp1* mutants are able to progress to later developmental stages, which correlates with the slightly yellow pigmentation of the *pbp1* plants, indicating low levels of chlorophyll biosynthesis.

As shown in Table 1, the *EMB1241* gene codes for a chloroplastic GrpE-containing protein. GrpE proteins are bacterial co-chaperones that function as nucleotide-exchange factors in the chaperone/co-chaperone system DnaK/DnaJ/GrpE (reviewed in [52,53]). They enhance the activity of DnaK chaperones (such as Hsp70s) by improving the rate of release of the hydrolyzed ATP from the chaperon's ATPase domain [54,55]. It is likely that the EMB1241 protein plays a role in the import of proteins into the chloroplast to the stroma, given that bacterial-like chaperones such as Hsp70 and DnaJ exist in association with the TOC/TIC import machinery [56–61]. Moreover, it has been demonstrated that mutant lines lacking GrpE in *Physcomitrella patens* are defective in translocating proteins into chloroplasts [62]. Our data strongly support the conclusion that EMB1241 plays an important but not yet characterized role in the importation of proteins into *Arabidopsis* chloroplasts.

In the case of the *pbp1* mutant, we observed important defects in the endomembrane system, which contained only a few scattered thylakoids. At the transcription level, we found a slight down-regulation of the early transcriptional marker *rrn16S*, but strong down-regulation of late marker genes, which indicate that these plastids are able to progress to later developmental stages, compared to the *pbp1* mutant. This is supported by the yellow pigmentation of these mutants. Interestingly, the PBP1 protein is the major interacting protein of the inactive form of PYK10, a very well-characterized β-glucosidase enzyme that is involved in the interactions of plant roots and the mutualistic fungus *Piriformospora indica* [63]. PBP1 and PYK10 are predicted to have endoplasmic reticulum localization, and it is thought that PBP1 functions as a chaperone that is necessary for the proper folding of PYK10 that is required for activity [63,64]. Despite the fact that PBP1 has been studied in the past, the pigment-deficient phenotype displayed by *pbp1* mutant plants has not been previously reported. Interestingly, we observed only mild down-regulation (79%) of *accD* transcript levels in *pbp1* plants. The *accD* gene encodes for the Acetyl-CoA Carboxylase, an enzyme that catalyzes the synthesis of Malonil-CoA, which is the first committed metabolite of the chloroplastic fatty acid synthesis pathway [65]. This observation, in addition to the existence of contact sites between ER and chloroplast membranes that mediate lipid trafficking between both organelles and thus impacts thylakoid membrane composition [66–69], suggest that *pbp1* plants might contain altered lipid levels that affect the composition and function of thylakoid membranes. This possibility will be addressed in a future analysis. Furthermore, in 2005, Villarejo et al. reported that the plastid localized carbon anhydrase 1 (CA1) is imported through a secretory pathway. This finding provided evidence for the existence of a novel protein import pathway to the chloroplasts that depend on the endoplasmic reticulum and Golgi [46]. Taking into account the strong molecular and cellular chloroplast-development defects displayed by the *pbp1* mutant plants, the extensive evidence showing PBP1 endoplasmic reticulum localization and the existence of ER-dependent pathways to deliver proteins and lipids into the chloroplasts, it is possible that the PBP1 protein plays a role mediating one or both transport systems.

Finally, the ATRABE1B protein is a chloroplast resident bacterial-like Tu-type translation elongation factor (Table 1). Participation of putative bacterial-like translation elongation factors in chloroplast development has been previously documented; the SVR3 (suppressor of variegation 3) protein is a chloroplastic putative bacterial-like typA translation elongation

factor, and mutant lines affected in the expression of the *SVR3* gene display a pale green phenotype under normal conditions. Moreover, this phenotype is accentuated when mutants are challenged to cold stress [70]. ATRABE1B is part of the GTP-binding elongation-factor protein family that is composed of 6 members of *Arabidopsis*; given the slight variegation phenotype shown by the *atrabe1b* mutant (Fig. 6B), it is possible that functional redundancy exists within other members of the protein family, attenuating an otherwise strong phenotype.

5. Concluding remarks

In this study, using four pigment deficient mutants, we were able to identify proteins that were commonly or specifically affected among these lines. Further analysis allowed the identification of three novel proteins whose mutant lines displayed pigment-deficient phenotypes; transcriptional and electron microscopy analysis of these mutant plants showed that the identified proteins modulate the development or function of chloroplasts. Also, our analysis revealed clear evidence of heterotrophy as the *clb* mutant energy production strategy, as well as their severe impairment on photosynthesis.

Supplementary data to this article can be found online at http://dx.doi.org/10.1016/j.jprot.2014.07.003.

Transparency document

The Transparency document associated with this article can be found, in the online version.

Acknowledgments

The authors thank Patricia Jarillo for the technical support, Alma Lidia Martínez, Juan Manuel Hurtado, Roberto Rodríguez Bahena and Arturo Ocádiz for computer support, Paul Gaytan and Eugenio López for oligonucleotide synthesis and Guadalupe Zavala Padilla (UME, Instituto de Biotecnolgía, UNAM) and Fernando García Hernández (UM, Instituto de Fisiología Celular, UNAM) for chloroplast electron microscopy analysis. This work was supported by UNAM-DGAPA-PAPIIT (grants IN217111 to AGG and IN208211 to PL) and CONACYT-México (CB-129266 to AGG and 127546 to PL).

REFERENCES

[1] Kannangara C, Henningsen K, Stumpf P, Appelqvist L, von Wettstein D. Lipid biosynthesis by isolated barley chloroplasts in relation to plastid development. Plant Physiol 1971;48:526–31.
[2] Lichtenthaler H. The 1-deoxy-d-xylulose-5-phosphate pathway of isoprenoid biosynthesis in plants. Plant Mol Biol 1999;50:47–65.
[3] Kirk PR, Leech RM. Amino acid biosynthesis by isolated chloroplasts during photosynthesis. Plant Physiol 1972;50:228–34.
[4] Baldwin A, Wardle A, Patel R, Dudley P, Park SK, Twell D, et al. A molecular–genetic study of the Arabidopsis Toc75 gene family. Plant Physiol 2005;138:715–33.
[5] Hust B, Gutensohn M. Deletion of core components of the plastid protein import machinery causes differential arrest of embryo development in *Arabidopsis thaliana*. Plant Biol 2006;7:18–30.
[6] Chou ML, Fitzpatrick LM, Tu SL, Budziszewski G, Potter-Lewis S, Akita M, et al. Tic40, a membrane-anchored co-chaperone homolog in the chloroplast protein translocon. EMBO J 2003;22:2970–80.
[7] Kovacheva S, Bedard J, Patel R, Dudley P, Twell D, Rios G, et al. In vivo studies on the roles of Tic110, Tic40 and Hsp93 during chloroplast protein import. Plant J 2005;41:412–28.
[8] Constan D, Froehlich JE, Rangarajan S, Keegstra K. A stromal Hsp100 protein is required for normal chloroplast development and function in *Arabidopsis*. Plant Physiol 2004;136:3605–15.
[9] Mandel MA, Feldmann KA, Herrera-Estrella L, Rocha-Sosa M, Leon P. CLA1, a novel gene required for chloroplast development, is highly conserved in evolution. Plant J 1996;9:649–58.
[10] Guevara-Garcia A, San Román C, Arroyo A, Cortés ME, De La Luz Gutiérrez-Nava M, León P. Characterization of the *Arabidopsis* clb6 mutant illustrates the importance of posttranscriptional regulation of the methyl-D-erythritol 4-phosphate pathway. Plant Cell 2005;17(2):628–43.
[11] Chateigner-Boutin AL, Ramos-Vega M, Guevara-García A, Andrés C, De La Luz Gutiérrez-Nava M, Cantero A, et al. CLB19, a pentatricopeptide repeat protein required for editing of rpoA and clpP chloroplast transcripts. Plant J 2008;56(4):590–602.
[12] Koussevitzky S, Stanne TM, Peto CA, Giap T, Sjögren LL, Zhao Y, et al. An *Arabidopsis thaliana* virescent mutant reveals a role for ClpR1 in plastid development. Plant Mol Biol 2007;63(1):85–96.
[13] Schweer J, Türkeri H, Kolpack A, Link G. Role and regulation of plastid sigma factors and their functional interactors during chloroplast transcription—recent lessons from *Arabidopsis thaliana*. Eur J Cell Biol 2010;89:940–6.
[14] Ishizaki Y, Tsunoyama Y, Hatano K, Ando K, Kato K, Shinmyo A, et al. A nuclear-encoded sigma factor *Arabidopsis* SIG6, recognizes sigma-70 type chloroplast promoters and regulates early chloroplast development in cotyledons. Plant J 2005;42:133–44.
[15] Kroll D, Meierhoff K, Bechtold N, Kinoshita M, Westphal S, Vothknecht UC, et al. VIPP1, a nuclear gene of *Arabidopsis thaliana* essential for thylakoid membrane formation. Proc Natl Acad Sci U S A 2001;98(7):4238–42.
[16] Zhang L, Kato Y, Otters S, Vothknecht UC, Sakamoto W. Essential role of VIPP1 in chloroplast envelope maintenance in *Arabidopsis*. Plant Cell 2012;24(9):3695–707.
[17] Wang Q, Sullivan RW, Kight A, Henry RL, Huang J, Jones AM, et al. Deletion of the chloroplast-localized thylakoid formation1 gene product in *Arabidopsis* leads to deficient thylakoid formation and variegated leaves1. Plant Physiol 2004;136(3):3594–604.
[18] Larkin RM, Alonso JM, Ecker JR, Chory J. GUN4, a regulator of chlorophyll synthesis and intracellular signaling. Science 2003;299:902–6.
[19] Gutierrez-Nava M, Gillmor CS, Jiménez LF, Guevara-García A, León P. CHLOROPLAST BIOGENESIS genes act cell and noncell autonomously in early chloroplast development. Plant Physiol 2004;135(1):471–82.
[20] Tian L, DellaPenna D, Dixon R. The pds2 mutation is a lesion in the *Arabidopsis* homogentisate solanesyltransferase gene involved in plastoquinone biosynthesis. Planta 2007;226(4):1067–73.
[21] Avendaño-Vázquez AO, Cordoba E, Llamas E, San Román C, Nisar N, de la Torre S, et al. An uncharacterized apocarotenoid-derived signal generated in ζ-carotene

desaturase mutants regulates leaf development and the expression of chloroplast and nuclear genes in *Arabidopsis*. Plant Cell 2014;26:2524–37.
[22] Waters MT, Langdale JA. The making of a chloroplast. EMBO J 2009;28(19):2861–73.
[23] Pogson BJ, Albrecht V. Genetic dissection of chloroplast biogenesis and development: an overview. Plant Physiol 2011; 155(4):1545–51.
[24] Rho J, Mead JR, Wright WS, Brenner DE, Stave JW, Gildersleeve JC, et al. Discovery of sialyl Lewis a and Lewis X modified protein cancer biomarkers using high density antibody arrays. J Proteomics 2013;96:291–9.
[25] Kim PY, Tan O, Diakiw SM, Carter D, Sekerye EO, Wasinger VC, et al. Identification of plasma complement C3 as a potential biomarker for neuroblastoma using a quantitative proteomic approach. J Proteomics 2013;96:1–12.
[26] Bianchi L, Gagliardi A, Campanella G, Landi C, Capaldo A, Carleo A, et al. A methodological and functional proteomic approach of human follicular fluid en route for oocyte quality evaluation. J Proteomics 2013;90:61–76.
[27] Wang G, Guo Y, Zhou T, Shi X, Yu J, Yang Y, et al. In-depth proteomic analysis of the human sperm reveals complex protein compositions. J Proteomics 2013;79:114–22.
[28] Abreu IA, Farinha AP, Negrão S, Gonçalves N, Fonseca C, Rodrigues M, et al. Coping with abiotic stress: proteome changes for crop improvement. J Proteomics 2013;93:145–68.
[29] Sobhanian H, Aghaei K, Komatsu S. Changes in the plant proteome resulting from salt stress: toward the creation of salt-tolerant crops? J Proteomics 2011;74:1323–37.
[30] Kleffmann T, Russenberger D, von Zychlinski A, Christopher W, Sjolander K, Gruissem W, et al. The *Arabidopsis thaliana* chloroplast proteome reveals pathway abundance and novel protein functions. Curr Biol 2004;14:354–62.
[31] Friso G, Giacomelli L, Ytterberg A, Peltier J, Rudella A, Sun Q, et al. In-depth analysis of the thylakoid membrane proteome of *Arabidopsis thaliana* chloroplasts: new proteins, new functions, and a plastid proteome database. Plant Cell 2004; 16:478–99 [Online].
[32] Sun Q, Emanuelsson O, van Wijk K. Analysis of curated and predicted plastid subproteomes of *Arabidopsis*. Subcellular compartmentalization leads to distinctive proteome properties. Plant Physiol 2004;135(2):723–34.
[33] Kleffmann T, von Zychlinski A, Russenberger D, Hirsch-Hoffmann M, Gehrig P, Gruissem W, et al. Proteome dynamics during plastid differentiation in rice. Plant Physiol 2007;143:912–23.
[34] Majeran W, Cai Y, Sun Q, van Wijk K. Functional differentiation of bundle sheath and mesophyll maize chloroplasts determined by comparative proteomics. Plant Cell 2005;17:3111–40.
[35] Majeran W, Zybailov B, Ytterberg AJ, Dunsmore J, Sun Q, van Wijk K. Consequences of C4 differentiation for chloroplast membrane proteomes in maize mesophyll and bundle sheath cells. Mol Cell Proteomics 2008;7:1609–38.
[36] Kamal AH, Cho K, Choi JS, Bae KH, Komatsu S, Uozumi N, et al. The wheat chloroplastic proteome. J Proteomics 2013;93: 326–42.
[37] Bischof S, Baerenfaller K, Wildhaber T, Troesch R, Vidi PA, Roschitzki B, et al. Plastid proteome assembly without Toc159: photosynthetic protein import and accumulation of N-acetylated plastid precursor proteins. Plant Cell 2011;11: 3928–39113.
[38] Kim J, Rudella A, Ramirez-Rodriguez V, Zybailov B, Olinares PDB, van Wijk K. Subunits of the plastid ClpPR protease complex have differential contributions to embryogenesis, plastid biogenesis, and plant development in *Arabidopsis*. Plant Cell 2009;21(6):1669–92.
[39] Rutschow H, Ytterberg AJ, Friso G, Nilsson R, van Wijk KJ. Quantitative proteomics of a chloroplast SRP54 sorting mutant and its genetic interactions with CLPC1 in *Arabidopsis*. Plant Physiol 2008;148(1):156–75.
[40] Motohashi R, Rodiger A, Agne B, Baerenfaller K, Baginsky S. Common and specific protein accumulation patterns in different albino/pale-green mutants reveals regulon organization at the proteome level. Plant Physiol 2012;160(4): 2189–201.
[41] Hurkman WJ, Tanaka CK. Solubilization of plant membrane proteins for analysis by two-dimensional gel electrophoresis. Plant Physiol 1986;81(3):802–6.
[42] Encarnación S, Hernández M, Martínez-Batallar G, Contreras S, Del Carmen Vargas M, Mora J. Comparative proteomics using 2-D gel electrophoresis and mass spectrometry as tools to dissect stimulons and regulons in bacteria with sequenced or partially sequenced genomes. Biol Proced 2005;7(1):117–35 [online].
[43] Huang DW, Sherman BT, Lempicki RA. Systematic and integrative analysis of large gene lists using DAVID Bioinformatics Resources. Nat Protoc 2009;4(1):44–57.
[44] de Luna-Valdez LA, Martínez-Batallar AG, Hernández-Ortiz M, Encarnación-Guevara S, Ramos-Vega M, López-Bucio JS, et al. Data for proteomic analysis of chloroplast biogenesis(clb) mutants uncovers novel proteins potentially involved in the development of Arabidopsis thaliana chloroplasts 2014. http://dx.doi.org/10.1016/j.dib.2014.07.001 [In Press, Accepted Manuscript, Available online 12 August 2014].
[45] Li Q, Huang J, Liu S, Li J, Yang X, Liu Y, et al. Proteomic analysis of young leaves at three developmental stages in an albino tea cultivar. Proteome Sci 2011;9(1):44.
[46] Villarejo A, Burén S, Larsson S, Déjardin A, Monné M, Rudhe C, et al. Evidence for a protein transported through the secretory pathway en route to the higher plant chloroplast. Nat Cell Biol 2005;7(12):1224–31.
[47] Izumi M, Tsunoda H, Suzuki Y, Makino A, Ishida H. RBCS1A and RBCS3B, two major members within the Arabidopsis RBCS multigene family, function to yield sufficient RuBisCO content for leaf photosynthetic capacity. J Exp Bot 2012;63(5):2159–70.
[48] Suzuki K, Nakanishi H, Bower J, Yoder D, Osteryoung K, Miyagishima S. Plastid chaperonin proteins Cpn60α and Cpn60β are required for plastid division in *Arabidopsis thaliana*. BMC Plant Biol 2009;9(38). http://dx.doi.org/10.1186/1471-2229-9-38.
[49] Albrecht V, Ingenfeld A, Apel K. Characterization of the snowy cotyledon 1 mutant of *Arabidopsis thaliana*: the impact of chloroplast elongation factor G on chloroplast development and plant vitality. Plant Mol Biol 2006;60(4):507–18.
[50] Somerville C, Portis A, Ogren W. A mutant of *Arabidopsis thaliana* which lacks activation of RuBP carboxylase in vivo. Plant Physiol 1982;70(2):381–7.
[51] Horlitz M, Klaff P. Gene-specific trans-regulatory functions of magnesium for chloroplast mRNA stability in higher plants. J Biol Chem 2000;275(45):35638–45.
[52] Flores-Pérez Ú, Jarvis P. Molecular chaperone involvement in chloroplast protein import. Biochim Biophys Acta 2013; 1833(2):332–40.
[53] Fink A. Chaperone-mediated protein folding. Physiol Rev 1999;70(2):425–42.
[54] Liberek K, Marszalek J, Ang D, Georgopoulos C, Zylicz M. *Escherichia coli* DnaJ and GrpE heat shock proteins jointly stimulate ATPase activity of DnaK. Proc Natl Acad Sci 1991; 88(7):2874–8.
[55] Harrison CJ, Hayer-Hartl M, Di Liberto M, Hartl FU, Kuriyan J. Crystal structure of the nucleotide exchange factor GrpE bound to the ATPase domain of the molecular chaperone DnaK. Science 1997;276:431–5.
[56] Becker T, Hritz J, Vogel M, Caliebe A, Bukau B, Soll J, et al. Toc12, a novel subunit of the intermembrane space preprotein translocon of chloroplasts. Mol Biol Cell 2004;15: 5130–44.

[57] Sohrt K, Soll J. Toc64, a new component of the protein translocon of chloroplasts. J Cell Biol 2000;148:1213–21.
[58] Ivey III RA, Bruce BD. In vivo and in vitro interaction of DnaK and a chloroplast transit peptide. Cell Stress Chaperones 2000;5:62–71.
[59] Ivey III RA, Subramanian C, Bruce BD. Identification of a Hsp70 recognition domain within the RuBisCO small subunit transit peptide. Plant Physiol 2000;122:1289–99.
[60] Rial DV, Arakaki AK, Ceccarelli EA. Interaction of the targeting sequence of chloroplast precursors with Hsp70 molecular chaperones. Eur J Biochem 2000;267:6239–48.
[61] Zhang XP, Glaser E. Interaction of plant mitochondrial and chloroplast signal peptides with the Hsp70 molecular chaperone. Trends Plant Sci 2002;7:14–21.
[62] Shi LX, Theg SM. A stromal heat shock protein 70 system functions in protein import into chloroplasts in the moss *Physcomitrella patens*. Plant Cell 2010;22(1):205–20.
[63] Ahn YO, Shimizu B, Sakata K, Gantulga D, Zhou Z, Bevan DR, et al. Scopolin-hydrolyzing-glucosidases in roots of *Arabidopsis*. Plant Cell Physiol 2010;51(1):132–43.
[64] Nagano AJ, Matsushima R, Hara-Nishimura I. Activation of an ER-body-localized β-glucosidase via a cytosolic binding partner in damaged tissues of *Arabidopsis thaliana*. Plant Cell Physiol 2005;46(7):1140–8.
[65] Li-Beisson Y, Shorrosh B, Beisson F, Andersson MX, Arondel V, Bates PD, et al. Acyl-lipid metabolism. Arabidopsis Book 2013;11:e0161.
[66] Wang Z, Benning C. Chloroplast lipid synthesis and lipid trafficking through ER–plastid membrane contact sites. Biochem Soc Trans 2012;40(2):457–63.
[67] Andersson MX, Goksor M, Sandelius AS. Optical manipulation reveals strong attracting forces at membrane contact sites between endoplasmic reticulum and chloroplasts. J Biol Chem 2006;282(2):1170–4.
[68] Roughan PG, Holland R, Slack CR. The role of chloroplasts and microsomal fractions in polar-lipid synthesis from [1-14C] acetate by cell-free preparations from spinach (*Spinacia oleracea*) leaves. Biochem J 1980;188(1):17–24.
[69] Benning C. Mechanisms of lipid transport involved in organelle biogenesis in plant cells. Annu Rev Cell Dev Biol 2009;25(1):71–91.
[70] Liu X, Rodermel SR, Yu F. A var2 leaf variegation suppressor locus, SUPPRESSOR OF VARIEGATION3, encodes a putative chloroplast translation elongation factor that is important for chloroplast development in the cold. BMC Plant Biol 2010; 10(1):287.

MPMI Vol. 28, No. 6, 2015, pp. 701–710. http://dx.doi.org/10.1094/MPMI-01-15-0005-R

e-Xtra*

Mitogen-Activated Protein Kinase 6 and Ethylene and Auxin Signaling Pathways Are Involved in *Arabidopsis* Root-System Architecture Alterations by *Trichoderma atroviride*

Hexon Angel Contreras-Cornejo,[1] Jesús Salvador López-Bucio,[2] Alejandro Méndez-Bravo,[1] Lourdes Macías-Rodríguez,[1] Maricela Ramos-Vega,[2] Ángel Arturo Guevara-García,[2] and José López-Bucio[1]

[1]Instituto de Investigaciones Químico-Biológicas, Universidad Michoacana de San Nicolás de Hidalgo. Edificio B3, Ciudad Universitaria. C. P. 58030, Morelia, Michoacán, México; [2]Instituto de Biotecnología, Universidad Nacional Autónoma de México, Apartado Postal 510-3, 62250 Cuernavaca, Morelos, México

Submitted 6 January 2015. Accepted 30 January 2015.

Trichoderma atroviride **is a symbiotic fungus that interacts with roots and stimulates plant growth and defense. Here, we show that *Arabidopsis* seedlings cocultivated with *T. atroviride* have an altered root architecture and greater biomass compared with axenically grown seedlings. These effects correlate with increased activity of mitogen-activated protein kinase 6 (MPK6). The primary roots of *mpk6* mutants showed an enhanced growth inhibition by *T. atroviride* when compared with wild-type (WT) plants, while *T. atroviride* increases MPK6 activity in WT roots. It was also found that *T. atroviride* produces ethylene (ET), which increases with L-methionine supply to the fungal growth medium. Analysis of growth and development of WT seedlings and *etr1*, *ein2*, and *ein3* ET-related *Arabidopsis* mutants indicates a role for ET in root responses to the fungus, since *etr1* and *ein2* mutants show defective root-hair induction and enhanced primary-root growth inhibition when cocultivated with *T. atroviride*. Increased MPK6 activity was evidenced in roots of *ctr1* mutants, which correlated with repression of primary root growth, thus connecting MPK6 signaling with an ET response pathway. Auxin-inducible gene expression analysis using the *DR5:uidA* reporter construct further revealed that ET affects auxin signaling through the central regulator CTR1 and that fungal-derived compounds, such as indole-3-acetic acid and indole-3-acetaldehyde, induce MPK6 activity. Our results suggest that *T. atroviride* likely alters root-system architecture modulating MPK6 activity and ET and auxin action.**

Plants integrate a network of external stimuli, including light, temperature, nutrients, soil pH, and the presence of organisms such as other plants, microbes, nematodes, and insects to adjust their growth and development. Plant developmental patterns are regulated by different phytohormones, mainly auxins, cytokinins and ethylene (ET), while interactions among hormonal pathways modulate morphogenesis (Acharya and Assmann 2009).

The rhizosphere is the soil region that is influenced by roots due to exudation of carbohydrates, amino acids, organic acids, and mucilage, which represent a rich source for nutrients for microbial populations. On the other hand, microorganisms inhabiting roots may have a strong influence on plant growth and health. Root-microbe communication occurs through release of diverse signaling molecules, leading to symbiosis events that improve plant fitness directly or indirectly. As an example, most angiosperms develop symbiotic interactions with fungal species, such as mycorrhizal fungi, *Piriformospora indica*, and *Trichoderma* spp., which may act in biocontrol of pathogens, activating defense responses, boosting nutrient uptake, or producing growth-regulating substances (Contreras-Cornejo et al. 2013; Khatabi et al. 2012).

Trichoderma species are frequently found in agricultural soils as common inhabitants of the rhizosphere. *T. virens* and *T. atroviride* produce auxins and auxin-like compounds that affect both root-hair and lateral-root development (Contreras-Cornejo et al. 2009, 2014). Root responses to auxin are mediated by three protein families, i.e., the AUXIN RESPONSE FACTOR (ARF) family of transcription factors, responsible for the regulation of auxin-inducible gene expression, the AUXIN/INDOLE-3-ACETIC ACID (AUX/IAA) transcriptional inhibitors, which interact with ARF to prevent their action, and F-box proteins that are part of the ubiquitin protein ligase SCF^{TIR1} complex controlling the rapid ubiquitin-mediated degradation of AUX/IAA proteins in response to auxin (Růzicka et al. 2007). Inside cells, auxin binds to the TRANSPORT INHIBITOR RESPONSE 1/AUXIN SIGNALING F-BOX (TIR1/AFB) family of F-box proteins, which are subunits of the SCF E3-ligase protein complex, to lead the ubiquitination and the proteasome-mediated specific degradation of AUX/IAA transcriptional repressors. Subsequently, the ARF are released to activate auxin-inducible gene expression (Dharmasiri et al. 2005).

In a recent report, the potential of *T. virens* and *T. atroviride* to confer salt tolerance to *Arabidopsis* seedlings through an auxin signaling pathway was explored. It was found that salt represses plant growth and root development in a dose-dependent manner blocking auxin signaling. Analysis of WT and ETHYLENE INSENSITIVE ROOT 1 (*eir1*), *aux1-7*,

Corresponding author: José López-Bucio; Telephone: +52 (443) 3265788; Fax: +52 (443) 3265788; E-mail: jbucio@umich.mx

*The *e*-Xtra logo stands for "electronic extra" and indicates that five supplementary figures are published online.

arf7arf19, and *tir1afb2afb3* auxin-related mutants, revealed a key role for IAA signaling in mediating salt tolerance. Interestingly, *T. virens* (Tv29.8) and *T. atroviride* (IMI 206040) promoted plant growth in both normal and saline conditions that was related to the induction of lateral roots and root hairs through auxin signaling (Contreras-Cornejo et al. 2014).

ET also regulates root developmental processes, acting either synergistically or independently of auxin signaling (Muday et al. 2012). For instance, ET promotes root-hair initiation and elongation but, in contrast to auxin, ET inhibits lateral root formation and elongation (Bleecker and Kende 2000; Johnson and Ecker 1998; Pitts et al. 1998). ET is perceived by ET-binding receptors, such as ETHYLENE RESPONSE 1 (ETR1) and ETHYLENE RECEPTOR SUBFAMILY 1 (ERS1). The activation of these receptors causes repression of CONSTITUTIVE TRIPLE RESPONSE 1 (CTR1), which, in turn, permits ETHYLENE INSENSITIVE 2 (EIN2) to relay the ET signal to the transcription factors EIN3 and ETHYLENE-INSENSITIVE3-LIKE (EIL). EIN3 activates ETHYLENE RESPONSE FACTOR 1 (ERF1), inducing the expression of ET-responsive genes (Huang et al. 2003; Kieber et al. 1993; Sánchez-Rodríguez et al. 2010). Loss-of-function mutations in *ETHYLENE-INSENSITIVE 2* and *3* severely limit the plant's response to ET (Chao et al. 1997).

Intracellular signaling processes that translate microbial perception into genetic, metabolic, and developmental responses in roots are the focus of current plant-microbe interactions research. Important signaling pathways involved in recognition of microbial elicitors, such as pathogen- or microbe-associated molecular patterns, as well as growth regulating substances such as auxins or ET or both include mitogen-activated protein kinase (MAPK) cascades (Zhang et al. 2006). MAPKs act through phosphorylation events in which a MAPK kinase kinase (MPKKK) phosphorylates a MAPK kinase and this, in turn, activates a MAPK (MPK6) to translate external stimuli into cellular responses (Colcombet and Hirt 2008). MAPKs mediate responses to a variety of signaling molecules, such as reactive oxygen species, flagellin, UV light, brassinosteroids, ET, and nitric oxide. Indeed, MAPKs phosphorylate different substrates, including other kinases, phosphatases, or transcription factors, to regulate stomatal, embryo, and root development (Brader et al. 2007; Yoo et al. 2008). In a recent study, the role of MPK6 in *Arabidopsis* embryo development and in postembryonic root system architecture was unraveled (López-Bucio et al. 2014). The *mpk6* mutation caused alterations in embryo development and in root architecture characterized by a primary root longer than that of the WT, accompanied by significantly increased lateral root initiation and more and longer root hairs. Apparently, the increment in primary root growth resulted from an enhanced cell production and cell elongation. These data demonstrated that MPK6 acts as a repressor of primary and lateral root development as well as root-hair differentiation and growth (López-Bucio et al. 2014).

So far, all described information indicates that *Trichoderma* spp. improve plant growth and modulate root architecture by producing auxins and other signaling molecules, while the mechanisms by which the plant senses the fungal signals remain to be characterized. In this work, we show that *T. atroviride* regulates root architecture and increases MPK6 activity, likely depending on ET and auxin signaling. It was found that ET, IAA, and IAAld (indole-3-acetaldehyde) produced by the fungus induce MPK6 activity. Also, molecular and phenotypical analysis of ET-related mutants *ctr1*, *ein2*, *ein3*, and *etr1* indicate an important role of ET in *T. atroviride* modulation of root architecture. Further analysis of auxin-related gene expression in WT seedlings and *ctr1* mutants expressing the *DR5:uidA* construct showed that the effect of ET on root growth and differentiation is apparently mediated by auxin signaling, thus indicating that an auxin-ET crosstalk involving MPK6 fine-tunes seedling growth and development in response to a beneficial soil fungus.

RESULTS

T. atroviride regulates root architecture and increases MPK6 activity.

The effects of *T. atroviride* on *Arabidopsis* growth and development were investigated using an in vitro fungus-plant interaction system. To test the possibility that some volatile or diffusible fungal compounds could be involved in promoting plant growth, fungal spores were placed at a distance of 5 cm from the primary root tip. In such experimental conditions, without any root-mycelium physical contact, *T. atroviride* clearly promoted lateral-root and root-hair formation and increased total plant biomass production (Supplementary Fig. S1).

MPK6 regulates plant responses during plant-microbe interactions (Merkouropoulos et al. 2008; Ren et al. 2008), and recently, it was considered as a negative regulator of root development, as the *mpk6* mutant produced more lateral roots and root hairs than WT seedlings (López-Bucio et al. 2014). Here, the possible involvement of MPK6 in root responses to *T. atroviride* was investigated. In experiments in which WT (Col-0) and *mpk6* mutant seedlings were grown side by side on axenic agar-solidified Murashige and Skoog (MS) 0.2× medium and in the same conditions but in the presence of the fungus, root-hair parameters were analyzed 2 days after inoculation (d.a.i.). It was found that *T. atroviride* increased 50% the length of root hairs and 25% the root-hair density in WT plants (Fig. 1A to F). Meanwhile, when grown under axenic conditions, *mpk6* mutants produced significantly longer root hairs and increased root-hair density than WT seedlings, but when cocultivated with *T. atroviride*, the increase in the length of root hairs and root-hair density was similar to the WT (Fig. 1A to F).

In contrast to root hairs, the primary roots of inoculated *mpk6* plants showed an enhanced growth inhibition by *T. atroviride* when compared with WT plants, whose primary root growth was unaffected by the presence of the fungus (Fig. 2A). In addition, in relation to their respective axenic controls, the lateral root number of WT plants cocultivated with *T. atroviride* increased 400%, while inoculated *mpk6* plants increased only 40% (Fig. 2B). The greater ability of *mpk6* mutants to develop lateral root meristems under axenic conditions may explain why *T. atroviride* did not increase further the number of lateral roots in the mutant as compared with the WT.

To test if *T. atroviride* has some effect on MPK6 activity, an in-gel MAPK assay was performed, using fungus-challenged plant material from *Arabidopsis* WT seedlings in which no contact between the mycelium and the primary root had been established (4 d.a.i.) and another in which 30% of the root system was covered by the fungal colony (6 d.a.i.). In both cases, we found that MPK6 activity increases after inoculation (Fig. 2C). The induction of MPK6 activity by *T. atroviride* was absent in *mpk6 Arabidopsis* mutants (Supplementary Fig. S2). These results show that *T. atroviride* modulates plant growth and that MPK6 probably is involved in this signaling pathway.

T. atroviride releases ET in response to L-methionine supply.

Several rhizospheric fungi are able to produce plant hormones (Barbieri and Galli 1993; Contreras-Cornejo et al. 2009; Malhotra and Srivastava 2008; Patten and Glick 2002; Splivallo

et al. 2009; Suzuki et al. 2003). A major effect of *T. atroviride* is regulating root-hair morphogenesis, a trait that is under ET and auxin control, opening the possibility that the fungus could produce this kind of compound. As we already identified IAA and auxin-related compounds produced by *Trichoderma* spp. (Contreras-Cornejo et al. 2009), we now conducted experiments aimed at evaluating whether these compounds were present in the growth medium after growth of *T. atroviride* colonies by gas chromatography (GC)-mass spectrometry. All three compounds, namely IAA, IAAld, and ICAld (indole-3-carboxaldehyde), could be identified as some of the metabolites produced by *T. atroviride* (Supplementary Fig. S3). ET production by *T. atroviride* was also determined by GC-mass spectrometry analyses. For this, the fungus was grown on petri dishes and the volatile compound was released to the headspace of the plates. We identified ET (retention time: 2.39 min) released by the fungal colony at 4 and 6 days of growth (Fig. 3A and B). Importantly, when 1 mM L-methionine was added to the culture medium, the production of ET was substantially increased (Fig. 3B). These data confirm that *T. atroviride* produces auxins and show that it could induce root architectural changes by producing ET.

T. atroviride modulates root-hair development through ET signaling.

ET regulates root-hair elongation through binding to the ET receptor ETR1, which regulates CTR1, EIN2, and EIN3 downstream (Pitts et al. 1998; Yoo et al. 2008). To determine whether *T. atroviride* induced root-hair formation through ET signaling, we analyzed the effects of fungal cocultivation on root-hair length and density in WT and *etr1-1*, *ein2-1*, and *ein3-1* ET-related mutant lines. As previously reported (Pitts et al. 1998), axenically grown *etr1-1* and *ein2-1* mutants showed a significant reduction in root-hair length and density when compared with WT plants, whereas the *ein3-1* mutant showed only a small but yet significant reduction (Fig. 4A to J). In these experiments, *T. atroviride* clearly increased root-hair length and density in the WT, an effect that was absent in the three ET-related mutants analyzed (Fig. 4A to J). Treatment with silver nitrate ($AgNO_3$), an ET inhibitor, impaired root-hair development in WT and *mpk6* mutants grown under axenic conditions or cocultivated with *T. atroviride*. In contrast, treatment with the auxin transport inhibitor *N*-1-naphthylphthalamic acid (NPA) stimulated root-hair growth in both WT and *mpk6* seedlings (Supplementary Fig. S4). Our results indicate that an intact ET signaling pathway is required for mediating the effects of *T. atroviride* on root-hair development, likely involving MPK6.

T. atroviride modifies lateral root formation through a MPK6 and ET-independent mechanism.

To further investigate whether all the effects of *T. atroviride* on root-system architecture involved components of the ET signaling pathway, we cocultivated WT *Arabidopsis* seedlings and ET-related mutants with the fungus and primary root growth and lateral root formation were analyzed. When grown under axenic conditions, the primary roots of *etr1*, *ein2*, and *ein3* mutants were longer than WT. In contrast, when cocultivated with *T. atroviride,* the growth of the primary roots of WT plants was unaffected, whereas primary root growth of *ein 2* and *ein3* was inhibited (Fig. 5A). The analysis of lateral root formation showed that the *etr1*, *ein2*, and *ein3* mutants already produced three- to sixfold more lateral roots than WT seedlings and manifested a normal induction of lateral roots by *T. atroviride* (Fig. 5B). Similar effects were observed in the analysis performed with the *mpk6* mutant (Fig. 2). These data suggest that, in contrast to root-hair growth, induction of lateral root

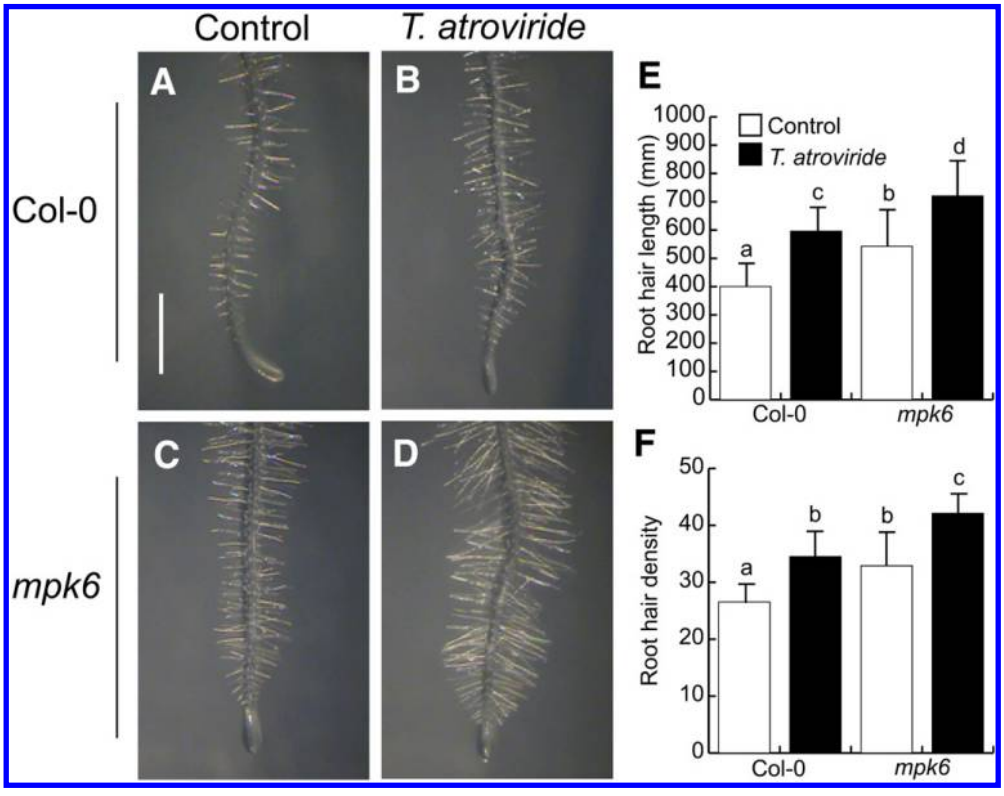

Fig. 1. *Trichoderma atroviride* effects on root-hair density and development. **A** to **D,** Representative roots from wild-type (Col-0) and *mpk6* mutant seedlings 6 days after germination, uninoculated (A and C) or inoculated with *T. atroviride* (B and D). Bar = 500 µm. **E,** Average length of root hairs. **F,** Root-hair density (number of root hairs per cemtimeter). Values shown represent the mean of 100 root hairs ± standard deviation. Different letters are used to indicate means that differ significantly ($P < 0.05$).

formation by *T. atroviride* is an MPK6 and ET-independent process.

MPK6 activity is induced in the *ctr1* mutant of *Arabidopsis*.

The ET signaling pathway is negatively controlled by the master regulator CONSTITUTIVE TRIPLE RESPONSE 1 (CTR1), which encodes a Raf-like MPKKK (Huang et al. 2003; Kieber et al. 1993). To investigate the contribution of the ET signaling pathway on the MPK6 activity through CTR1, we performed gel kinase assays on the mutant line *ctr1*, growing both under standard light and in darkness conditions. Under a 16-h light and 8-h dark photoperiod, MPK6 activity in the shoots of Col-0 and the *ctr1* mutant was similar but the kinase activity was increased in the root of the *ctr1* mutant (Fig. 6A). In the case of shoots and etiolated conditions, no significant differences in MPK6 activity were found between Col-0 and *ctr1* seedlings. Interestingly, a positive correlation could be established between the increase of MPK6 activity and the repression of the primary root growth in *ctr1* seedlings (Fig. 6B). In *ein2* mutants, a normal or slightly decreased MPK6 activity could be determined (Fig. 6C). These results indicate

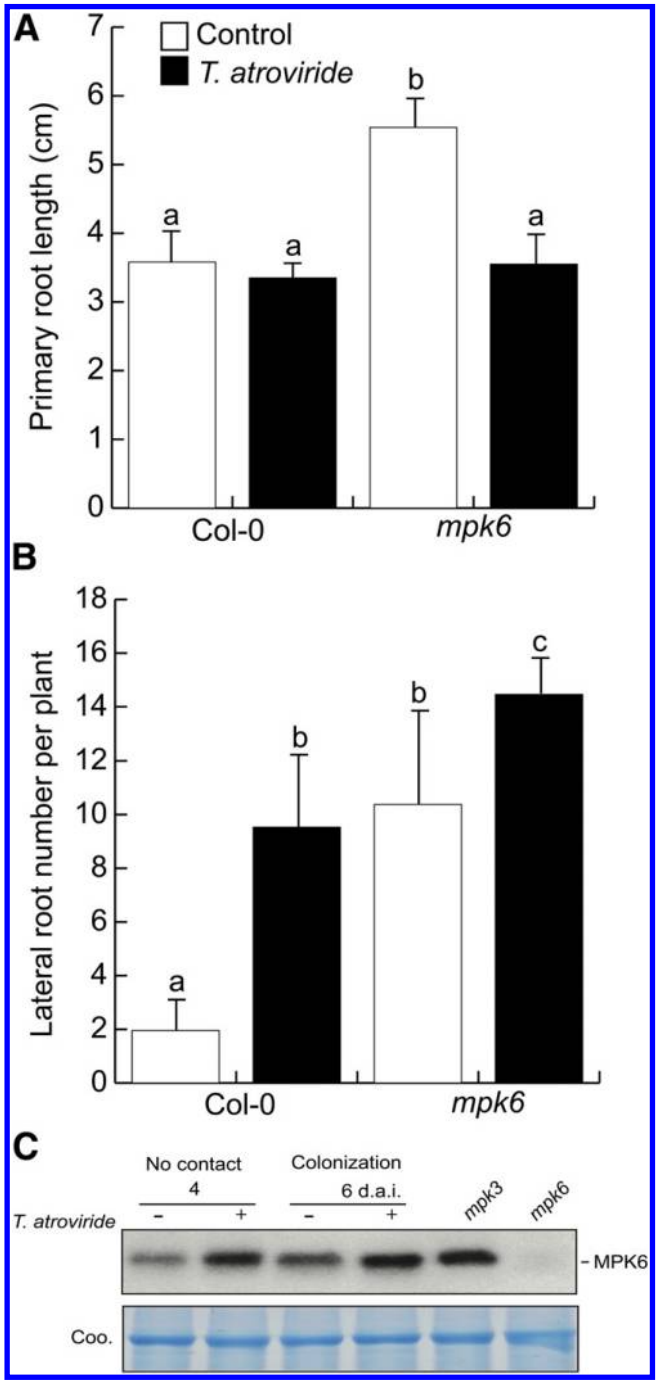

Fig. 2. *Trichoderma atroviride* effects on root-system architecture and MPK6 activity. **A,** Primary root length and **B,** lateral root number of wild-type (Col-0) and *mpk6* mutant seedlings 10 days after germination. Root system parameters were quantified for 15 seedlings and different letters are used to indicate means that differ significantly ($P < 0.05$). The experiment was repeated three times with similar results. **C,** In-gel mitogen-activated protein kinase assays using total protein extracts (30 µg) from Col-0 seedlings growing in the presence of *T. atroviride* by 4 and 6 days. The Coomassie stained gel (Coo) is shown as loading control and *mpk6* and *mpk3* mutants were included as reference of MPK6 activity.

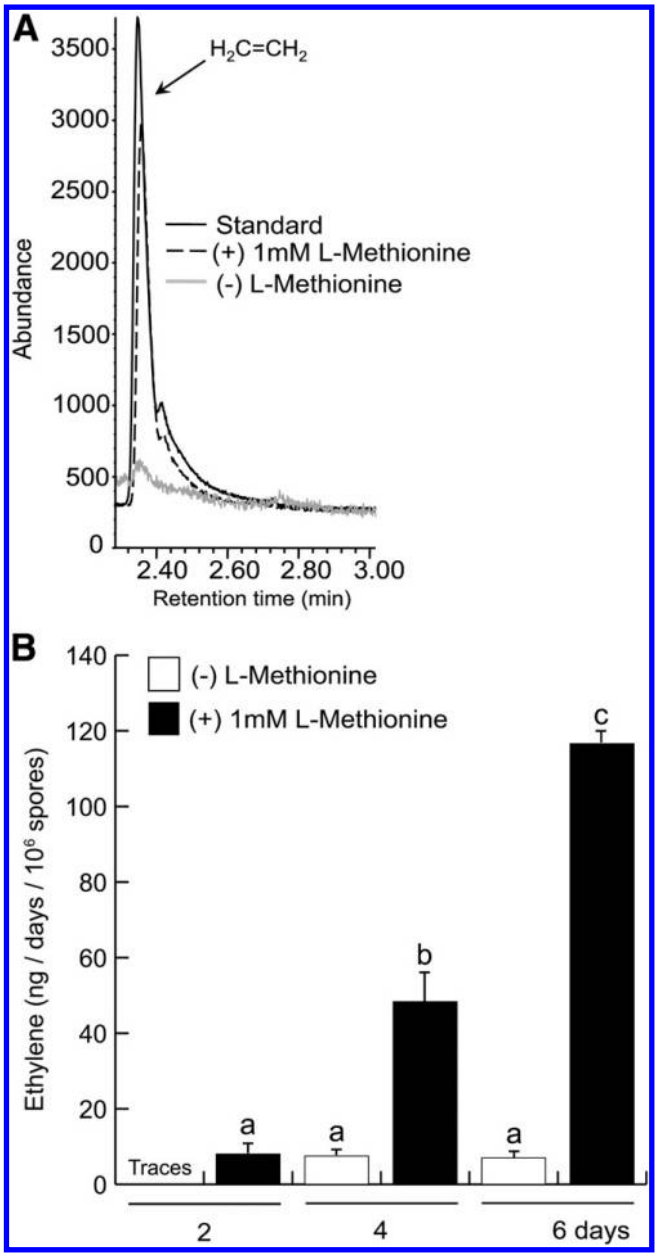

Fig. 3. *Trichoderma atroviride* ethylene (ET) production. **A,** ET chromatogram from a gaseous sample obtained of the headspace of a *T. atroviride* culture medium. **B,** Production of ET at different intervals of time with or without 1 mM L-methionine. Determinations were from at least four independent samples. Different letters are used to indicate means that differ significantly ($P < 0.05$).

that MPK6 activity is differentially regulated in shoot and in root systems and that ET signaling influences MPK6 activity particularly in roots.

***T. atroviride* regulates the activity of MPK6.**

Previously, we identified IAA and auxin-related compounds produced by *Trichoderma* spp. (Contreras-Cornejo et al. 2009), and we here demonstrate that the indolic compounds accumulate in the growth medium and the fungus also produces ET (Fig. 3). Next, we tested whether *T. atroviride* compounds with auxin activity (IAA, IAAld, and ICAld) affect MPK6 activity. We then evaluated the kinase activity on 10-day-old *Arabidopsis* seedlings grown in MS 0.2× medium supplied with different concentrations of these three compounds. The gel kinase assays showed that the MPK6 activity was induced in response to 10 and 100 µM IAA, 100 µM IAAld, and, slightly, with all concentrations of ICAld assayed (Fig. 7A). Since IAA is the main auxin in plants, we next tested the effect of 1 µM IAA on MAPK activity in a short period of time. It was found that MPK6 activity is rapidly activated by IAA (Fig. 7B). These results indicate that auxin-like compounds produced by *Trichoderma* spp. regulate MPK6 activity.

Expression pattern of the auxin reporter *DR5:uidA* gene is altered in the *ctr1* mutant.

Our results highlighted that *T. atroviride* alters root-system architecture, possibly via activation of MPK6, which was previously shown to be a negative regulator of primary root growth and lateral root formation (López-Bucio et al. 2014). To investigate a possible ET-auxin crosstalk in this phenomenon, we analyzed the effect of the loss of function of CTR1, a MPKKK considered a master regulator of the ET signaling pathway (Huang et al. 2003; Kieber et al. 1993), on auxin-inducible expression of the *DR5:uidA* auxin marker (Ulmasov et al. 1997). Then, we generated homozygous F3 *ctr1* × *DR5:uidA* seedlings to compare their β-glucuronidase (GUS) expression with that of *DR5:uidA* (WT_{DR5}) plants. In WT_{DR5} plants, GUS expression was located in root tips and shoot meristems at 3, 6, and 9 days after germination (d.a.g.) (Fig. 8A to F). Interestingly, *ctr1/DR5:uidA* seedlings of the same age showed short hypocotyls and primary roots, probably correlated with increased accumulation of auxins in the shoot and in the root system (Fig. 8G to L). Particularly, the increased GUS expression in *ctr1/DR5:uidA* primary roots suggests that both auxin and ET could be related with the prolific growth of root hairs (Fig. 8L). In *ctr1/DR5:uidA* seedlings cocultivated with *T. atroviride*, an increased auxin response in root tips was further evidenced (Supplementary Fig. S5). These data show that an ET-auxin crosstalk is involved in the regulation of primary root growth and formation of root hairs in *Arabidopsis* roots.

DISCUSSION

In natural environments, plants are continuously exposed to both pathogenic and symbiotic microorganisms that influence their growth and health. Rhizospheric fungi are able to colonize the root system and modulate plant growth and development with implications in crop productivity. Our previous research documented that *T. virens* and *T. atroviride* promote *Arabidopsis* root growth directly by producing auxin-like compounds (Contreras-Cornejo et al. 2009). However, the molecular

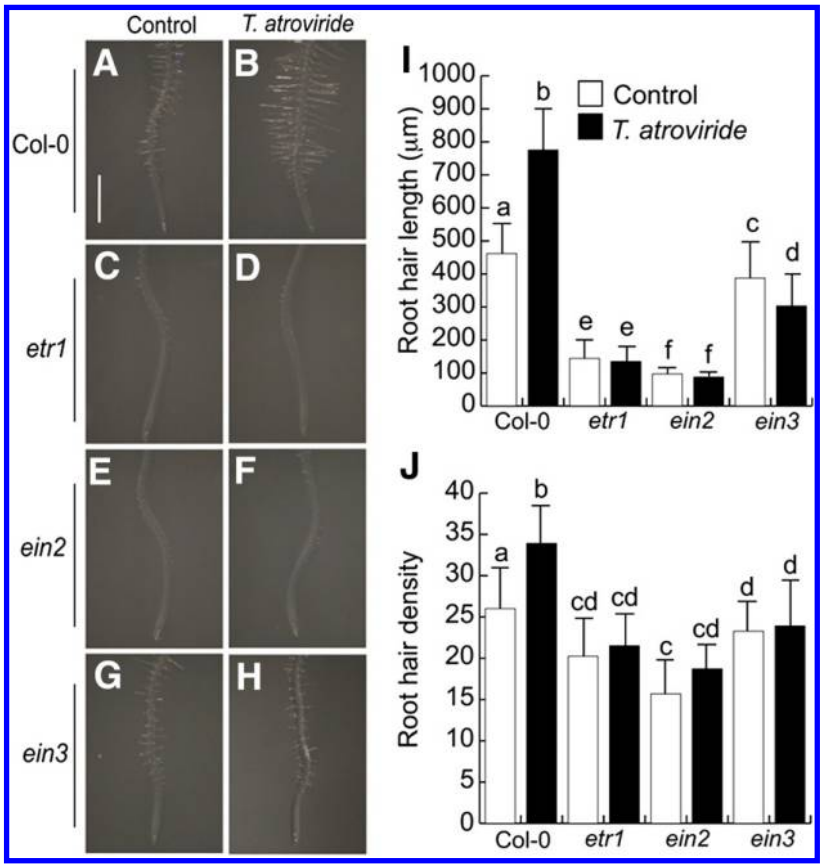

Fig. 4. *Trichoderma atroviride* effects on root-hair development in ethylene perception mutants. **A** to **H,** Representative roots from indicated seedlings grown on Murashige and Skoog 0.2× medium uninoculated or inoculated with *T. atroviride*. Bar = 500 µm. **I,** Average length of root hairs. **J,** Root-hair density. Values shown represent the mean of 100 root hairs ± standard deviation. Different letters are used to indicate means that differ significantly ($P < 0.05$).

mechanisms that coordinate root responses influenced by these fungi remain to be characterized. There is evidence that external signals from microbes often converge on a set of plant hormones such as auxin and ET, which are responsible for the execution of specific morphogenetic responses in the root (Kazan 2013; Lynch 1972). The large array of responses mediated by these signals is probably achieved by a combinatorial mechanism at the level of biosynthesis, transport, and sensitivity among different tissues (Bennett et al. 2005). MAPKs are classic regulators of most aspects of plant development, including hormone action, cell division, and perception of biotic and abiotic stimuli (Colcombet and Hirt 2008). For instance, plant recognition of microbes leads to rapid activation of MPK3 and MPK6 in *Arabidopsis* (Bögre et al. 1999; Jonak et al. 1996; Knetsch et al. 1996; Wilson et al. 1997) and, after activation of MPK6, an increase in camalexin levels is detected in *Arabidopsis* (Ren et al. 2008). In this signaling pathway, a pathogen-inducible transcription factor (WRKY33) is a MPK6 phosphorylation substrate regulating the camalexin biosynthesis (Mao et al. 2011). Our previous and current data show that, through MPK6 activation by *T. atroviride*, both plant defense responses and root differentiation can be concomitantly regulated. In a previous work, it was reported that *Trichoderma* spp. induced the accumulation of camalexin (Contreras-Cornejo et al. 2011; Velázquez-Robledo et al. 2011). In this work, we showed that *T. atroviride* regulates *Arabidopsis* root development by the production of ET and auxins involving MPK6 activation, events known to regulate plant responses during plant-microbe interactions (Merkouropoulos et al. 2008; Ren et al. 2008). Recently, it was reported that the MPK6 is a negative regulator of root development, because *mpk6* mutants had a longer primary root with more lateral roots and root-hair production than the WT (López-Bucio et al. 2014). Here, our analysis of the previously characterized *mpk6* mutant inoculated with *T. atroviride* showed that the number and the length of root hairs increases in a similar fashion in both *mpk6* and WT seedlings (Fig. 1), being that increment dependent on ET signaling. Interestingly, the induction of lateral roots in fungus-inoculated *mpk6* plants was slightly higher than in WT plants and the primary root growth of the *mpk6* mutant was inhibited by inoculation with *T. atroviride*, whereas the primary

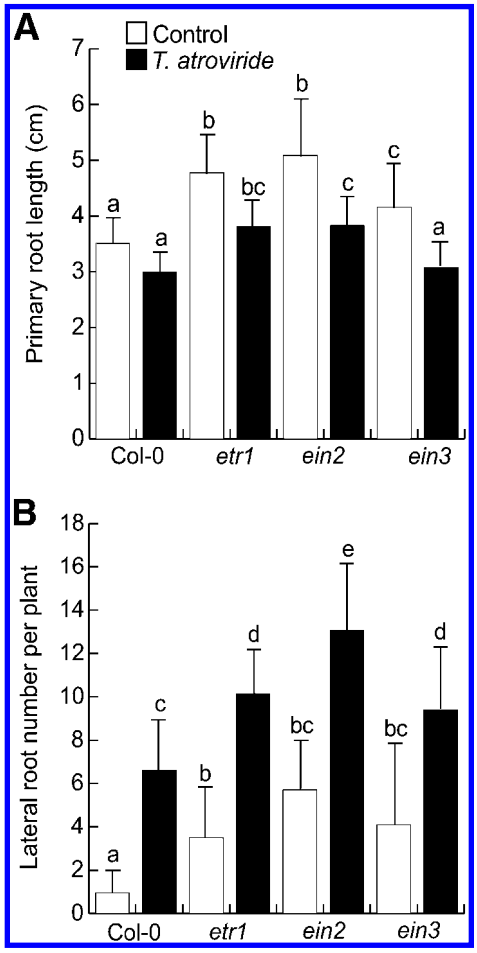

Fig. 5. *Trichoderma atroviride* effects on the root-system architecture in ethylene perception mutants. **A,** Primary root length and **B,** lateral root number of seedlings 10 days after germination. Root-system parameters were quantified for 15 seedlings and different letters are used to indicate means that differ significantly ($P < 0.05$). The experiment was repeated three times with similar results.

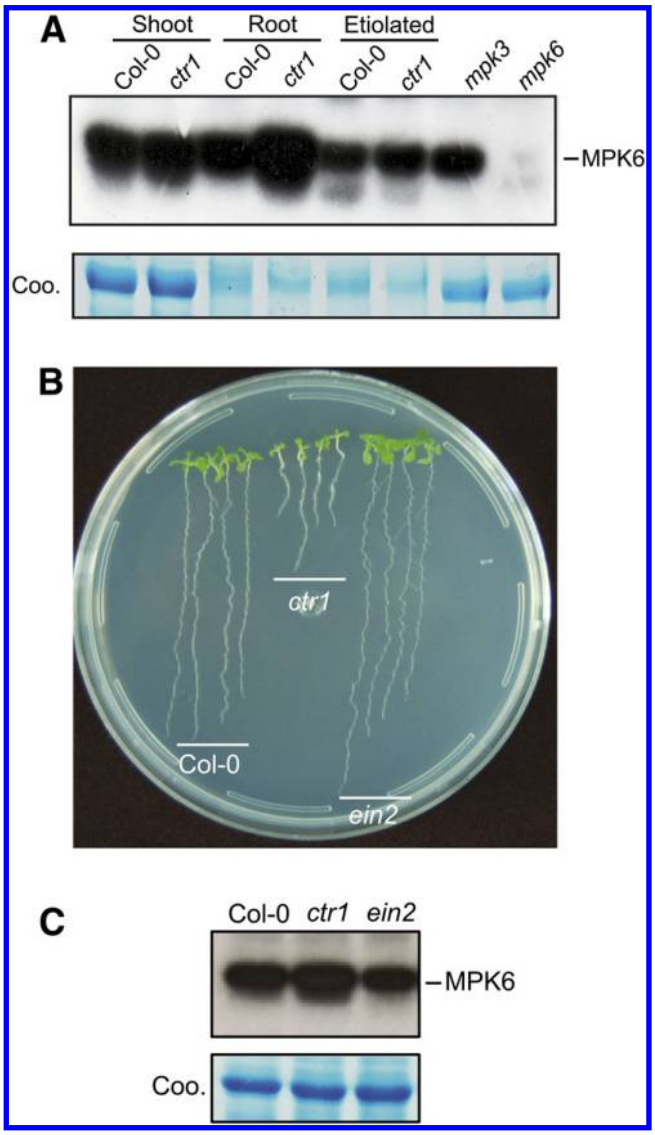

Fig. 6. MPK6 activity in ethylene signaling mutants. **A,** Mitogen-activated protein kinase activity in organs and etiolated seedlings. Notice that MPK6 activity is increased in the root of the *ctr1* mutant compared with the wild type (Col-0). **B,** Root phenotypes of wild type (Col-0), *ctr1* and *ein2* mutants of 12-day-old seedlings grown in Murashige and Skoog 0.2× medium. Compared with Col-0, *ctr1* has a shorter primary root and *ein2* shows a prolific formation of lateral roots. **C,** MPK6 activity in Col-0 and the *ctr1* and *ein2* mutants. The Coomassie stained gels (Coo) are shown as loading control and *mpk6* and *mpk3* mutants were included as reference of MPK6 activity.

roots of WT seedlings were insensitive to this treatment (Fig. 2). These observations underscore the complexity of signaling networks controlling the various root morphogenetic events led by *T. atroviride* and support the notion that *T. atroviride* induces changes of the root system likely involving a MAPK signaling pathway.

Root hairs are differentiated epidermal cells directly involved in water and nutrient uptake as well as in interactions with soil microorganisms. As Pitts et al. (1998) reported that ET promoted root-hair elongation in *Arabidopsis* and we observed that plants inoculated with *T. atroviride* increase the number of root hairs at early stages of the interaction, prior to their physical contact, we hypothesized that *T. atroviride* could increase the root-hair development by ET production. Then, using gas chromatography-mass spectrometry (GC-mass spectrometry) analysis, we identified *T. atroviride* ET production in 4- and 6-day fungus cultures. Moreover, the ET production increased when *T. atroviride* culture media was supplemented with L-methionine (Fig. 3), suggesting a canonical biosynthesis pathway. Further, we found that the root-hair induction required an intact ET signaling pathway, as no increased root-hair length or density in response to fungal stimulation was observed on ET-signaling mutants *etr1, ein2*, and *ein3* (Fig. 4) or after treatment with ET inhibitor silver nitrate. Interestingly, the auxin transport inhibitor NPA did not inhibit root-hair development in axenically grown WT seedlings but, rather, stimulated root-hair growth, in contrast to silver nitrate, which inhibits root-hair growth. In response to *Trichoderma* spp., the combination of NPA with silver nitrate results in root-hair growth inhibition, clearly indicating that ET signaling is important for root-hair responses to *Trichoderma* spp.

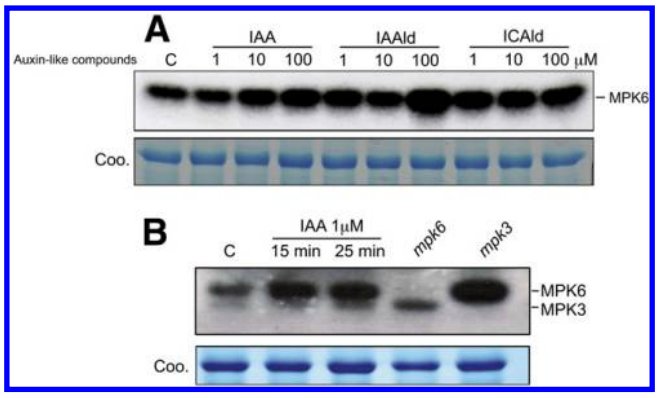

Fig. 7. Compounds with auxin activity produced by *Trichoderma atroviride* activate MPK6. **A,** Germination and growth of *Arabidopsis* seedlings in Murashige and Skoog 0.2× medium supplied with indole-3-acetic acid (IAA), indole-3-acetaldehyde (IAAld), and indole-3-carboxaldehyde (ICAld) induce MPK6 activity. **B,** IAA induces a rapid and sustained activation of MPK6. Total protein extracts were prepared from seedlings treated as indicated and 30 μg were used for an in-gel mitogen-activate protein kinase assay. The Coomassie stained gels (Coo) are shown as loading control and *mpk6* and *mpk3* mutants were included as reference of MPK6 activity.

Regarding the effects of *T. atroviride* on lateral root formation and primary root length, we found similar responses in the *mpk6* mutant and ET signaling mutants with a slight induction of lateral root production and primary root inhibition caused by fungal cocultivation (Fig. 5). These data indicate that particular root developmental cues are affected by all signals emitted by the fungi and that the net root architectural configuration of plants interacting with *Trichoderma* spp. likely depends on the timing and degree of root colonization.

It has been reported that auxin and ET act synergistically during root development (Muday et al. 2012). The effect of ET on root growth can be mediated by regulation of auxin biosynthesis or auxin distribution; in turn, elevated levels of auxins enhance ET biosynthesis (Abel et al. 1995; Negi et al. 2008; Yoo et al. 2008). The crosstalk between ET and auxins during fungus-plant interaction is emerging as a key element in signal integration processes. *Tuber borchii* induces primary root shortening, lateral root, and root-hair production on the host

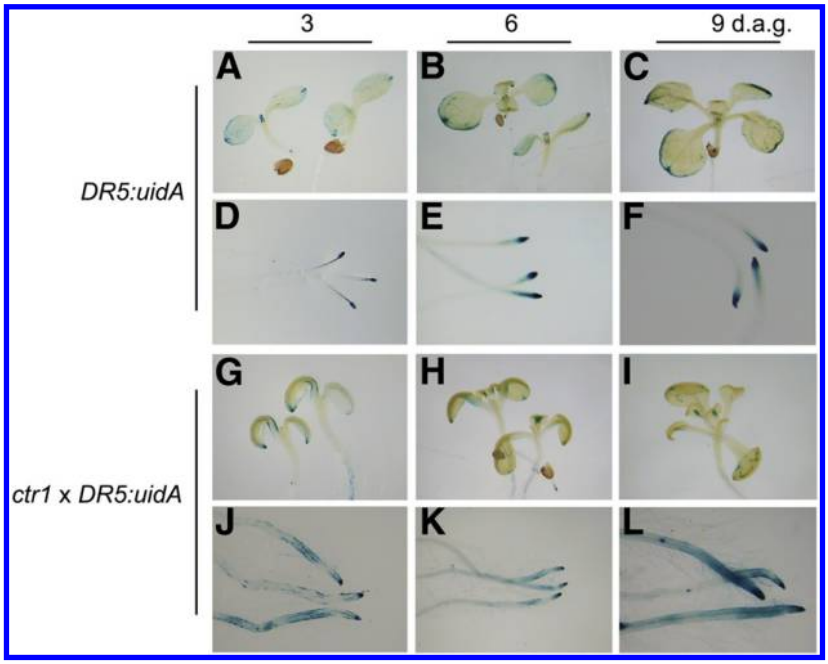

Fig. 8. Ethylene modulates the expression of the *DR5* auxin marker gene through CTR1. β-Glucuronidase (GUS) activity of indicated *Arabidopsis* seedlings grown for 3, 6, and 9 days after germination (d.a.g.) on Murashige and Skoog 0.2× medium. **A** to **F,** Wild-type (*DR5:uidA*) GUS expression in the shoot and the primary root. **G** to **L,** *ctr1:DR5:uidA* GUS expression in the shoot and the primary root. GUS activity reveals an increased auxin response in the primary root of the *ctr1* mutant. Representative individuals of at least 10 stained seedlings are shown. The experiment was repeated twice with similar results.

Cistus incanus and the nonhost *Arabidopsis thaliana* (Splivallo et al. 2009). The authors demonstrated that the application of a mixture of aminocyclopropane-1-carboxylic acid (ACC) and IAA fully mimicked the root morphology induced by *Tuber borchii* colony for both host and nonhost plants. Moreover, primary root growth was not inhibited in the *Arabidopsis* auxin transport mutant *aux1-7* by truffle metabolites, while root branching was less affected in the ET-insensitive mutant *ein2-1*. Similarly, IAA secreted by *Trichoderma* strains may promote root growth directly, by stimulating plant cell elongation or cell division, or indirectly, by influencing ET emissions (Viterbo et al. 2010).

MPK6 activity seems to play a central role during *T. atroviride* root development regulation. It has been demonstrated that MPK6 is activated, supplying the ET precursor ACC to plants. This activation leads to a rapid induction of ET biosynthesis, which is associated with an increase in 1-aminocyclopropane-1-carboxylic acid synthase activity in *Arabidopsis* (Liu and Zhang 2004). MPK6 also participates in the ET signaling regulating the stability of the transcription factor EIN3 in response to ET (Ouaked et al. 2003; Yoo et al. 2008). Phosphorylation assays in the *ctr1* mutant suggest that MPK6 could have a key role in the short root phenotype of this mutant, which deserves further attention (Fig. 6). We also found that the compounds with auxin activity released by *Trichoderma* spp. induce MPK6 activity (Fig. 7). Then, it is tempting to speculate that MPK6 could be acting as an integrator of auxin and ET signals. This speculation is supported by an auxin-inducible gene expression analysis on homozygous *ctr1/DR5:uidA* seedlings, which clearly shows an increased auxin-inducible expression independent of fungal colonization (Fig. 8). According to these data, we propose a model in which *T. atroviride* induces MPK6 accompanied by ET and auxin production (Fig. 9). *T. atroviride* affects root morphogenetic programs, apparently inducing the MPK6 activation through ET and indolic compound biosynthesis. ET and auxins induce root-hair production in an ET-dependent pathway, whereas ET could regulate the auxin biosynthesis and distribution to enhance lateral root production. These two hormones can act synergistically to inhibit primary root growth by an overactivation of MPK6, which acts as a negative regulator of primary root growth and lateral root formation (Fig. 9). In consequence, MPK6 and its MAPK associated cascade, likely including CTR1, seems to be a regulation node to one or both maintain or amplify the hormonal effects underlying plant development or defense or both. To our knowledge, the short-root phenotype of *ctr1* mutants has not been previously reported. Apparently, *ctr1* primary roots enter a determinate developmental pathway caused by quiescent center-cell differentiation and halted cell division in primary root meristems (A. Méndez-Bravo and J. López-Bucio, *personal communication*). We cannot exclude the possibility that other molecules, such as small peptides, volatiles, or diffusibles, may also affect root development through MPK6 signaling. Our work provides conclusive data demonstrating that a MAPK module including MPK6 acts as a signal transducer during root development mediated by *Trichoderma* spp. In this scenario, the induction of MPK6 activity by *T. atroviride* auxin-like compounds could enhance ET biosynthesis, thus regulating the root-hair development in an ET-dependent pathway. In turn, the enhanced ET production could influence auxin biosynthesis or distribution impacting the initiation of lateral roots, all together suggesting a positive feedback between auxins and ET during a beneficial fungal-plant interaction.

MATERIALS AND METHODS

Plant material and growth conditions.

Arabidopsis thaliana ecotype Columbia-0 (Col-0) and several mutant lines were used in this work. Lines *mpk6-2* (Liu and Zhang 2004) and *mpk3-1* (Wang et al. 2007) are mutants affected in protein kinases; *etr1-3* (Hua and Meyerowitz 1998), *ein2-1* (Guzmán and Ecker 1990), *ein3-1* (Chao et al. 1997), and *ctr1-1* (Kieber et al. 1993) are ET-related mutants. *DR5:uidA* (Ulmasov et al. 1997) is an auxin-responsive marker. A homozygous *ctr1/DR5:uidA* line used to analyze auxin signaling in the root system as affected by the ET pathway was generated in this work. All the seeds were surface-sterilized, and were then germinated and grown on agar plates containing 0.2× MS medium (MS basal salts mixture; Sigma), basal or supplied with the indicated compounds. Plates were placed vertically at a 65-degree angle to allow root growth along the agar surface and unimpeded aerial growth of the hypocotyls. Plants were grown at 24°C in a chamber with a 16-h light (200 μmol m^2 s^{-1}), 8-h dark photoperiod.

Fungal growth and plant inoculation experiments.

Trichoderma atroviride IMI 206040 used in this was previously evaluated in vitro for their ability to promote plant growth in *Arabidopsis*. Fungal spore densities of 10^6 were inoculated placing the spores at 5 cm in the opposite ends of agar plates containing 4-d.a.g. *Arabidopsis* seedlings (10 seedlings per plate). Plates were arranged in a completely randomized design. The seedlings were cultivated in a Percival AR95L growth chamber at the temperature and photoperiod conditions already indicated.

Plant growth measurements.

At 4 d.a.i., total fresh weight was determined on an analytical scale for three groups of 10 plants. Growth of primary roots was registered using a ruler. Lateral root numbers were determined by counting the lateral roots present in the primary root. To analyze the effect of *T. atroviride* on root cell differentiation, the primary root zone was photographed 2 days after inoculation, using a stereoscopic microscope (Leica MZ6; Leica Microsystems). Measurements were determined using Image J Tool software; pixel areas were calibrated based on a known distance. Root hairs were measured in a region of 500 μm at

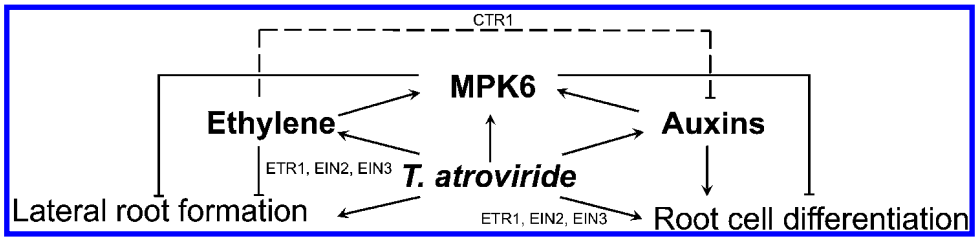

Fig. 9. Proposed model for the signaling pathways controlled by *Trichoderma atroviride* in *Arabidopsis* for modulating the root-system architecture. *T. atroviride* induces the activation of plant MPK6 that translates fungal signals into cellular responses. Plant growth regulators, such as auxins and ethylene, produced by the fungus control several aspects of the root growth but, simultaneously, can modulate the MPK6 activity, which also affects root development.

approximately 1 cm from the primary root tip. The average length of root hairs was determined measuring 100 hairs for each root, taking as a reference the root protoxylematic plane to locate the radical hair base in the epidermal cell.

Indolic compound determinations.

Arabidopsis WT seedlings (Col-0) were grown and inoculated as described above. IAA and indolic compound determinations were done by GC-mass spectrometry from the MS agar portion of the petri dishes after 6 days of fungal growth. Seedlings and mycelia were removed from the agar surface. A quantity of 20 to 28 g of MS agar was removed from each plate with a spatula, was placed in a flask with 100 ml of deionized water, and was homogenized and filtered. To recover IAA, samples were acidified to pH 3 with concentrated HCl. IAAld and ICAld were obtained when the aqueous extracts from the agar were adjusted to pH 7, using 10% KOH. Aqueous solutions were mixed with 100 ml of ethyl acetate and were vortexed for 1 min. The upper phase was concentrated to dryness at 55°C, was redissolved in 3.0 ml of ethyl acetate, was trasferred to vials, and was evaporated to dryness under a stream on nitrogen. Samples containing IAAld and ICAld were redissolved in 50 µl of ethyl acetate. For IAA determinations, IAA was methyl esterified with 500 µl of acetyl chloride in 2 ml of dry methanol, was sonicated for 15 min, and was heated at 75°C for 1 h. The IAA methyl ester was evaporated under a stream of nitrogen and redissolved in 50 µl of ethyl acetate.

The indolic compounds were analyzed in an Agilent 6850 Series II gas chromatograph equipped with an Agilent MS detector model 5973 and a 30 m × 0.2 µm × 0.25 mm, 5% phenyl methyl silicone capillary column (HP-5 MS). Operating conditions used helium at a rate of 1 ml min^{-1} as carrier gas, 300°C detector temperature, and 250°C injector temperature. The volume of the injected sample was 1 µl. The column was held for 5 min at 150°C and was programmed at 5°C per minute to a final temperature of 278°C for 5 min. Indolic compounds were identified by comparison with a mass spectra library (National Institute of Standards and Technology, Environmental Protection Agency, National Institutes of Health; Chem Station; Hewlett-Packard). The identities of the indolic compounds were further confirmed by comparison of the retention time (Rt) in the fungal extract with samples of the pure IAAld (Rt = 8.88 min), ICAld (Rt = 10.98 min), and IAA (Rt = 11.02 min) standards (Sigma). A selected ion-monitoring analysis was used to verify the presence of these indolic compounds in the samples. The molecular ions were monitored after electron impact ionization (70 eV). For IAAld, mass-to-charge ratios (*m/z*) were *m/z* 130 and 159 [M^+]; for ICAld, they were *m/z* 116 and 145 [M^+]; and for IAA methyl ester, they were *m/z* 130 and 189 [M^+]. To estimate the amount of compounds produced by *T. atroviride*, we constructed individual calibration curves for each compound.

ET collection and analysis.

T. atroviride was inoculated on petri dishes containing MS 0.2× medium for 2, 4, and 6 days days, for measuring the accumulation of ET in the head-space. Gaseous hormone was collected using a gas-tight (Batch H08-A9817) syringe. The identification and determination of ET were performed using an Agilent 6850 Series II gas chromatograph equipped with a 30-m MS Q-Plot column GC-mass spectrometry system. GC–selected ion monitoring mass spectrometry and retention time were established for ET (*m/z* 26 and 27, 2.39 min). The operating conditions used were: 1 ml min^{-1} of helium as carrier gas, 250°C detector temperature, and 110°C injector temperature. The column was held for 4 min at 60°C and the samples were run at isotermic conditions in the splitless mode. To estimate the amount of ET, columns were injected with 200 µl of gas taken from 2 ml of sample treated previously with 2 ml of KOH 1N to eliminate the CO_2 produced by the fungus that could interfere with the peak of the ET. Additionally, we constructed a curve with a pure standard (Sigma).

Protein extraction.

Frozen seedlings were ground in liquid nitrogen and were thawed in extraction buffer (100 mM HEPES [pH 7.5], 5 mM EDTA, 5 mM EGTA, 10 mM dithiothreitol [DTT], 10 mM Na_3VO4, 10 mM NaF, 50 mM β-glycerophosphate, 10% glycerol, 7.5% polyvinylpolypyrrolidone), supplied with a protease inhibitor mixture (as recommended by Sigma). The ground slurry was centrifuged at 20,000 × *g* for 20 min at 4°C. Supernatants were collected into new tubes, were frozen in liquid nitrogen, and were stored at –80°C until their use. The protein concentration was determined using the Bio-Rad protein assay kit with bovine serum albumin (BSA) as standard.

In-gel kinase assays.

The in-gel kinase assay was performed as described by Lu et al. (2002). Briefly, 50-µg aliquots of total protein extracted from plant tissue were fractionated on a sodium dodecyl sulfate 10% polyacrylamide gel containing 0.25 mg myelin basic protein per milliliter (Sigma) as substrate for the MAPKs. After electrophoresis, the gel was washed three times for 30 min each with 25 mM Tris, pH 7.5, 0.5 mM DTT, 0.1 mM Na_3VO_4, 5 mM NaF, 0.5 mg of BSA per milliliter, and 0.1% (vol/vol) Triton X-100, at room temperature. Proteins in the gel were renatured by incubating the gel in 25 mM Tris, pH 7.5, 1 mM DTT, 0.1 mM Na_3VO_4, and 5 mM NaF at 4°C overnight with three changes of buffer. The kinase reactions were carried out by incubating the gel in 30 ml of reaction buffer (25 mM Tris, pH 7.5, 2 mM EGTA, 12 mM $MgCl_2$, 1 mM DTT, 0.1 mM Na_3VO_4, 200 nM ATP, and 50 µCi of [γ-^{32}P] ATP with >4,000 Ci/mmol; 1 Ci = 37 GBq) for 60 min at room temperature. To remove free ^{32}P, the gel was repeatedly washed at room temperature with several changes of 5% (wt/vol) trichloroacetic acid and 1% (wt/vol) $NaPP_i$ until ^{32}P radioactivity in the wash solution was barely detectable. Then, the gel was dried under vacuum on Whatman 3MM paper and was used to expose an X-ray film. Protein sizes were estimated by using molecular mass markers (Bio-Rad).

Data analysis.

Experiments were statistically analyzed in the SPSS 10 program (SPSS, Chicago). Multivariate analyses with a Tukey's post hoc test were used for testing differences in the root system architecure. Different letters were used to indicate means that differed significantly ($P \leq 0.05$).

ACKNOWLEDGMENTS

We thank J. Altamirano for his support and technical improvement for ET determination. We are thankful to P. Guzmán and T. Guilfoyle for kindly providing us with *Arabidopsis* mutant seeds. H. A. Contreras-Cornejo is indebted to CONACYT for a doctoral fellowship. This work was supported by grants from the Consejo Nacional de Ciencia y Tecnología (CONACYT, México, grant number 43978), the Consejo de la Investigación Científica (UMSNH, México, grant number CIC 2.26), and the UNAM-DGAPA-PAPIIT (grant IN207014 to Á. A. Guevara-García, J. S. López-Bucio, and M. Ramos-Vega).

LITERATURE CITED

Abel, S., Nguyen, M. D., Chow, W., and Theologis, A. 1995. ACS4, a primary indoleacetic acid-responsive gene encoding 1-aminocyclopropane-1-carboxylate synthase in *Arabidopsis thaliana*. Structural characterization, expression in *Escherichia coli*, and expression characteristics in response to auxin [corrected]. J. Biol. Chem. 270:19093-19099.

Acharya, B. R., and Assmann, S. M. 2009. Hormone interactions in stomatal function. Plant Mol. Biol. 69:451-462.

Barbieri, P., and Galli, E. 1993. Effect on wheat root development of inoculation with an *Azospirillum brasilense* mutant with altered indole-3-acetic acid production. Res. Microbiol. 144:69-75.

Bennett, M., Bellini, C., and Van Der Straeten, D. 2005. Integrative biology: Dissecting cross-talk between plant signaling pathways. Physiol. Plant. 123:109.

Bleecker, A. B., and Kende, H. 2000. Ethylene: A gaseous signal molecule in plants. Annu. Rev. Cell Dev. Biol. 16:1-18.

Bögre, L., Calderini, O., Binarova, P., Mattauch, M., Till, S., Kiegerl, S., Jonak, C., Pollaschek, C., Barker, P., Huskisson, N. S., Hirt, H., and Heberle-Bors, E. 1999. A MAP kinase is activated late in plant mitosis and becomes localized to the plane of cell division. Plant Cell 11:101-113.

Brader, G., Djamei, A., Teige, M., Palva, E. T., and Hirt, H. 2007. The MAP kinase kinase MKK2 affects disease resistance in *Arabidopsis*. Mol. Plant-Microbe Interact. 20:589-596.

Chao, Q., Rothenberg, M., Solano, R., Roman, G., Terzaghi, W., and Ecker, J. R. 1997. Activation of the ethylene gas response pathway in Arabidopsis by the nuclear protein ETHYLENE-INSENSITIVE3 and related proteins. Cell 89:1133-1144.

Colcombet, J., and Hirt, H. 2008. Arabidopsis MAPKs: A complex signalling network involved in multiple biological processes. Biochem. J. 413:217-226.

Contreras-Cornejo, H. A., Macías-Rodríguez, L., Cortés-Penagos, C., and López-Bucio, J. 2009. *Trichoderma virens*, a plant beneficial fungus, enhances biomass production and promotes lateral root growth through an auxin-dependent mechanism in *Arabidopsis*. Plant Physiol. 149: 1579-1592.

Contreras-Cornejo, H. A., Macías-Rodríguez, L., Beltrán-Peña, E., Herrera-Estrella, A., and López-Bucio, J. 2011. *Trichoderma*-induced plant immunity likely involves both hormonal- and camalexin-dependent mechanisms in *Arabidopsis thaliana* and confers resistance against necrotrophic fungi *Botrytis cinerea*. Plant Signal. Behav. 6:1554-1563.

Contreras-Cornejo, H. A., Ortiz-Castro, R., and López-Bucio, J. 2013. Promotion of plant growth and the induction of systemic defence by *Trichoderma*: Physiology, genetics and gene expression. Pages 175-196 in: Trichoderma Biology and Applications. P. K. Mukherjee,ed. CAB International, London.

Contreras-Cornejo, H. A., Macías-Rodríguez, L., Alfaro-Cuevas, R., and López-Bucio, J. 2014. Trichoderma spp. improve growth of *Arabidopsis* seedlings under salt stress through enhanced root development, osmolite production, and Na^+ elimination through root exudates. Mol. Plant-Microbe Interact. 27:503-514.

Dharmasiri, N., Dharmasiri, S., Weijers, D., Lechner, E., Yamada, M., Hobbie, L., Ehrismann, J. S., Jürgens, G., and Estelle, M. 2005. Plant development is regulated by a family of auxin receptor F box proteins. Dev. Cell 9:109-119.

Guzmán, P., and Ecker, J. R. 1990. Exploiting the triple response of Arabidopsis to identify ethylene-related mutants. Plant Cell 2:513-523.

Hua, J., and Meyerowitz, E. M. 1998. Ethylene responses are negatively regulated by a receptor gene family in *Arabidopsis thaliana*. Cell 94: 261-271.

Huang, Y., Li, H., Hutchison, C. E., Laskey, J., and Kieber, J. J. 2003. Biochemical and functional analysis of CTR1, a protein kinase that negatively regulates ethylene signaling in *Arabidopsis*. Plant J. 33:221-233.

Johnson, P. R., and Ecker, J. R. 1998. The ethylene gas signal transduction pathway: A molecular perspective. Annu. Rev. Genet. 32:227-254.

Jonak, C., Kiegerl, S., Ligterink, W., Barker, P. J., Huskisson, N. S., and Hirt, H. 1996. Stress signaling in plants: A mitogen-activated protein kinase pathway is activated by cold and drought. Proc. Natl. Acad. Sci. U.S.A. 93:11274-11279.

Kazan, K. 2013. Auxin and the integration of environmental signals into plant root development. Ann. Bot. (Lond.) 112:1655-1665.

Khatabi, B., Molitor, A., Lindermayr, C., Pfiffi, S., Durner, J., von Wettstein, D., Kogel, K. H., and Schäfer, P. 2012. Ethylene supports colonization of plant roots by the mutualistic fungus *Piriformospora indica*. PLoS ONE 7:e35502.

Kieber, J. J., Rothenberg, M., Roman, G., Feldmann, K. A., and Ecker, J. R. 1993. CTR1, a negative regulator of the ethylene response pathway in Arabidopsis, encodes a member of the raf family of protein kinases. Cell 72:427-441.

Knetsch, M., Wang, M., Snaar-Jagalska, B. E., and Heimovaara-Dijkstra, S. 1996. Abscisic acid induces mitogen-activated protein kinase activation in barley aleurone protoplasts. Plant Cell 8:1061-1067.

Liu, Y., and Zhang, S. 2004. Phosphorylation of 1-aminocyclopropane-1-carboxylic acid synthase by MPK6, a stress-responsive mitogen-activated protein kinase, induces ethylene biosynthesis in Arabidopsis. Plant Cell 16:3386-3399.

López-Bucio, J. S., Dubrovsky, J. G., Raya-González, J., Ugartechea-Chirino, Y., López-Bucio, J., de Luna-Valdez, L. A., Ramos-Vega, M., León, P., and Guevara-García, A. A. 2014. *Arabidopsis thaliana* mitogen-activated protein kinase 6 is involved in seed formation and modulation of primary and lateral root development. J. Exp. Bot. 65: 169-183.

Lu, C., Han, M. H., Guevara-Garcia, A., and Fedoroff, N. V. 2002. Mitogen-activated protein kinase signaling in postgermination arrest of development by abscisic acid. Proc. Natl. Acad. Sci. U.S.A. 99:15812-15817.

Lynch, J. M. 1972. Identification of substrates and isolation of microorganisms responsible for ethylene production in the soil. Nature 240:45-46.

Malhotra, M., and Srivastava, S. 2008. An *ipdC* gene knock-out of *Azospirillum brasilense* strain SM and its implications on indole-3-acetic acid biosynthesis and plant growth promotion. Antonie van Leeuwenhoek 93:425-433.

Mao, G., Meng, X., Liu, Y., Zheng, Z., Chen, Z., and Zhang, S. 2011. Phosphorylation of a WRKY transcription factor by two pathogen-responsive MAPKs drives phytoalexin biosynthesis in Arabidopsis. Plant Cell 23:1639-1653.

Merkouropoulos, G., Andreasson, E., Hess, D., Boller, T., and Peck, S. C. 2008. An Arabidopsis protein phosphorylated in response to microbial elicitation, AtPHOS32, is a substrate of MAP kinases 3 and 6. J. Biol. Chem. 283:10493-10499.

Muday, G. K., Rahman, A., and Binder, B. M. 2012. Auxin and ethylene: Collaborators or competitors? Trends Plant Sci. 17:181-195.

Negi, S., Ivanchenko, M. G., and Muday, G. K. 2008. Ethylene regulates lateral root formation and auxin transport in *Arabidopsis thaliana*. Plant J. 55:175-187.

Ouaked, F., Rozhon, W., Lecourieux, D., and Hirt, H. 2003. A MAPK pathway mediates ethylene signaling in plants. EMBO (Eur. Mol. Biol. Organ.) J. 22:1282-1288.

Patten, C. L., and Glick, B. R. 2002. Role of *Pseudomonas putida* indoleacetic acid in development of the host plant root system. Appl. Environ. Microbiol. 68:3795-3801.

Pitts, R. J., Cernac, A., and Estelle, M. 1998. Auxin and ethylene promote root hair elongation in *Arabidopsis*. Plant J. 16:553-560.

Ren, D., Liu, Y., Yang, K. Y., Han, L., Mao, G., Glazebrook, J., and Zhang, S. 2008. A fungal-responsive MAPK cascade regulates phytoalexin biosynthesis in *Arabidopsis*. Proc. Natl. Acad. Sci. U.S.A. 105: 5638-5643.

Růzicka, K., Ljung, K., Vanneste, S., Podhorská, R., Beeckman, T., Friml, J., and Benková, E. 2007. Ethylene regulates root growth through effects on auxin biosynthesis and transport-dependent auxin distribution. Plant Cell 19:2197-2212.

Sánchez-Rodríguez, C., Rubio-Somoza, I., Sibout, R., and Persson, S. 2010. Phytohormones and the cell wall in Arabidopsis during seedling growth. Trends Plant Sci. 15:291-301.

Splivallo, R., Fischer, U., Göbel, C., Feussner, I., and Karlovsky, P. 2009. Truffles regulate plant root morphogenesis via the production of auxin and ethylene. Plant Physiol. 150:2018-2029.

Suzuki, S., He, Y., and Oyaizu, H. 2003. Indole-3-Acetic acid production in *Pseudomonas fluorescens* HP72 and its association with suppression of creeping bentgrass brown patch. Curr. Microbiol. 47:138-143.

Ulmasov, T., Murfett, J., Hagen, G., and Guilfoyle, T. J. 1997. Aux/IAA proteins repress expression of reporter genes containing natural and highly active synthetic auxin response elements. Plant Cell 9:1963-1971.

Velázquez-Robledo, R., Contreras-Cornejo, H. A., Macías-Rodriguez, L., Hernández-Morales, A., Aguirre, J., Casas-Flores, S., López-Bucio, J., and Herrera-Estrella, A. 2011. Role of the 4-phosphopantetheinyl transferase of *Trichoderma virens* in secondary metabolism and induction of plant defense responses. Mol. Plant-Microbe Interact. 24:1459-1471.

Viterbo, A., Landau, U., Kim, S., Chernin, L., and Chet, I. 2010. Characterization of ACC deaminase from the biocontrol and plant growth-promoting agent *Trichoderma asperellum* T203. FEMS Microbiol. Lett. 305:42-48.

Wang, H., Ngwenyama, N., Liu, Y., Walker, J. C., and Zhang, S. 2007. Stomatal development and patterning are regulated by environmentally responsive mitogen-activated protein kinases in *Arabidopsis*. Plant Cell 19:63-73.

Wilson, C., Voronin, V., Touraev, A., Vicente, O., and Heberle-Bors, E. 1997. A developmentally regulated MAP kinase activated by hydration in tobacco pollen. Plant Cell 9:2093-2100.

Yoo, S. D., Cho, Y. H., Tena, G., Xiong, Y., and Sheen, J. 2008. Dual control of nuclear EIN3 by bifurcate MAPK cascades in C_2H_4 signalling. Nature 451:789-795.

Zhang, T., Liu, Y., Yang, T., Zhang, L., Xu, S., Xue, L., and An, L. 2006. Diverse signals converge at MAPK cascades in plant. Plant Physiol. Biochem. 44:274-283.

Springer

Dear Author,

Here are the proofs of your article.

- You can submit your corrections **online**, via **e-mail** or by **fax**.
- For **online** submission please insert your corrections in the online correction form. Always indicate the line number to which the correction refers.
- You can also insert your corrections in the proof PDF and **email** the annotated PDF.
- For fax submission, please ensure that your corrections are clearly legible. Use a fine black pen and write the correction in the margin, not too close to the edge of the page.
- Remember to note the **journal title**, **article number**, and **your name** when sending your response via e-mail or fax.
- **Check** the metadata sheet to make sure that the header information, especially author names and the corresponding affiliations are correctly shown.
- **Check** the questions that may have arisen during copy editing and insert your answers/ corrections.
- **Check** that the text is complete and that all figures, tables and their legends are included. Also check the accuracy of special characters, equations, and electronic supplementary material if applicable. If necessary refer to the *Edited manuscript*.
- The publication of inaccurate data such as dosages and units can have serious consequences. Please take particular care that all such details are correct.
- Please **do not** make changes that involve only matters of style. We have generally introduced forms that follow the journal's style.
  Substantial changes in content, e.g., new results, corrected values, title and authorship are not allowed without the approval of the responsible editor. In such a case, please contact the Editorial Office and return his/her consent together with the proof.
- If we do not receive your corrections **within 48 hours**, we will send you a reminder.
- Your article will be published **Online First** approximately one week after receipt of your corrected proofs. This is the **official first publication** citable with the DOI. **Further changes are, therefore, not possible.**
- The **printed version** will follow in a forthcoming issue.

Please note

After online publication, subscribers (personal/institutional) to this journal will have access to the complete article via the DOI using the URL: http://dx.doi.org/[DOI].
If you would like to know when your article has been published online, take advantage of our free alert service. For registration and further information go to: http://www.link.springer.com.

Due to the electronic nature of the procedure, the manuscript and the original figures will only be returned to you on special request. When you return your corrections, please inform us if you would like to have these documents returned.

Metadata of the article that will be visualized in OnlineFirst

Please note: Images will appear in color online but will be printed in black and white.

ArticleTitle	*ALTERED MERISTEM PROGRAM 1* Plays a Role in Seed Coat Development, Root Growth, and Post-Embryonic Epidermal Cell Elongation in *Arabidopsis*	
Article Sub-Title		
Article CopyRight	Springer Science+Business Media New York (This will be the copyright line in the final PDF)	
Journal Name	Journal of Plant Growth Regulation	
Corresponding Author	Family Name	**López-Bucio**
	Particle	
	Given Name	**José**
	Suffix	
	Division	Instituto de Investigaciones Químico-Biológicas
	Organization	Universidad Michoacana de San Nicolás de Hidalgo
	Address	Edificio B3, Ciudad Universitaria, C. P. 58030, Morelia, Michoacán, México
	Email	jbucio@umich.mx
	ORCID	
Author	Family Name	**López-García**
	Particle	
	Given Name	**Claudia Marina**
	Suffix	
	Division	Instituto de Investigaciones Químico-Biológicas
	Organization	Universidad Michoacana de San Nicolás de Hidalgo
	Address	Edificio B3, Ciudad Universitaria, C. P. 58030, Morelia, Michoacán, México
	Email	
	ORCID	
Author	Family Name	**Raya-González**
	Particle	
	Given Name	**Javier**
	Suffix	
	Division	Instituto de Investigaciones Químico-Biológicas
	Organization	Universidad Michoacana de San Nicolás de Hidalgo
	Address	Edificio B3, Ciudad Universitaria, C. P. 58030, Morelia, Michoacán, México
	Email	
	ORCID	
Author	Family Name	**López-Bucio**
	Particle	
	Given Name	**Jesús Salvador**
	Suffix	

	Division	
	Organization	Instituto de Biotecnología-UNAM
	Address	Av. Universidad No. 2001, Col. Chamilpa, Cuernavaca, Morelos, México
	Email	
	ORCID	
Author	Family Name	**Guevara-García**
	Particle	
	Given Name	**Ángel Arturo**
	Suffix	
	Division	
	Organization	Instituto de Biotecnología-UNAM
	Address	Av. Universidad No. 2001, Col. Chamilpa, Cuernavaca, Morelos, México
	Email	
	ORCID	

Schedule	Received	4 September 2015
	Revised	
	Accepted	19 April 2016

Abstract	Plant development relies on the capacity of cells to interpret positional information and translate it into proliferation, elongation, and differentiation programs. *ALTERED MERISTEM PROGRAM 1 (AMP1)* encodes a putative glutamate carboxypeptidase involved in embryo development, plant growth, and phytohormone homeostasis. Here, we show that mutations of *AMP1* cause defective seed coat formation, which correlates with increased frequency of embryo abortion, low seed production, and retarded germination. Seed alterations in *amp1* mutants were related to decreased production of trichomes on leaves and increased ratio of short or bifurcated root hairs in primary roots and primary root growth inhibition. Expression analyses of hormone-related gene constructs *TCS::GFP*, *DR5:uidA*, and *pABI4:uidA* indicated that slow root growth is likely independent of cytokinin and auxin signaling and involves changes in abscisic acid responsiveness. Our data show that *AMP1* is necessary for normal seed coat and embryo establishment during seed development and plays an important role in post-embryonic root growth and epidermal cell elongation.

Keywords (separated by '-')	*Arabidopsis* - Cell differentiation - Seed coat - Root hairs - Trichomes - Root growth
Footnote Information	**Electronic supplementary material** The online version of this article (doi:10.1007/s00344-016-9612-3) contains supplementary material, which is available to authorized users.

Metadata of the article that will be visualized in OnlineAlone

Electronic supplementary material	Below is the link to the electronic supplementary material. Supplementary material 1 (PDF 3443 kb)

J Plant Growth Regul
DOI 10.1007/s00344-016-9612-3

ALTERED MERISTEM PROGRAM 1 Plays a Role in Seed Coat Development, Root Growth, and Post-Embryonic Epidermal Cell Elongation in *Arabidopsis*

Claudia Marina López-García[1] · Javier Raya-González[1] · Jesús Salvador López-Bucio[2] · Ángel Arturo Guevara-García[2] · José López-Bucio[1]

Received: 4 September 2015 / Accepted: 19 April 2016

Abstract Plant development relies on the capacity of cells to interpret positional information and translate it into proliferation, elongation, and differentiation programs. *ALTERED MERISTEM PROGRAM 1 (AMP1)* encodes a putative glutamate carboxypeptidase involved in embryo development, plant growth, and phytohormone homeostasis. Here, we show that mutations of *AMP1* cause defective seed coat formation, which correlates with increased frequency of embryo abortion, low seed production, and retarded germination. Seed alterations in *amp1* mutants were related to decreased production of trichomes on leaves and increased ratio of short or bifurcated root hairs in primary roots and primary root growth inhibition. Expression analyses of hormone-related gene constructs *TCS::GFP*, *DR5:uidA*, and *pABI4:uidA* indicated that slow root growth is likely independent of cytokinin and auxin signaling and involves changes in abscisic acid responsiveness. Our data show that *AMP1* is necessary for normal seed coat and embryo establishment during seed development and plays an important role in post-embryonic root growth and epidermal cell elongation.

Keywords *Arabidopsis* · Cell differentiation · Seed coat · Root hairs · Trichomes · Root growth

Introduction

Plant form and function require specialization of cells through acquisition of distinct morphological, biochemical, and physiological properties. Growth and differentiation programs are tightly coordinated to develop the shoot system, which performs the basic functions of photosynthesis and reproduction, whereas the root system specializes in anchoring the plant to the soil and absorbs water and mineral nutrients (Gallavotti 2013; Ruiz-Herrera and others 2015). The epidermis is the protective outer layer of clonally related cells covering all plant organs at most developmental stages. It is composed of cells that differentiate in adaptively significant frequencies and patterns (Glover 2000; Javelle and others 2011). The seed coat and seedling epidermis arise from the outer cell layer during embryogenesis. The leaf and stem epidermis originate after germination from the shoot apical meristem, whereas the root epidermis develops from the root apical meristem. Epidermal-differentiated cells include stomatal guard cells that allow gas exchange, trichomes that protect the aerial parts from herbivores, and root hairs that increase the root surface area for water and nutrient uptake (Ishida and others 2008; Casson and Hetherington 2010; Bruex and others 2012).

Seeds ensure the propagation of angiosperms via embryo protection and geographical dispersion. Seed development initiates after a double fertilization event that gives rise to the three major components of the seed, (i) the embryo, which comes from egg cell fertilization, (ii) the endosperm, which comes from central cell fertilization and

Electronic supplementary material The online version of this article (doi:10.1007/s00344-016-9612-3) contains supplementary material, which is available to authorized users.

✉ José López-Bucio
jbucio@umich.mx; joselopezbucio@yahoo.com.mx

[1] Instituto de Investigaciones Químico-Biológicas, Universidad Michoacana de San Nicolás de Hidalgo, Edificio B3, Ciudad Universitaria, C. P. 58030 Morelia, Michoacán, México

[2] Instituto de Biotecnología-UNAM, Av. Universidad No. 2001, Col. Chamilpa, Cuernavaca, Morelos, México

Journal : Large 344 | Dispatch : 13-6-2016 | Pages : 18
Article No. : 9612 | LE | TYPESET
MS Code : JPGR-15-0354 | CP | DISK

provides a supply of nutrients to the developing embryo, and (iii) the seed coat, which originates from maternal integuments and acts as a mechanical and protective barrier (Haughn and Chaudhury 2005; Dekkers and others 2013). After fertilization, cell division begins yielding an apical and a larger basal cell, and the apical cell continues dividing to finally produce the hypocotyl, the shoot meristem, and cotyledons. The basal cell divides horizontally producing the suspensor, whose hypophyseal cell participates in the formation of the embryonic root meristem (Breuninger and others 2008; Lau and others 2012; Locascio and others 2014). The final seed size, weight, and form are coordinately determined by endosperm development, growth of the embryo, and differentiation of the integuments (Berger and others 2006; Zhou and others 2009). The proper embryo development depends on an adequate provision of sucrose and nutrients by the endosperm and seed coat; if endosperm development fails or transport of sucrose via the seed coat is affected, embryo development does not proceed normally (Hehenberger and others 2012; Lafon and Köhler 2014; Chen and others 2015). Genetic analysis suggests that the endosperm produces a signal that initiates the differentiation of the integuments to produce the seed coat (Berger and others 2006; Ingouff and others 2006; Figueiredo and Köhler 2014). A few loci have been implicated in the development of the seed coat in *Arabidopsis*, including *APETALA 2* (*AP2*) and *TRANSPARENT TESTA GLABRA 1* (*TTG1*), which regulates elongation of seed coat cells, protoanthocyanidin, and mucilage biosynthesis (Debeaujon and others 2000; Orozco-Arroyo and others 2015). Moreover, *TTG1* and *AP2* loss-of-function causes limited and prolonged cell proliferation of the endosperm, respectively, indicating an endosperm seed coat cross-talk during seed development (Koornneef 1981; Koornneef and others 1982; Jofuku and others 1994; Figueiredo and Köhler 2014).

Following germination, the plant epidermis plays important structural and adaptive roles. In primary and lateral roots, epidermal cells differentiate into two cell types following a file-specific program, root hair cells, also named trichoblast or H (Hairy) cells, and non-hair cells, termed atrichoblasts, or N (Non-hair) cells. Trichoblasts are commonly located between two cortical cells and are thought to control root hair determination and differentiation via signal exchange (Rerie and others 1994; Masucci and others 1996; Ishida and others 2008; Libault and others 2010). TTG1 and GLABRA 2 (GL2*)* transcription factors are important regulators of root hair specification that control the expression of genes encoding cell wall components, such as *CELLULOSE SYNTHASE 5 (CESA5)* and *XYLOGLUCAN ENDOTRANSGLUCOSYLASE* 17 (XTH17) (Tominaga-Wada and others 2009; Libault and others 2010). After root hair specification, several processes including cytoskeleton dynamics, vesicle trafficking and ion or metabolite exchange regulate the polarized growth of root hairs (Rerie and others 1994; Masucci and others 1996; Ishida and others 2008; Libault and others 2010). In leaves, some epidermal cells differentiate as trichomes, which act in defense against herbivores, in protection against UV light, and in production of protective chemicals (Hülskamp and others 1994; Pattanaik and others 2014). In *Arabidopsis,* trichome cells are three branched structures, whose specification depends on a signaling network involving *GLABRA 3 (GL3), GLABRA 1 (GL1*), and *TTG1* (Pattanaik and others 2014).

Plant growth regulators control epidermal cell differentiation and elongation thoroughly. Auxin, ethylene, cytokinin CK, abscisic acid ABA, and gibberellin signaling pathways play crucial roles in seed development, dormancy, and germination. Phytohormones regulate both root hair and trichome development via changes in expression of genes encoding transcription factors, enzymes, and structural components, such as cellulases and expansions required to achieve the final morphology and function of epidermal cells (Hülskamp and others 1994; Ishida and others 2008; Pattanaik and others 2014). Although seed coat differentiation, root hair, and trichome development rely on the expression of a common set of genes, very little is known about the specific role of each gene product in coordination of growth and cell patterning specification (Casson and Hetherington 2010; Bruex and others 2012).

ALTERED MERISTEM PROGRAM 1 (AMP1) encodes an endoplasmic reticulum (ER) membrane-localized glutamate carboxypeptidase involved in several developmental processes in plants. Recently, it has been found that *AMP1* and *ARGONAUTE 1*, a key component of the plant micro-RNA (miRNA) effector complex, both localize to the ER and interact to inhibit translation. In *amp1* mutants, mRNA cleavage and decay occur normally, whereas the translation rate of micro-RNA (miRNA)-controlled proteins is enhanced at ER-located polysomes, suggesting an important role of *AMP1* on the plant signaling pathways controlled by miRNAS (Liu and others 2013).

In accordance with its critical role in plant signaling, mutations in the *Arabidopsis AMP1* gene cause large-scale alterations in phenotype including abnormal embryo development, altered number of cotyledons, de-etiolation of dark grown seedlings, increased leaf initiation, dwarfing, earlier flowering, semi-sterility, and increased cell proliferation (Chaudhury and others 1993; Mordhorst and others 1998; Nogué and others 2000a, b; Vidaurre and others 2007; Kong and others 2015). These alterations have been related to increased levels of endogenous phytohormones, including CKs and/or ABA, as well as nitric oxide or *AUXIN RESPONSE FACTOR 5* (*ARF5*) acting downstream in a signaling cascade affecting cell cycle gene expression

Journal : Large 344 | Dispatch : 13-6-2016 | Pages : 18
Article No. : 9612 | LE | TYPESET
MS Code : JPGR-15-0354 | CP | DISK

(Vidaurre and others 2007; Griffiths and others 2011; Liu and others 2013; Shi and others Shi and others 2013a, b). An increased CK content in *amp1* mutant seedlings likely explains the constitutive photomorphogenesis, enhanced shoot regeneration, and increased branching already reported for these mutants, whereas the enhanced shoot meristem size and leaf initiation rate phenotype appears to be independent of the altered CK levels (Chin-Atkins and others 1996; Nogué and others 2000b; Huang and others 2015). Mutation of the *amp1–31* allele resulted in both greater accumulation of ABA than the WT and increased ABA sensitivity in seed germination and root growth inhibition; this later response was correlated with more lateral roots being formed in the mutants and improved drought resistance (Yao and others 2014). Hence, AMP1 represents a key regulator of plant development and hormonal responses; however, how the diverse functions of this protein converge at the molecular and cellular level is not resolved.

In this study, we provide evidence that *AMP1* plays a pleiotropic role in epidermal tissue differentiation leading to seed coat development, and report four distinct and stable seed phenotypes that were not previously described for these mutants. We also found that *amp1* seedlings produce less trichomes per leaf and short or bifurcated root hairs in primary roots and shorter primary roots. The indicated root or shoot phenotypes are unlikely caused by enhanced CK or auxin response, and correlated with increased ABA responsiveness in root tips and, surprisingly, with *AP2* and *MUM3* overexpression. Our data suggest a primary role of this putative glutamate carboxypeptidase not only in coordinating embryo development to the formation of the seed coat, but also in post-embryonic root growth and epidermal cell elongation programs.

Materials and Methods

Plant Material and Growth Conditions

Arabidopsis (*Arabidopsis thaliana*) ecotypes Columbia (Col-0), Landsberg erecta and Wassilewskija, and the single, double, and triple mutant lines *amp1–10* (SALK_021406), *amp1–20* (SALK_138749), *cre1–12* (Inoue and others 2001), *ahk2-2* (Ueguchi and others 2001), *ahk3-3* (Ueguchi and others 2001), *det2-1* (Chory and others 1991), *rpn12* (Smalle and others 2002), *ein2* (Guzman and Ecker 1990), *ein3* (Chao and others 1997), *etr1* (Bleecker and others 1988), *eto3* (Woeste and others 1999), *ctr1* (Kieber and others 1993), *Atnoa1* (Guo and others 2003), *nia1nia2* (Wilkinson and Crawford 1993), *jar1* (Tiryaki and Staswick 2002), *pft1,2* (Raya-González and others 2014), *aux1–7* (Pickett and others 1990), *axr2-1* (Wilson and others 1990), *slr1* (Fukaki and others 2002), *arf7arf19* (Okushima and others 2007), *tir1afb2afb3* (Parry and others 2009), *abi1* (Leung and others 1997), *abi2* (Leung and others 1997), *abi3* (Nambara and others 1992), *abi4* (Finkelstein and others 1998), *abi5* (Finkelstein 1994), and *drr1* (Morquecho-Contreras and others 2010) were used for the experiments reported here. To generate the wild-type and *amp1* lines expressing CK, auxin or ABA reporter gene constructs, *TCS::GFP* (Zürcher and others 2013), *DR5:uidA* (Ulmasov and others 1997), and *pABI4:uidA* (Bossi and others 2009), respectively, crosses were made between transgenic plants expressing these constructs and homozygous *amp1* mutants. F3 populations from the crosses were screened for seedlings with slow growing roots, and homozygous lines harboring the marker constructs were used in subsequent experiments. For histochemical analysis of GUS activity and detection of GFP expression, we used the protocols reported by Raya-González and others (2014).

Seeds were surface sterilized with ethanol 95 % and sodium hypochlorite 20 % for 5 and 7 min, respectively, then washed five times with 1 ml sterile distilled water, and incubated for 7 days at 4 °C. The seeds were plated into 0.2X solidified MS medium containing MS basal salts (Murashige and Skoog Basal Salts Mixture, Sigma-Aldrich, St Louis, MO), 1 % agar (Phytagar Gibco-BRL), and 1 % sucrose (Sigma-Aldrich, St Louis, MO) and incubated in a plant growth chamber (Percival AR-95L) at 22 °C with a photoperiod of 16-h light/8-h darkness under light intensity of 105 μmol/m^2/s.

Seed Coat Analysis

The seed phenotype analysis was performed using a stereoscopic microscope MZ6 (Leica Microsystems). Seed phenotypes of the *amp1* mutant were classified and photographed with a camera adapted to the microscope (Cyber-shot DSC-S75; Sony Electronics), and the seed length and width were determined with Image J program (Wayne Rasband National Institutes of Health, USA). For the analysis of the seed coat, dry WT and *amp1–10* seeds were covered with a copper layer and analyzed and photographed using a Jeol JSM-7600F field emission scanning electron microscope, equipped with a Bruker X-Flash6/30 camera.

Seed Germination Assays

For germination assays, mature seeds from WT and the four *amp1–10* mutant classes were sterilized and plated into 0.2X MS medium and/or the same medium supplemented with 1 μM GA, and incubated in a plant growth

Journal : Large 344 | Dispatch : 13-6-2016 | Pages : 18
Article No. : 9612 | LE | TYPESET
MS Code : JPGR-15-0354 | CP | DISK

chamber to register germination at the time when radicle was completely emerged.

Trichome, Root Hair, and Silique Analyses

Arabidopsis WT and *amp1–10* mutant seeds were surface disinfected and plated as described above and then grown into a plant growth chamber (Percival AR-95L). Root hairs were analyzed from primary roots of 7-day-old seedlings and trichomes were counted and photographed from 14-day-old leaves. For embryo development analysis, WT and *amp1* mutant seedlings were grown in Petri plates for 12 days and then transferred to soil until fruit production. Ten siliques were dissected with a needle and the developing seeds and embryos photographed with a stereoscopic microscope (MZ6, Leica Microsystems), and with a DM5000B differential contrast microscope, respectively.

Mucilage Detection

Dry seeds of *Arabidopsis* WT and *amp1* mutants were incubated in 1 ml 50 mM EDTA at 1000 rpm during 2 h and then incubated in agitation in 0.01 % (w/v) Ruthenium Red at 1000 rpm during 1 h. Stained seeds were mounted on glass slides, analyzed, and photographed with an optic microscope DM5000B (Leica Microsystems) using differential interference contrast (DIC) microscopy.

Embryo Analysis

Arabidopsis WT and *amp1* embryos were dissected from the silique using a needle and then incubated for 2 days in Hoyeŕs solution (prepared as described in Seed Genes Project database; http://www.seedgenes.org). After clearing, the seeds were analyzed and photographed by DIC microscopy in a DM5000B optic microscope (Leica Microsystems).

Northern Blotting

For RNA hybridization analysis, 12-day-old seedlings were frozen and grinded into liquid nitrogen, and total RNA was extracted from 50 mg of grinded tissue using TRIzol according to the protocol of the manufacturer (Invitrogen, Carlsbad, CA, USA). RNA (10 µg) was separated in 1.2 % formaldehyde agarose gel electrophoresis according to the protocol adapted from Rneasy Mini Handbook (QIAGEN) and transferred to Hybond-N+nylon membrane (GE, Healthcare) and fixed in an UV crosslinker at 70,000 microjoules/cm^2. Different probes were ^{32}P radiolabeled with α^{32}P dCTP (Perkin Elmer Life Science Inc.) using Klenow DNA polymerase 1 according to the protocol of the manufacturer (NEW ENGLAND, Biolabs). Membranes containing RNA were hybridized for 4 h with the different probes tested and washed with a solution of sodium chloride (7.5 mM)/sodium citrate (8.75 mM). The probe was detected after 8 h of exposure in an X-Ray film (GE, Healthcare). The assayed probes were amplified by PCR reactions from DNA using the indicated oligonucleotides, AP2 forward 5′ GGGATCTAAACGACGCAC 3′ and reverse 5′ACGCCGGTAAAACGTAAC 3′; TTG1 forward 5′ CACTCTACGCCATGGCTT 3′ and reverse 5′TGATGC GAAAACCCTAGC 3′; MUM3 forward 5′GATGGATGA GGGAAGGCA 3′ and reverse 5′CATTCGGGAGCTCGT GGC 3′.

Results

AMP1 Mutation Affects Fruit Size, Seed Production, and Seed Phenotype

Seed development is an important agricultural and adaptive trait. An analysis of *Arabidopsis* WT (Col-0) and *amp1–10* mutants grown in soil showed that *amp1* siliques were 65 % shorter than WT, which correlated with decreased seed production and ovule fertilization (Supplementary Fig. S1). To analyze seed viability, we obtained several seed pools from individual homozygous *amp1–10* and *amp1–22* mutants and compared to WT seeds. Surprisingly, both *amp1* mutant alleles exhibited four segregating phenotypically distinctive seed classes not previously described for these mutants (Fig. 1a–e and Supplementary Fig. S2), including seeds that we defined as "regular," "raisin," "irregular," and "burst." In the first class (∼80 % *amp1–10*/regular seeds), the loss-of-function of *AMP1* caused slight alterations in seed morphology (Fig. 1b and Supplementary Figs. S2 and S3). The second class (∼8 % *amp1–10*/raisin seeds) included seeds with rough coats (Fig. 1c and Supplementary Figs. S2 and S3). The third class (∼10 % *amp1–10*/irregular seeds) had alterations in shape, seed coat structure, and pigmentation (Fig. 1d and Supplementary Figs. S2 and S3), whereas the smaller class (∼2 % *amp1–10*/burst seeds phenotype) included seeds with protruding embryos (Fig. 1e and Supplementary Figs. S2 and S3). An *AMP1* overexpressing line AMP1 OX2 showed normal seed phenotypes both in form and size, whereas *amp1–10* mutants developed smaller and thinner seeds (Supplementary Figs. S3 and S4). These data show that although the loss-of-function in *AMP1* affects seed form and size, higher *AMP1* levels did not disrupt normal seed morphogenesis.

Because most phytohormones are known to participate in seed development, we tested whether the seed phenotype of *amp1* mutants could be observed in *Arabidopsis* mutants affected in auxin, ET, CK, ABA, nitric oxide, and jasmonic

Journal : Large 344 | Dispatch : 13-6-2016 | Pages : 18
Article No. : 9612 | LE | TYPESET
MS Code : JPGR-15-0354 | CP | DISK

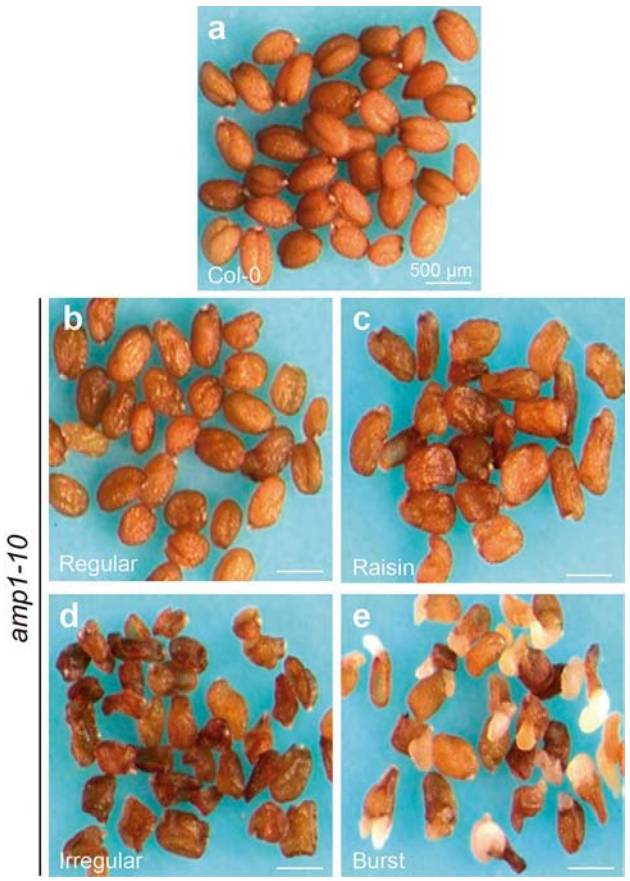

Fig. 1 *AMP1* mutation causes four different seed phenotypes. Seeds from wild-type plants (Col-0) are shown in (**a**). **b–e** *amp1–10* mutant seeds that were collected from individual homozygous plants and separated according to the seed phenotype using a dissection microscope: **b** Seeds with phenotype similar to WT ("regular"). **c** Seeds resembling raisins ("raisin"). **d** Seeds with clearly collapsed coats ("irregular"). **e** Seeds with embryos protruding from the seed coat ("burst"). *Scale bar* = 500 µM

acid signaling pathways. Dry seed screening, considering form, width, and length of *cre1–12*, *ahk2-2*, *ahk3-3*, *det2-1*, *rpn12*, *ein2*, *ein3*, *etr1*, *eto3*, *ctr1*, *Atnoa1*, *nia1nia2*, *jar1*, *pft1*,*2*, *sag13*, *aux1–7*, *axr2-1*, *slr1*, *arf7arf19*, *tir1afb2afb3*, *abi1*, *abi2*, *abi3*, *abi4*, *abi5*, and *drr1,* hormone-related mutants, revealed that the *abi5* and *tir1afb2afb3* single and triple mutants, respectively, were longer than WT seeds (Supplementary Fig. S5). However, none of the above-mentioned mutants showed the seed phenotypes already found in the *amp1* mutants.

amp1 Seeds Show Defects in Seed Coat Structure and Mucilage Production

The outer cell layer of *Arabidopsis* seeds consists of polygonal structures that form a donut-shaped pocket with a volcano-shaped central elevation known as columella, which results from deposition of mucilage between the primary cell wall and protoplasm (Windsor and others 2000; Volodymyr and Boriskuj 2014). To determine if *AMP1* modulates seed morphology through modifications on seed coat cells, we performed an ultra-structure scanning electron microscopy analysis on mature WT and *amp1–10* seeds. This analysis revealed the characteristic polygonal cells with thickened radial cell walls and well-defined columella in WT seeds (Fig. 2a–c). In contrast, the seed coat of the four different *amp1–10* seed classes exhibited unusual epidermal cells (Fig. 2d–o). Although no significant differences in size were evident, "regular" and "raisin" seeds showed more robust columella than the WT (Fig. 2f, i, p, and q), whereas "burst" seeds had an abnormal organization of seed coat cells, lacking well-defined cell walls and columella (Fig. 2m–q).

Mucilage mainly consists of pectin, which contains large amounts of galacturonic acid and rhamnose, and low amounts of monosaccharides such as arabinose, galactose, glucose, xylose, and mannose forming complex polysaccharides (Voiniciuc and others 2015). Seed mucilage content can be estimated via ruthenium red staining, which reveals the acidic biopolymers found in the seed coat (Hanke and Northcote 1975). A ruthenium red staining assay on WT seeds revealed inner and outer domains; the inner domain was defined by a characteristic magenta color, which radiates out from the mucilage pocket, whereas the outer mucilage domain is defined by an unstained halo surrounding the inner layer (Fig. 3a–c). The staining assay in *amp1–10* "regular" and "raisin" seeds showed similar staining patterns as in WT seeds (Fig. 3d–i), but in the "irregular" and "burst" seeds, regions without mucilage staining could be observed (Fig. 3j–o), indicating a direct link between *amp1* seed phenotypes and the proper formation of the mucilage capsule during seed development.

Relationship Between Seed Coat and Embryo Development in *Arabidopsis amp1* Mutants

Some *amp1* embryos are affected during the globular stage, producing new organs with cotyledon identity via ectopic cell divisions (Vidaurre and others 2007). This was further confirmed through an analysis of embryo development in which *amp1–10* mutants with "regular" seed coats commonly developed embryos with three cotyledons (Fig. 4a–s). These abnormal embryos were able to fill the seed and the development of the seed proceeded normally, giving rise to the testa with phenotype similar to the WT (Fig. 4b–j and l–t). A more detailed microscopic analysis of mature *amp1–10* seeds revealed that "irregular" seeds contained embryos arrested at early stages during their development (Fig. 5e–h). Other "irregular" seeds apparently lacked embryos (Fig. 5c and d), whereas "burst" seeds often

Journal : Large 344 | Dispatch : 13-6-2016 | Pages : 18
Article No. : 9612 | LE | TYPESET
MS Code : JPGR-15-0354 | CP | DISK

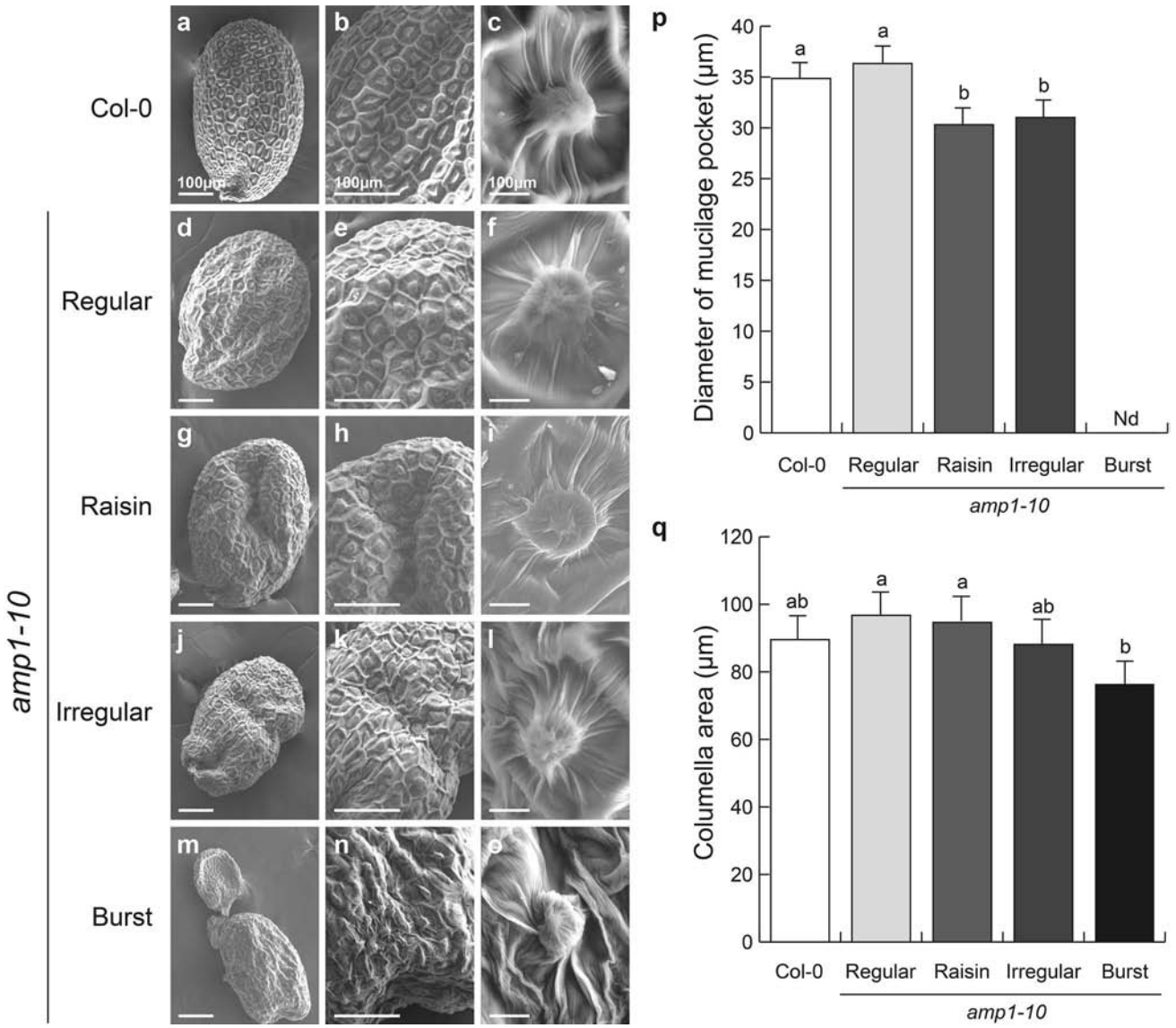

Fig. 2 *AMP1* mutation affects seed coat structure. Dry seeds were covered with a copper layer and observed with a scanning electron microscopy. **a–c** Seed phenotype of *Arabidopsis* WT (Col-0). Note hexagonal epidermal cells with thickened radial cell walls and volcano-shaped columella at the center of each cell. **c** Close-up of WT seed coat. *amp1* mutant seed photographs with "regular" (**d–f**), "raisin" (**g–i**), "irregular" (**j–l**), and "burst" (**m–o**) phenotypes. Raisin, irregular, and burst *amp1* phenotypes show altered seed coat shape and columella structure. (**p**) Diameter of mucilage pocket. (**q**) Columella area (measured from electronic micrographs using the image J program). *Error bars* represent SD from 30 seeds analyzed. *Different letters* indicate statistical differences at $P < 0.05$. This analysis was performed from three individual *amp1* seed harvests with similar results

included cell masses protruding from the seed coat (Supplementary Fig. S6). In most cases, altered embryo development in *amp1–10* mutants correlated with a defective seed testa (Fig. 5c–j).

Altered Seed Shape in *amp1* Mutants Correlates with Viability

AMP1 has been involved in seed dormancy, germination, and ABA responses (Griffiths and others 2011; Shi and others 2013b). To determine if the seed coat alterations of *amp1* mutants could be related to viability, we compared germination frequencies between WT and *amp1* seeds at 24, 28, and 32 h. WT seeds started germination 24 h after shown (Fig. 6a) and reached 100 % around 32 h (Fig. 6b and c). On the other hand, *amp1* seeds with a "regular" phenotype germinated at similar frequencies as WT, but showed decreased viability as about 25 % of the seeds did not germinate (Fig. 6a–c). Only around 40, 15, and 8 % of "raisin," "irregular," and "burst" *amp1* seeds,

Journal : Large 344 Dispatch : 13-6-2016 Pages : 18
Article No. : 9612 LE TYPESET
MS Code : JPGR-15-0354 CP DISK

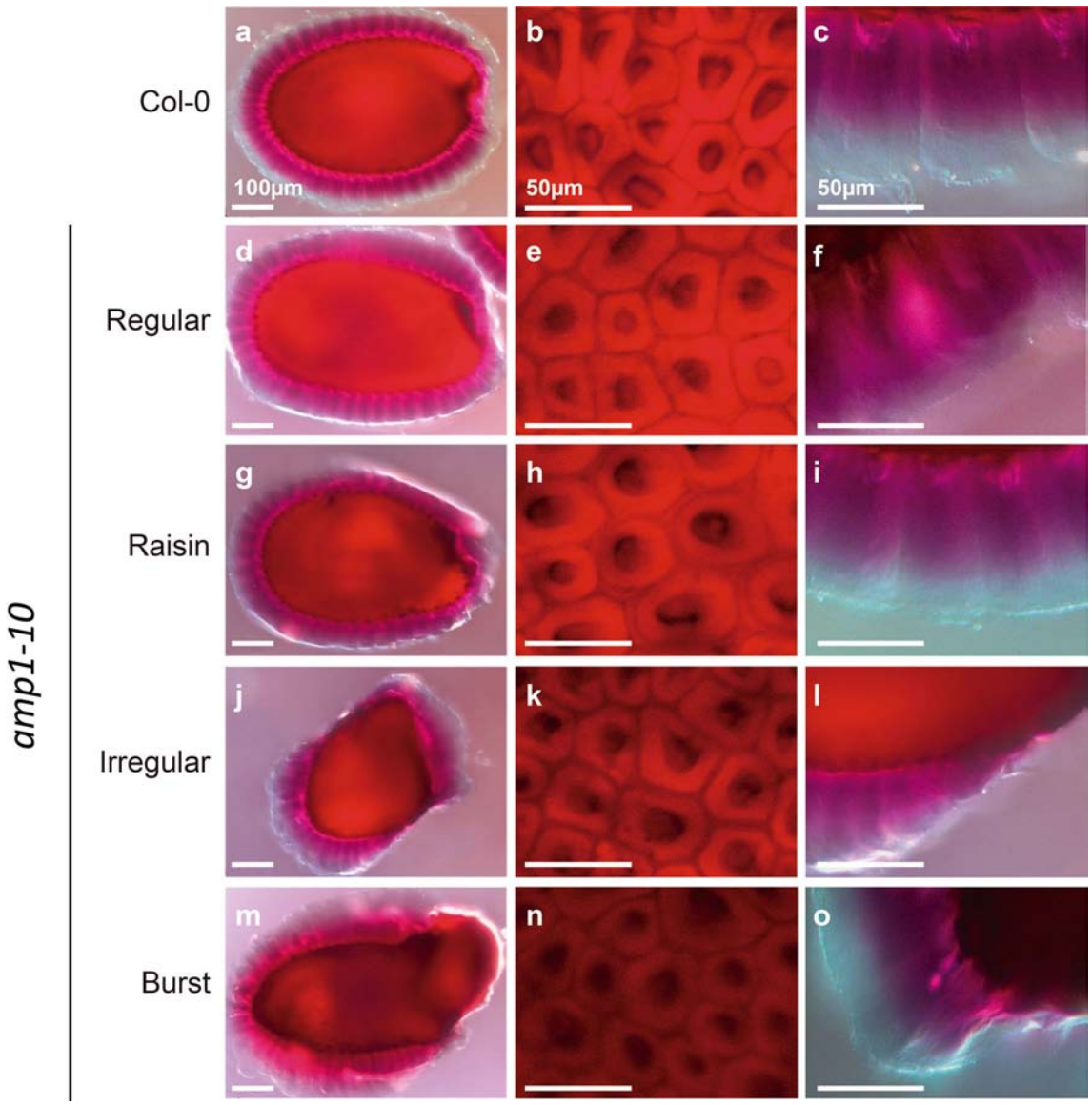

Fig. 3 The mucilage capsule of seeds is altered in *amp1* mutant. *Arabidopsis* WT and *amp1–10* mutant seeds were staining with ruthenium red and observed in a Leica DM5000B microscope. The mucilage capsule from WT (Col-0) seeds shows the characteristic outer and inner domains; the inner region stained in *magenta color* radiates out from the mucilage pocket, and the outer, unstained mucilage domain covers the inner layer. The coat of "irregular" and "burst" *amp1* seeds show decreased mucilage capsule width in some areas of the seed coat. *Scale bars* indicated in **a–c**, are the same for all photographs in a column

respectively, were able to germinate (Fig. 6c). Because gibberellic acid (GA) induced germination (Ullah and others 2002; Holdsworth and others 2008), we tested if GA addition could normalize germination in *amp1* seeds. Indeed, GA promoted germination of both WT and *amp1* "regular" seeds at earlier stages (Fig. 6a and b) and "raisin" seeds at 32 h but failed to improve germination in "irregular" and "burst" a*mp1* seeds at any of the stages tested (Fig. 6c). These results indicate that *amp1* seeds have decreased viability, which is apparently related to altered seed coat and embryo development.

AMP1 is Involved in Post-Embryonic Shoot and Root Epidermal Cell Differentiation

The plant epidermis plays important roles during post-embryonic development. Trichomes are specialized epidermal cells formed on leaves and stems that protect the aerial parts from herbivores. Root hairs also are specialized epidermal cells developed in primary and lateral roots that play a critical role in water and nutrient acquisition (Javelle and others 2011). To determine if *AMP1* could have a function in differentiation of root and shoot epidermal

Journal : Large 344 Dispatch : 13-6-2016 Pages : 18
Article No. : 9612 LE TYPESET
MS Code : JPGR-15-0354 CP DISK

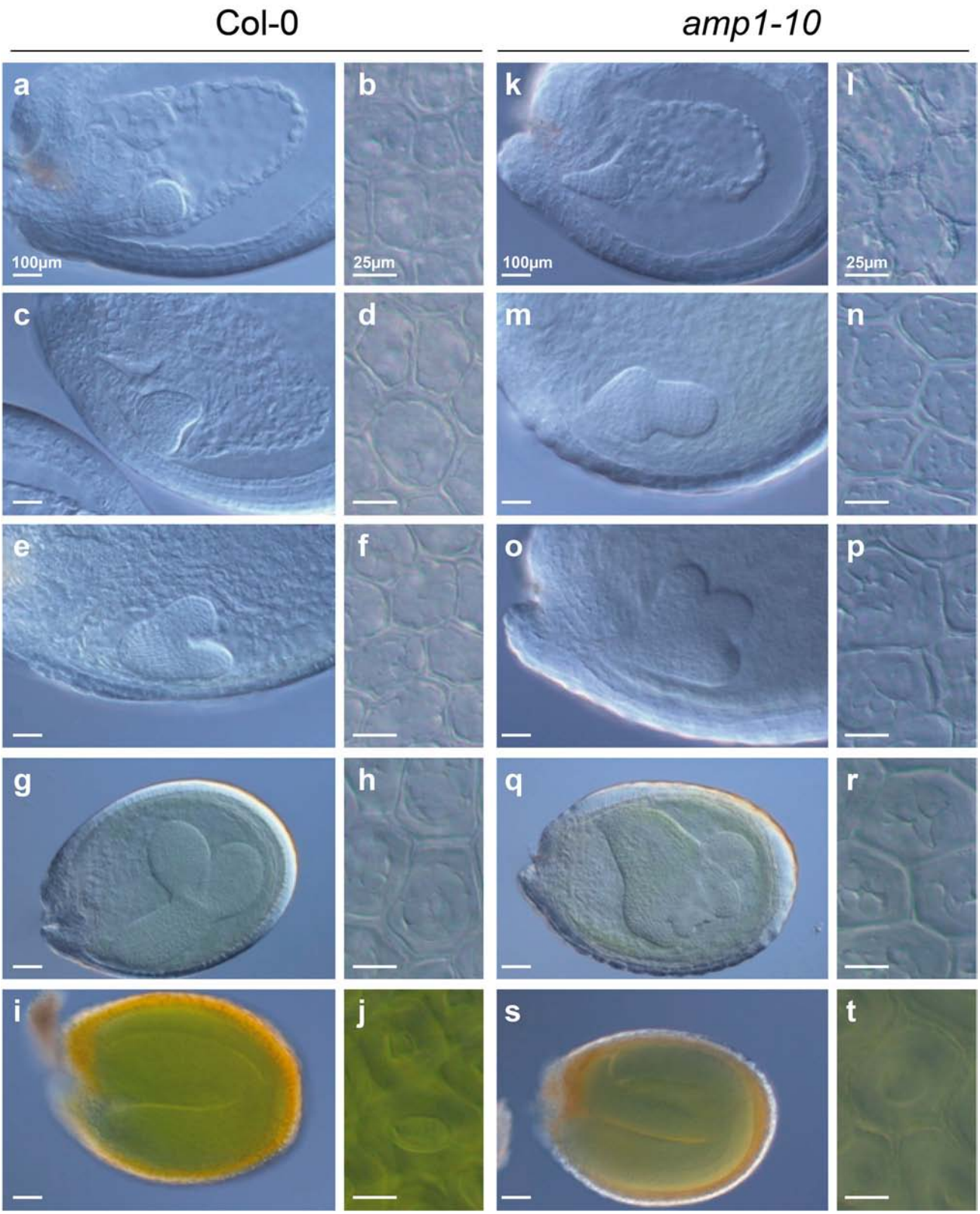

Journal : Large 344 Dispatch : 13-6-2016 Pages : 18
Article No. : 9612 ☐ LE ☐ TYPESET
MS Code : JPGR-15-0354 ☑ CP ☑ DISK

◄**Fig. 4** *amp1* embryos are affected in development. *Arabidopsis* WT (Col-0) embryos at different developmental stages are shown: globular (**a),** pre-heart (**c**), heart (**e),** cotyledon (**g**), and blend (**i)** stages. *amp1–10* mutant embryos are shown in **k**, **m**, **o**, **q**, and **s** panels. WT and *amp1–10* embryos in the same file were taken from siliques at a similar stage of development. To the right of each embryo picture, a close-up of the corresponding seed coat is shown. All the pictures were taken using Nomarsky optics. *Scale bars* indicated in **a**, **b**, **k**, and **l** are for all pictures within the same column

cells, we compared root hair and trichome formation in 7- and 14-day-old WT and *amp1* seedlings, respectively. Compared to the WT (Col-0), *amp1* seedlings germinated from "regular" and "raisin" seeds produced 50 % less trichomes per leaf (Fig. 7a–k). Trichome production was even lower (75 %) in seedlings from "irregular" and "burst" seeds (Fig. 7k). Additionally, *amp1* produced abnormal trichomes, which fail to branch (Fig. 7l). When

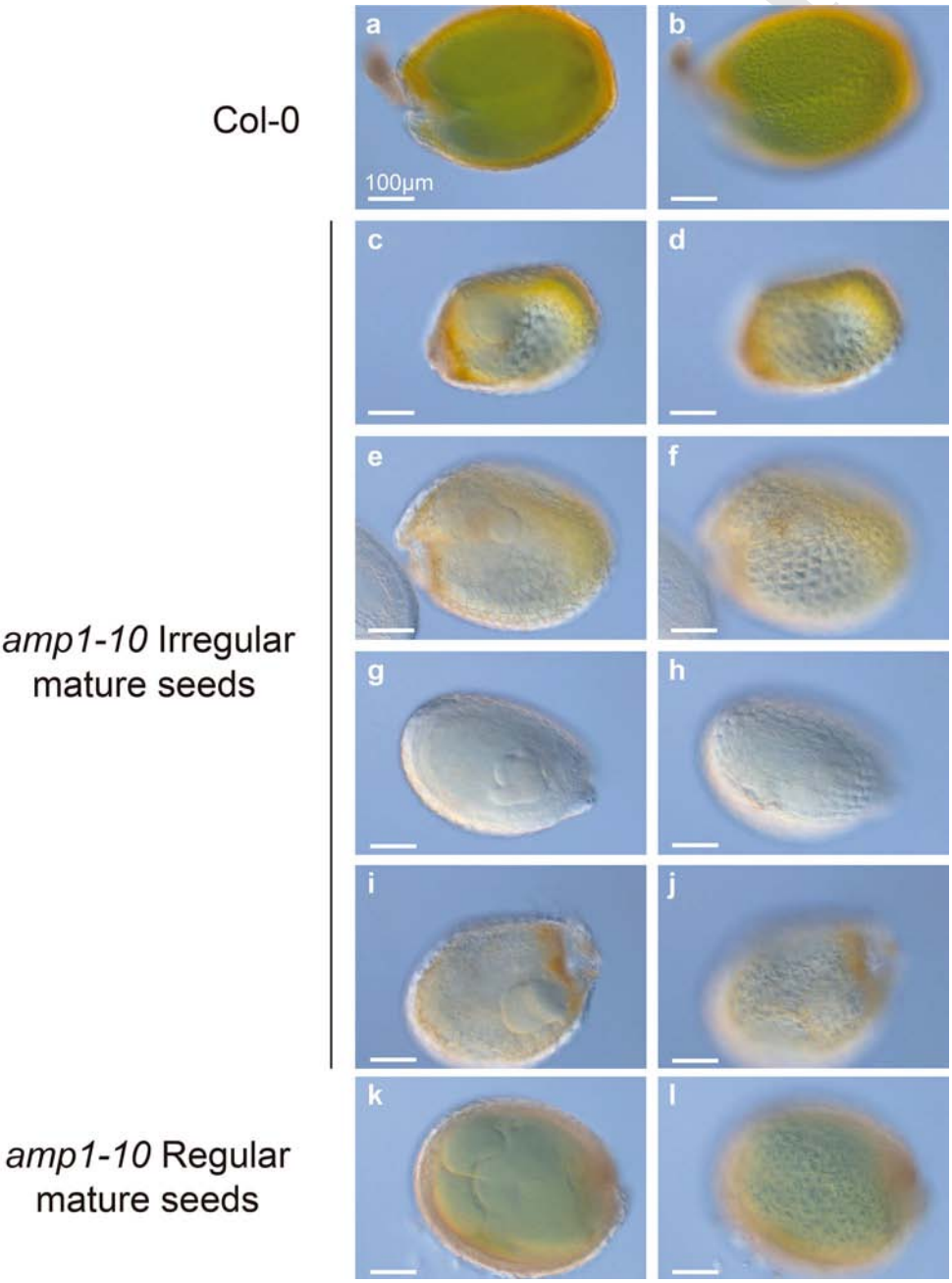

Fig. 5 Halted embryo development and defective seed testa in *amp1* mutants appear to be related. *Arabidopsis* WT (Col-0) and *amp1* seeds were taken from the same silique and clarified with chloral hydrate. WT embryos and their corresponding seed coats are shown (Col-0; **a, b**), *amp1–10* mutant (**c–i** embryos; **d–j** seed coats). Note that defective embryo development in *amp1–10* "irregular" seeds seems to be related to an altered seed testa. *Scale bar* indicated in **a** is the same in all the pictures

Journal : Large 344 Dispatch : 13-6-2016 Pages : 18
Article No. : 9612 LE TYPESET
MS Code : JPGR-15-0354 CP DISK

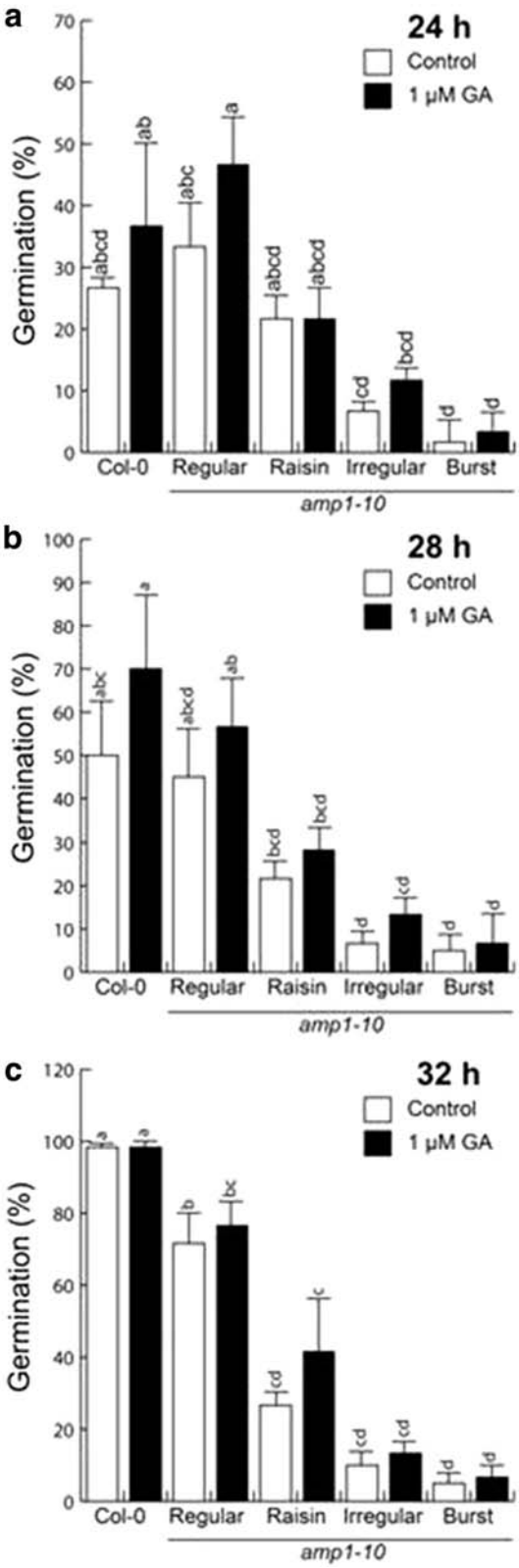

◀**Fig. 6** Seed germination in WT *amp1* mutants. *Arabidopsis* WT (Col-0) and *amp1* seeds were collected from individual plants. *amp1* seeds were grouped according to the different seed phenotypes. Seeds were shown on 0.2X MS medium or the same medium supplemented with 1 µM GA and the percentage of germination (radicle protrusion) was evaluated at 24 (**a**), 28 (**b**), and 32 h (**c**). Note the germination percentages of all seed classes of *amp1* mutant are lower and that GA fails to rescue the germination of "irregular" and "burst" seeds

comparing root hair development in WT and *amp1* seedlings, no alterations in root hair density were evident, but interestingly, the root hair length decreased in *amp1* seedlings (Fig. 8a–o), and some of these root hairs were abnormally bifurcated (Fig. 8k–m and p). These results suggest that *AMP1* plays an important role in epidermal cell differentiation, not only during seed coat development, but also in trichome and root hair differentiation.

To investigate the possible role of AMP1 in regulating the expression of genes involved in seed coat, trichome, and root hair development, we monitored the transcript levels of *APETALA 2* (*AP2*), *TRANSPARENT TESTA GLABRA 1* (*TTG1*), and *CELLULOSE SYNTHASE 5* (*CESA5/MUM3*) genes in 12-day-old WT seedlings or in *amp1–10* and *amp1–22* mutant seedlings by Northern blot analysis. Our results show that in *amp1* mutants, the transcript levels of *AP2* and *MUM3* were induced, whereas *TTG1* expression was not affected when compared to WT seedlings (Supplementary Fig. S7). These data suggest that *AMP1* is a repressor of *AP2* and *MUM3* during post-embrionary plant development.

Expression of *ABI4:uidA* Gene Marker Is Increased in Roots and Shoots of *amp1* Mutant Seedlings

Phenotypical alterations in *amp1* seedlings have been related to altered levels and/or response to CKs, auxin, and ABA (Vidaurre and others 2007; Griffiths and others 2011; Liu and others 2013; Shi and others 2013a, b). We focused on the short root phenotype of *amp1* seedlings already reported by Yao and others (2014, Fig. 9a and b) to compare the expression of hormone-related gene constructs *TCS::GFP* (Zürcher and others 2013), *DR5:uidA* (Ulmasov and others 1997), and *pABI4:uidA* (Bossi and others 2009), which are inducible by CKs, auxin, and ABA, respectively, in WT or *amp1* seedlings. In our experiments, the expression domains of *TCS::GFP* and *DR5:uidA* did not change in *amp1* seedlings when compared to the WT, whereas *pABI4:uidA* was clearly increased in primary root tips of *amp1* seedlings (Fig. 9c–h). An analysis of the expression of these hormone-inducible gene markers in the shoot system provided similar results (Supplementary Fig. S8), suggesting that AMP1 negatively regulates in

Journal : Large 344 Dispatch : 13-6-2016 Pages : 18
Article No. : 9612 LE TYPESET
MS Code : JPGR-15-0354 CP DISK

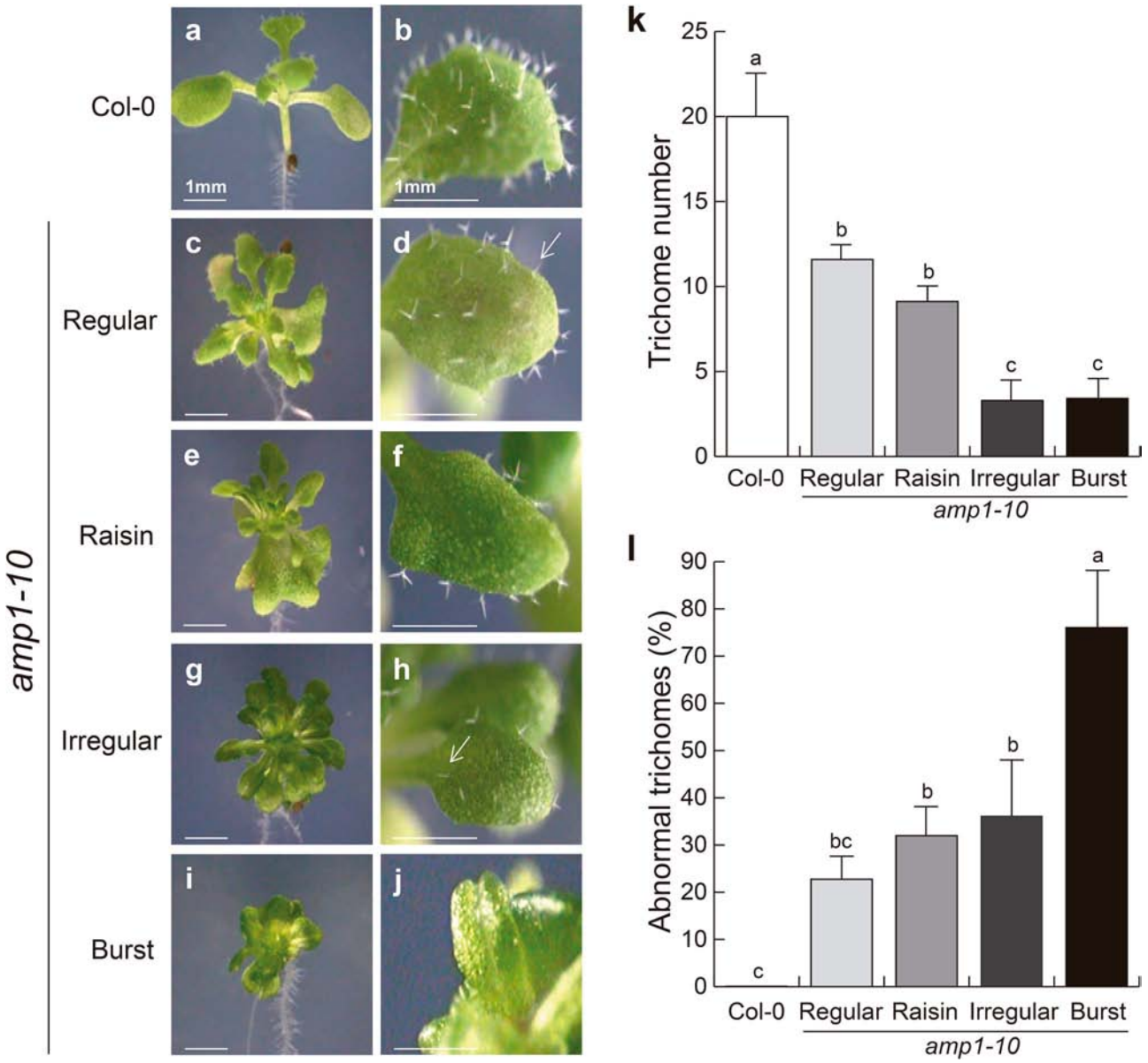

Fig. 7 Trichome development is affected in *amp1* mutant. Trichomes of *Arabidopsis* WT (Col-0) and *amp1* seedlings germinated and shown on 0.2X MS medium were analyzed using a stereomicroscope. Seedling (**a, c, e, g, and i**) and leaf close-up (**b, d, f, h, and j**) phenotypes of WT (**a** and **b**) and *amp1* mutant **c–j** are shown. *Scale bars* shown in **a and b** are the same for the corresponding column. Arrows in **d, h** are used to show abnormal trichomes. Note that besides the evident reduction in the number of trichome per leaf (**k**), an abnormal trichome branching (without branches or less branched than WT) is observed in all *amp1* seedling classes **l**. *Error bars* represent SD from 10 leaves analyzed. *Different letters* indicate statistical differences at $P < 0.05$. The experiment was repeated three times with similar results

ABA biosynthesis and/or responsiveness, affecting ABA-mediated developmental programs.

Discussion

Genes controlling cell growth or differentiation is important for coordinating the activities of specialized tissues and organs; mutations in these genes can cause large-scale changes in the structure of an organism. Mutation of *AMP1* leads to several defects in embryo development, germination, photomorphogenesis, shoot apical meristem, flowering, and hormonal responses (Chaudhury and others 1993; Helliwell and others 2001; Saibo and others 2007; Vidaurre and others 2007; Griffiths and others 2011; Shi and others 2013b). In this work, we performed a detailed analysis of seed morphology in two *amp1* mutant alleles (*amp1–10* and *amp1–22*) and established a correlation between

Journal : Large 344 Dispatch : 13-6-2016 Pages : 18
Article No. : 9612 LE TYPESET
MS Code : JPGR-15-0354 CP DISK

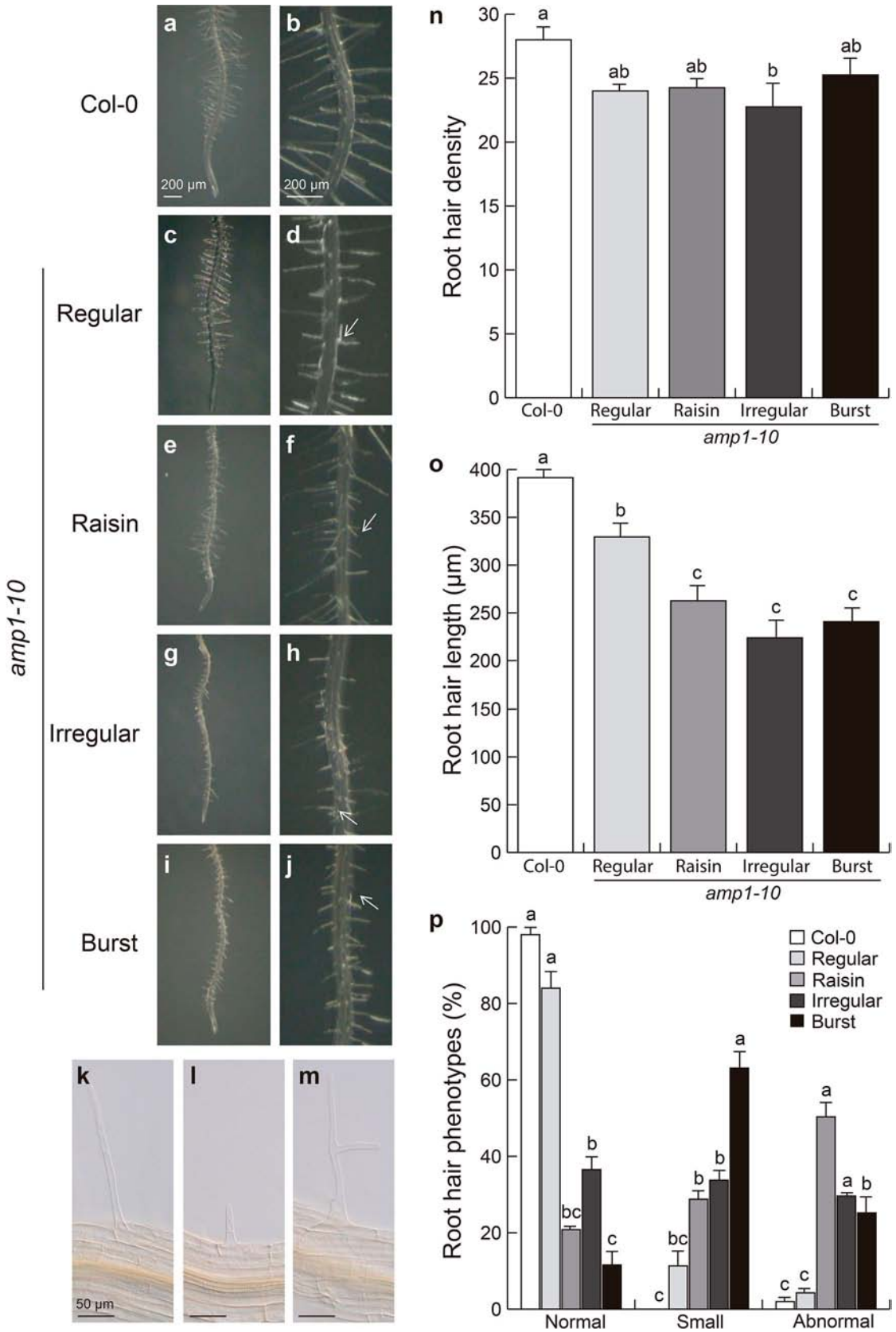

Journal : Large 344 Dispatch : 13-6-2016 Pages : 18
Article No. : 9612 LE TYPESET
MS Code : JPGR-15-0354 CP DISK

◀**Fig. 8** Root hair development is affected in *amp1* mutant. Root hairs of *Arabidopsis* WT (Col-0) and *amp1* mutant seedlings were scored 7 days after germination from a primary root using a stereomicroscope (**a–j**) or mounted on slides and visualized with the Nomarsky optics (**k–m**) then measured with image J program (http://imagej.nih.gov/ij/). Root hairs from WT (**a, b**), *amp1* "regular" seeds (**c, d**), "raisin" seeds (**e, f**), "irregular" seeds (**g, h**), or "burst" seeds (**i, j**) are shown. *Arrows* in **d, f**, and **j** are used to show small (**f**) and branched root hairs (**d and j**). Representative photographs of WT (**k**) and small (**l**) and branched root hairs (**m**) from *amp1* mutant seedlings using Nomarsky optics are shown. Root hair density (number of root hairs/mm of root), length and percentage of normal, small, and branched root hairs from each *amp1* seed classes are plotted in **n, o**, and **p** panels, respectively. *Error bars* represent SD from 10 plants analyzed. *Different letters* indicate statistical differences at $P < 0.05$. The experiment was repeated three times with similar results

defective embryo development, seed coat structure, and viability. Four phenotypic seed classes were identified in the progeny of homozygous *amp1* seedlings, including seeds with "regular" (WT) appearance along with seeds showing rough or very irregular coats and with protruding embryos. The alterations in seed structure and embryo development were reproducible in at least four generations of homozygous *AMP1* plants and could be traced back to early seed development in siliques from *amp1* plants showing the reported phenotypes of altered shoot development and early flowering (Chaudhury and others 1993; Vidaurre and others 2007; Griffiths and others 2011; Shi and others 2013b). Thus, we conclude that *amp1* seed phenotypes are genetically stable and are apparently related to the previously reported embryo defects in this mutant.

Arabidopsis seed development is controlled by several genes, including *FUSCA 3* (*FUS3*), *ABSCISIC ACID INSENSITIVE 3* (*ABI3*), *LEAFY COTYLEDON 1* and 2 (*LEC1, 2*), *AP2*, *TTG1*, and *GL2*. All four *abi3*, *lec1*, *lec2*, and *fus3* mutants are severely affected in seed maturation (Bäumlein and others 1994; Parcy and others 1997; Nambara and others 1995; Brarybrook and others 2006; Chiu and others 2012; Koornneef 1981; Koornneef and others 1982; Jofuku and others 1994). To the best of our knowledge, none of these mutants display the *amp1* seed coat phenotypes described here. Scanning electron microscopy analysis of epidermis of *amp1* seeds revealed that "raisin," "irregular," and "burst" classes of *amp1* seeds had a deformed surface, which is phenotypically similar to the *wrinkled 1* (*wri1*) mutant defective in an APETALA 2/ETHYLENE RESPONSIVE ELEMENT BINDING (AP2/EREB) transcription factor involved in seed storage metabolism (Focks and Benning 1998; Cernac and Benning 2004). Any possible relationship between *WRI1* and *AMP1* cannot be excluded based on the similarity of seed phenotypes. Another interesting connection between defective embryo development, seed coat specification, and sugar transport was recently revealed from characterization of *Arabidopsis* mutants defective on sucrose transporters SWEET11, 12, and 15. The corresponding mutants exhibited specific tissue and temporal expression patterns in developing seeds, and a *sweet11;12;15* triple mutant showed severe seed defects, including retarded embryo development, reduced seed weight, and reduced starch and lipid content that result in a "wrinkled" seed phenotype similar to that of *amp1* "raisin" or "irregular" seeds. In *sweet11;12;15* triple mutant, starch accumulates in the seed coat but not in the embryo, implicating SWEET-mediated sucrose efflux in the transfer of sugars from seed coat to embryo. An open possibility waiting to be demonstrated is that *AMP1* could regulate SWEET family sucrose transporters for sugar portioning to embryos and in this way affect the seed developmental program.

Previous research documented that mutation in the *MITOGEN-ACTIVATED PROTEIN KINASE 6 (MPK6)* affects seed morphology and embryo development leading to formation of three distinct seed phenotypes including rough seed coats and seeds with protruding embryos, which correlate with defects in seedling root development (López-Bucio and others 2014). Here, taking into account previous findings by Chaudhury and others (1993), and our analysis of embryo development in WT and *amp1–10* mutants, we propose that the absence of embryos in some "irregular" seeds of *amp1* is likely explained because of a failure in the fertilization process of egg and/or central cell. Abortion events were observed in *amp1* siliques, particularly from "irregular" seeds, as these contained embryos with retarded growth or lacked an embryo. In contrast, the analysis of less affected "regular" *amp1* seeds confirmed that this mutation causes an exaggerated activity of the shoot apical meristem, yielding embryos with three cotyledons (Chaudhury and others 1993; Nogué and others 2000a).

The closest *AMP1* homologous protein is a human glutamate carboxypeptidase II (GCPII), which is up-regulated in many tumors but its role in cancer development or the cell cycle is currently unknown (Hlouchova and others 2012). It is possible that the abnormal divisions during embryo development in *amp1* embryos arose through changes in the proteins controlling the plant cell cycle, but this hypothesis needs to be verified experimentally. The *Arabidopsis* mature seed coat consists of epidermal cells that produce mucilage, and its proper development is important to seed dispersion, water retention, and embryo protection (Arsovski and others 2010; Haughn and Western 2012). During germination, the mucilage is hydrated to form a gelatinous capsule composed by two layers: an inner one strongly adhered to the coat and another water soluble. Using electronic scanning microscopy and ruthenium red staining, we determined that *amp1* seed coats are

Journal : Large 344 Dispatch : 13-6-2016 Pages : 18
Article No. : 9612 LE TYPESET
MS Code : JPGR-15-0354 CP DISK

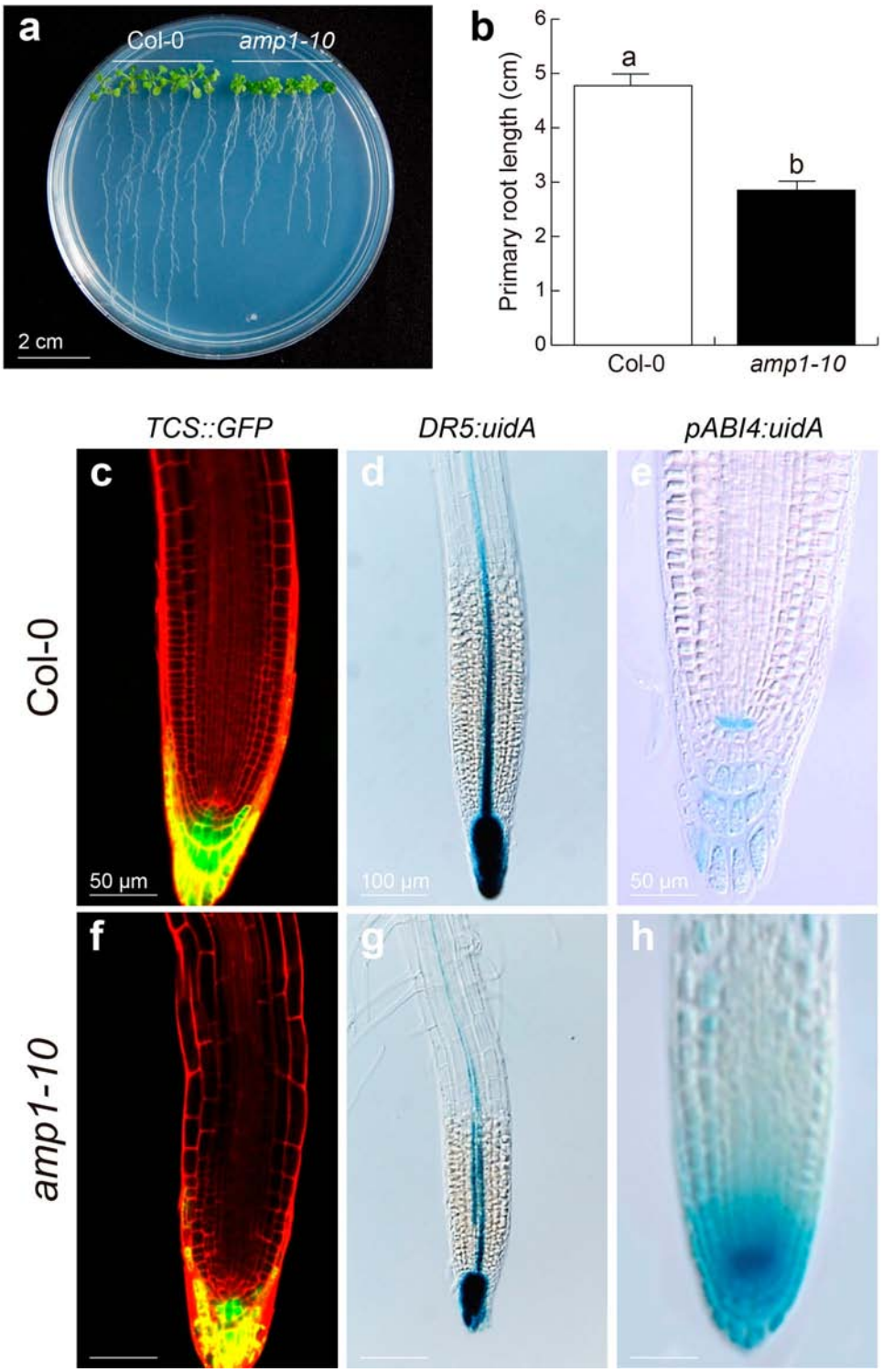

Fig. 9 Expression analyses of hormone-related gene markers in roots of WT and *amp1* seedlings. The phenotype of WT and *amp1* seedlings grown side by side (**a**) and mean primary root 7 days after germination (**b**). Expression of *TCS::GFP* (**c and f**) *DR5:uidA* (**d and g**) and *pABI4:uidA* (**e and h**) in primary roots of WT and *amp1* mutants. *Scale bars* in (**a**–**c**) are the same for all photographs in a column. Images are representative photographs of 15 seedlings analyzed

defective not only in epidermal cell structure, but also in formation of mucilage pocket. *amp1* "irregular" and "burst" phenotypical classes have areas of mucilage pocket thinner than the WT, and in some seed areas, the mucilage layers are missing. Interestingly, the outer layer increased its size in "regular" *amp1* seeds suggesting that *AMP1* is important for correct differentiation of the seed coat. Mutations on MUM genes cause defects in both mucilage production and chemical seed composition (Western and others 2001). In particular, the MUM3 and MUM4 genes are necessary for columella formation. MUM3 encodes *CELLULASE SYNTHASE 5*, whereas

Journal : Large 344 | Dispatch : 13-6-2016 | Pages : 18
Article No. : 9612 | LE | TYPESET
MS Code : JPGR-15-0354 | CP | DISK

MUM4 encodes an enzyme implicated in rhamnose biosynthesis and are thought to be regulated by *GL2* and *TTG* (Western and others 2004). One interesting possibility arising from our previous and current data is that *AMP1* could regulate the expression and/or activity of transcription factors regulating seed coat development or genes acting downstream. Contrary to our expectations, the gene expression analysis of *AP2*, *TTG*, and *MUM3* showed that decreased root growth as well as deformed root hairs and trichomes in *amp1* seedlings cannot be explained by reduced expression of these cell differentiation marker genes.

The similar seed phenotypes caused by mutations in *AMP1* and *MPK6* raises the significant question about the identity of the growth regulator mediating both seed coat and embryo development defects. To address this question, we compared the seed phenotypes of WT, *amp1*, and 27 hormone-related mutants. None of these mutants showed the *amp1* seed phenotypes described here, suggesting that *AMP1* controls seed development independently of the classical hormonal pathways, which evidently regulate other aspects of seed development, dormancy, or germination. Our observations further suggest a possible genetic link with MAPK signaling. Mutations in the MPKKK4 (YDA) protein kinase gene cause defects in embryo development resulting in protruding embryos similar to those observed in *mpk6* and *amp1* mutants (Lukowitz and others 2004). Besides, *MPKKK4* and *MPK6* are components of a common MAPK cascade involved in regulation of the embryo (Bush and Krysan 2007), stomata (Wang and others 2007), and root hair development (López-Bucio and others 2014), indicating their important role in epidermal developmental programs.

Germination begins with water uptake by the seed and proceeds to radicle emergence through the epidermis. The embryo, seed coat, and endosperm coordinately regulate seed dormancy and germination, independently or synergistically depending of the plant species (Bewley 1997). In a previous report, treatments with GA improved by 60 % *amp1* germination (Griffiths and others 2011). The data from "regular" *amp1* seeds are in agreement with this previous report. However, GA failed to normalize seed germination of most *amp1* seeds with "raisin," "irregular," and "burst" phenotypes, suggesting that the seed coat defects in these mutants likely occur independently of GA signaling and that seed germination did not proceed because the embryos failed to develop.

In *Arabidopsis*, some common genes are involved in the production of seed mucilage, root hair, and trichome development, including *TTG1* and *GL2* (Walker and others 1999; Rerie and others 1994). *ttg1* and *gl2* mutants lack the mucilage pocket in the seed coat, whereas the trichomes and root hairs are defective in these mutants. This prompted us to investigate whether *amp1* mutants could have any developmental alteration during trichome and root hair development. The *amp1* mutants had reduced numbers of trichomes on leaves, which were shorter and less branched than the WT. In contrast, when compared to WT seedlings, *amp1* mutants developed short, abnormally branched root hairs. Together, these observations support a function of *AMP1* on epidermal cell differentiation programs on leaves and in determining root hair elongation. The opposite phenotypes of trichomes and root hairs observed in *amp1* mutants cannot be explained by changes in gene cassettes regulating trichome cell fate or root hair organization. In the leaf epidermis, *TTG*, *GL2*, and an upstream myb family factor (*GL1* or *CAPRICE*, *CPC*) induce trichome differentiation. In roots, *TTG*, *GL2*, and *CPC* are used to block root hair differentiation (Benfey 1999; Schiefelbein 2003). Lin and Schiefelbein (2001) found that the *GL2* expression starts in the protoderm stage during embryo development and concluded that the cell pattern of trichomes and root hairs is established early during embryogenesis. Indeed, *GL2* and *TTG1* are required for both mucilage synthesis and columella formation. The seed coat phenotypes of *amp1* mutants correlate with embryo malformation and even abortion at relatively early developmental stages suggesting that the seed coat defect is rather a unspecific consequence derived from the embryo defect. Another important difference between *amp1* and the *gl2/ttg1* class of epidermal differentiation mutants is that in the severe *amp1* seed class, a columella is still recognizable and mucilage staining present in the majority of the seed coat. Moreover, whereas *amp1* shows a reduction in trichome density similar to *gl2/ttg1* their other hallmark, ectopic root hair formation from normally atrichoblastic cells is apparently not present in *amp1*. We rather observed shorter root hairs and occasional branching but the root hair density is not increased as in *gl2* mutants. From these evidences, it seems that *AMP1* acts independently from TTG to impact the epidermal differentiation program during post-embryonic development. The fact that AP2 is overexpressed in *amp1* mutants shows another level of interaction possibly mediating cell phase transitions during vegetative/reproductive development such as the flowering time, but this possibility merits further research.

The prevalent explanation of the shoot apical meristem defects in *amp1* mutants takes into account the reported increments in CK levels. However, recent data have failed to coherently attribute the shoot and root phenotypes of *amp1* to a single hormonal pathway, because the corresponding mutants show alterations in ABA and auxin-related gene programs (Yao and others 2014; Huang and others 2015). An analysis of WT and *amp1* lines expressing CKs, auxin or ABA reporter gene constructs revealed a clear induction of *pABI:uidA* in roots and shoots of *amp1*

Journal : Large 344 | Dispatch : 13-6-2016 | Pages : 18
Article No. : 9612 | LE | TYPESET
MS Code : JPGR-15-0354 | CP | DISK

mutants, suggesting that ABA synthesis and/or response is a critical factor underlying post-embryonic developmental alterations associated with the function of this master regulator.

In summary, our results indicate that *AMP1* serve in the differentiation of epidermal cells from the embryo, root, and leaf likely via ABA signaling. Future studies to examine *AMP1* gene expression and function in *Arabidopsis* mutants with seed coat and epidermal phenotypes such as *yoda* and *mpk6* could shed much light on MAPK signaling involved in root growth and epidermal patterning.

Acknowledgments We are thankful to the *Arabidopsis* stock center for kindly providing us with *Arabidopsis* mutant seeds and Jose Antonio Rodríguez-Torres and Víctor López-Morelos for permission and advice for the use of electronic microscope, and León F. Ruiz-Herrera for support in confocal imaging. Drs. Shuhua Yang, Tom Guilfoyle, Bruno Müller, and Patricia León are thanked for providing us *Arabidopsis* mutant and transgenic lines. This work was supported by grants from the Consejo Nacional de Ciencia y Tecnología (CONACYT, México, Grant no. 177775), the Consejo de la Investigación Científica (UMSNH, México, Grant No. CIC 2.26), and the AQ2 UNAM-DGAPA-PAPIIT (Grant IN207014 to AAGG and JSLB).

References

Arc E, Sechet J, Corbineau F, Rajjou L, Marion-Poll A (2013) ABA crosstalk with ethylene and nitric oxide in seed dormancy and germination. Front Plant Sci 4:1–19

Arsovski AA, Haughn GW, Western TL (2010) Seed coat mucilage cells of *Arabidopsis thaliana* as a model for plant cell wall research. Plant Signal Behav 5:796–801

Bäumlein H, Miséra S, Luerssen H, Kölle K, Horstmann C, Wobus U, Müller AJ (1994) The FUS3 gene of *Arabidopsis thaliana* is a regulator of gene expression during late embryogenesis. Plant J 6:379–387

Benfey P (1999) Is the shoot a root with a view? Curr Opin Plant Biol 2:39–43

Berger F, Grini PE, Schnittger A (2006) Endosperm: an integrator of seed growth and development. Curr Opin Plant Biol 9:664–670

Bewley JD (1997) Seed germination and dormancy. Plant Cell 9:1055–1066

Bleecker AB, Estelle MA, Somerville C, Kende H (1988) Insensitivity to ethylene conferred by a dominant mutation in *Arabidopsis thaliana*. Science 241:1086–1089

Bossi F, Cordoba E, Dupre P, Santos M, San Roman C, León P (2009) The *Arabidopsis* ABA-INSENSITIVE (ABI) 4 factor acts as a central transcription activator of the expression of its own gene, and for the induction of *ABI5* and *SBE2.2* genes during sugar signaling. Plant J 59:359–374

Brarybrook S, Stone L, Park S, Bur AQ, Lee BH Fischer RL, Goldberg RB, Harada JJ (2006) Genes directly regulated by leaf cotyledon 2 provides insight into the control of embryo maturation and somatic embryogenesis. Proc Natl Acad Sci USA 103:3468–3473

Breuninger H, Rikirsch E, Hermann M, Ueda M, Laux T (2008) Differential expression of *WOX* genes mediates apical-basal axis formation in the *Arabidopsis* embryo. Dev Cell 14:867–876

Bruex A, Kainkaryam RM, Wieckowski Y, Kang YH, Bernhardt C, Xia Y, Zheng X, Wang JY, Lee MM, Benfey P, Woolf PJ, Schiefelbein J (2012) A gene regulatory network for root epidermis cell differentiation in *Arabidopsis*. PLoS Genet 8:e1002446

Bush SM, Krysan PJ (2007) Mutational evidence that the *Arabidopsis* MAP kinase MPK6 is involved in another, inflorescence, and embryo development. J Exp Bot 58:2181–2191

Casson SA, Hetherington AM (2010) Environmental regulation of stomatal development. Curr Opin Plant Biol 13:90–95

Cernac A, Benning C (2004) WRINKLED1 encodes an AP2/EREB domain protein involved in the control of storage compound biosynthesis in *Arabidopsis*. Plant J 40:575–585

Chao Q, Rothenberg M, Solano R, Roman G, Terzaghi W, Ecker J (1997) Activation of the ethylene gas response pathway in *Arabidopsis* by the nuclear protein ETHYLENE-INSENSITIVE3 and related proteins. Cell 89:1133–1144

Chaudhury AM, Letham S, Craig S, Dennis ES (1993) *AMP1* a mutant with high cytokinin levels and altered embryonic pattern, faster vegetative growth, constitutive photomorphogenesis and precocious flowering. Plant J 4:907–916

Chen LQ, Lin W, Qu XQ, Sosso D, McFarlane HE, Londoño A, Samuels L, Frommer W (2015) A cascade of sequentially expressed sucrose transporters in the seed coat and endosperm provides nutrition for the *Arabidopsis* embryo. Plant Cell 27:607–619

Chin-Atkins A, Craig S, Hocart C, Dennis E, Chaudhury A (1996) Increased endogenous cytokinin in the *Arabidopsis amp1* mutant corresponds with de-etiolation responses. Planta 198:549–556

Chiu RS, Nahal H, Provart NJ, Gazzarrini S (2012) The role of the *Arabidopsis* FUSCA3 transcription factor during inhibition of seed germination at high temperature. BMC Plant Biol 12:15

Chory J, Nagpal P, Peto CA (1991) Phenotypic and genetic analysis of *det2,* a new mutant that affects light-regulated seedling development in *Arabidopsis*. Plant Cell 3:445–459

Debeaujon I, Léon-Kloosterziel KM, Koornneef M (2000) Influence of the testa on seed dormancy, germination, and longevity in *Arabidopsis*. Plant Physiol 122:403–414

Dekkers BJ, Pearce S, van Bolderen-Veldkamp RP et al (2013) Transcriptional dynamics of two seed compartments with opposing roles in *Arabidopsis* seed germination. Plant Physiol 163:205–215

Figueiredo DD, Köhler C (2014) Signalling events regulating seed coat development. Biochem Soc Trans 42:358–363

Finkelstein R (1994) Mutations at two new Arabidopsis ABA response loci are similar to the *abi3* mutations. Plant J 5:765–771

Finkelstein RR, Wang ML, Lynch TJ, Rao S, Goodman HM (1998) The Arabidopsis abscisic acid response locus *ABI4* encodes an APETALA2 domain protein. Plant Cell 10:1043–1054

Focks N, Benning C (1998) *wrinkled1*: a novel, low-seed-oil mutant of *Arabidopsis* with a deficiency in the seed-specific regulation of carbohydrate metabolism. Plant Physiol 118:91–101

Fukaki H, Tameda S, Masuda H, Tasaka M (2002) Lateral root formation is blocked by a gain-of-function mutation in the SOLITARY-ROOT/IAA14 gene of *Arabidopsis*. Plant J 29:153–168

Gallavotti A (2013) The role of auxin in shaping shoot architecture. J Exp Bot 64:2593–2608

Glover B (2000) Differentiation in plant epidermal cells. J Exp Bot 51:497–505

Griffiths J, Barrero JM, Taylor J, Helliwell CA, Gubler F (2011) ALTERED MERISTEM PROGRAM 1 is involved in development of seed dormancy in Arabidopsis. PLoS One 6:e20408

Guo FQ, Okamoto M, Crawford NM (2003) Identification of a plant nitric oxide synthase gene involved in hormonal signaling. Science 302:100–103

Guzman P, Ecker JR (1990) Exploiting the triple response of *Arabidopsis* to identify ethylene-related mutants. Plant Cell 2:513–523

Journal : Large 344 | Dispatch : 13-6-2016 | Pages : 18
Article No. : 9612 | ☐ LE | ☐ TYPESET
MS Code : JPGR-15-0354 | ☑ CP | ☑ DISK

Hanke DE, Northcote DH (1975) Molecular visualization of pectin and DNA by ruthenium red. Biopolymers 14:1–17

Haughn G, Chaudhury A (2005) Genetic analysis of seed coat development in *Arabidopsis*. Trends Plant Sci 10:472–477

Haughn G, Western T (2012) *Arabidopsis* seed coat mucilage is a specialized cell wall that can be used as a model for genetic analysis of plant cell wall structure and function. Front Plant Sci 3:64

Hehenberger E, Kradolfer D, Köhler C (2012) Endosperm cellularization defines an important developmental transition for embryo development. Development 139:2031–2039

Helliwell CA, Chin-Atkins AN, Wilson IW, Chapple R, Dennis ES, Chaudhury A (2001) The *Arabidopsis AMP1* gene encodes a putative glutamate carboxypeptidase. Plant Cell 13:2115–2125

Hlouchova K, Navratil V, Tykvart J, Sacha P, Konvalinka J (2012) GCPII variants, paralogs and orthologs. Curr Med Chem 19:1316–1322

Holdsworth MJ, Bentsink L, Soppe WJJ (2008) Molecular networks regulating *Arabidopsis* seed maturation, after-ripening, dormancy and germination. New Phytol 179:33–54

Huang W, Pitorre D, Poretska O, Marizzi C, Winter N, Poppenberger B, Sieberer T (2015) *ALTERED MERISTEM PROGRAM1* suppresses ectopic stem cell niche formation in the shoot apical meristem in a largely cytokinin-independent manner. Plant Physiol 167:1471–1486

Hülskamp M, Misra S, Jürgens G (1994) Genetic dissection of trichome cell development in *Arabidopsis*. Cell 76:555–566

Ingouff M, Jullien PE, Berger F (2006) The female gametophyte and the endosperm control cell proliferation and differentiation of the seed coat in *Arabidopsis*. Plant Cell 18:3491–3501

Inoue T, Higuchi M, Hashimoto Y, Seki M, Kobayashi M, Kato T, Tabata S, Shinozaki K, Kakimoto T (2001) Identification of CRE1 as a cytokinin receptor from *Arabidopsis*. Nature 409:1060–1063

Ishida T, Kurata T, Okada K, Wada TA (2008) Genetic regulatory network in the development of trichomes and root hairs. Annu Rev Plant Biol 59:365–386

Javelle M, Vernoud V, Rogowsky PM, Ingram GC (2011) Epidermis: the formation and functions of a fundamental plant tissue. New Phytol 189:17–39

Jofuku D, den Boer BGW, Van Montagu M, Okamuro JK (1994) Control of *Arabidopsis* flower and seed development by the homeotic gene *APETALA2*. Plant Cell 6:1211–1225

Kieber JJ, Rotheberg M, Roman G, Feldmann KA, Ecker JR (1993) CTR a negative regulator of the ethylene response pathway in *Arabidopsis*, encodes a member of the Raf family of protein kinases. Cell 72:1–20

Kong J, Lau S, Jurgens G (2015) Twin plants from supernumerary egg cells in *Arabidopsis*. Curr Biol 25:225–230

Koornneef M (1981) The complex syndrome of the *ttg* mutants. Arabid Inf Serv 18:45–51

Koornneef M, Dellaert LWM, Vanderveen JH (1982) EMS-induced and radiation-induced mutation frequencies at individual loci in *Arabidopsis thaliana* (L) heynh. Mutat Res 93:109–123

Lafon C, Köhler C (2014) Embryo and endosperm, partners in seed development. Curr Opin Plant Biol 17:64–69

Lau S, Slane D, Herud O, Kong J, Jürgens G (2012) Early embryogenesis in flowering plants: settings up the basic body pattern. Annu Rev Plant Biol 63:483–506

Leung J, Merlot S, Giraudat J (1997) The Arabidopsis ABSCISIC ACID-INSENSITIVE2 (ABI2) and ABI1 genes encode homologous protein phosphatases 2C involved in abscisic acid signal transduction. Plant Cell 9:759–771

Libault M, Brechenmacher L, Cheng J, Xu D, Stacey G (2010) Root hairs systems biology. Trends Plant Sci 15:641–650

Lin Y, Schiefelbein J (2001) Embryonic control of epidermal cell patterning in the root and hypocotyl of *Arabidopsis*. Development 128:3697–3705

Liu WZ, Kong DD, Gu XX, Gao HB, Wang JZ, Xia M, Gao Q, Tian LL, Xu ZH, Bao F, Hu Y, Ye NS, Pei ZM, He YK (2013) Cytokinins can act as suppressors of nitric oxide in Arabidopsis. Proc Natl Acad Sci U S A 110:1548–1553

Locascio A, Roig-Villanova I, Bernardi J, Varotto S (2014) Current perspectives on the hormonal control of seed development in Arabidopsis and maize: a focus on auxin. Front Plant Sci 5:1–22

López-Bucio JS, Dubrovsky JG, Raya-González J, Ugartechea-Chirino Y, López-Bucio J, de Luna-Valdez LA, Ramos-Vega M, León P, Guevara-García AA (2014) *Arabidopsis thaliana* mitogen-activated protein kinase 6 is involved in seed formation and modulation of primary and lateral root development. J Exp Bot 65:169–183

Lukowitz W, Roeder A, Parmenter D, Somerville C (2004) A MAPKK kinase gene regulates extra-embryonic cell fate in *Arabidopsis*. Cell 116:109–119

Masucci JD, Rerie WG, Foreman DR, Zhang M, Galway ME, Marks MD, Schiefelbein JW (1996) The homeobox gene *GLABRA 2* is required for position-dependent cell differentiation in the root epidermis of *Arabidopsis thaliana*. Development 122:1252–1260

Mordhorst AP, Voerman KJ, Hartog MV, Meijer EA, van Went J, Koornneef M, de Vries SC (1998) Somatic embryogenesis in *Arabidopsis thaliana* is facilitated by mutations in genes repressing meristematic cell divisions. Genetics 149:549–563

Morquecho-Contreras A, Méndez-Bravo A, Pelagio-Flores R, Raya-González J, Ortíz-Castro R, López-Bucio J (2010) Characterization of *drr1*, an alkamide-resistant mutant of *Arabidopsis*, reveals an important role for small lipid amides in lateral root development and plant senescence. Plant Physiol 152:1659–1673

Nambara E, Naito S, McCourt P (1992) A mutant of Arabidopsis which is defective in seed development and storage protein accumulation is a new *abi3* allele. Plant J 2:435–441

Nambara E, Keith K, McCourt P, Naito S (1995) A regulatory role for the ABI3 gene in the establishment of embryo maturation in *Arabidopsis thaliana*. Development 121:629–636

Nogué F, Grandjean O, Craig S, Dennis E, Chaudhury AM (2000a) Higher level of cell proliferation rate and cyclin CycD3 expression in the *Arabidopsis amp1* mutant. Plant Growth Regul 32:275–283

Nogué F, Hocart C, Letham DS, Dennis ES, Chaudhury AM (2000b) Cytokinin synthesis is higher in the *Arabidopsis amp1* mutant. Plant Growth Regul 32:267–273

Okushima Y, Fukaki H, OnadaM Theologis A, Tasaka M (2007) ARF7 and ARF19 regulate lateral root formation via direct activation of LBD/ASL genes in *Arabidopsis*. Plant Cell 19:118–1340

Orozco-Arroyo G, Paolo D, Ezquer I, Colombo L (2015) Networks controlling seed size in *Arabidopsis*. Plant Reprod 28:17–32

Parcy F, Valon C, Kohara A, Miséra S, Giraudat J (1997) The ABSCISIC ACID-INSENSITIVE 3 (ABI3), FUSCA 3 (FUS3) and LEAFY COTYLEDON 1 (LEC1) loci act in concert to control multiple aspects of Arabidopsis seed development. Plant Cell 9:1265–1277

Parry G, Calderon-Villalobos LI, Prigge M, Peret B, Dharmasiri S, Itoh H, Lechner E, Gray WM, Bennett M, Estelle M (2009) Complex regulation of the TIR/AFB family of auxin receptors. Proc Natl Acad Sci USA 106:22540–22545

Pattanaik S, Patra B, Kumar S, Yuan L (2014) An overview of the gene regulatory network controlling trichome development in the model plant, Arabidopsis. Front Plant Sci 5:1–8

Pickett FB, Wilson AK, Estelle M (1990) The *aux1* mutation of Arabidopsis confers both auxin and ethylene resistance. Plant Physiol 94:1462–1466

Raya-González J, Ortiz-Castro R, Ruiz-Herrera LF, Kazan K, López-Bucio J (2014) Phytochrome and flowering time1/mediator25 regulates lateral root formation via auxin signaling in *Arabidopsis*. Plant Physiol 165:880–894

Journal : Large 344 | Dispatch : 13-6-2016 | Pages : 18
Article No. : 9612 | LE | TYPESET
MS Code : JPGR-15-0354 | CP | DISK

Rerie WG, Feldman DD, Carrington JC (1994) The GLABRA2 gene encodes a homeodomain protein required for normal trichome development in *Arabidopsis*. Genes Dev 8:1388–1399

Roszak P, Köhler C (2011) Polycomb group proteins are required to couple seed coat initiation to fertilization. Proc Natl Acad Sci USA 108:20826–20832

Ruiz-Herrera LF, Shane M, López-Bucio J (2015) Nutritional regulation of root development. Wires Dev Biol 4:431–443

Saibo NJ, Vriezen WH, De Grauwe L, Azmi A, Prinsen E, Van Der Straeten D (2007) A comparative analysis of the *Arabidopsis* mutant *amp1-1* and a novel weak *amp1* allele reveals new functions of the AMP1 protein. Planta 225:831–842

Schiefelbein J (2003) Cell-fate specification in the epidermis: a common patterning mechanism in the root and shoot. Curr Opin Plant Biol 6:74–78

Shi H, Ye T, Wang Y, Chan Z (2013a) Arabidopsis ALTERED MERISTEM PROGRAM 1 negatively modulates plant responses to abscisic acid and dehydration stress. Plant Physiol Biochem 67:209–216

Shi Y, Wang Z, Meng P, Tian S, Zhang X, Yang S (2013b) The glutamate carboxypeptidase AMP1 mediates abscisic acid and abiotic stress responses in *Arabidopsis*. New Phytol 199:135–150

Smalle J, Kurepa J, Yang P, Babiychuk E, Kushnir S, Durski A, Vierstra RD (2002) Cytokinin growth responses in *Arabidopsis* involve the 26S proteasome subunit RPN12. Plant Cell 14:17–32

Tiryaki I, Staswick P (2002) An Arabidopsis mutant defective in jasmonate response is allelic to the auxin-signaling mutant *axr1*. Plant Physiol 130:887–894

Tominaga-Wada R, Iwata M, Sugiyama J, Katoke T, Ishida T, Yokoyama R, Nishitani K, Kiyotaka Okada, Wada T (2009) The GLABRA2 hoeodomain protein directly regulates CESA5 and XTH17 gene expression in *Arabidopsis* Roots. Plant J 60:564–574

Ueguchi C, Koizumi H, Suzuki T, Mizuno T (2001) Novel family of sensor histidine kinase genes in *Arabidopsis thaliana*. Plant Cell Physiol 42:231–235

Ullah H, Chen JG, Wang S, Jones AM (2002) Role of a heterotrimeric G protein in regulation of Arabidopsis seed germination. Plant Physiol 129:897–907

Ulmasov T, Murfett J, Hagen G, Guilfoyle TJ (1997) Aux/IAA proteins repress expression of reporter genes containing natural and highly active synthetic auxin response elements. Plant Cell 9:1963–1971

Vidaurre DP, Ploense S, Krogan NT, Berleth T (2007) AMP1 and MP antagonistically regulate embryo and meristem development in *Arabidopsis*. Development 134:2561–2567

Voiniciuc C, Yang B, Schmidt MHW, Günl M, Usadel B (2015) Starting to gel: how *Arabidopsis* seed coat epidermal cells produce specialized secondary cell walls. Int J Mol Sci 16:3452–3473

Volodymyr R, Boriskuj L (2014) Physical, metabolic and developmental functions of the seed coat. Front Plant Sci 5:1–17

Walker AR, Davidson PA, Bolognesi-Winfield AC, James CM, Srinivasan N, Blundellb TL, Esche JJ, Marks MD, Gray JC (1999) The TRANSPARENT TESTA GLABRA1 locus, which regulates trichome differentiation and anthocyanin biosynthesis in *Arabidopsis*, encodes a WD40 repeat protein. Plant Cell 11:1337–1350

Wang H, Ngwenyama N, Liu Y, Walker JC, Zhang S (2007) Stomatal development and patterning are regulated by environmentally responsive mitogen-activated protein kinases in *Arabidopsis*. Plant Cell 19:63–73

Western TL, Burn J, Skinner DJ, Martin-McCaffrey L, Moffatt BA, Haughn GW (2001) Isolation and characterization of mutants defective in seed coat mucilage secretory cell development in *Arabidopsis*. Plant Physiol 127:998–1011

Western TL, Young DS, Dean GH, Tan WL, Samuels AL, Haughn GW (2004) MUCILAGE-MODIFIED4 encodes a putative pectin biosynthetic enzyme developmentally regulated by APETALA2, TRANSPARENT TESTA GLABRA1, and GLABRA2 in *Arabidopsis* seed coat. Plant Physiol 134:296–306

Wilkinson JQ, Crawford NM (1993) Identification and characterization of a chlorate-resistant mutant of *Arabidopsis thaliana* with mutations in both nitrate reductase structural genes *NIA1* and *NIA2*. Mol Gen Genet 239:289–297

Wilson AK, Pickett FB, Turner JC, Estelle M (1990) A dominant mutation in Arabidopsis confers resistance to auxin, ethylene and abscisic acid. Mol Gen Genet 222:377–383

Windsor J, Symonds V, Mendenhall J, Lloyd A (2000) *Arabidopsis* seed coat development: morphological differentiation of the outer integument. Plant J 22:483–493

Woeste KE, Ye C, Kieber JJ (1999) Two Arabidopsis mutant that overproduce ethylene are affected in the posttranscriptional regulation of 1-aminocyclopropane-1-carboxylic acid synthase. Plant Physiol 119:521–530

Yao Y, Dong CH, Yi Y, Li X, Zhang X, Liu J (2014) Regulatory function of *AMP1* in ABA biosynthesis and drought resistance in *Arabidopsis*. J Plant Biol 57:117–126

Zhou Z, Wang L, Li J, Song X, Yang C (2009) Study on programmed cell death and dynamic changes of starch accumulation in pericarp cells of *Triticum aestivum* L. Protoplasma 236:49–58

Zürcher E, Tavor-Deslex D, Lituiev D, Enkerli K, Tarr P, Müller B (2013) A robust and sensitive synthetic sensor to monitor the transcriptional output of the cytokinin signaling network in planta. Plant Physiol 161:1066–1075

Journal : Large 344 | Dispatch : 13-6-2016 | Pages : 18
Article No. : 9612 | ☐ LE | ☐ TYPESET
MS Code : JPGR-15-0354 | ☑ CP | ☑ DISK

Journal : **344**
Article : **9612**

Springer
the language of science

Author Query Form

Please ensure you fill out your response to the queries raised below and return this form along with your corrections

Dear Author

During the process of typesetting your article, the following queries have arisen. Please check your typeset proof carefully against the queries listed below and mark the necessary changes either directly on the proof/online grid or in the 'Author's response' area provided below

Query	Details Required	Author's Response
AQ1	Please check the edit made in the article title.	
AQ2	Reference: Reference (E Arc 2013, P Roszak 2011) was provided in the reference list; however, this was not mentioned or cited in the manuscript. As a rule, if a citation is present in the text, then it should be present in the list. Please provide the location of where to insert the reference citation in the main body text.	